Regulation of virulence-associated traits of the human fungal pathogen *Candida albicans* by nitrogen availability

Regulation Virulenz-assoziierter Faktoren im humanpathogenen Pilz *Candida albicans* durch Stickstoffverfügbarkeit

Doctoral thesis for a doctoral degree

at the Graduate School of Life Sciences (GSLS),

University of Würzburg

Section: Infection and Immunity

Submitted by

Nico Dunkel

from Dresden, Germany

Würzburg, 2013

Submitted on:

Members of the Supervisory Committee:

Chairperson: Prof. Dr. Thomas Dandekar

Primary Supervisor: Prof. Dr. Joachim Morschhäuser

Supervisor (Second): Prof. Dr. Sven Krappmann

Supervisor (Third): Prof. Dr. Roy Gross

Supervisor (Fourth) (if applicable):

Date of Public Defense:

Date of receipt of Certificate:

Eingereicht am:

Mitglieder des Promotionskomitees:

Vorsitzender: Prof. Dr. Thomas Dandekar

1. Gutachter: Prof. Dr. Joachim Morschhäuser
2. Gutachter: Prof. Dr. Sven Krappmann
3. Gutachter: Prof. Dr. Roy Gross
4. Gutachter (falls zutreffend):

Tag des Promotionskolloqiums:

Doktorurkunde ausgehändigt am:

Affidavit

I hereby confirm that my thesis entitled “Regulation of virulence-associated traits of the human fungal pathogen *Candida albicans* by nitrogen availability” is the result of my own work. I did not receive any help or support from commercial consultants. All sources and/or materials applied are listed and specified in the thesis

Furthermore, I confirm that this thesis has not been submitted as a part of another examination process neither in identical nor similar form.

Würzburg, 15 July, 2013 Nico Dunkel

Eidesstattliche Erklärung

Hiermit erkläre ich an Eides statt, die Dissertation „Regulation Virulenz-assoziierter Faktoren im humanpathogenen Pilz *Candida albicans* durch Stickstoffverfügbarkeit“ eigenständig, d.h. insbesondere selbständig und ohne Hilfe eines kommerziellen Promotionsberaters, angefertigt und keine anderen als die von mir angegebenen Quellen und Hilfsmittel verwndet zu haben.

Ich erkläre außerdem, dass die Dissertation weder in gleicher noch in ähnlicher Form bereits in einem anderem Prüfungsverfahren vorgelegen hat.

Würzburg, 15 Juli 2013 Nico Dunkel

Acknowledgments

Hereby I express my deep sense of gratitude to my doctoral supervisor Prof. Dr. Joachim Morschhäuser for his sublime guidance and paramount support. I also deeply thank the members of my Supervisory Committee, Prof. Dr. Sven Krappmann and Prof. Dr. Roy Gross, for their supportive suggestions and valuable help during my dissertation. Moreover, I gratefully appreciate the affiliation at the Institute for Molecular Infection Biology, under direction of Prof. Dr. Dr. h.c. mult. Jörg Hacker and Prof. Dr. Jörg Vogel, which gave me the chance to discuss and socialize with remarkable scientists. Further I thank the Graduate School of Life Sciences (GSLS) for providing an excellent research and education environment that strongly promoted my scientific skills.

I am also indepted to Tina Schäfer, who thoroughly helped me with the mouse experiments, and Dr. Oliver Reuss, Dr. Christoph Sasse, Renate Franz, and Tobias Hertlein, who generated the peptide transporter mutant strains.

Moreover, I owe special thanks to Prof. Dr. Martine Raymond and her group at the IRIC (Institute for Research in Immunology and Cancer), Université de Montréal, Canada, for the unique chance to perform ChIP-on-chip experiments and the wonderful time I had. Especially, I cherish the exceptional supervision by Sandra Weber and the pleasing conversations with Fatiha Louhichi.

I further yield thanks to all former and present members of the Candida working group who accompanied my dissertation, particularly (in alphabetical order) Anna-Lena, Benjamin, Bernardo, Christa, Christina, Christoph, Dagmar, Eva, Fatima, Heide, Irene, Jens, Julia, Kristina, Michael, Sabrina Schneider, Sabrina Schubert, Selene, Srisuda, Sven, Tina, and Rebecca for a splendid time in and outside the laboratory.

I feel also blessed to have such a wonderful family behind myself, who supported me financially and mentaly during the ups and downs of my PhD thesis.

From the bottom of my heart I thank my magnificient fiancée Lisa for her love and patience with me over the years.

Danksagung

Hiermit drücke ich meine tiefste Dankbarkeit gegenüber meinem Doktorvater Prof. Dr. Joachim Morschhäuser aus, für seine großartige Anleitung und hervorragende Unterstützung. Ich danke weiterhin meinen Komiteemitgliedern, Prof. Dr. Sven Krappmann and Prof. Dr. Roy Gross, für ihre unterstützenden Vorschläge und wertvolle Hilfe während meiner Promotion. Des Weiteren schätze ich die Zugehörigkeit am Institut für Molekulare Infektionsbiologie, unter der Leitung von Prof. Dr. Dr. h.c. mult. Jörg Hacker and Prof. Dr. Jörg Vogel, welches mir die Chance ermöglichte aussergewöhnliche Wissenschaftler kennenzulernen. Ausserdem danke ich der Graduate School of Life Sciences (GSLS) für die Bereitstellung einer exzellenten Forschungs- und Bildungsumgebung, welche meine wissenschaftlichen Fähigkeiten stark gefördert haben.

Zu großem Dank verpflichtet bin ich auch Dr. Tina Schäfer für die tolle Hilfe bei der Durchführung der Mausexperimente und Dr. Oliver Reuss, Dr. Christoph Sasse, Renate Franz und Tobias Hertlein, für die Herstellung der Peptidtransportermutanten.

Insbesondere danke ich Prof. Dr. Martine Raymond und ihrer Arbeitsgruppe am IRIC (Institute for Research in Immunology and Cancer), Université de Montréal, Kanada, für die einmalige Möglichkeit ChIP-on-chip Experimente durchzuführen und für die wundervolle Zeit. Spezielle Wertschätzung gilt dabei der außergewöhnlichen Betreuung durch Sandra Weber und den angenehmen Gesprächen mit Fatiha Louhichi.

Besonderer Dank gilt auch allen ehemaligen und aktuellen Mitgliedern der Candida-Arbeitsgruppe, die mich während meiner Promotion begleitet haben, speziell (in alphabetischer Reihenfolge) Anna-Lena, Benjamin, Bernardo, Christa, Christina, Christoph, Dagmar, Eva, Fatima, Heide, Irene, Jens, Julia, Kristina, Michael, Sabrina Schneider, Sabrina Schubert, Selene, Srisuda, Sven, Tina, und Rebecca für eine blendende Zeit innerhalb und außerhalb des Labors.

Zu guter Letzt fühle ich mich gesegnet eine solch wundervolle Familie zu haben, die mich immer, sowohl finanziell als auch mental während aller Hochs und Tiefs meiner Promotion, unterstützt haben.

Aus tiefstem Herzen danke ich meiner großartigen Verlobten Lisa für ihre Liebe und ihre Geduld mit mir über die Jahre.

Dedicated to my parents

Gewidmet meinen Eltern

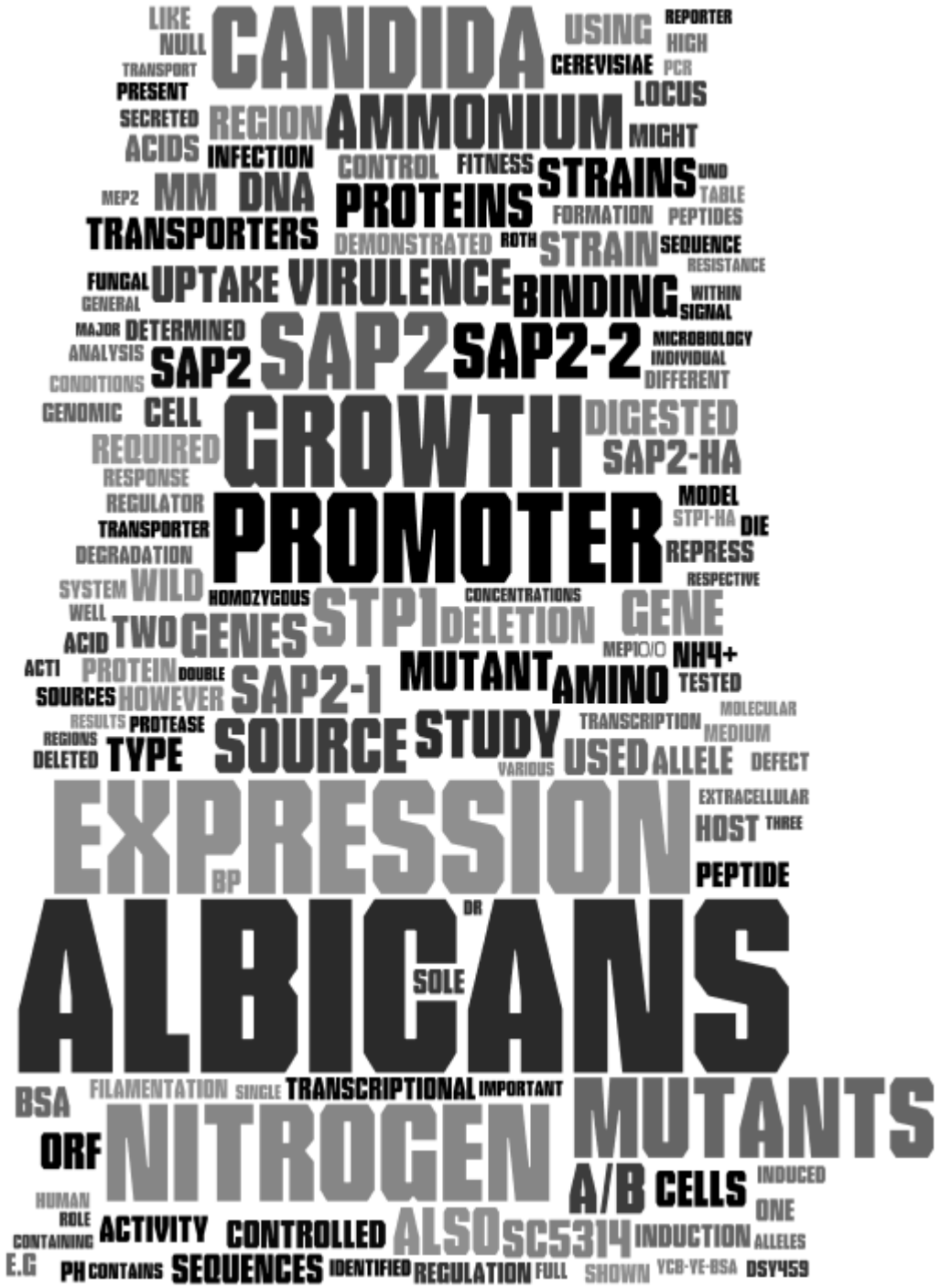

Created with www.wordle.net

Content

Summary

Nitrogen-regulated pathogenesis describes the expression of virulence attributes as direct response to the quantity and quality of an available nitrogen source. As consequence of nitrogen availability, the opportunistic human fungal pathogen *Candida albicans* changes its morphology and secretes aspartic proteases [SAPs], both well characterized virulence attributes. *C. albicans*, contrarily to its normally non-pathogenic relative *Saccharomyces cerevisiae*, is able to utilize proteins, which are considered as abundant and important nitrogen source within the human host. To assimilate complex proteinaceous matter, extracellular proteolysis is followed by uptake of the degradation products through dedicated peptide transporters (di-/tripeptide transporters [PTRs] and oligopeptide transporters [OPTs]). The expression of both traits is transcriptionally controlled by Stp1 - the global regulator of protein utilization - in *C. albicans*.

The aim of the present study was to elucidate the regulation of virulence attributes of the pathogenic fungus *C. albicans* by nitrogen availability in more detail.

Within a genome wide binding profile of Stp1, during growth with proteins, more than 600 Stp1 target genes were identified, thereby confirming its role in the usage of proteins, but also other nitrogenous compounds as nitrogen source. Moreover, the revealed targets suggest an involvement of Stp1 in the general adaption to nutrient availability as well as in the environmental stress response. With the focus on protein utilization and nitrogen-regulated pathogenesis, the regulation of the major secreted aspartic protease Sap2 - additionally one of the prime examples of allelic heterogeneity in *C. albicans* - was investigated in detail. Thereby, the heterogezygous *SAP2* promoter helped to identify an unintended genomic alteration as the true cause of a growth defect of a *C. albicans* mutant. Additionally, the promoter region, which was responsible for the differential activation of the *SAP2* alleles, was delimited. Furthermore, general Sap2 induction was demonstrated to be mediated by distinct *cis*-acting elements that are required for a high or a low activity of *SAP2* expression.

For the utilization of proteins as nitrogen source it is also crucial to take up the peptides that are produced by extracellular proteolysis. Therefore, the function and importance of specific peptide transporters was investigated in *C. albicans* mutants, unable to use peptides as nitrogen source (*opt1*Δ/Δ *opt2*Δ/Δ *opt3*Δ/Δ *opt4*Δ/Δ *opt5*Δ/Δ *ptr2*Δ/Δ *ptr22*Δ/Δ

septuple null mutants). The overexpression of individual transporters in these mutants revealed differential substrate specificities and expanded the specificity of the OPTs to dipeptides, a completely new facet of these transporters. The peptide-uptake deficient mutants were further used to elucidate, whether indeed proteins and peptides are an important *in vivo* nitrogen source for *C. albicans*. It was found that during competitive colonization of the mouse intestine these mutants exhibited wild-type fitness, indicating that neither proteins nor peptides are primary nitrogen sources required to efficiently support growth of *C. albicans* in the mouse gut.

Adequate availability of the preferred nitrogen source ammonium represses the utilization of proteins and other alternative nitrogen sources, but also the expression of virulence attributes, like Sap secretion and nitrogen-starvation induced filamentation. In order to discriminate, whether ammonium availability is externally sensed or determined inside the cell by *C. albicans,* the response to exterior ammonium concentrations of ammonium-uptake deficient mutants (*mep1*Δ/Δ *mep2*Δ/Δ null mutants) was investigated. This study showed that presence of an otherwise suppressing ammonium concentration did not inhibit Sap2 proteases secretion and arginine-induced filamentation in these mutants. Conclusively, ammonium availability is primarily determined inside the cell in order to control the expression of virulence traits.

In sum, the present work contributes to the current understanding of how *C. albicans* regulates expression of virulence-associated traits in response to the presence of available nitrogen sources - especially proteins and peptides - in order to adapt its lifestyle within a human host.

Zusammenfassung

Stickstoffregulierte Pathogenität bezeichnet die Kontrolle von Virulenz-assoziierten Eigenschaften als direkte Folge der verfügbaren Quantität und Qualität einer Stickstoffquelle. Im Zusammenhang mit der Stickstoffverfügbarkeit verändert der opportunistisch krankheitserregende Pilz *Candida albicans* seine Morphologie und sekretiert Aspartat-Proteasen [SAPs], beides gut charakterisierte Virulenzattribute. Im Gegensatz zu seinem normalerweise apathogenen Verwandten *Saccharomyces cerevisiae* ist *C. albicans* in der Lage Proteine zu verwerten, welche als sehr häufige und wichtige Stickstoffquelle im menschlichen Wirt angesehen werden. Zur Nutzung von Proteinen sekretiert *C. albicans* Aspartat-Proteasen für den außerzellulären Verdau der Proteine und exprimiert Peptidtransporter (Di- /Tripeptidtransporter [PTRs] und Oligopeptidtransporter [OPTs]) um die Abbauprodukte aufzunehmen. Beide Eigenschaften werden transkriptionell von Stp1 - dem globalen Regulator zur Verwertung von Proteinen - kontrolliert.

Ziel der vorliegenden Arbeit war es, die Regulation von Virulenzattributen im pathogenen Pilz *C. albicans* durch die Verfügbarkeit von Stickstoff genauer zu untersuchen.

Innerhalb einer genomweiten Bindestudie von Stp1 wurden mehr als 600 Stp1-Zielgene während des Wachstums mit Proteinen identifiziert. Dadurch bestätigte sich die Funktion von Stp1 in der Proteinverwertung und wurde zudem auch auf die allgemeine Verwertung von Stickstoffquellen erweitert. Des Weiteren deuten die aufgedeckten Zielgene an, dass Stp1 womöglich in der Adaption an die generelle Nährstoffverfügbarkeit sowie in der Antwort auf Stresssignale beteiligt ist. Mit dem Fokus auf die Proteinverwertung und stickstoffregulierter Pathogenität wurde die Regulation der wichtigsten sekretierten Protease Sap2 - welche außerdem ein Paradebeispiel für allelische Heterogenität ist - im Detail untersucht. Dabei half der heterogene *SAP2*-Promoter bei der Identifizierung einer unbeabsichtigten genomischen Veränderung als wahren Grund eines Wachstumsdefektes einer *C. albicans* Mutante. Zusätzlich wurde der Promotorbereich eingegrenzt, welcher für die unterschiedliche Aktivierung der beiden *SAP2* Allele verantwortlich ist. Weiterhin wurden verschiedene *cis*-aktive Elemente identifiziert, die entweder für eine hohe oder eine niedrige *SAP2* Expression benötigt werden.

Die Aufnahme von Peptiden, die durch den außerzellulären Verdau entstehen, ist für die Verwertung von Proteinen ebenso wichtig. Deshalb wurde die Funktion und Bedeutung der spezifischen Peptidtransporter anhand von *C. albicans* Mutanten untersucht, welche Peptide nicht aufnehmen können (*opt1*Δ/Δ *opt2*Δ/Δ *opt3*Δ/Δ *opt4*Δ/Δ *opt5*Δ/Δ *ptr2*Δ/Δ *ptr22*Δ/Δ Septuplemutanten). Die Überexpression von individuellen Transportern in diesen Septuplemutanten offenbarte unterschiedliche Substratspezifitäten und erweiterte die Spezifität für die OPTs auf Dipeptide, eine komplett neue Facette dieser Transporter. Des Weiteren ermöglichten die Septuplemutanten eine Aufklärung, ob Proteine und Peptide tatsächlich eine wichtige *In Vivo* Stickstoffquelle für *C. albicans* sind. Dieses Arbeit zeigte, dass während der kompetitiven Kolonisierung des Mäusedarms die Septuplemutanten wildtypische Fitness aufwiesen. Dies deutet daraufhin, dass weder Proteine noch Peptide eine wichtige Stickstoffquelle für ein effizientes Wachstum in diesem *In Vivo* Model sind.

Die ausreichende Verfügbarkeit der bevorzugten Stickstoffquelle Ammonium unterdrückt die Verwertung von Proteinen und anderen alternativen Stickstoffquellen. Aber auch die Expression von Virulenzattributen, wie die Proteasesekretion und die stickstoffmangel-induzierte Filamentierung, wird durch Ammonium inhibiert. Um zu unterscheiden, ob *C. albicans* die Ammoniumverfügbarkeit außerzellulär oder in der Zelle bestimmt, wurde das Verhalten auf außerzelluläre Ammoniumkonzentrationen in Mutanten untersucht, welche Ammonium nicht aufnehmen können (*mep1*Δ/Δ *mep2*Δ/Δ Mutanten). Diese Arbeit zeigte, dass in diesen Mutanten eine ansonsten inhibierende Ammoniumkonzentration nicht in der Lage war, die Sekretion der Sap2-Protease oder die Arginin-induzierte Hyphenbildung zu unterdrücken. Folglich wird, um die Expression von Virulenzattributen zu regulieren, die Ammoniumverfügbarkeit vorrangig in der Zelle bestimmt.

Zusammenfassend erweitert die vorliegende Arbeit das Verständnis zur Regulation der Expression von Virulenzattributen durch die Verfügbarkeit von Stickstoffquellen - insbesondere Proteine und Peptide - die eine Anpassung von *C. albicans* an ein Leben im menschlichen Wirt ermöglichen.

1 Introduction

Infectious diseases are a leading cause of death worldwide. Despite steady medical improvements these are still a major threat for human health. According to the World Health Organization (WHO) infectious diseases kill almost 9 million people every year, many of them children under five years old, and cause enormous burdens through life long disabilities (WHO, 2012). Among the infectious agents, bacterial and parasitic pathogens draw the most attention while the global burden of fungal infections is currently underestimated and not widely recognized by the public or by influential funding agencies. Only the U.S. Center for Disease Control and Prevention (CDC) has established a fungal research and surveillance program while other public health organizations, like the WHO, contribute only minimal or not at all to fungal surveillance and research (Brown *et al.*, 2012b). It is also noteworthy that a variety of fungal plant pathogens have major economic impacts on the agricultural landscape (e.g. crop failures).

The most common fungal diseases in humans are caused by dermatophytes, which affect one quarter of the world population (~1.7 billion people) by milder, superficial infections. The second most common agents are members of the *Candida* spp. also causing a wide range of superficial infections. Invasive fungal infections are of greater concern since their mortality rate often exceeds 50%. “In fact, at least as many, if not more, people die from the top 10 invasive fungal diseases than from tuberculosis or malaria” citing the review on human fungal infections by G. Brown and colleagues (Brown *et al.*, 2012a). A rising importance of giving attention to fungal infections is largely attributed to the pandemia of HIV and the rise of chemotherapy, transplantations, and immunosuppression in modern medicine. The higher numbers of hospitalized and immunocompromised individuals together with frequent usage of broad-spectrum antibiotics, immunosuppressive and corticosteroid-based agents increases the patient’s susceptibility to mycotic infections.

Clinically relevant fungal species, with regard to invasiveness and mortality, are members of the genera *Aspergillus*, *Cryptococcus*, and *Candida*, with the latter being the most isolated agent of invasive fungal infections in Northern America, Europe and China (Lass-Flörl, 2009, Liao *et al.*, 2013, Perlroth *et al.*, 2007, Pfaller & Diekema, 2010). The clinical manifestation of a *Candida* spp. infection is termed candidiasis with a clinical spectrum ranging from

local/superficial oropharyngeal/esophageal ("thrush") or genital/vulvovaginal to life-threatening systemic manifestations (Calderone & Clancy, 2012). “Thrush” is not very common in healthy people but among HIV-infected patients prevalence is estimated from 9% to 31% and nearly 20% in cancer patients (CDC, 2012). In contrast, vulvovaginal candidiasis is quite common and it is estimated that 75% of all adult women will have at least one episode in their lifetime, where 5% of them were faced with recurrent infection cycles (Sobel, 2007). Invasive candidiasis occurrence is extremely rare in healthy people but in immunosuppressed individuals *Candida* spp. cells can disseminate and infect virtually every organ, mostly kidneys and liver but also the central nervous system. The mortality rate of invasive candidiasis is 15% up to 50% and *Candida* spp. are the 4th most common cause of hospital acquired systemic infections (Pfaller & Diekema, 2007, Pfaller & Diekema, 2010).

The genus *Candida* has around 200 members, but only a dozen of them have been described as pathogenic. The important members thereto are *C. albicans*, *C. dubliniensis*, *C. glabrata*, *C. krusei*, *C. lusitaniae*, *C. parapsilosis*, and *C. tropicalis* (Figure 1.1). The most prevalent one in nearly every study worldwide is *C. albicans*, but the non-albicans species have emerged during the last decades, which may be a result of improved diagnostics of *non-albicans* species (Falagas *et al.*, 2010). Nevertheless, *C. albicans* still dominates invasive and superficial infections caused by *Candida* species.

1.1 *Candida albicans*

The white plaque from the clinical picture of “thrush”, gives this *Candida* species its suffix *albicans*, derived from the word for white in Latin. It is estimated that 30% to 75% of the world population are symptom-less carriers of *C. albicans* at any given moment by some means or other (Pappas *et al.*, 2009, Perlroth *et al.*, 2007). The exclusively warm blooded host associated lifestyle distinguishes *C. albicans* from the majority of other *Candida* spp. and other opportunistic fungal pathogens like *Aspergillus* and *Cryptococcus*, which are usually accidentally acquired from the environment. During a commensal lifestyle the permanent interactions with host defense mechanisms creates a hostile environment that requires a balance between *Candida* growth rate and clearance by the immune system. An imbalance or disturbance of the normal microbial flora or the host immune system promotes the change of *C. albicans* from a commensal to a pathogenic and dangerous aggressor.

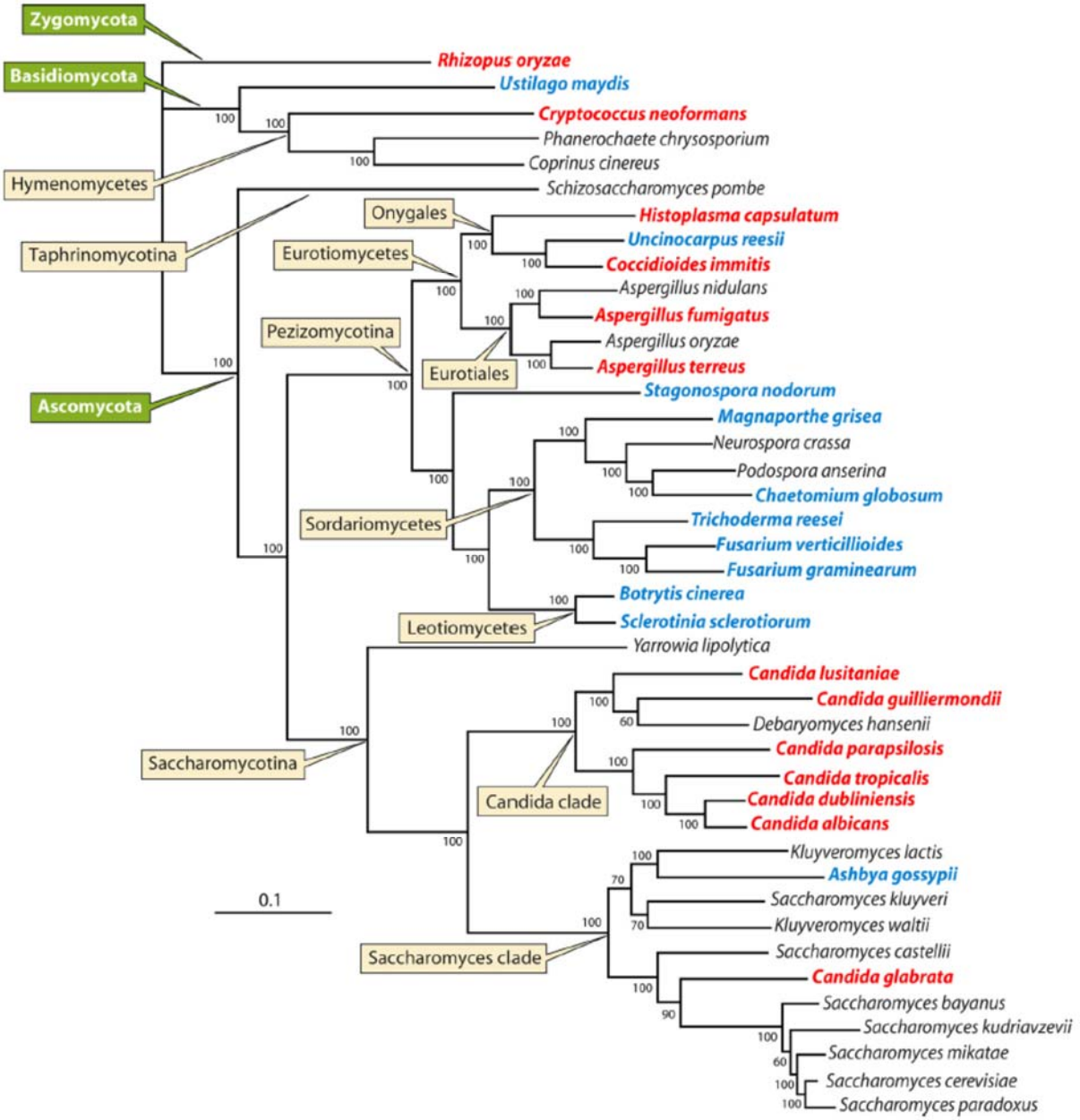

Figure 1.1: Phylogenetic tree of 42 fully sequenced fungal species with plant pathogens in blue and human pathogens in red (from (Butler, 2010)). Bootstrap scores are shown at all nodes.

1.2 Genetics

For every living organism the genetic information encoded in its genome provides the fundament for its life and characteristic features. Under most conditions *C. albicans* propagates asexually with a diploid set of eight chromosomes (chromosome 1 - 7 and chromosome R). The currently annotated (haploid) genome of *C. albicans* (online available at

www.candidagenome.org; CGD) encompasses approx. 15,845,000 base pairs, including the mitochondrial genome, based on the redefined assembly 21 from reference strains SC5314 (van het Hoog *et al.*, 2007). From a total of 6,215 predicted protein coding open reading frames (ORFs) only 24.09% (1,497) are verified, leaving 73.47% uncharacterized (4,570) or dubious (2.45% or 152) (CGD webpage accessed on May 23th 2013). Approximately 12% of the encoded ORFs are unique to *C. albican*s thereby probably determining its specific characteristics (Kabir & Hussain, 2009). An interesting genetic feature of the *Candida* clade is its unusual codon usage (or non-canonical genetic code), so is the triplet CUG translated into serine and not leucine (Massey *et al.*, 2003, Ohama *et al.*, 1993). Furthermore, throughout the whole genome of *C. albicans* a high degree of heterozygosity is present, leading on average to one single nucleotide polymorphism (SNP) per 330–390 bases in the sequenced reference strains SC5314 and WO-1 (Forche *et al.*, 2004, Jones *et al.*, 2004, Massey *et al.*, 2003). Such high diversity is especially surprising when considering a predominantly clonal or asexual mode of propagation. It is therefore suggested that *C. albicans* developed mechanisms to maintain and even gain heterozygosity as means of adaption and evolution (Calderone., 2008). A high degree of heterozygosity also opens new facets of regulating gene expression or gene function. One prominent example is the heterozygous mating type locus (MTL**a**/MTLα) that generates the **a**1-α2 repressor, which blocks the formation of mating-competent cells, e.g., in the reference strain SC5314. Strains homozygous for the MTL, e.g. the reference strain WO-1, can undergo mating due to the absence of the **a**1-α2 repressor (Morschhäuser, 2010b). Moreover, differential induction of the two alleles of the major secreted protease gene *SAP2* is a consequence of their highly heterozygous promoter sequences (Staib *et al.*, 2002a). Furthermore, heterozygosity was reported for *HIS4*, where only one of the two gene copies encoded a functional protein in SC5314 (Gómez-Raja *et al.*, 2008).

The high genomic flexibility of *C. albicans* gives rise to large-scale genetic alterations like chromosomal rearrangements, aneuploidy, and loss of heterozygosity (LOH). It was also proposed “that *C. albicans* and other pathogens may have evolved mechanisms not only to tolerate but also to generate large-scale genetic variation as a means of adaptation” (Selmecki *et al.*, 2010). Additional genetic diversity of *C. albicans* arises from a parasexual cycle, the importance of which is currently not understood. It relies on a homozygous MTL, the mating competent opaque state and the actual mating followed by unconventional meiotic or “concerted” chromosome loss (Magee & Magee, 2004, Sherwood & Bennett, 2009). Until

February 2013 *C. albicans* was considered to be obligate diploid with no haploid phase, but disproved by the discovery of viable *C. albicans* haploids (Hickman *et al.*, 2013). The impact of this finding on general *Candida* research is not yet foreseeable, but this study provides evidence that a high degree of heterozygosity is generally beneficial for growth. Although unusual codon usage, absence of a true sexual cycle, and the long assumed obligate diploidity hamper genetic manipulation, there are many tools to genetically modify and manipulate *C. albicans*. Creation of knockout mutants and usage of common molecular techniques, *in vivo* infections models, as well as global profiling analysis are available and have been applied to study *C. albicans* making it a model pathogenic fungus (Brand & MacCallum, 2012). In addition, discoveries in other well-studied pathogenic fungi (Figure 1.1) increased the current understanding of genetics and fungal pathogenicity mechanisms, especially findings in *Aspergillus fumigatus*, *Cryptococcus neoformans* and, in the normally non-pathogenic but more extensively studied relative, *Saccharomyces cerevisiae* (beer or baker's yeast). Indeed, two third of *C. albcians'* genes have clear orthologs in *S. cerevisiae*.

1.3 Drug resistance

Severely *Candida*-infected patients are treated with only a small set of antifungals currently available. The first antifungal drug, the polyene amphotericin B was introduced in 1958, later fluorocytosine, azoles and most recently, in the year 2001, the echinocandins were approved for clinical treatment. The mode of action of most antifungals based on the interference with the cell wall and cell membrane. For example the biosynthesis of the fungal sterol ergosterol, a major component of the cell membrane, is targeted by the widely used azoles (Ghannoum & Rice, 1999, Shapiro *et al.*, 2011). The lack of new antifungal drugs with novel targets together with the broad and prophylactic usage of the available drugs fostered the development of resistance in *C. albicans*. Hence, current research focuses on unraveling antifungal resistance mechanisms, which occur for all antifungals. The main resistance mechanisms in *C. albicans* are drug uptake inhibition/alteration, modification or overexpression of the antifungal drug target or lowering intracellular antifungal concentration by overexpression of efflux pumps, like Mdr1, Cdr1, and Cdr2 (Morschhäuser, 2010a, Shapiro *et al.*, 2011).

1.4 Adherence

Adherence to host cells, other *Candida* cells, microorganisms, and to abiotic surfaces, like catheters and dentures, strongly depends on specialized proteins, designated adhesins. To facilitate cell-surface interaction they are surface attached, mostly by a GPI-anchor (Als1-7, Als9, Ecm33, Hwp1, Eap1, Iff4, Sap9, and Sap10), but also through non-covalent cell surface/wall association (Mp65, Phr1) or as integrin (Int1). Two of them, namely Als3 and Hwp1, have been ascribed a high importance for adhesions.

Besides mere adherence *C. albicans* cells can also gain entry into the cells by two mechanistically different ways, (a) induced endocytosis or (b) active penetration. (a) Induced endocytosis depends on the presence of invasins on the fungal cell surface that mediate binding to host ligands, which trigger cell engulfment. The fate of engulfed cells is unknown. (b) The process of active penetration is so far uncharacterized, but adhesion, sheer physical force, and secreted aspartic proteases, which degrade tissue barriers, have been related with this mechanism (Mayer *et al.*, 2013). Interestingly, active penetration is currently the only known option by which *C. albicans* invades intestinal cells highlighting this route, since systemic candidiasis originate mainly from their natural reservoir in the gastrointestinal tract (Dalle *et al.*, 2010, Nucci & Anaissie, 2001).

1.5 Biofilm formation

Another key for the success of *C. albicans* is its ability to form biofilms on virtually any surface. Routine usage of implanted medical devices (over 10 million recipients per year) fostered device-associated *Candida* infections (Kojic & Darouiche, 2004). Biofilm formation proceeds in four sequential steps which are: adherence, initiation, maturation, and dispersal. Mature biofilms demonstrate much higher resistance to antifungals and help *C. albicans* to effectively evade host defense mechanisms. Formation of biofilms is based on a complex intertwined network of the transcriptional regulators Bcr1, Tec1, Efg1, Ndt80, Rob1, and Brg1. (Finkel & Mitchell, 2011, Fox & Nobile, 2012).

1.6 Morphogenesis

The possibly most striking pathogenicity attribute of *C. albicans* is its ability to change its morphology (Sudbery *et al.*, 2004). As members of the Saccharomycotina (Figure 1.1), *C. albicans* forms typical ovoid-shaped cells, termed yeast or white cells, which are prominent under most routine laboratory conditions. One morphology transition is the formation of large (approx. 6–10 µm) thick-walled spore-like structures, termed chlamydospores, whose biological function is currently unknown (Staib & Morschhäuser, 2007).

A further morphology is the opaque state, formed by phenotypic switching and a prerequisite for mating. Opaque cells are elongated or bean-shaped and are predominantly formed in MTL homozygous strains (see section "1.2 Genetics"), however natural MTL heterozygous strains were very recently reported to be able to switch to the opaque phase (Xie *et al.*, 2013). Besides the spontaneous white (yeast) to opaque switching rate (10^3-10^4), several environmental signals are known to increase this rate dramatically, among them *N*-acetyl-D-glucosamine (GlnNAc), UV radiation, oxidants, elevated CO_2, and anaerobic conditions. The implications of switching to the opaque form, besides mating, are thought to enhance the persistence of a mixed population (with other phenotypic forms of *Candida* cells) in infected tissues and host niches. Opaque cells differ from the white (yeast) cells also in their ability to colonize and infect specific host tissues and are differentially recognized by neutrophils (Morschhäuser, 2010b, Sasse *et al.*, 2013, Soll, 2009).

Finally, the most important morphological transition, while it is often only referred to as dimorphism, is the yeast-to-hyphae transition. The terms filamentation or filamentous/hyphal/hyphae growth or hyphae/hyphal formation are generally used to describe the formation of true hyphae and pseudohyphae (Figure 1.2). The physiological role of pseudohyphae formation for a *C. albicans* infection is rather unclear, but they might represent an intermediate between yeast and true hyphae (Shapiro *et al.*, 2011, Sudbery, 2011).

Yeast cells are mainly found on mucosal and skin epithelial cell surfaces, where they are usually tolerated by the host immune system and grow as commensals. In addition, yeast cells are present in the bloodstream of *Candida* infected patients as dispersed cells from biofilms and infection loci. On the contrary, hyphal forms are not tolerated by the immune system. The morphogenetic switch to the hyphae morphology is mandatory for invasion of *C. albicans* cells and to escape from macrophages. However, neither one single morphology *per se* (yeast or

hyphae) is required for pathogenicity (see below), but rather the transition-ability in general is crucial for infection. Hence, both forms are found at infection sites.

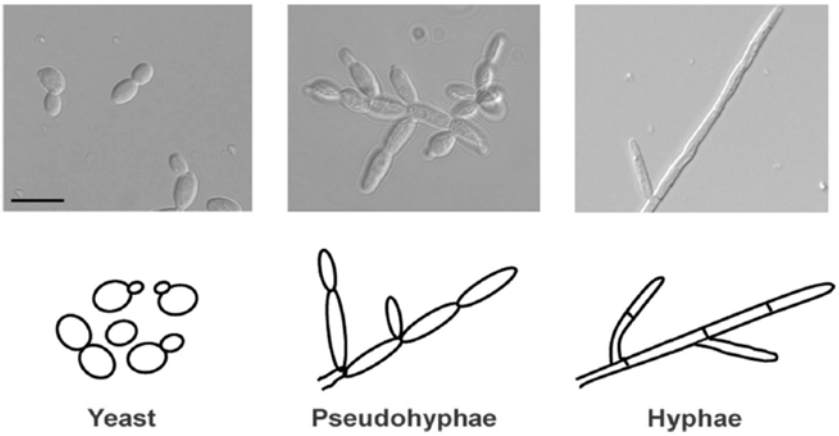

Figure 1.2: Morphological states of *Candida albicans* cells depicted as light microscopic pictures (top row; bar = 10 µm) and schematic drawings (bottom row) from (Thompson *et al.*, 2011). Yeast cells are typically ovoid-shaped. Pseudohyphae are elongated, still attached strings of yeast-like budding cells (branched chains of elongated buds), which occur by polarized cell division and produces constrictions at their cell junctions. Hyphae are long septated, multinucleated thread-like cells that emerge from short polarized outgrowths, called germ tubes, of a yeast cell by polarized tip-growth.

The hyphal transition is generally accepted as the backbone for *C. albicans* virulence. Thus, research concentrated on this phenomenon providing now a detailed picture of how hyphae are induced, formed, and maintained, as well as their cell biology and the complex regulation of hyphal development (Shapiro *et al.*, 2011, Sudbery, 2011).

Hyphae formation is induced by a wide range of diverse environmental cues, reflecting the adaption to the host and the broad spectrum of niches colonized by *C. albicans.* Generally human body temperature (above 35°C) is required for filamentation with two exceptions, matrix-embedded or hypoxia-induced filamentation, which occur at 25°C. The presence of serum is a strong hyphae formation signal as well as the partial CO_2 pressure present in the bloodstream (5% CO_2). The presence of GlcNAc, a shift towards neutral/alkaline pH, contact sensing and genotoxic stress were also shown to induce filamentation. Interestingly, the starvation for carbon and nitrogen induces the emergence of hyphae, creating a direct link between the nutritional status and pathogenesis (Shapiro *et al.*, 2011, Sudbery, 2011).

On the other hand, some signals repress hyphae formation, e.g. lower temperatures (below 35°C) block hyphae formation via the temperature sensitive chaperone Hsp90. Farnesol, a quorum sensing molecule secreted by *C. albicans* cells also inhibits at high concentrations filamentation (>10^7 cells/ml). In biofilm communities the quorum sensing molecule

homoserine lactone from *Pseudomonas aeruginosa* blocks filamentation. Lastly, hyperosmotic stress is also capable to repress serum-induced yeast-to-hyphae transition (Gow *et al.*, 2012, Sudbery, 2011).

Synchronistic with the yeast-to-hyphae transition also gene expression changes drastically, hence, dramatically altering the functional properties of *C. albicans* cells. Many hypha-specific genes, dispensable for hyphae formation and maintenance *per se* have been implicated with virulence attributes. For example *HWP1* and *ALS3*, whose gene products are required for adherence (see section "1.4 Adherence"), are expressed in the hyphae state. In addition Ece1, Hyr1, Sod5, and the three secreted aspartic proteases Sap4 to Sap6 are expressed during the hyphae program. Saps contribute to tissue penetrations and nutrient acquisition from proteins (see section "1.7 Hydrolytic enzymes").

Several transcriptional regulatory networks have been characterized integrating the variety of environmental signals via specific and overlapping signal transduction pathways to the hypha-specific developmental program (Figure 1.3). The transcription factors Efg1, Cph1, Cph2, Tec1, Flo8, Czf1, Rim101, and Ndt80 were described as positive regulators of hyphal formation through induction of hypha-specific gene expression in response to environmental cues.

The transcription factor Efg1 is considered as one of the major regulators for filamentation since *efg1*Δ/Δ mutants do not filament in response to several inducing signals, including serum, CO_2, neutral pH, GlcNAc and nitrogen starvation. The activation of Efg1 is integrated via the PKA/cAMP signaling pathway (Figure 1.3). Additionally, inducing signals are also transduced via the MAPK pathway, where Cph1 is the transcriptional effector. As depicted in Figure 1.3 the signal of nitrogen starvation (low N) can be transduced via both pathways through the activation of the guanine nucleotide binding protein Ras1. Ras1 is activated by signaling of the integral membrane ammonium permease or transceptor Mep2 (see section "1.10 Nitrogen regulation"). The other pathways that integrate signals to hypha-specific gene expression are designated pH pathway (acting via Rim101), (matrix-) embedded pathway (activating Czf1), and cell cycle arrest pathway (not depicted in Figure 1.3). The importance of hyphal formation is highlighted by absent or attenuated virulence in mice infection models of individual null mutation for the respective positive regulator (*efg1*Δ/Δ, *flo8*Δ/Δ, *tec1*Δ/Δ, and *rim101*Δ/Δ), with the exception of the *cph1*Δ/Δ deletion mutant, which retained the ability to kill mice (Shapiro *et al.*, 2011). Recently, Mfg1 was identified as new player in this complex network (Ryan *et al.*, 2012). Tup1 together with either Rfg1 or Nrg1 are described as negative

regulators inhibiting hyphal formation and hypha-specific gene expression. The respective null mutants for all three negative regulators grow permanently in the filamentous form and express hyphae-specific genes under non-inducing conditions and are avirulent (Ryan *et al.*, 2012, Shapiro *et al.*, 2011).

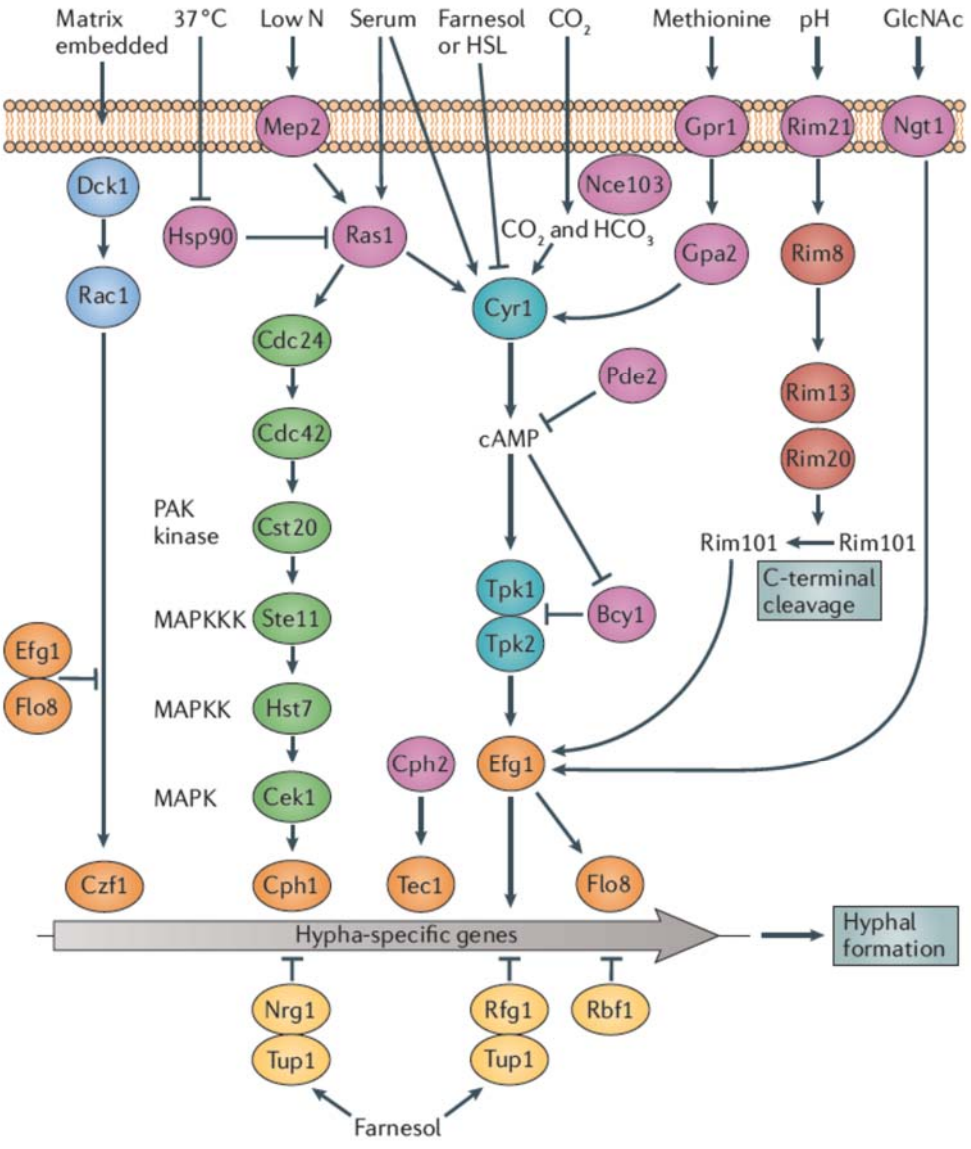

Figure 1.3: Network of signaling pathways integrating environmental cues to hypha-specific gene expression. Taken from (Sudbery, 2011). Color code is as follows: factors involved in signal transduction (mauve); matrix-embedded sensing pathway (blue); pH sensing pathway (brown); mitogen-activated protein kinase (MAPK) pathway (green); protein kinase A (PKA)/cAMP pathway (turquoise); transcriptional activators (orange), transcriptional repressors (yellow). Abbreviations are as followed: nitrogen starvation (Low N); 3-oxo-homoserine lactone (HSL); *N*-acetyl-D-glucosmaine (GlnNAc); p21-activated kinase (PAK); mitogen-activated protein kinase (MAPK), MAPK kinase (MAPKK), MAPKK kinase (MAPKK)

So taken that cells unable to form hyphae and cells permanently locked in the hyphae state are avirulent in various infection models suggests that the morphological switch or both forms are necessary for a successful infection (Shapiro *et al.*, 2011, Sudbery, 2011).
Unquestionable the hyphae formation and hypha-specific gene expression are key features in *C. albicans* pathogenicity.

1.7 Secreted hydrolytic enzymes

A high degree of hydrolytic power is found to be enriched in pathogenic species, suggesting an evolutionary adaption to a pathogenic lifestyle. Moreover, *C. albicans* appears to have a higher hydrolytic activity than other *Candida* spp., additionally *C. albicans* isolates recovered from infected patients exhibited higher hydrolytic activity than those from symptom-less carriers (Naglik *et al.*, 2003, Schaller *et al.*, 2005).
One of the main functions of digestive hydrolases is to provide nutrients from otherwise indigestible sources, which are too voluminous or not accessible. The variety and heterogeneity of natural available nutrient sources demands a variety of mechanisms to utilize them. Hence, the *C. albicans* genome harbors several gene families encoding many slightly distinct isoenzymes/isotransporters in order to cover the variety of nutrient sources.
Interestingly, *C. albicans* and other fungi have adopted the biochemical properties of their hydrolases to directly influence and modulate their immediate surroundings in order to aid a successful infection process. For example extracellular hydrolases help to gain entry into cells during active penetration and tissue invasion (see section “1.4 Adherence”) by disrupting the membranes phospholipid bilayer or actively destroy host defense molecules and cells (Mayer *et al.*, 2013, Schaller *et al.*, 2005).
The major secreted hydrolase families, each with 5 to 10 members, of *C. albicans* are (a) lipases, (b) phosphoslipases and (c) proteases.
(a) The lipase family consist of ten members (*LIP1 - 10*), with *LIP8* being important for pathogenicity, as shown by attenuated virulence of a *lip8*Δ/Δ mutant (Gácser *et al.*, 2007). The individual members of the *LIP* genes were differentially expressed in various *in vitro* and *in vivo* models as well as in several clinical samples. Overall broad and highly flexible lipolytic activities of *C. albicans* suggest their involvement in the establishment and manifestation of an infection (Mayer *et al.*, 2013, Schaller *et al.*, 2005).

(b) The phospholipases (PL) family is, based on their mode of action and substrates, partitioned into 4 subclasses (A, B, C, and D). Only the five members from the B-class (*PLB1 - 5*) are secreted and *PLB1* expression is regulated by environmental cues and the nutritional status. *PLB1* and *PLB5* are important for pathogenicity as evident from attenuated virulence of *plb1*Δ/Δ and *plb5*Δ/Δ single mutants in a mouse model of systemic infection (Mayer *et al.*, 2013, Schaller *et al.*, 2005).

(c) Since almost 50 years extracellular proteolytic activities are associated to *C. albicans* (Staib, 1965, Staib, 1969). Albeit phospholipase secretion was discovered simultaneously (Werner, 1966), research strongly focused on the characterization of secreted proteases. Since the first successful purification (Remold *et al.*, 1968) and genetic characterization (Hube *et al.*, 1991) of *C. albicans* extracellular proteases, 10 members of the *SAP* (*SAP1 – SAP10*) gene family were characterized (Figure 1.4).

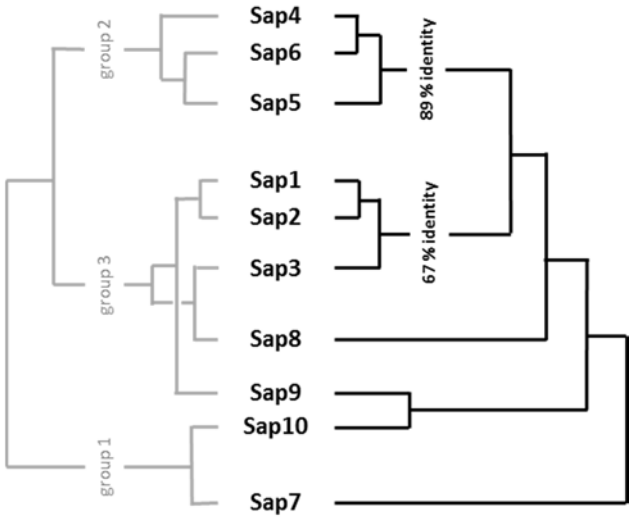

Figure 1.4: Schematic dendrogram depicting the relationship between the 10 *SAP* gene family members. Right side: Sequence homologies with *SAP1* to *SAP3* sharing up to 67% identical sequences and *SAP4* to *SAP6* being up to 89% identical (adapted from (Naglik *et al.*, 2003)). Left side: Substrate specificity homologies grouping the Sap isoenzymes in 3 categories, where Sap7 and Sap10 have a narrower substrate specificity compared to the broad specificity of the other Sap isoenzymes (adapted from (Aoki *et al.*, 2011)).

All ten *SAP* members are transcribed as preproenzymes, starting with a signal peptide sequence, which targets the proenzymes for secretion. The proenzymes are activated in the Golgi-apparatus by the Kex2 protease followed by vesicle-mediated release into the extracellular space (Naglik *et al.*, 2003). The function of Kex2 processing seems to be critical for pathogenicity, evident from filamentation defects under several hyphae-inducing conditions, highly attenuated virulence, and reduced kidney damage and invasion by a *kex2*Δ/Δ null mutant (Naglik *et al.*, 2003). However, deficiency of the multifunctional and globally processing protease Kex2 has several pleiotropic effects. Thus, inefficient processing

in the *kex2*Δ/Δ mutant affects several other Kex2 target substrates, apart from the Saps. For example malfunction of the adhesion-required proteins Hwp1 and Mp65, and the pH responding proteins Phr1 and Phr2, have been suggested to account for the observed virulence attenuation (Newport *et al.*, 2003). Interestingly, active but abnormally processed Sap2 is also secreted by this *kex2*Δ/Δ null mutant implying an alternative activation mechanism.

In addition to the shared Kex2-processing step, all Sap isoenzymes have two highly conserved aspartate residues in their active site, which leads to general Sap inhibition by Pepstatin A (except for Sap7). A functional difference between the Sap isoenzymes is the different pH optimum within an interval from pH 2 to pH 7, with Sap1-3 at lower and Sap4-6 at higher pH values. This reflects the broad activity spectrum of individual Saps and suggests a differential contribution depending on the host niche, e.g. the pH of the vaginal mucosa is more acidic than that of the oral cavity (Aoki *et al.*, 2011, Schaller *et al.*, 2005). Beyond degrading proteins for nutrition Saps degrade a wide range of other molecules, which results in additional benefits for fungal survival and infection (Table 1.1). The degradation of host cell structures and extracellular matrix components, including the hardly digestible keratin, is considered to facilitate active penetration during invasion. Hydrolysis of complement factors (C3b, C4b, and C5), as well as all types of immunoglobulins help *C. albicans* to evade attacks by the host immune system. Moreover, destruction of protease inhibitors, like α2-microglobulin and cystatin A, promotes extracellular proteolytic activity. Lastly, the interference with host signaling pathways, e.g. by activating Il-1β from its precursor or cleavage of prothrombin, might modulate the host immune response advantageous for *C. albicans*.

In sum, secreted aspartic protease support *C. albicans* survival and infection within the host beyond mere nutrition supply. It is noteworthy that almost all named hydrolyzed substrates (Table 1.1) were based on the *in vitro* identification as Sap2 substrates, which is dominantly expressed under most *in vitro* conditions (Naglik *et al.*, 2003, Schaller *et al.*, 2005).

Table 1.1: Substrates hydrolyzed by secreted aspartic proteases (Saps) of *C. albicans*

Extracellular matrix proteins	Host defense molecules	Host (immune) signaling cascades	Protease inhibitors
Keratin	Secretory Immunoglobulin A (IgA)	Il-1β	α2-microglobulin
Laminin	Complement factors C3b, C4b, C5	Prothrombin	Cystatin A
Collagen	Salivary Lactoferrin	Coagulation factor X	
Fibronectin	Lactoperoxidase	Clotting factor XII	
Vimentin	Cathepsin B	Hageman factor	
Albumin	Mucin		
Stratum corneum	Histatin-5		

A recent study analyzed the substrate specificity of all 10 Sap isoenzymes and showed that Sap7, Sap9 and Sap10 have a narrower substrate specificity compared to the broad specificity of the other Sap isoenzymes (Figure 1.4; left side) (Aoki *et al.*, 2011). The proteases Sap9 and Sap10 are actually not secreted, but remain attached to the cell membrane / wall via a GPI-anchor. Both are necessary for cell surface integrity and cell separation during budding (Albrecht *et al.*, 2006) and are considered to modify the cell wall and cell wall proteins, e.g. cell wall remodeling enzymes (Cht2, Pga4, Ecm33, Rhd3) and host-cell interacting proteins (Ywp1, Als2, Rhd3) (Schild *et al.*, 2011). It was shown that Sap9 and Sap10 play a role in adhesion and cell damage (Albrecht *et al.*, 2006), while Sap9 additionally modulated the interaction with human neutrophils (Hornbach *et al.*, 2009) and cleaved the antimicrobial peptide Histatin-5 (Meiller *et al.*, 2009). But neither Histatin-5 uptake nor survival rates were altered in the *sap9*Δ/Δ, *sap10*Δ/Δ single and double deletion mutants compared to a wild type, unlike the impairment seen for deletion of their orthologs (yapsins) in *C. glabrata* (Kaur *et al.*, 2007, Schild *et al.*, 2011). Sap8 was identified as one mediator that facilitates Msb2 shedding, a process required to activate the Cek1 MAPK pathway and necessary for full virulence (Puri *et al.*, 2012). Additionally, did the extracellular Msb2 domain effectively protected cells from the antimicrobial peptides Histatin-5 and LL-37 (Szafranski-Schneider *et al.*, 2012).

The role of the Sap proteins, especially Sap1 to Sap6, in *C. albicans* pathogenicity has been the subject of several studies. Differential *SAP* gene and Sap isoenzyme expression patterns were demonstrated in a variety of different stages and sites of infection using common reporter systems. These studies strongly suggested differential roles for the various Sap isoenzymes depending on the host niches and were reasonably connected to *C. albicans* pathogenicity. The characterization of single and multiple deletions mutants for almost all individual *SAP* genes allowed to elucidate their role in a variety of infection models (Naglik *et al.*, 2003,

Schaller *et al.*, 2005). The myriad studies done to evaluate the role of the Sap proteins in *C. albicans* pathogenicity produced congruent, but also controversial results, strongly dependent on the infection model used. The most reasonable evidences connecting Sap enzymes and virulence arose from attenuated virulence of *sap1*Δ/Δ, *sap2*Δ/Δ, or *sap3*Δ/Δ, single deletion mutants in models of acute systemic candidiasis (Hube *et al.*, 1997) and strongly impaired virulence of the *sap4*Δ/Δ *sap5*Δ/Δ *sap6*Δ/Δ triple deletion mutant (DSY459) in a systemic infection model in guinea pigs and mice (Sanglard *et al.*, 1997). However, the use of the *URA3* marker for mutant construction, as done for the above mentioned *sap* deletion mutants, complicates the interpretation of virulence studies since the ectopic expression of *URA3* can significantly alter virulence behavior of the respective mutants (Brand *et al.*, 2004, Lay *et al.*, 1998). Nowadays this can be overcome by, e.g., integration of *URA3* into *ENO1* (Staab & Sundstrom, 2003) or *RPS10* (Brand *et al.*, 2004) locus, using other auxotrophic markers or by simply using the dominant selective marker *caSAT1* (Reuss *et al.*, 2004). Indeed, triple mutants for *sap1*Δ/Δ, *sap2*Δ/Δ, *sap3*Δ/Δ, that were reconstructed based on the *caSAT1* marker in the wild type background, demonstrated wild-type like invasion and damage of vaginal reconstituted human epithelium (vRHE) (Lermann & Morschhäuser, 2008). This was in striking contrast to the clear impaired invasion and damage of RHE observed for the equivalent *URA3* marker derived *sap1*Δ/Δ and *sap2*Δ/Δ mutants (Schaller *et al.*, 2003). Based on this discrepancies and possible misinterpretation of virulence defects in *URA3* marker derived *sap* mutants a comprehensive re-evaluation of the so far investigated *sap* mutants was performed in 2010 to shed light on their controversial role for *C. albicans* virulence (Correia *et al.*, 2010). In this study both the *URA3* marker and the *caSAT1* marker triple deletions (for *SAP1* to *SAP3* and *SAP4* to *SAP6*) were simultaneously tested for virulence in a murine model of hematogenously disseminated candidiasis. There it became clear that the Sap enzymes may not be as important for *C. albicans* virulence as long assumed. Colonization of various host niches might require Sap isoenzymes, but the general pathogenicity does not rely on Sap activity.

Sap enzymes assuredly aid *C. albicans* pathogenicity as evident from reduced virulence in intranasal (Fallon *et al.*, 1997) and intraperitoneal (Kretschmar *et al.*, 1999) models, when Sap activity was inhibited with Pepstatin A. Many clinical data illustrated protective effects of HIV protease inhibitors against *C. albicans* prevalence on mucosal surfaces in human patients (Schaller *et al.*, 2005). In these patients the level of immune cells remained low so that cross-

inhibition of Sap activity is considered to reduce the fungal load. Furthermore, Sap2, together with Sap1 and Sap3, is important for a successful infection in a rat vaginal model, while Sap4 to Sap6 are not required (De Bernardis *et al.*, 1999). On the other hand Sap4 to Sap6 are needed for virulence in murine models of *Candida* peritonitis and keratitis (Felk *et al.*, 2002, Jackson *et al.*, 2007). Moreover, high titres of anti-Sap antibodies can be detected in patients with systemic or superficial candidiasis and anti-Sap2-antibody treatment protects against *C. albicans* in vaginal, oral, and peritoneal experimental infection models (De Bernardis *et al.*, 2002, Rahman *et al.*, 2007, Vilanova *et al.*, 2004). Lastly, expression of *SAP2* and *SAP4* - *SAP6* was detected in oral cavity samples of *C. albicans*-infected patients and asymptomatic carriers, whereas expression of *SAP1, SAP3, SAP4, SAP7,* and *SAP8* was predominantly restricted to infected patients (Schaller *et al.*, 2005). Although Sap1 to Sap6 may not be essential for pathogenicity they contribute to the success of *C. albicans* in colonizing and thriving within the hostile environment of the host.

So far the role of other secreted proteases, e.g. one metalloprotease and one serine protease is unclear (dos Santos *et al.*, 2006).

1.8 Stress response

Another key for the success of *C. albicans* is its ability to colonize many different host niches and to rapidly adapt to changes in a very dynamic environment. Environmental conditions inside warm-blooded host organisms exposes *C. albicans* to many different stresses that have to be tolerated. Mainly *C. albicans* is faced with (a) osmotic-, (b) pH-, (c) temperature-, (d) oxidative- and (e) nitrosative stresses. (a) Osmotic stress response, where glycerol is intracellularily accumulated to reduce the water efflux, seemed important for oral epithelial cell damage (Wächtler *et al.*, 2011). (b) Proper adaption to changes in the pH is crucial for colonizing different body locations (e.g. pH 7.4 in human blood and pH 4.0 in the vagina). Adaptation to pH changes is mediated, e.g., through the action of Phr1 and Phr2. These two cell wall glycosidases are differentially expressed at different pH. Phr2 is essential for infections of the vagina, whereas Phr1 is required during systemic infections. The response to extracellular pH leads to proteolytic activation of the major pH-responsive regulator Rim101, which also participates in hypha-specific gene regulation (Figure 1.3). Once activated Rim101 enters the nucleus and mediates expression of pH-response genes. Under nutrient starvation conditions the extracellular pH is also actively alkalinized by the excretion of ammonium and

alkaline pH in turn induces hyphal growth. The transcriptional regulator Stp2, the urea amidolyase Dur1,2 and the Ato (ammonia transport outward) export proteins are involved this process (Vylkova *et al.*, 2011). (c) Response to temperature stress is a highly conserved mechanism in all phyla and heat shock proteins (Hsps), also called chaperones, are the mediators that ensure proper protein folding and prevent protein unfolding and aggregation. *C. albicans* possesses six major Hsps (Hsp90, Hsp104, Hsp78, Hsp60, Ssa1, and Ssa2,) and several small Hsps (e.g. Hsp21), whose expression is mainly controlled by the transcription factor Hsf1 (heat shock factor 1). Hsf1 is essential for viability and mutants with reduced Hsf1 activity demonstrated attenuated virulence in a murine model of systemic infection. Additionally, Hsp90 has a central role in regulating morphogenesis (Figure 1.3), biofilm formation, drug resistance, and virulence (Mayer *et al.*, 2013).

A major weapon of professional phagocytic cells, like neutrophils and macrophages, to fight against *C. albicans* are (a) ROS (reactive oxygen species) and (b) RNS (reactive nitrogen species). In consequence, *C. albicans* has developed mechanism to defend against such attacks. (d) ROS are neutralized by the action of the Catalase Cat1 and the superoxide dismutases Sod1 and Sod5, and all three are individually required for full virulence in a mouse model of systemic candidiasis (Chauhan *et al.*, 2006). (e) RNS are neutralized by the action of Yhb1, which is induced during infections and required for full virulence in a mouse model of systemic candidiasis (Hromatka *et al.*, 2005). Although effectors are important, also involved signal transduction pathways are crucial to evoke an appropriate stress response. MAPK pathways have a central role in stress response mainly mediated through the action of the MAP kinases Mkc1, Hog1, and Cek1. Single mutants for all three MAP kinases are attenuated in virulence in mouse infection models, highlighting the essential need for a proper stress response in *C. albicans* during an infection (Mayer *et al.*, 2013).

1.9 Metabolic adaption

Unquestionable highly developed metabolic adaption is mandatory to survive and thrive within the human host. The bloodstream, as main nutrient distributer in the host, is rich in glucose, amino acids and proteins. Likewise the mucosal surfaces are considered nutrient rich, but because of the presence of other microorganisms and the mucosal immune system, they represent a highly competitive surrounding. In contrast, other niches (e.g. necrotic tissue) might be extremely depleted for nutrients and *C. albicans* cells are exposed to extreme starvation after phagocytosis by macrophages and neutrophils (Mayer *et al.*, 2013).

The acquisition of metals like iron, zinc, copper, and manganese is essential because these elements act as cofactors for several key enzymes and proteins in the metabolic networks. The restricted access to iron within the human host links iron acquisition to virulence in many bacterial and fungal pathogens. *C. albicans* acquires iron via a reductive system, but also uptake of siderophores or heme molecules from the host is known. Uptake of zinc by zincophores was described and putative copper (Crp1) and manganese (Smf2) transporters were also identified, but not characterized so far (Mayer *et al.*, 2013).

Like most organisms *C. albicans* prefers glucose as carbon and energy source. Alternatively, other sugars and so-called gluconeogenic carbon sources can be used, e.g. lactate, citrate, glycerol, and amino acids. To save energy and metabolites in the presence of sufficient amount of the preferred glucose, the utilization of alternative carbon and energy sources is repressed. This phenomenon is called carbon catabolite repression and mainly executed by the transcriptional repressor Mig1. Growth on alternative gluconeogenic carbon sources, like proteins, peptides, amino acids, lactate, fatty acids, and lipids require the glyoxylate cycle, which depends on the action of the malate synthase Mls1 and Icl1, the isocitrate lyase. Therefore, activation of glyoxylate cycle enzymes indicates non-fermentable carbon sources and generally signals (carbon) starvation in *C. albicans*. Importance of this cycle for pathogenicity is evident from *ICL1* upregulation during infections and the attenuated virulence of the *icl1*Δ/Δ null mutant (Lorenz & Fink, 2001). Further support that links pathogenicity to alternative carbon source metabolism is provided by the attenuated virulence of a *C. albicans* mutant (*fox2*Δ/Δ), which was unable to use fatty acids or ethanol, citric acid as carbon source, in systemic infection models (Ramírez & Lorenz, 2007). Lastly, growth on lactate, an abundant carbon source in the gut and vaginal mucosa, modulates cell wall structure, increases drug

and stress resistance, affects phagocytic recognition, and renders the cells more virulent in a systemic and vaginal mouse model (Ene *et al.*, 2012, Ene *et al.*, 2013).

Another key nutrient which limits microbial life in virtually all microorganisms is nitrogen. The utilization, the regulatory networks, and the recognition of the various nitrogen sources by *C. albicans* are outlined in more detail in the next section.

1.10 Nitrogen regulation

A great variety of different nitrogen sources (e.g. proteins, peptides, amino acids, amides, purines, urea, and ammonium) can be used by *C. albicans* as source of cellular nitrogen. Hence, several uptake mechanisms and specific assimilation pathways incorporate nitrogen into the cellular metabolism and provide the nitrogen needed to maintain the cell's economy. All of the distinct assimilation pathways share one core pathway, which consists of the conversion of α-ketoglutarate (α-KG) to glutamate (Glu) and glutamate to glutamine (Gln) (Figure 1.5) (Ljungdahl & Daignan-Fornier, 2012, Magasanik & Kaiser, 2002). The various nitrogen sources are hierarchical categorized into quality classes, with preferred and non-preferred ones. Identical to the carbon catabolite repression, a preferred nitrogen source represses expression of genes, which are necessary for the utilization of non-preferred nitrogen sources, and this regulation is designated nitrogen catabolite repression (NCR) or, in filamentous fungi, nitrogen metabolite repression (NMR) (Magasanik & Kaiser, 2002). Amino acids and proteins are considered as abundant and therefore important nitrogen source for *C. albicans* within the human host. Additionally, urea is present at very high concentrations in the human blood, cerebrospinal fluid, and might be plenty available during colonization of the genital/vulvovaginal mucosae (Lee *et al.*, 2013).

The genomic repertoire of *C. albicans* enables the utilization of many different nitrogen sources. The transcriptional regulation of such nitrogen-responsive genes is mainly mediated by members of the GATA zinc finger transcriptional regulator family. These factors bind to GATA sequences in regulatory sequences and activate or repress transcription of NCR-responsive genes (Marzluf, 1997). The central role of GATA factors in nitrogen regulation is well conserved among fungal species, e.g. nitrogen regulation in the filamentous fungus *Aspergillus nidulans* is mediated by the GATA family activator AreA and the repressor AreB. AreA orthologes, denoted Gat1 or Nit2, are present in all ascomycetes and are functionally conserved. Whereas filamentous fungi rely on a single set of GATA factors the

Saccharomycotina clade had evolved a second, partially redundant, copy of both activating and repressing regulators. Conclusively, in *S. cerevisiae* expression of NCR-responsive genes is activated by Gat1 and Gln3 and repressed by Dal80 and Gzf3. In *C. albicans* both activators Gat1 and Gln3 were identified and investigated, whereas function of the repressors remain uncharacterized (Dabas & Morschhäuser, 2007, Liao *et al.*, 2008, Limjindaporn *et al.*, 2003).

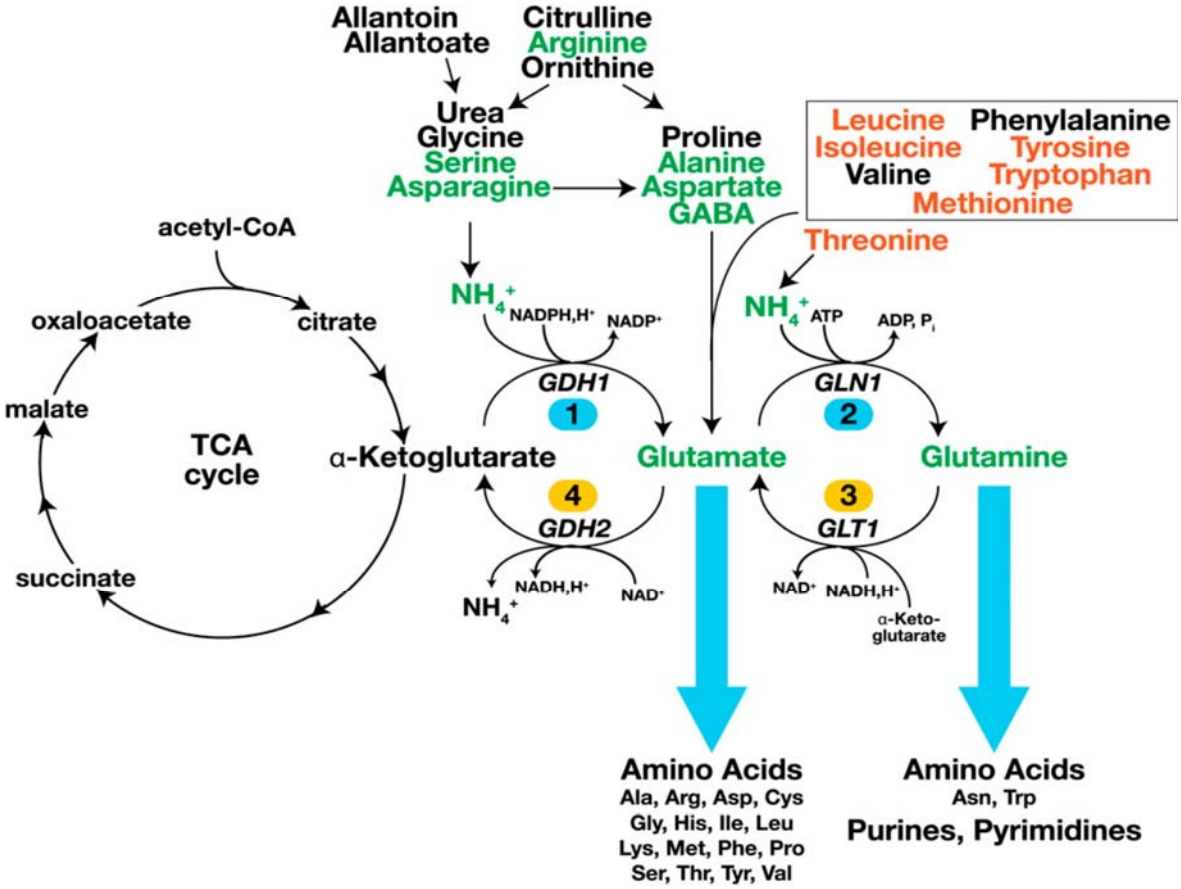

Figure 1.5: Main metabolic pathways for various nitrogen sources in *S. cerevisiae* from (Ljungdahl & Daignan-Fornier, 2012). Usable nitrogen sources are categorized into ones that are preferred (green), nonpreferred (red), or undetermined (black). Cellular nitrogenous compounds are synthesized using glutamine and glutamate as nitrogen donors. Key anabolic enzymatic reactions (blue 1 and 2) are facilitated by Gdh1 (NADPH-glutamate dehydrogenase) and Gln1 (glutamine synthase). Central catabolic reactions (yellow 3 and 4) are catalyzed by Gdh2 (NAD-glutamate dehydrogenase) and Glt1 (glutamate synthase). Ammonium, derived from different assimilation pathways, is either Gdh1-mediated attached to α-Ketoglutarate resulting in glutamate or Gln1-mediated attached to glutamate resulting in glutamine. Glutamine donates one ammonium group to α-KG to produce glutamate, which is catalyzed by Glt1. Gdh2 then catalyzes the reformation of α-KG out of glutamate. Resupply of α-KG is provided TCA cycle.

In the same way as for carbon, the acquisition of nitrogen as nutrient impacts *C. albicans* morphogenesis and expression of virulence-associated traits. Hence, quality and quantity of a nitrogen source is directly linked to pathogenicity. As previously mentioned nitrogen starvation is one signal that triggers the yeast-to-hyphae transition (see section "1.6 Morphogenesis") and is a prerequisite for Sap2 secretion (Morschhäuser, 2011). The importance of nitrogen regulation in pathogenicity is further emphasized by the behavior of null mutants for the central NCR regulators Gln3 and Gat1, which exhibited attenuated, for *gln3*Δ/Δ (Liao *et al.*, 2008), or absent virulence, for *gat1*Δ/Δ (Limjindaporn *et al.*, 2003) in a murine model of disseminated candidiasis. Furthermore, the *gln3*Δ/Δ null mutant demonstrated strong reduction of nitrogen starvation induced filamentous growth (Dabas & Morschhäuser, 2007). Additionally, the positive NCR regulator AfAreA and the Gcn4 ortholog AfCpcA are required for full virulence of *A. fumigatus* in mice (Hensel *et al.*, 1998, Krappmann *et al.*, 2004) and the orthologous regulator AreA/Gat1 in *C. neoformans* positively regulates the formation of the virulence determinant capsule. Contrarily, however, deletion of AreA/Gat1 in *C. neoformans* enhanced infectious basidiospore formation, melanin production, growth at high body temperatures, and resulted in a slightly more virulent *C. neoformans* mutant strain (Lee *et al.*, 2011).

These and other studies strongly suggest a general linkage, whether positive or negative, of virulence and nitrogen regulation in *C. albicans* and other clinically relevant fungal species (Lee *et al.*, 2013). In *C. albicans* nitrogen-regulated pathogenesis is a pivotal feature, which influences the critical step of the commensal-to-pathogen transition in various host niches.

The *C. albicans* genome encodes >20 amino acid permease plus many amino acid metabolism related enzymes. This is not surprising since uptake and assimilation of free amino acids is a common feature in all phyla. Most of these genes are NCR-responsive and expression of, at least, the permeases *CAN1, GAP1*, and *GAP2,* was shown to require additionally the transcriptional activator Stp2. However, the largest reservoir of amino acids is fixed in proteins. The utilization of proteins as nitrogen source is more complex, because degradation into digestible pieces is mandatory prior to uptake and assimilation by the cell. Consequently, when proteins are a nitrogen source *C. albicans* secretes aspartic proteases and induces expression of several oligopeptide and di/-tripeptide transporters. Here too, an additional transcriptional activator, namely Stp1, is crucial for the protease secretion and transporter expression and transcription of Stp1 is regulated by Gat1 and Gln3 (Dabas & Morschhäuser,

2008). Thus, apart from the global NCR regulators Gat1 and Gln3, pathway specific factors like Stp1 and Stp2 have a key role in nitrogen acquisition and regulation.

Both factors Stp1 and Stp2 are expressed as latent precursors and activated via proteolytic cleavage upon signaling of the SPS sensor. The mechanism of SPS signaling is well studied in *S. cerevisiae* and is functionally remarkable similar in *C. albicans* (Ljungdahl, 2009, Ljungdahl & Daignan-Fornier, 2012). The SPS sensor is built on three components, the integral membrane associated sensor Ssy1 (or Csy1), the effector protease Ssy5, and a predicted mediator Ptr3. Upon presence of micromolar concentrations of amino acids the SPS sensor activates the Ssy5 protease, which proteolytically cleaves Stp1 and Stp2 therefore liberates both from cytoplasmic retention, facilitating nuclear localization and consequently activating transcription (Martínez & Ljungdahl, 2005). Another example of cytoplasmic retention is ScGln3 in *S.* cerevisiae, which is sequestered in the cytoplasm by physically interacting with Ure2 and only liberated during nitrogen deprivation and this might be also true for ScGat1 (Broach, 2012). A *C. albicans* mutant (*csh3*Δ/Δ) with a non-functional SPS-sensor demonstrated greatly impaired amino acid uptake and reduced virulence (Martínez & Ljungdahl, 2004).

Interestingly, a recent study by Davis and co-workers showed reduced virulence of a *C. albicans stp1*Δ/Δ, but not a *stp2*Δ/Δ, null mutant during infection of the model host *Drosophila melanogaster* (Davis *et al.*, 2011). This was somewhat surprising since the concentrations of free amino acids, circulating in the *Drosophila* hemolymph (Piyankarage *et al.*, 2010), were thought to repress *STP1* transcription, so that Stp1 should be dispensable. However, this work demonstrated that Stp1 and its target genes, e.g. *SAP2*, are required for pathogenesis of *C. albicans* and further implied that rather protein than amino acid utilization was important to thrive inside this model host. On the contrary, prtT, an *A. fumigatus* global regulator of extracellular proteolytic activity was crucial for growth on proteins as sole nitrogen source, but dispensable for virulence in a leukopenic mouse model (Bergmann *et al.*, 2009).

Nevertheless, the role of Stp1 and its target genes in *C. albicans*, besides its importance for protein utilization, has not been studied so far.

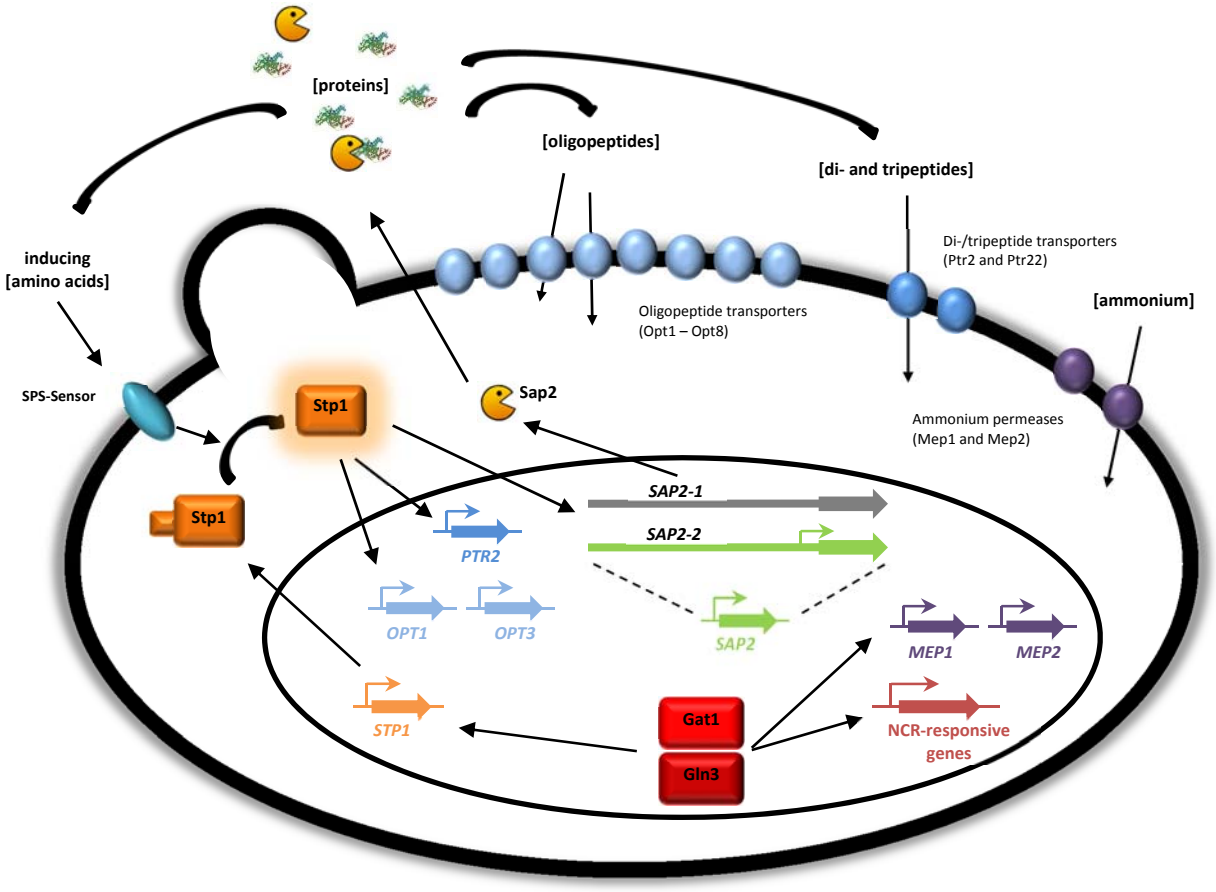

Figure 1.6: Regulation by proteins as sole nitrogen source. To utilize proteins proteolytic degradation by Sap2 and uptake of the produced peptides via the oligopeptide (Opt) or di-/tripeptide (Ptr) transporters is required. Presumably basal proteolytic Sap2 activity, solely derived from basal transcription the *SAP2-2* allele, degrades proteins thereby producing few amino acids. These amino acids in turn act as inducers to activate the SPS-sensor which leads to activation of the transcription factor Stp1 by proteolytic cleavage. Active Stp1 fully induces expression from both *SAP2* alleles and induces transcription of oligopeptide (*OPT1, OPT3*) and di-/tripeptide (*PTR2*) transporter genes, thus enabling growth on proteins. Stp1 expression is controlled by the activity of the global positive NCR regulators Gat1 and Gln3, which are induced under limiting nitrogen conditions. Mep1 and Mep2, two ammonium permeases needed to acquire ammonium, are Gat1-Gln3 dependent induced under nitrogen starvation.

Under *in vitro* laboratory conditions with proteins as sole nitrogen source Sap2 protease secretion (Hube *et al.*, 1997) and oligopeptide transporter expression (Reuss & Morschhäuser, 2006) are essential for *C. albicans* growth. Hence, mutants unable to induce their expression, e.g. *stp1*Δ/Δ single mutants (Martínez & Ljungdahl, 2005) and *gat1*Δ/Δ *gln3*Δ/Δ double mutants (Dabas & Morschhäuser, 2008), exhibited a similar growth defect. Under this growth conditions the need for amino acids to induce SPS signaling and consequently protease secretion seems puzzling. The current model suggests that basal Sap2 expression and secretion in the wild type strain SC5314 leads to basal proteolytic protein degradation, which

then provides the needed inducing amino acids. This model is further delimited to differential expression of the *SAP2* alleles, where only the *SAP2-2* allele has this basal transcriptional activity and/or is more easily induced (Figure 1.6). Data that support this model are provided by the fact that deletion of *sap2-2* alone resulted in the growth defect on BSA as sole nitrogen, whereas deletion of *sap2-1* had no effect (Staib *et al.*, 2002a). Thus, expression from the *SAP2-1* allele requires a functional *SAP2-2* allele. Since both alleles encode functional identical Sap2 enzymes (protein sequence differs in two conserved amino acid substitutions: A9G and V258L), their expression must be differentially induced, presumably due to differences in the promoter regions. The sequence of both promoters differ markedly in various SNPs and prominently in two pentameric repeat regions, designated as R1 (GCTTT) and R2 (TTGAT/A). The *SAP2-1* allele harbors 4 copies of R1 and 6 copies of R2, whereas the *SAP2-2* allele harbors 5 copies of R1 and R2. Although the total repeat number is always 10 only the 5/5 combination have been implicated with an earlier and easier induction of the *SAP2-2* allele *in vivo* and *in vitro* (Staib *et al.*, 2002a). Beyond that nothing more is known about other *cis*-acting elements that influence expression of this virulence trait.

Sap2 and the other related Saps are endoproteases that mainly produce peptides of various length and amino acid combinations. Accordingly, all the proteolytic capacity of *C. albicans* is only useful when there is an appropriate uptake system for the enormous variety of produced di-, tri-, and oligopeptides. Peptide uptake in *C. albicans* mainly depends on two distinct proton-coupled transport systems. The ubiquitously widespread PTR (peptide transport) system, which mediates uptake of di- and tripeptides, and the OPT (oligopeptide transport) system, which mediates uptake of longer peptides and is restricted to fungal species and plants (Hartmann *et al.*, 2011, Hauser *et al.*, 2001, Reuss & Morschhäuser, 2006). Furthermore, in *S. cerevisiae* the allantoate/ureidosuccinate transporter Dal5 was ascribed a di-/tripeptide-uptake capacity (Cai *et al.*, 2007, Homann *et al.*, 2005). Whereas *S. cerevisiae* has two functional Opts (Opt1 and Opt2) and one Ptr transporter (Ptr2) *C. albicans* possesses a battery of eight oligopeptides transporters (*OPT1 – OPT8*) and two di-/tripeptide transporters (*PTR2* and *PTR22*). It is highly probable that the gene family of *OPT*s co-evolved along with the gene family of Sap proteases. The eight Opts have somewhat redundant substrate specificities so that a single deletion for each individual *OPT* gene did not affect growth on proteins. Significantly reduced growth on BSA as sole nitrogen source was consequently only observed in *C. albicans* mutants deleted for the three transporters Opt1, Opt2, and Opt3 and the growth

defect was further exacerbated when additionally Opt4 and Opt5 were deleted (Reuss & Morschhäuser, 2006). These results indicated that, due to proteolytic degradation of BSA by Sap2, mainly oligopeptides and marginally di- and tripeptides are produced. Accordingly, the PTR system was dispensable as demonstrated by wild-type like growth of the single and double deletion mutants for *ptr2*Δ/Δ and/or *ptr22*Δ/Δ under these conditions (Hertlein, 2008). Similarly, an additional deletion for *ptr2* and *ptr22* in the *opt1*Δ/Δ *opt2*Δ/Δ *opt3*Δ/Δ *opt4*Δ/Δ *opt5*Δ/Δ quintuple mutant did not further reduce growth (Hertlein, 2008). The functionality and substrate preferences for individual transporters remained difficult to elucidate, mainly due to the high redundancy and overlapping substrate spectra within and between both peptide-uptake systems. So far individual transporters were characterized when each of the *OPT* genes was overexpressed in the *opt1*Δ/Δ *opt2*Δ/Δ *opt3*Δ/Δ triple mutants and tested for restored growth on BSA or defined peptides as sole nitrogen source. Overexpression of Opt1 to Opt5 restored growth on BSA, consequently verifying them as functional peptide transporters, whereas Opt6 to Opt8 remained unverified, but might have a more specific substrate spectrum (Reuss & Morschhäuser, 2006). Opt7 was characterized as transporter for glutathione (Desai *et al.*, 2011). *C. albicans* depends on the transporters Opt1 to Opt3 to use oligopeptides as a nitrogen source. Thus, contrarily to the wild type SC5314, the *opt1*Δ/Δ *opt2*Δ/Δ *opt3*Δ/Δ triple mutants were unable to grow on defined tetra-, penta-, hepta-, and octapeptides (Reuss & Morschhäuser, 2006).

In *A. fumigatus* it was recently shown that oligopeptide transport was dispensable for virulence in a murine infection model (Hartmann *et al.*, 2011). Consistently, preliminary studies showed no virulence attenuation of *C. albicans opt1*Δ/Δ *opt2*Δ/Δ *opt3*Δ/Δ *opt4*Δ/Δ *opt5*Δ/Δ quintuple mutants during systemic infection of mice (K. Schröppel, personal communication with J. Morschhäuser). However, the role of the peptide uptake during *C. albicans* infection and establishment within other host niches has not been determined so far.

Ammonium exemplifies a high quality nitrogen source, which is preferentially taken up by *C. albicans*, at least under laboratory conditions. If ammonium indeed represents an available nitrogen source within the host, the high pk_a value (9.2) then presumably favor the protonated NH_4^+ rather than NH_3. Hence, not passive diffusion of gaseous NH_3 across the membrane, but active uptake via the two ammonium permeases Mep1 and Mep2 facilitates intracellular ammonium accumulation. Furthermore, retrieval of leaking metabolic ammonium seemed to

be an important function of Mep permeases in *S. cerevisiae* (Boeckstaens *et al.*, 2007). Exceptionally interesting is that besides transport activity the Mep2 permease functions as a transceptor (see section “1.6 Morphogenesis”). Thereby, Mep2 combines its transport function with an ammonium sensing and signaling function, which is essential for nitrogen starvation induced hyphal growth (Figure 1.3). However, the regulation of the signaling activity of Mep2 is still debated (Morschhäuser, 2011). Evident from studies in *S. cerevisiae*, one model proposes that sensing of extracellular ammonium correlates with the transport activity of Mep2. This was suggested because mutated Mep2 with enhanced transport activity resulted in hyperfilamentous growth and Mep2 mutations, which decreased ammonium transport, inhibited pseudohyphal growth in response to nitrogen limitation. Contrarily, in *C. albicans* a Mep2 mutation which blocked filamentation but only slightly reduced ammonium transport contradict this hypothesis and suggest an alternative model (Dabas *et al.*, 2009). In this alternative scenario non-transporting Mep2 proteins permanently signal hyphae induction whereas transporting Mep2 proteins do not. Thus, absent or low ammonium concentrations leave many Mep2 proteins non-transporting and in the signalling status, which finally triggers hypha-specific gene expression. Higher ammonium concentration involves more Mep2 proteins in transport and consequently fewer Mep2 proteins signal hyphae induction, finally not inducing filamentation. At high ammonium concentration *MEP2* is repressed and thus filamentation is not induced. Nevertheless, this phenomenon highlights once again the tight link of nitrogen regulation and pathogenesis in *C. albicans*.

Besides hypha induction, sensing of ammonium availability by Mep2 is thought to fine tune the nitrogen starvation response, based on the general determination of the intracellular nitrogen status. This is evident as Mep2 itself is subject to NCR and regulated by Gat1 and Gln3 in response to nitrogen availability (Dabas & Morschhäuser, 2007). Monitoring the availability of nutrients by both an external sensor and the intracellular status is known for glucose sensing in *S. cerevisiae* (Broach, 2012). There, extracellular glucose is sensed by the G-protein coupled receptor, ScGpr1, and intracellular glucose levels are determined by the glucose phosphorylation-dependent system. Similarly, extracellular amino acids are sensed by the ScSsy1 protein of the SPS sensor in the exterior and intracellularily by the GCN (general amino acid control response) system (Zaman *et al.*, 2008). The signal for the GCN response are uncharged tRNAs, which increase in abundance when intracellular amino acids became depleted due to nitrogen starvation. A complex phosphorylation cascade together with uORF

regulation finally activates the transcriptional regulator ScGcn4, which then induces expression of amino acid permease and biosynthesis genes (Zaman *et al.*, 2008). Besides uncharged tRNAs the internal nitrogen status is probably determined by the ratio of Gln/Glu and/or α-KG/Glu and there is strong evidence from *S. cerevisiae* that intracytoplasmic glutamine concentration is the signal controlling NCR, indeed, Gln3 activity is inversely proportional to intracellular glutamine levels (Magasanik, 2005).

As previously mentioned NCR is a powerful way to repress unnecessary gene expression, when sufficient amounts of preferred ammonium are available. As a result ammonium is also capable to repress expression of virulence-associated attributes, like Sap2 enzyme secretion and hyphae formation by certain signals (e.g. amino acids) in *C. albicans* (Morschhäuser, 2011). Similarly, ammonium reduces also the size of the virulence determinant capsule in *C. neoformans* (Lee *et al.*, 2011).

However, the way how ammonium availability is sensed and actually regulates NCR is poorly understood. There could be an external sensor that recognizes ammonium in the medium or ammonium availability is determined by a different mechanism inside the cell.

1.11 Aim of this study

Starvation for nutrients may represent a key signal unmasking the disease-causing attributes of opportunistic pathogens, like *Candida albicans*. Foremost nitrogen starvation boost the commensal-to-pathogen transition, which is evident from numerous nitrogen source controlled virulence attributes. Hyphae formation, the backbone of *C. albicans* pathogenicity, is induced under nitrogen starvation and the secretion of extracellular aspartic protease is directly regulated by nitrogen source availability. Moreover, rapid and versatile adaption to different nitrogen sources, next to mere survival, is also fundamental for infection establishment within the human host. Notably interesting is the remarkably overrepresented size and expansion of gene families for nitrogen acquisition (e.g. secreted aspartic proteases and oligopeptide transporters) in pathogenic fungi, like *C. albicans* compared to *S. cerevisiae*, which conceivably represent means of adaption to a pathogenic lifestyle (Moran *et al.*, 2011). Nevertheless, current knowledge on the concept of nitrogen-regulated pathogenesis in *C. albicans,* where quality and quantity of nitrogen source directly impacts virulence-associated traits, still leaves many unsolved questions. So the main issues addressed in this dissertation are:

a) What role possesses the regulator of protein utilization, Stp1, in the intertwined network of nitrogen-regulated pathogenesis?

b) How is the regulation of one major virulence attribute, exemplified by the expression of the protease Sap2, facilitated in detail?

c) What role possesses the peptide-uptake capacity for protein utilization within a host niche?

d) How does the preferred nitrogen source ammonium repress virulence-associated traits, like protease secretion or filamentation?

2 Results

2.1 Stp1, a transcriptional regulator required for growth on proteins

An appropriate cellular response is essential to use various nitrogen sources as nutrients in a steadily and rapidly changing environment, especially when living inside mammalian hosts. Proteins and complex proteinaceous structures are abundant in the host and may represent a main source of cellular nitrogen for *C. albicans*. Utilization of proteins strongly relies on the transcriptional regulator Stp1, which controls expression of secreted proteases (*SAP2*) and oligopeptide transporters (*OPT1, OPT3*) (Dabas & Morschhäuser, 2008, Martínez & Ljungdahl, 2005). The ability to degrade extracellular proteins is additionally adopted to directly influence the immediate surroundings in a beneficial manner for *C. albicans* establishment and infections, e.g., by evading from host immune attacks and degrading tissue barriers. Therefore, by controlling protein utilization and protease secretion Stp1 contributes to the great success of *C. albicans* as commensal as well as pathogen.

Uncovering Stp1 target genes will shed light on the function and involvement of Stp1 in response to proteins as nitrogen source. To determine Stp1 target genes the *in vivo* identification of Stp1 binding sites was accomplished in collaboration with the working group of Prof. Dr. Martine Raymond (IRIC, Université de Montréal, Canada) by ChIP-on-chip experiments.

2.1.1 Construction of the HA-tagged transcriptional regulator Stp1

Prior to the ChIP-on-chip experiments Stp1 was tagged for specific pull down during chromatin immunoprecipitation. The commonly used human influenza hemagglutinin (HA) surface glycoprotein was used as C-terminal epitope tag. In detail, three sequential repeats (without any linking sequence) of the amino acid sequence were attached to Stp1. Therefore, the stop codon of the *STP1* ORF was replaced by a BamHI-restriction site, thereby producing a GS-linker sequence. To obtain a HA-tagged Stp1 variant the coding region of *STP1* was amplified using the primer pair STP1-5/STP1-10 and genomic DNA from SC5314 as template. The PCR-product was digested at the introduced ApaI and BamHI sites and cloned together with the BamHI-PstI fragment from pGAT1H1 into the ApaI-PstI digested vector pSTP1PG2. The resulting plasmid was designated pSTP1H1 and now harbored *STP1* fused with the 3xHA-tag under control of its

own promoter. The ApaI-SacI fragment from pSTP1H1 was used to transform two times independently the *stp1*Δ/Δ single mutants (STP1M4 A/B). Correct integration of the cassette into the *STP1* locus was verified via Southern hybridization of EcoRI-digested genomic DNA with *STP1*-specific probes (not shown). The resulting mutants were denoted *stp1*ΔSTP1H1 A/B and harbored the HA-tagged variant of Stp1 as only *STP1* copy in the genome.

2.1.2 HA-tagged Stp1 is a functional transcription factor

Prior to the genome wide binding study the functionality of the HA-tagged Stp1 transcriptional regulator was tested. Therefore, (a) the ability of Stp1-HA to complement the growth defect of the *stp1*Δ/Δ mutant was assessed in medium containing BSA as sole nitrogen source and (b) the expression of the Stp1-HA protein was determined by Western immnunoblotting in both *stp1*ΔSTP1H1 A/B mutants (Figure 2.1).

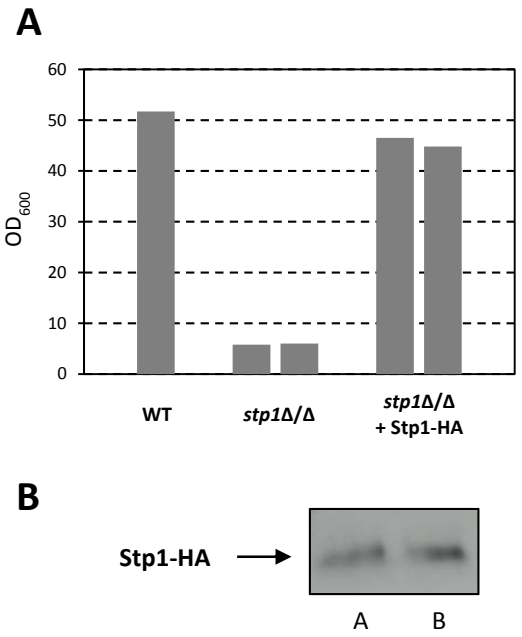

Figure 2.1: Growth restored by Stp1-HA and expression of Stp1-HA in the *stp1*Δ/Δ background (*stp1*ΔSTP1H1 A/B). (A) Growth on BSA as sole nitrogen source was tested. YPD-overnight cultures were 1:100 inoculated in fresh YCB-BSA and grown at 30°C for 24 hours. Growth was determined by measuring the optical density (OD_{600}) of the cultures. For comparison the wild type SC5314 and the parental *stp1*Δ/Δ single mutants (STP1M4 A/B) were included. Note: Only the results from one experiment are shown and similar results were obtained in an independent repeat experiment. (B) For testing expression of the HA-tagged Stp1 protein YPD-overnight cultures were 1:200 inoculated in fresh YCB-YE-BSA and grown at 30°C for 7 hours. Raw protein extracts of the cells were prepared and separated by SDS-PAGE and transferred to a nylon membrane. Stp1-HA was detected with an anti-HA-Peroxidase antibody.

The growth defect of the *stp1*Δ/Δ single mutants on BSA as sole nitrogen source in YCB-BSA was restored by the introduction of the HA-tagged Stp1 transcription factor (Figure 2.1 A). This demonstrated the functionality of Stp1-HA and detectable expression of Stp1-HA protein in raw protein extracts further confirmed expression of Stp1-HA during growth in YCB-YE-BSA (Figure 2.1 B).

2.1.3 Genome-wide binding of Stp1-HA to target sequences

To identify genome-wide binding of Stp1-HA to target sequences a ChIP-on-chip analysis as described in material and methods was performed using only the A strain, *stp1*ΔSTP1H1 A. After growth in YCB-YE-BSA, Stp1-HA bound DNA-fragments were immunoprecipitated and hybridized to *C. albicans* whole genome tiling microarrays. The background noise of unspecific signals was corrected by simultaneous hybridization of DNA-fragments from mock precipitates of the wild type SC5314, which contained untagged Stp1. The combined data from three independent experiments was uploaded to the *Candida albicans* Montréal Database (https://www.candida-montreal.ca) using a p-value cut-off of ≤0.01 and a Log_2 signal threshold for the binding intensity of ≥1.5. Genome-wide location of Stp1-HA binding was visualized in the Genome Browser of the database as individual hit as well as a binding map. The binding map illustrated binding intensities for each individual bound oligomer represented by intensity bars. An example of the data output in the Genome Browser is given in Figure 2.2.

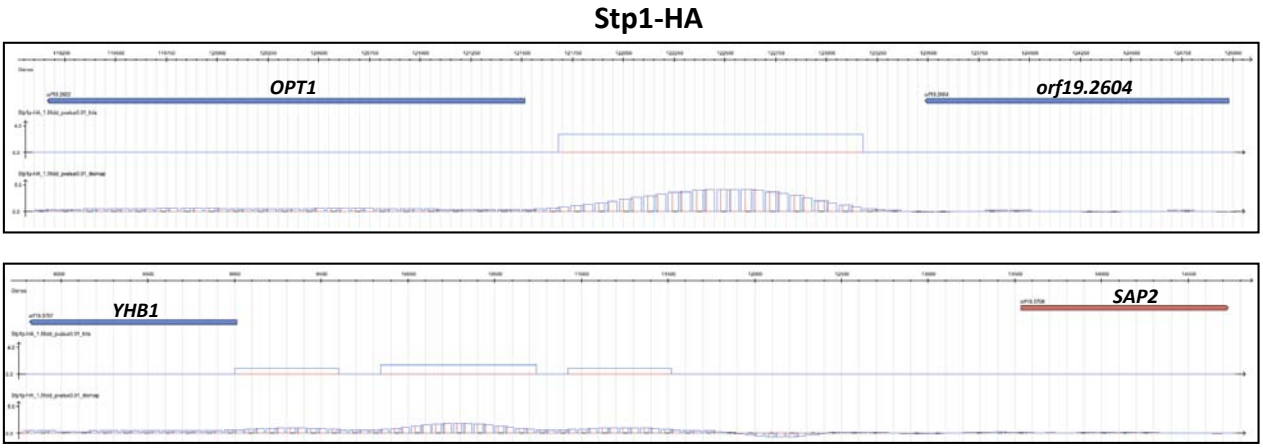

Figure 2.2: Stp1-HA binding visualized in the Genome Browser of the *C. albicans* Montréal Database. Binding of Stp1-HA to target sequences in strain *stp1*ΔSTP1H1 A after growth in YCB-YE-BSA to OD_{600} = 2.0. Stp1-HA binding is represented by single hits (wide single bars) and binding maps (hills of small bars). Blue and red filled arrows are ORFs and the upper scale is the position within the respective contig of assembly 19. On the left axis the binding intensity scale is indicated. Depicted is Stp1-HA binding to the promoters of *OPT1* (top) and *SAP2* as well as *YHB1* (bottom).

The analysis of the ChIP-on-chip data for Stp1-HA revealed 656 binding events showing ≥1.5 fold binding ratios. Manual assignment of these hits to neighboring ORFs, which might be regulated by Stp1, were done using following criteria: ORFs within a maximal distance of 5 kb upstream were assigned to an individual hit and also upstream binding events with a slight overlap to the ORF coding sequence were included. Since classical transcriptional regulators control gene expression primarily by binding to the upstream promoter region, Stp1-HA binding events downstream and within ORFs were excluded. It is noteworthy that the output was based on the assembly 19 and not the current assembly 21, which complicated interpretation, e.g., some ORFs have been re-annotated or removed in assembly 21 and individual positions were based on contig19 numbers and not chromosomal locations.

After merging ORFs, which were assigned to multiple binding events and the removal of duplicates finally 610 ORFs were identified, whose promoters were bound by Stp1-HA during growth in YCB-YE-BSA (Appendix A1). However, only 315 hits were exclusively assignable to only one ORF leaving the rest with two possibly regulated neighboring ORFs (e.g. see Figure 2.2 bottom; Stp1-HA binding events were concurrently in the promoters of *YHB1* and *SAP2*). The complete list containing all identified Stp1-HA targets is provided in Appendix A1.

All of the 610 Stp1-targets were analyzed and grouped for their biological process and function in *C. albicans* using the CGD Gene Ontology Slim Mapper (http://www.candidagenome.org/cgi-bin/GO/goTermMapper). A summary of some representative GO term groupings and respective genes annotated to the terms is provided in Table 2.1.

Table 2.1: Selection of relevant process gene ontology (GO) annotations of Stp1 targets using the CGD Gene Ontology Slim Mapper. Genes were annotated directly or indirectly (via a parent:child relationship) to the GO Slim terms. Note that the gene annotations bases on the standard names, which not necessarily reflect the commonly used annotations, e.g. the standard name for Stp1 is Stp3 in the CGD.

GO term	Cluster frequency	Genes annotated to the term
regulation of biological process	140 out of 610 genes, 23%	*AAF1, ACO1, ADAEC, ADH1, AHR1, BCR1, BCY1, BRG1, BUD14, CBF1, CDC19, CLB4, CLG1, CRZ2, CTA24, CTA4, CUP9, CYP1, CZF1, DBF2, DOT5, DYN1, EFG1, ENO1, EPL1, ESA1, FBA1, FCR3, FKH2, FLO8, GAL1, GAL10, GAP1, GCN4, GLN3, GPR1, GRF10, GRR1, GSC1, GTR1, HAP41, HMS1, HMT1, HOF1, HSL1, HSP60, HSP70, HSP78, HSP90, HXK2, INO2, LAP3, LPD1, MDM34, MIG1, MIH1, MP65, NCE102, NRG1, OPI1, PDS5, PGK1, PHO4, PIL1, RAS2, RAX1, RCK2, REG1, RFG1, RGS2, RGT1, RHB1, RPL30, SAP2, SBP1, SEC14, SEF1, SFU1, SGS1, SHA3, SIM1, SIR2, SOD1, SSN6, SSU81, SSZ1, STB3, STP2, STP3, STP4, SUA71, SUI2, SWE1, TAR1, TCC1, TDH3, TPS2, TRX1, TRY3, TSA1, TSA1B, TYE7, UBC8, WOR2, WSC2, ZCF18, ZCF2, ZCF21, ZCF3, ZCF31, ZRT2, orf19.1028, orf19.1150, orf19.1363, orf19.1434, orf19.1604, orf19.1835, orf19.2222, orf19.2308, orf19.2458, orf19.2726, orf19.3533, orf19.3854, orf19.3945, orf19.430, orf19.4342, orf19.4701, orf19.4792, orf19.4906, orf19.4913, orf19.5131, orf19.5605, orf19.5953, orf19.6003, orf19.6539, orf19.6769, orf19.6874, orf19.7196, orf19.7445, orf19.92*
response to stress	100 out of 610 genes, 16.4%	*ADAEC, AGP2, AHR1, APN2, ATC1, BCR1, BCY1, BRG1, CAT1, CDC19, CDR1, CEK2, CRZ2, CZF1, DAC1, DDR48, DOT5, DYN1, EAF6, ECM33, EFG1, EPL1, ESA1, FGR3, FGR30, FGR6, FGR6-10, FGR6-3, FGR6-4, GAL10, GCN4, GCY1, GLN3, GPD1, GPR1, GPX2, GRR1, HMS1, HOF1, HPR5, HSL1, HSP60, HSP70, HSP78, HSP90, KAR2, MDR1, MP65, NRG1, OLE1, OPI1, OSM2, PDS5, PHO4, PIL1, PTC8, RAD10, RAD32, RAS2, RCK2, REG1, RFG1, RHB1, RHR2, SBP1, SFU1, SGS1, SHA3, SIR2, SOD1, SSA2, SSN6, SSU1, SSU81, STP2, SUI2, TPS2, TPS3, TRX1, TSA1, TSA1B, TYE7, WSC2, YHB1, YIM1, ZRT2, orf19.1434, orf19.2458, orf19.345, orf19.3854, orf19.4246, orf19.4409, orf19.461, orf19.4914, orf19.5438, orf19.5576, orf19.5844, orf19.5917.3, orf19.6816, orf19.7196*
transport	97 out of 610 genes, 15.9%	*AGP2, CAN2, CAN3, CDR1, CNT1, CRP1, DBP5, DIP5, FCY21, FLC1, FLU1, FRP3, FTH1, GAL1, GAP1, GAP6, GEF2, GIT1, GIT3, GLK1, GNP1, GTR1, HGT2, HGT6, HGT7, HIP1, HMT1, HSP60, HSP70, HSP78, HXK2, KAR2, MDH1-1, MDJ2, MDM34, MDR1, NCE102, OPT1, OPT2, OPT3, PDR16, PET9, PEX7, PFK1, PFK2, PHO84, PHO87, PIL1, PMA1, PMC1, PTR2, PTR22, QDR1, RCH1, RGT1, RHB1, SDS24, SEC14, SFC1, SHA3, SIT1, SMF12, SSA2, SSU1, STP2, TIM21, TPO3, TRX1, VMA13, XUT1, YHB1, YOR1, ZRT2, orf19.1312, orf19.1355, orf19.1544, orf19.1655.3, orf19.1867, orf19.2026, orf19.2222, orf19.2333, orf19.304, orf19.3043, orf19.430, orf19.474, orf19.4940, orf19.5022, orf19.5114, orf19.5539, orf19.5628, orf19.5917.3, orf19.6209, orf19.6343, orf19.6804, orf19.7445, orf19.932*

GO term	Cluster frequency	Genes annotated to the term
response to chemical stimulus	84 out of 610 genes, 13.8%	*AHR1, APN2, BCR1, CAT1, CBF1, CDR1, CNT, CRZ2, CTA4, DAC1, DDR48, DIP5, DOT5, EFG1, FCY21, FKH2, FLO8, FLU1, GAL1, GAL10, GAL102, GCN4, GCY1, GLN3, GPR1, GRR1, GSC1, GSL1, HGT7, HMS1, HSL1, HSP70, HSP90, HXK2, KAR2, LAP3, MDR1, MIG1, MSI3, NRG1, OLE1, OPI1, OPT1, OSM2, PDR16, PGA62, PHO4, PMC1, QDR1, RCK2, RHB1, SFU1, SHA3, SIR2, SIT1, SOD1, SSA2, SSN6, SSU81, STB3, STP2, STP3, SWE1, TPO3, TPS2, TRX1, TSA1, TSA1B, TUB2, TYE7, YHB1, YTH1, ZCF3, ZCF31, orf19.2047, orf19.2827, orf19.304, orf19.345, orf19.3854, orf19.3945, orf19.5587, orf19.6586, orf19.6816, orf19.7029*
filamentous growth	84 out of 610 genes, 13.8%	*AAF1, AHR1, BCR1, BCY1, BRG1, CAT1, CDC19, CEK2, CLB4, CTA4, CUP9, CZF1, DAC1, DBF2, DDR48, DYN1, ECM33, EFG1, ENO1, ESA1, FGR3, FGR30, FGR6, FGR6-1, FGR6-10, FGR6-3, FGR6-4, FKH2, FLO8, GAL10, GAP1, GCN4, GLN3, GPR1, GRF10, GRR1, HMS1, HPR5, HSL1, HSP90, KAP114, LPD1, MNT2, MP65, NAG1, NRG1, OLE1, PDX1, PGA59, PHO4, PTC8, RAS2, RCK2, RFG1, RGT1, RHB1, SEF1, SGS1, SHA3, SOD1, SSN6, SSU1, SSU81, STP2, STP3, STP4, SUN41, TCC1, TPS2, TRX1, TSA1, TSA1B, TYE7, WOR2, YHB1, ZCF18, ZCF2, ZCF3, orf19.1835, orf19.2397.3, orf19.4246, orf19.461, orf19.5576, orf19.6874*
organelle organization	55 out of 610 genes, 9.0%	*ACO1, BUD14, CBF1, COF1, CYP1, DBF2, DNM1, DYN1, EAF6, EPL1, ESA1, FKH2, GRF10, HOF1, HSP60, HSP78, HSP90, IFC3, ILV5, KAR2, KGD2, MDH1, MDJ2, MDM34, NHP6A, OLE1, PDS5, PEX7, PHO4, RAD32, RPL10, RPL5, SEC14, SGS1, SSN6, TIM21, TIM23, TRX1, TUB2, orf19.1972, orf19.2726, orf19.2827, orf19.2938, orf19.3431, orf19.3533, orf19.4273, orf19.430, orf19.474, orf19.475, orf19.5438, orf19.5772, orf19.6246, orf19.6539, orf19.7196, orf19.7445*
carbohydrate metabolic process	50 out of 610 genes, 8.2%	*ADH1, ALG1, ATC1, BGL2, CDC19, CIT1, ENO1, FBA1, FOX2, GAL1, GAL10, GAL7, GCY1, GLK1, GPD1, GPD2, GPH1, GPM1, GSC1, GSL1, GUT2, HXK2, ICL1, MDH1, MDH1-1, MLS1, MNT2, MP65, NAG1, OST1, PCK1, PDC11, PFK1, PFK2, PGA56, PGI1, PGK1, RGT1, RHD1, RHR2, RKI1, TDH3, TPS2, TPS3, orf19.1355, orf19.2308, orf19.3060, orf19.3325, orf19.6816, orf19.6996*
response to drug	40 out of 610 genes, 6.6%	*AHR1, CDR1, CNT, DIP5, EFG1, FCY21, FLU1, GAL102, GCY1, GLN3, GSC1, GSL1, HGT7, HSL1, HSP90, MDR1, MIG1, MSI3, NRG1, OPT1, PDR16, PGA62, PMC1, QDR1, RHB1, SIT1, SSN6, STP2, STP3, SWE1, TPO3, TUB2, YTH1, ZCF3, ZCF31, orf19.2047, orf19.304, orf19.3854, orf19.6586, orf19.7029*
pathogenesis	35 out of 610 genes, 5.7%	*AHR1, BGL2, BRG1, CAT1, CSP37, DAC1, ECM33, EFG1, FLO8, FOX2, GLN3, GNA1, GSC1, HSL1, HSP90, ICL1, IFF11, MDR1, MIT1, MNT2, MP65, MSI3, NAG1, NRG1, OLE1, RCK2, RFG1, SAP2, SOD1, SSN6, SUN41, SWE1, TCC1, TPS2, YHB1*
biofilm formation	22 out of 610 genes, 3.6%	*ADH1, ADH5, AHR1, BCR1, BGL2, BRG1, CRZ2, CZF1, ECM33, EFG1, FCR3, FLO8, GCN4, IFD6, MP65, NRG1, PDX1, SUN41, TRY3, TYE7, YWP1, ZCF31*
signal transduction	15 out of 610 genes, 2.5%	*BCY1, DBF2, GPR1, HMS1, HSP90, OPI1, RAS2, RCK2, RGS2, RHB1, SSU81, WSC2, orf19.2726, orf19.430, orf19.6003*
protein catabolic process	12 out of 610 genes, 2%	*GRR1, KAR2, REG1, SAP2, UBC8, orf19.1028, orf19.2026, orf19.5131, orf19.6630, orf19.7196, orf19.7445, orf19.7497*
DNA binding	45 out of 610 genes, 7.4%	*ACO1, ADAEC, AHR1, APN2, BCR1, BRG1, CBF1, CTA4, CUP9, CZF1, EFG1, FCR3, FKH2, FLO8, GCN4, GLN3, GRF10, HAP41, HMS1, HSP60, ILV5, INO2, LAP3, MIG1, NHP6A, NRG1, PHO4, RAD10, RAD32, RFG1, RGT1, SBP1, SEF1, SFU1, STB3, STP2, STP3, STP4, TYE7, orf19.1150, orf19.1363, orf19.3431, orf19.4601, orf19.4914, orf19.6626, orf19.6874*

The most significant Stp1-HA binding events, bound with the highest intensities, were located in the promoters of the peptide transporter genes *PTR22, OPT1*, and *OPT2*, which was consistent with upregulation of peptide transport in YCB-YE-BSA. Binding of Stp1-HA to the promoters of known target genes, like *OPT1, OPT3*, *PTR2,* and *SAP2* was observed (Appendix A1), which strengthens the reliability of the obtained results.

Additionally, genes encoding core enzymes that were required to incorporate nitrogenous compounds into cellular nitrogen were among the hits (e.g. *GDH1, GDH2, GLN1, CIT1, and ACO1*) (Table A). Also enzymes involved in amino acid metabolism (e.g. Bat22, Lys4, Met10, Aat1, Dap2, and Ape2) as well as regulators, which are responsive to amino acids, like Gcn4 and Stp2 were Stp1-HA targets. Taken together this underlines the function of Stp1 for gene expression needed to assimilate proteins and other nitrogenous compounds as source for cellular nitrogen. Stp1-HA bound further in the promoter of the repressor Cup9, which has role in the regulation of peptide uptake. Moreover, Stp1 bound to its own promoter, suggesting auto regulation, which is frequently observed for transcriptional activators in order to amplify the transcriptional response.

Almost 16% of all genes were involved in transport processes (Table 2.1) including the mentioned peptide transporters, several amino acid permeases (e.g. Gap1, Gap3, Gap5, Can2, Agp1, Agp2, Dip5), transporters for the uptake of chloride (Gef2), manganese (Smf2), zinc (Zrt2), phosphate (Pho84, Pho87), copper (Crp1), iron siderophores (Sit1), heme (Flc1), and three glucose transporters (Hgt2, Hgt6, Hgt7). This, together with many hits for genes involved in carbohydrate or lipid metabolism as well as the global carbon catabolite repressor Mig1, indicates a general involvement of Stp1 in nutrient acquisition and metabolic adaption. Supportive evidence is provided by binding to the promoters of both genes encoding the enzymes of the anaplerotic glyoxylate cycle, *MLS1* and *ICL1*. The anaplerotic cycle is required to incorporate alternative carbon and nitrogen sources into cellular metabolism.

Interestingly, more than 16% of bound target genes were assigned a function involved in stress response, including starvations stress (*CBF1, STP2, GCN4, GAL10, GPR1, MP65, SFU1,* …) oxidative stress (*YHB1, SOD1, CAT1, GPX2, TSA1, UGA2, TRX1*), osmotic stress (*RHR2*) and temperature stress (*HSP60, HSP70, HSP78, HSP90*, and *SSA2*). This suggested a role for Stp1 in cellular stress adaptation and response to external stimuli which was further underlined by overrepresented hits for genes involved in response to chemical stimuli and drugs (Table 2.1). Although believed to be a pathway specific transcriptional regulator controlled by the global

regulators Gat1 and Gln3, Stp1 targets include more than 40 putative and verified transcription factors. Some of them have major roles in *C. albicans* pathogenicity, e.g., Efg1, Bcr1, Gln3, Nrg1, Flo8, Rgt1, and Czf1 or are important in other cellular processes (Sef1, Wor2, Stp2, Mig1, Stp1 …). Lastly, a major part of promoters bound by Stp1-HA controlled genes important for filamentous growth, biofilm formation and pathogenesis, possibly creating a direct link of Stp1 activity and *C. albicans* pathogenicity. How far Stp1 is involved in the regulation/modulation of the expression of these other transcriptional regulators is currently completely elusive.

Close inspection of Stp1-HA binding to the *SAP2* promoter (Figure 2.2 bottom) revealed three binding sites. As mentioned, also the adjacent *YHB1* ORF might be regulated by Stp1. However, experimental evidence indicated a regulation of *SAP2* expression by Stp1, e.g. *stp1*Δ/Δ null mutants are defective in *SAP2* expression and hyperactive $Stp1^{\Delta N61}$ induces Sap2 expression under normally repressive conditions (Dabas & Morschhäuser, 2008). The three possible *SAP2* regulating Stp1-HA binding sites are located between -4.3 kb and -2.0 kb upstream of the *SAP2* start codon, and at least one (presumably the binding event closest to the *SAP2* ATG^{start}) is likely to control *SAP2* expression.

With the extracted sequences from all Stp1 binding hits several web-based platforms (e.g. SCOPE: http://genie.dartmouth.edu/scope/ (Carlson *et al.*, 2007) or Peak-motifs: http://rsat.ulb.ac.be/peak-motifs_form.cgi (Thomas-Chollier *et al.*, 2012) were used in order to identify a Stp1 binding motif. However, no conclusive Stp1-motif was identified since all applied algorithms gave distinct or not significantly overrepresented motifs, in comparison to a random set of sequences. In addition, none of the motifs resembled the previously identified motif of the ortholog ScStp2 from *S. cerevisiae* (de Boer *et al.*, 2000, Zhu *et al.*, 2009).

Nevertheless, the genome wide binding profile of Stp1 during growth in YCB-YE-BSA confirmed direct regulation of known Stp1 targets, like *SAP2*, and revealed many new targets.

2.2 Sap2, a major secreted aspartic protease

The secreted aspartic protease Sap2 possesses a central role in growth on proteins as sole nitrogen source and has additionally been implicated as virulence trait in *C. albicans*. It serves therefore as an excellent example to illustrate nitrogen-regulated pathogenesis. The Sap2 protease is expressed from two polymorphic alleles which differ in many positions in the over 4 kb spanning promoter region. The current model proposes that only the promoter of *SAP2-2* is basally transcribed and more easily activated than *SAP2-1* upon signal input. Moreover, the basal expression from *SAP2-2* is necessary to provide the proteolytic degradation products that are required for full induction from both *SAP2* alleles (Figure 1.6). Thus, without the *SAP2-2* allele, the *SAP2-1* allele is not induced unless another source of proteolytic activity is applied in the exterior.

2.2.1 Protease dependent growth on proteins as sole nitrogen source

To study proteolytic activity of various Sap proteins in the laboratory, *C. albicans* mutants were commonly analyzed in medium where bovine serum albumin (BSA) served as sole nitrogen source. However, only Sap2, the major secreted protease, has been shown to be essential for the *in vitro* growth on BSA (Hube *et al.*, 1997).

2.2.1.1 Growth of different sap mutants with BSA as sole nitrogen source

The other Sap proteases are believed to contribute only minimal to the *in vitro* growth on BSA as sole nitrogen source. But based on the results, by Sanglard *et al.* (Sanglard *et al.*, 1997), also the proteases Sap4 to Sap6 seemed to be important. There, the *sap4*Δ/Δ *sap5*Δ/Δ *sap6*Δ/Δ triple deletion mutant, entitled DSY459, was impaired in growth on BSA, implying that these three proteases either are required for growth or play a role in providing the inducers needed for full *SAP2* induction (Figure 1.6). In contrast, however, other *sap4*Δ/Δ *sap5*Δ/Δ *sap6*Δ/Δ triple deletion mutants, named SAP456MS4A and B, constructed independently showed wild type like growth in YCB-BSA (Lermann & Morschhäuser, 2008).

Such striking phenotypic difference between theoretically similar mutants could have three main reasons (a) the genetic background, (b), variations in the experimental procedure or used supplements, or (c) unspecific genomic alterations, occurring while constructing or maintaining mutant strains.

(a) A distinct strain background was excluded as both triple mutants were derived from the reference strain SC5314 (Gillum *et al.*, 1984), where strain DSY459 was generated from an auxotrophic *ura3*Δ/Δ derivative of SC5314 by the URA-Blaster method (Fonzi & Irwin, 1993) and SAP456MS4 A/B were generated directly from SC5314 using the *SAT1*-flipper method (Reuss *et al.*, 2004, Sasse & Morschhäuser, 2012).

(b) To exclude variations in the experimental setup the growth of both triple deletion mutants (DSY459 vs. SAP456MS4 A/B) was directly evaluated in YCB-BSA medium from our laboratory. For comparison the wild type SC5314, the homozygous *sap2*Δ/Δ deletion mutants and the heterozygous mutants, deleted either for *SAP2-1* or *SAP2-2,* were included (Figure 2.3 A).

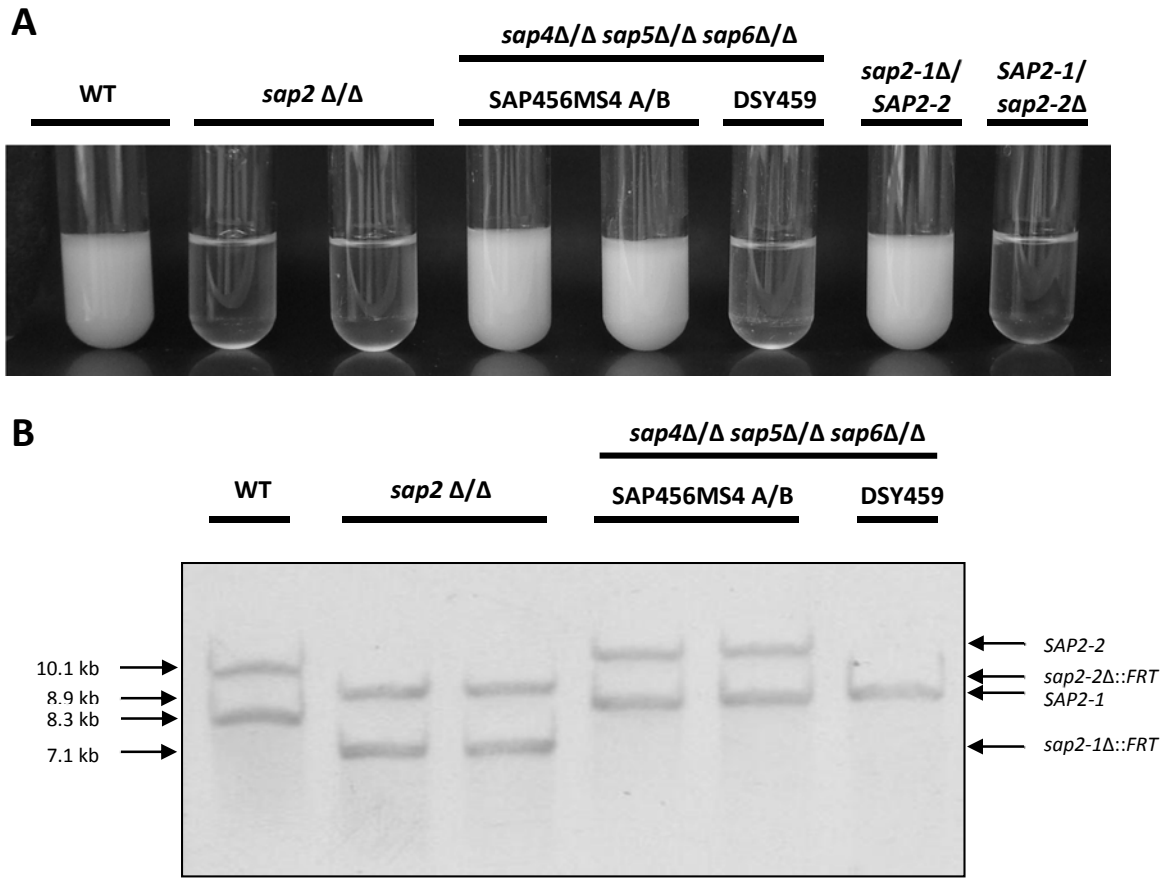

Figure 2.3: Growth and genomic differences of various *sap* deletion mutants. Following strains were used: SC5314 (WT); SAP2MS4A/B (*sap2*Δ/Δ); SAP456MS4A/B (*sap4*Δ/Δ *sap5*Δ/Δ *sap6*Δ/Δ); DSY459 (*sap4*Δ/Δ *sap5*Δ/Δ *sap6*Δ/Δ), SAP2MS4A (*sap2-1*Δ/*SAP2-2*), and SAP2MS4B (*SAP2-1*/*sap2-2*Δ). (A) Growth on BSA as sole nitrogen source was documented by photographing the cultures. YPD overnight cultures of the indicated strains were 1:1000 inoculated in fresh YCB-BSA medium and grown at 30°C for 4 days. (B) Analysis of the genomic ClaI polymorphism in the *SAP2* locus. Southern hybridization of ClaI-digested genomic DNA from indicated strains with a *SAP2*-specific probe. Individual identities and sizes of the hybridizing fragments are indicated.

The reported growth defect of DSY459, which grew as poorly as the *sap2*Δ/Δ mutants and the mutant lacking *SAP2-2* was confirmed (Figure 2.3 A). Also the wild type like growth of the SAP456MS4 A/B mutants was confirmed, which implied that the experimental setup was not responsible for the growth differences between the *sap4*Δ/Δ *sap5*Δ/Δ *sap6*Δ/Δ triple deletion mutants. Instead, the growth defect of DSY459 might be due to, (c), unspecific genomic alterations that may have occurred during strain construction. The fact, that loss of the *SAP2-2* allele alone impaired growth on YCB-BSA reasoned that DSY459 may have lost the *SAP2-2* allele. Therefore, the presence of *SAP2-2* in DSY459 was examined. Both *SAP2* alleles could be discriminated by a ClaI restriction site polymorphism, where only the *SAP2-1* allele contained the variable ClaI site (position -3178) (Staib *et al.*, 2002a). Southern hybridization of ClaI-digested genomic DNA with a *SAP2*-specific probe revealed the loss of the *SAP2-2* allele in DSY459 (Figure 2.3 B). Whereas the wild type SC5314 and the SAP456MS4 A/B strains had two fragments for both alleles (*SAP2-1*: approx. 8.3 kb; *SAP2-2*: approx. 10.1 kb), DSY459 has only the fragment corresponding to the *SAP2-1* allele. Consequently, DSY459 lost the *SAP2-2* allele and became homozygous for *SAP2-1* and thus, absence of *SAP2-2* arguable resulted in the growth defect of DSY459, when proteins are the sole nitrogen source in YCB-BSA.

2.2.1.2 DSY459 is homozygous for chromosome R

Loss of heterozygosity (LOH), like for the *SAP2-2* allele here, mainly results from either chromosomal rearrangements, including mitotic recombination and gene conversion or loss of a whole chromosome and duplication of the remaining one (Calderone., 2008, Selmecki *et al.*, 2010). To distinguish between these two possibilities a set of selected genes were analyzed, whether they had lost or retained their SNPs (SNP: single nucleotide polymorphism). The selected genes were distributed across the whole chromosome R, where *SAP2* is located on the left arm about 50 kb from the centromere (Figure 2.4 A) and harbored known SNPs. Local restricted loss of SNPs served as indicator for small-scale genomic rearrangements, whereas chromosome-wide LOH would indicate whole chromosome loss and duplication as cause for a *SAP2-2* allele loss.

Southern hybridization with genomic DNA from both strains, SC5314 and DSY459, was done to analyze the presence of SNPs that produced restriction site variability. The *OPT1* locus harbored a restriction site for HindIII and the *OPT4* locus for EcoRI (Reuss & Morschhäuser, 2006, Reuss *et al.*, 2004). Hybridization with a specific probe to the HindIII- / EcoRI-digested genomic DNA of DSY459 demonstrated that this strain was also homozygous for the *OPT1* and *OPT4* alleles (Figure 2.4 B).

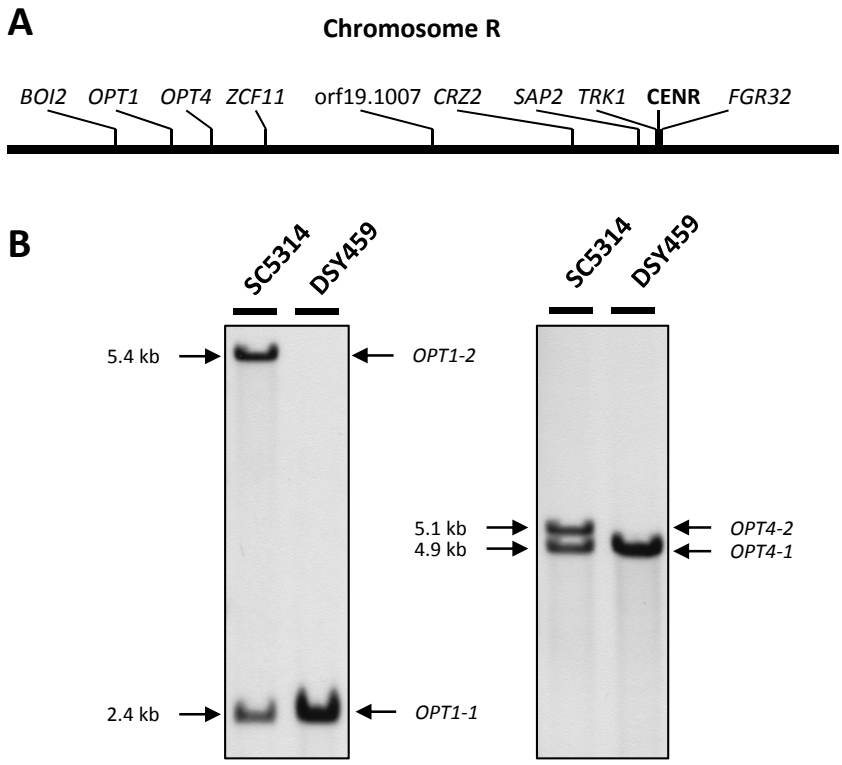

Figure 2.4: Differences in allelic polymorphisms of SC5314 and DSY459. (A) Schematic chromosome R with all analyzed polymorphic genes and their approximate position. CENR: centromere. (B) Analysis of genomic restriction site variability on chromosome R. Southern hybridization of genomic DNA digested with HindIII (*OPT1* locus; left panel) or EcoRI (*OPT4* locus; right panel) from the strains SC5314 and DSY459 with *OPT1*- or *OPT4*-specific probes, respectively. Polymorphic allele fragments and their size and arbitrarily designation in SC5314 are indicated.

Only the arbitrarily designated alleles *OPT1-1* and *OPT4-1* were detected in DSY459, whereas the wild type SC5314 possessed both alleles (Figure 2.4 B). Presence or absence of SNPs in DSY459 for the other genes was determined by sequencing. Therefore, the SNP containing regions were amplified with specific primers (Table 2.2) and the PCR product was directly sequenced. As control the SNPs were also determined for the wild type SC5314. Table 2.2 summarized all analyzed SNP location and the respective nucleotides found in DSY459 and SC5314.

Table 2.2: Single nucleotide polymorphisms (SNPs) in SC5314 and DSY459 for indicated genes on chromosme R. SNP locations were assigned according to the nucleotide positions, with regard to the start codon, in the *Candida* genome database (www.candidagenome.org). Gene IDs and the relative centromer position between *TRK1* and *FGR32* are indicated. Nucleotides for the respective positions in both strains were obtained by direct sequencing of PCR products. Primers used for amplification and sequencing are indicated.

Gene name	Gene ID	Primers	SNP location (nt position)	SC5314	DSY459
BOI2	orf19.3230	BOI2-1 / BOI2-2	2682 2731 2943	C/T A/G C/T	C G T
ZCF11	orf19.2423	ZCF11-1 / ZCF11-2	1035 1038 1041 1521 1689	C/T C/G A/G A/G G/T	T C G A T
-	orf19.1007	1007-1 / 1007-2	291 477 555 885	C/T A/G C/T C/T	C A C C
CRZ2	orf19.2356	CRZ2-1long / CRZ2-2long	76 84 168 172 191 193 258 447 450	A/G C/T C/G A/G C/T A/G C/T A/G A/G	G T C G T G C G A
TRK1	orf19.600	TRK1-1 / TRK1-2	465 563 801 989 1097 1131	A/G C/T A/G A/G A/G C/T	G C G G A C
CENR					
FGR32	orf19.593	FGR32-1 / FGR32-2	1327 1351 1579 1771 1882 1920 1938	A/G C/T A/G C/T C/T A/G G/T	G C A T C G G

The sequences of all analyzed genes revealed that all tested SNPs at all positions were lost in DSY459, in contrast to the wild type SC5314. SNPs of genes on both sides of the centromere (*TRK1* and *FGR32*) were also lost like SNPs at the extreme end of the chromosome (*BOI2*). It is therefore unlikely that LOH for all tested SNPs on both arms of the chromosome were a result from multiple local recombination events. So this strongly hinted that presumably the complete chromosome R was lost and the remaining one was consequently duplicated and therefore resulted in the loss of the *SAP2-2* allele (and all other SNPs) in DSY459.

2.2.1.3 Reintroduction of the *SAP2-2* allele restored growth of DSY459

Reasonably, loss of the *SAP2-2* allele, which was crucial for growth on BSA, may be the true cause of the impaired growth of the *sap4*Δ/Δ *sap5*Δ/Δ *sap6*Δ/Δ triple deletion mutant DSY459. To test this, the *SAP2-2* allele and the corresponding regulatory region was reintroduced into DSY459 using the cassette from pSAP2KS4. This cassette was obtained by amplification of the upstream and coding region of *SAP2-2* using genomic DNA from the heterozygous *sap2-1*Δ/*SAP2-2* mutant (SAP2MS2A) as template (Primers: SAP2P10 and SAP2ex2). The PCR-product was digested at the introduced ApaI and KpnI sites and ligated together with the KpnI-PstI fragment from pSAP2ex5 into the ApaI-PstI digested vector pSAP2H1 resulting in pSAP2KS4. This plasmid now harbored the complete (approx. 4.3 kb) *SAP2-2* regulatory region and also served as reference *SAP2-2* sequence for all further investigations (Appendix A2). It is noteworthy, that due to the cloning strategy, using the KpnI site at position +830, the *SAP2-2* ORF contained at position +1179 a Thymidine, a nucleotide present otherwise only in *SAP2-1*. Since this exchange is silent, resulting in no amino acid sequence alteration, the mature protein sequence remained unchanged. The ApaI-SacI fragment from pSAP2KS4 was used to transform two times independently DSY459 and a total of 12 DSY459-transformants were analyzed for correct integration by Southern hybridization of ClaI-digested genomic DNA with *SAP2*-specific probes (Figure 2.5). The hybridization with a *SAP2*-specific probe proved that in all DSY459-transformants the cassette had integrated correctly into the *SAP2* locus. It should be noted that the actual cross-over event within such long homologous regions, like the 5'*SAP2* sequences here, could have occurred at various sites resulting in a different extent of actual replacement (Figure 2.5 A). The loss of the ClaI-site in *SAP2-1*, indicated by a new hybridizing fragment of 7.7 kb, demonstrated that at least 3.2 kb of the *SAP2-1* promoter sequence has been replaced by the corresponding *SAP2-2* promoter sequences (Figure 2.5 B; DSY459-transformants A2, A4, B1, and B2).

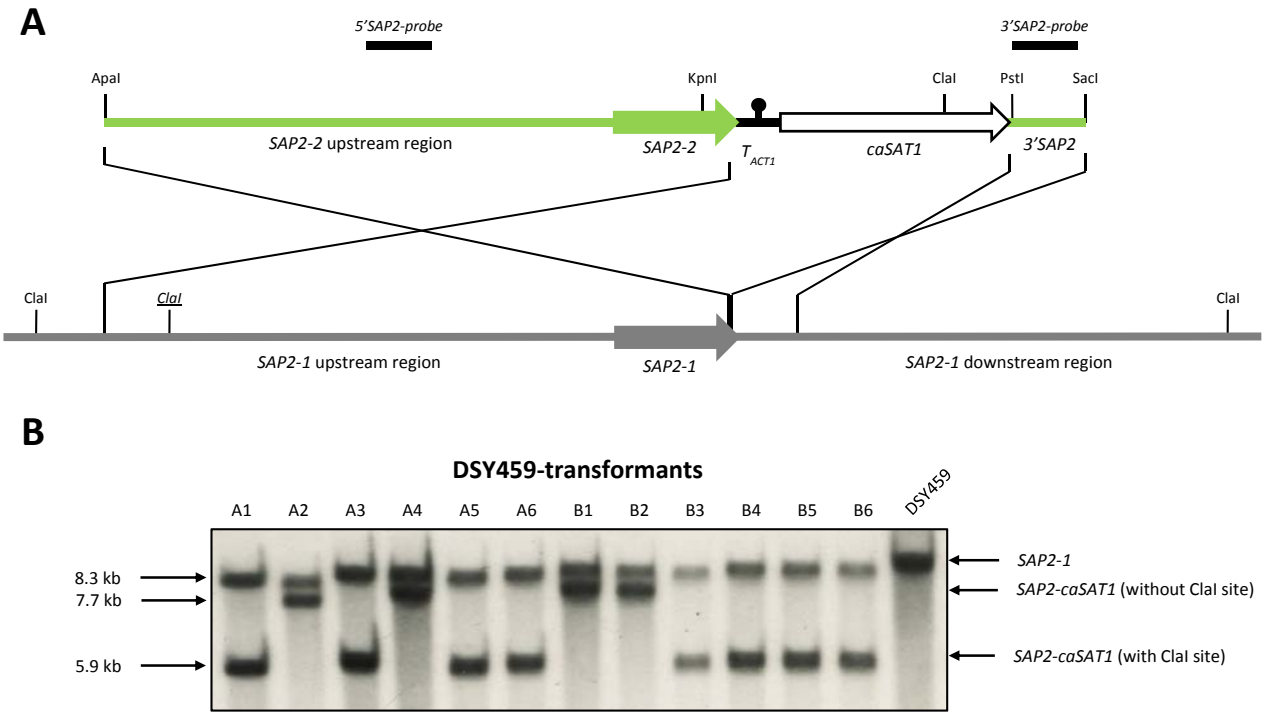

Figure 2.5: Integration of the *SAP2-2* sequences into one of the *SAP2-1* copies in DSY459. (A) Schematic drawing illustrating the integration of the ApaI-SacI fragment from pSAP2KS4 into one of the two *SAP2-1* copies in DSY459. *SAP2-2* sequences are colored in green and *SAP2-1* sequences in gray. The filled arrow depicts the *SAP2* gene and the unfilled arrow the ca*SAT1* selection marker. The black bar and circle symbolizes the transcription termination sequence of *ACT1* (T_{ACT1}). Relevant ClaI-sites are indicated with the ClaI-site only existing in *SAP2-1* underlined and in italics. The lines indicate homologous regions where a cross-over can occur while integrating the cassette. (B) Analysis of the genomic ClaI polymorphism in the *SAP2* locus. Southern hybridization with the 5'*SAP2*-specific probe of ClaI-digested genomic DNA, isolated from DSY459 and two independent sets of DSY459-transformants. Individual identities and size of the hybridizing fragments are indicated, whether the polymorphic ClaI site was retained or replaced.

On the other hand, preservation of the variable ClaI-site, indicated by a new hybridizing fragment of 5.9 kb, demonstrated a homologous recombination event proximal from this site (Figure 2.5 B; DSY459-transformants A1, A3, A5, A6, B3, B4, B5, and B6). To determine the exact extent of replacement for these DSY459-transformants the reintegrated *SAP2* copy was re-amplified with specific primers (SAP2P18 and ACT38) that only gave a PCR product for the cassette-containing *SAP2* allele. The ensued sequence analysis revealed the extent of replacement. DSY459-transformants A6, B3, and B6 had retained the complete *SAP2-1* promoter whereas A1, A3, A5, A4, and B5 contained proximal *SAP2-2* promoter sequences varying between 134 bp and 2.2 kb (Figure 2.6 left panel).

All 12 DSY459-transformants were then analyzed for their ability to grow on BSA as sole nitrogen source in YCB-BSA (Figure 2.6 right panel).

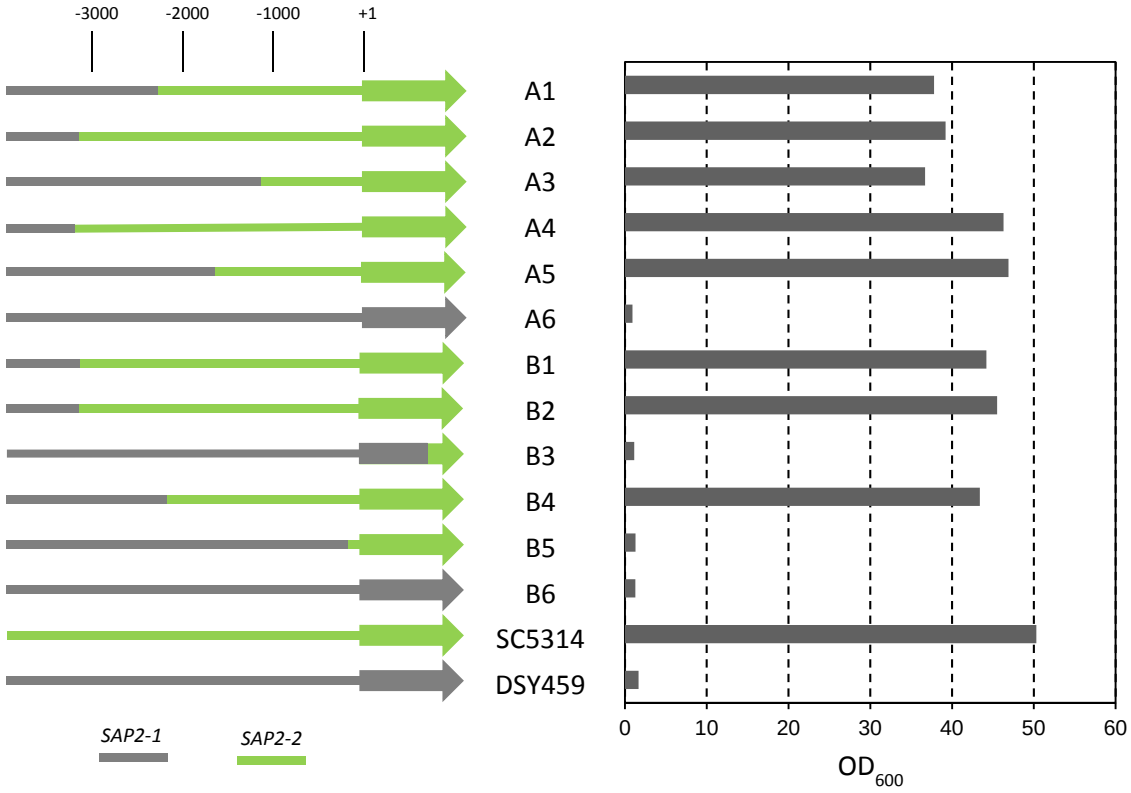

Figure 2.6: Growth and extent of *SAP2-1* sequence replacement in DSY459-transformants. The Left panel depicts the extent of replaced *SAP2-1* (gray) promoter (thick line) or gene (filled arrow) sequences by *SAP2-2* sequences (green) in the DSY459-transformants, respective to the *SAP2* ATG^{start} (+1). Note that only the relevant *SAP2* locus is shown and all strains also harbor one *SAP2-1* copy. The indicated *SAP2-2* sequences in the four DSY459-transformants A2, A4, B1, and B2 is the minimally replaced region (evident from replaced ClaI site) and was not further delimited. The extent of *SAP2-1* replacement in the other DSY459-transformants was determined by direct sequencing. The right panel shows the growth of all DSY459-transformants with BSA as sole nitrogen source in YCB-BSA. YPD overnight cultures of the indicated strains were 1:1000 inoculated in fresh YCB-BSA medium and grown at 30°C for 3 days. The parental strain DSY459 and the wild type SC5314 were included as control. Growth was determined by measuring the optical density (OD_{600}). Note: Only the results from one experiment is shown and similar results were obtained in an independent repeat experiment.

Eight DSY459-transformants demonstrated wild-type like growth in YCB-BSA medium (Figure 2.6) and all of them had integrated a minimum of 1.1 kb of the proximal *SAP2-2* promoter. The other four DSY459-transformants (A6, B3, B5, and B6) remained growth deficient. This clearly demonstrated that reintroduction of the *SAP2-2* promoter region restored growth of the *sap4*Δ/Δ *sap5*Δ/Δ *sap6*Δ/Δ triple deletion mutant DSY459. Consequently, not deletion for *sap4* to *sap6*, but the loss of *SAP2-2* due to homozygosity for the complete chromosome R, caused the growth defect in YCB-BSA.

2.2.1.4 Homozygosity for chromosome R and *SAP2-1* is sufficient to result in a growth defect with proteins as sole nitrogen source

Loss of the functional *SAP2-2* allele resulted in a growth defect in YCB-BSA medium. But the heterozygous *SAP2-1*/*sap2-2*Δ mutant (SCSAP2MS4B), harboring all three *SAP4* to *SAP6* genes, had retained only one copy of *SAP2-1* (Lermann & Morschhäuser, 2008, Staib *et al.*, 2002a), reasoning that a reduced gene dosage might be an additional requirement for a growth defect. Because DSY459 possessed two *SAP2-1* alleles, but is additionally deleted for *SAP4* to *SAP6*, their absence may impact activation of two *SAP2-1* copies, i.e. presence of Sap4 to Sap6 might be required for the induction from two *SAP2-1* copies and therefore enable growth. Thus, it was tested whether LOH of the *SAP2-2* allele and the chromosome R alone was sufficient to result in a growth defect. Therefore, the growth in YCB-BSA was tested for a mutant strain, which was homozygous for chromosome R and *SAP2-1*, but has the three *SAP4* to *SAP6* genes (Figure 2.7). This strain, designated YJB10698, is a derivative of SC5314 and arose after an *in vivo* passage and re-isolation from the kidneys of intravenously infected mouse (Forche *et al.*, 2009a, Legrand *et al.*, 2008).

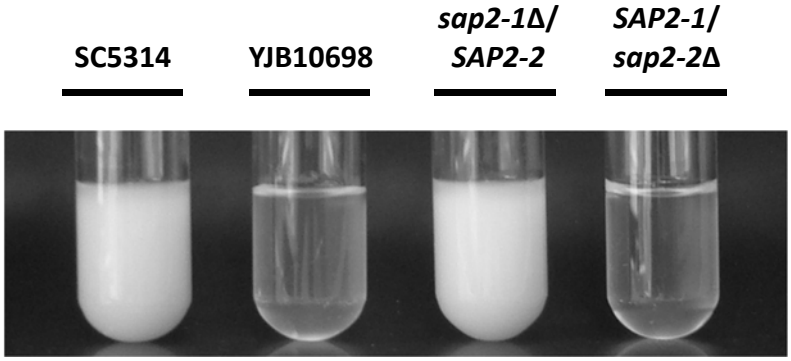

Figure 2.7: Growth on BSA as sole nitrogen source of YJB10698, which is homozygous for chromosome R and *SAP2-1*. As control the wild type SC5314 (WT) and both heterozygous *SAP2* mutants SAP2MS4A (*sap2-1*Δ/*SAP2-2*), and SAP2MS4B (*SAP2-1*/*sap2-2*Δ) were included. YPD overnight cultures of the indicated strains were 1:1000 inoculated in fresh YCB-BSA medium and grown at 30°C for 4 days. Growth was documented by photographing the cultures.

The strain YJB10698 exhibited the same growth defect as the heterozygous *SAP2-1*/*sap2-2*Δ mutant (Figure 2.7). This result consequently demonstrated that LOH of the *SAP2-2* allele and the chromosome R alone was sufficient to result in a growth defect on proteins as sole nitrogen source and indicated that the proteases Sap4 to Sap6 did not contribute to growth and *SAP2* activation.

2.2.1.5 Lack of the *SAP2-2* allele is sufficient to result in a growth defect with proteins as sole nitrogen source

LOH for the complete chromosome R could have also affected additional genes that might be required for growth in YCB-BSA, despite the loss of *SAP2-2*. To unambiguously prove that solely LOH for the *SAP2-2* allele and homozygosity for *SAP2-1* caused a growth defect on proteins as sole nitrogen source, the *SAP2-2* allele was replaced by the *SAP2-1* allele in the wild type strain SC5314. For the replacement of the *SAP2-2* allele with *SAP2-1* sequences the cassette from pSAP2KS5 was used. To obtain this cassette the identical cloning strategy as for pSAP2KS4, previously, was applied, except that amplification of the upstream and coding region of *SAP2-1* was done using genomic DNA from the heterozygous *SAP2-1/sap2-2*Δ mutant (SAP2MS2B) as template. This plasmid pSAP2KS5 now harbored the complete (approx. 4.3 kb) *SAP2-1* promoter and served as reference *SAP2-1* sequence for all further investigations (Appendix A2). The cassette from pSAP2KS5 was used to transform two times independently SC5314 and a total of 12 SC5314-transformants were analyzed for correct integration by Southern hybridization of ClaI-digested genomic DNA with *SAP2*-specific probes (Figure 2.8The hybridization with the 3'*SAP2*-specific probe proved that in all SC5314-transformants the cassette had integrated correctly into the *SAP2* locus (not shown). It should be noted that the actual cross-over event within such long homologous regions, like the 5'*SAP2* sequences here, could have occurred at various sites resulting in a different extent of actual replacement, which was checked with the 5'*SAP2*-probe (Figure 2.8 B).

Six SC5314-transformants had integrated the cassette into the *SAP2-1* allele, which was evident from the loss of the *SAP2-1* specific hybridizing fragment of 8.3 kb (Figure 2.8 B; SC5314-transformants A2, A3, A4, B2, B3 and B6). Loss of the *SAP2-2* specific hybridizing fragment of 10.1 kb and introduction of the variable ClaI-site, indicated by a new hybridizing fragment of 5.9 kb, demonstrated that at least 3.2 kb of the proximal *SAP2-2* promoter sequence has been replaced by the corresponding *SAP2-1* sequence (Figure 2.8 B; SC5314-transformants A1, B4, and B5).

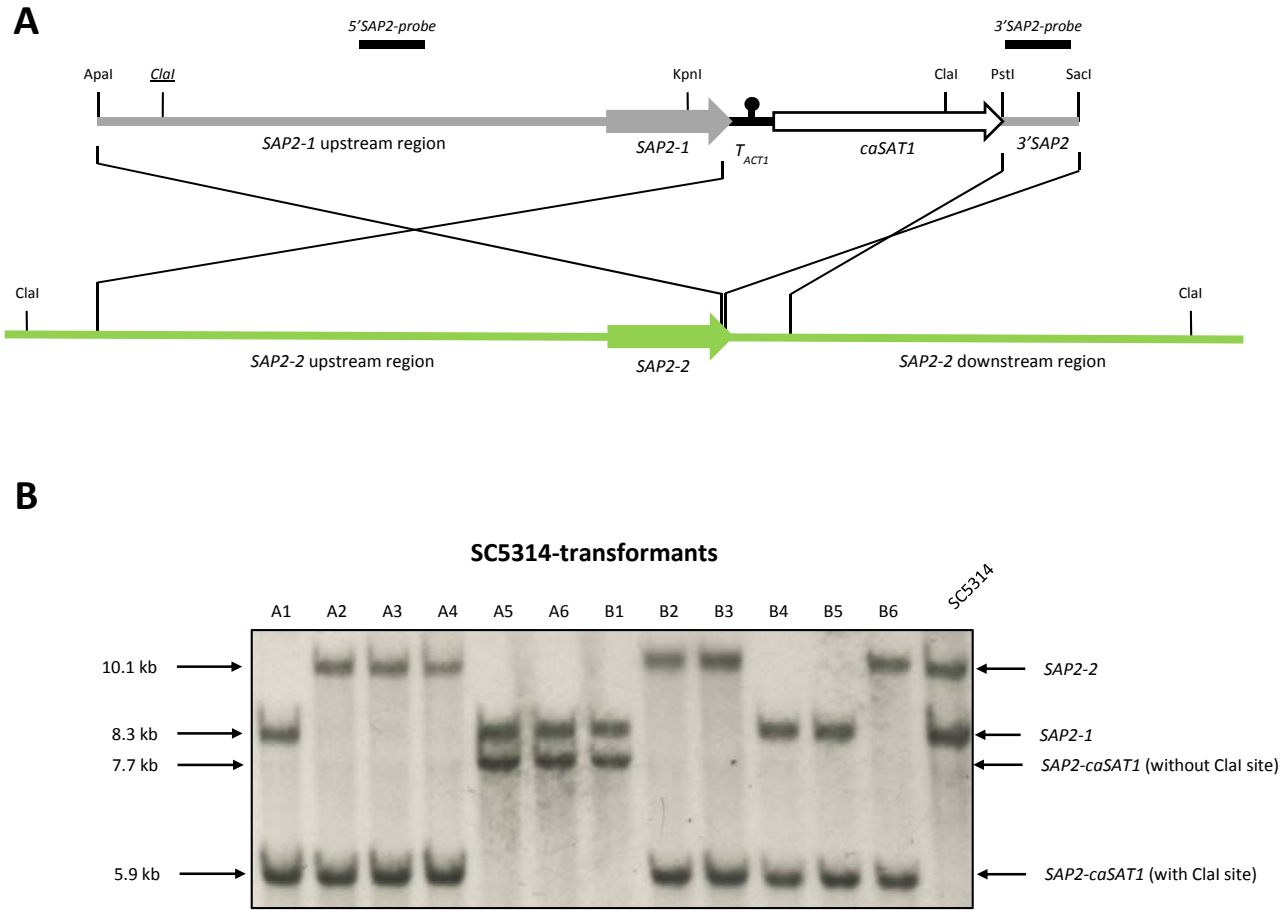

Figure 2.8: Integration of the *SAP2-1* sequences into the *SAP2-2* allele of the wild type SC5314. (A) Schematic drawing illustrating the integration of the ApaI-SacI fragment from pSAP2KS5 into the *SAP2-2* allele. *SAP2-2* sequences are colored in green and *SAP2-1* sequences in gray. The filled arrow depicts the *SAP2* gene and the unfilled arrow the ca*SAT1* selection marker. The black bar and circle symbolizes the transcription termination sequence of *ACT1* (T_{ACT1}). Relevant ClaI-sites are indicated with the ClaI-site only existing in *SAP2-1* underlined and in italics. The lines indicate homologous regions where a cross over can occur while integrating the cassette. (B) Analysis of the genomic ClaI polymorphism in the *SAP2* locus. Southern hybridization of ClaI-digested genomic DNA from SC5314 and from two independent sets of SC5314-transformants with the 5'*SAP2*-specific probe. Identities and sizes of the hybridizing fragments are indicated, whether the variable ClaI-site was introduced or not.

On the other hand, a new hybridizing fragment of 7.7 kb demonstrated that the variable ClaI-site was not introduced and thus hints that the actual cross-over event was located proximal from this site (Figure 2.8 B; SC5314-transformants A5, A6, and B1). To determine the exact extent of replacement the reintegrated *SAP2* copy was re-amplified with specific primers (SAP2P18 and ACT38) that only gave a PCR product for the cassette-containing *SAP2* allele. Sequence analysis revealed that the three SC5314-transformants, A5, A6, and B1, contained between 1.2 and around 3 kb of the proximal *SAP2-1* promoter (Figure 2.9 left panel).

All 12 SC5314-transformants were then analyzed for their ability to grow on BSA as sole nitrogen source (Figure 2.9 right panel). As control the wild type SC5314 and the heterozygous *SAP* mutants were included.

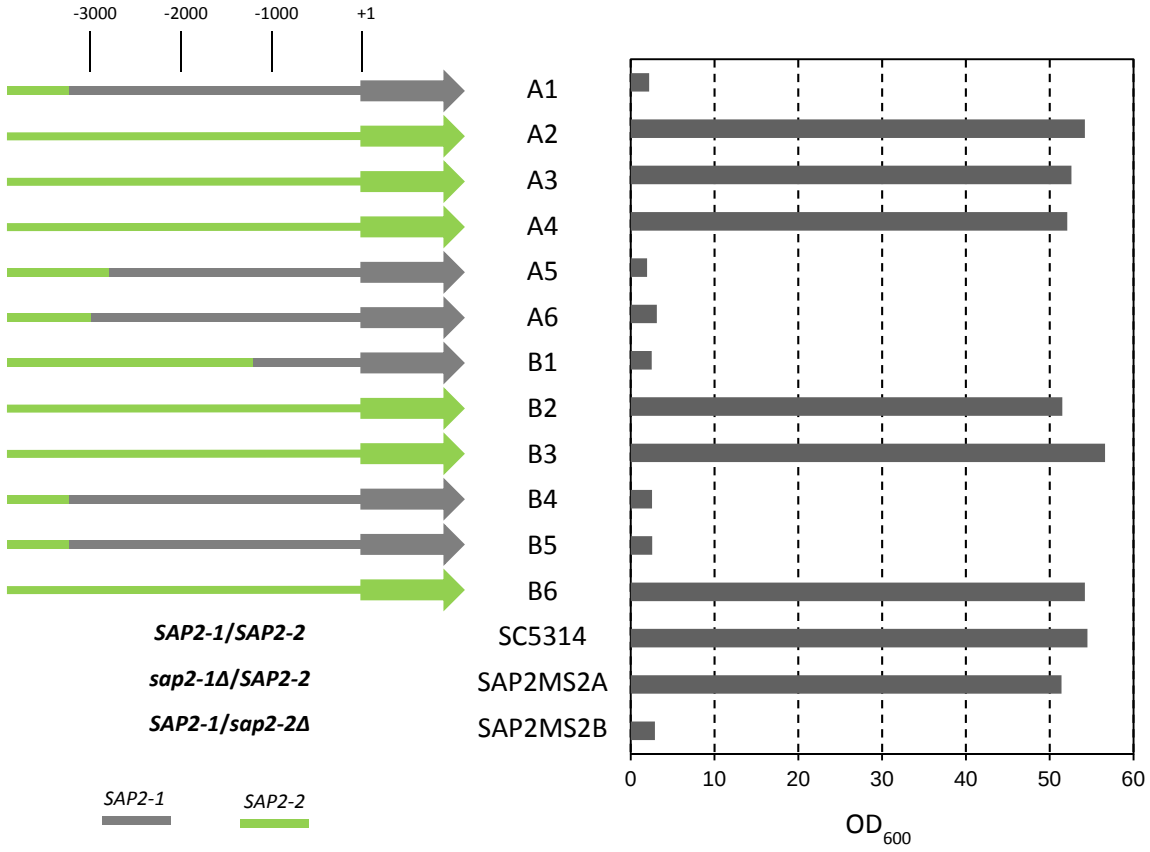

Figure 2.9: Growth and extent of *SAP2* sequence replacement in the *SAP2-2* locus of SC5314-transformants. The Left panel depicts the extent of replaced *SAP2-2* (green) promoter (thick line) or gene (filled arrow) sequences by *SAP2-1* sequences (gray) in the SC5314-transformants, respective to the *SAP2* ATG^{start} (+1). Heterozygous *SAP2* mutants SAP2MS2A (*sap2-1Δ/SAP2-2*), SAP2MS2B (*SAP2-1/sap2-2Δ*), and the wild type SC5314 (*SAP2-1/SAP2-2*) were included and their respective genotypes are indicated. The six SC5314-transformants A2, A3, A4, B2, B3, and B6 had integrated the cassette into the *SAP2-1* allele leaving the *SAP2-2* locus unaltered. The indicated *SAP2-1* sequence replacement in the three SC5314-transformants A1, B4, and B5 is the minimally replaced region (evident from the introduced ClaI site) and was not further delimited. The extent of *SAP2-2* replacement in the other SC5314-transformants was determined by direct sequencing. The right panel shows the growth of all SC5314-transformants with BSA as sole nitrogen source in YCB-BSA. YPD overnight cultures of the indicated strains were 1:1000 inoculated in fresh YCB-BSA medium and grown at 30°C for 3 days. Growth was determined by measuring the optical density (OD_{600}). Note: Only the results from one experiment is shown and similar results were obtained in an independent repeat experiment.

As expected all SC5314-transformants which had retained the complete *SAP2-2* allele grew as well as the wild type SC5314, whereas all SC5314-transformants exhibited a clear growth defect which had replaced the *SAP2-2* allele by at least 1.2 kb of the proximal *SAP2-1* promoter (Figure 2.9). This result unambiguously proved the replacement of *SAP2-2* sequences by the corresponding *SAP2-1* sequences was sufficient to cause a growth defect on proteins as sole nitrogen source. Moreover, replacing 1.2 kb of the proximal *SAP2-1* promoter region was sufficient to cause this growth defect.

2.2.2 *SAP2* promoter deletion analysis

Sap2 represents a well characterized virulence trait in *C. albicans* and it is therefore of general interest for nitrogen-regulated pathogenesis, how *SAP2* expression is controlled in detail.

Both *SAP2* ORFs encode functional secreted proteases, which differed only by two conserved amino acids exchanges. One is within the signal peptide sequence at residue 9 (*SAP2-1* encodes alanine; *SAP2-2* encodes glycine) and one at residue 258 (*SAP2-1* encodes valine; *SAP2-2* encodes leucine). Expression of both *SAP2* genes from the *ACT1* locus complemented the growth defect of a *sap2*Δ/Δ null mutant in YCB-BSA, thus demonstrating the functionality of both *SAP2* genes (Staib *et al.*, 2002a). Nevertheless, enzymatic difference between both Sap2 enzymes cannot be completely ruled out.

Over 80 polymorphisms distinguish the *SAP2-1* promoter from the *SAP2-2* promoter and two were shown to be important for *in vitro* and *in vivo SAP2* induction. These two pentameric tandem repeat regions were designated as R1 (GCTTT) and R2 (TTGAT/A). The *SAP2-1* allele harbors 4 copies of R1 and 6 copies of R2, whereas the *SAP2-2* allele harbors 5 copies of R1 and R2 (Staib *et al.*, 2002a). A promoter analysis done for *SAP2-1* showed that deletion of almost the entire promoter (in detail: deleted for sequences between -3.5 kb to -0.1 kb upstream of the *SAP2* ATG^{start}) abolished *SAP2-1* promoter activity in *ecaFLP* expression reporter system and quantitative RT-PCR (Lermann, 2008). In the *ecaFLP* reporter system the expression of the ecaFlp recombinase is controlled by the promoter of interest. Promoter activity leads to ecaFlp production, which mediates the recombination of FRT targets sequences thereby irreversible excising a mycophenolic acid resistance marker (MPA^R) and producing sensitive progenitor cells. These progenitor cells then form smaller colonies on agar plates containing low concentrations of mycophenolic acid. Thus, only promoter activity results in marker excision and smaller colonies, whose proportion is determined in comparison to not promoter-activated cells, which form big colonies. With the eca*FLP* system no promoter activity for *SAP2-1* was detected when deleted for the region between -2.5 kb to -0.1 kb, implying that *SAP2-1* promoter activity demands *cis*-acting elements within the upstream 2.5 kb. Indeed, the ChIP-on-chip global binding profile of Stp1-HA in the present work demonstrated binding to a region between -2.6 kb to -2.0 kb upstream of the *SAP2* start codon (Figure 2.2 bottom). This indicates that this promoter region is important for *SAP2* expression and furthermore suggests that the other two Stp1 binding events might be dispensable for *SAP2* expression, presumably they control expression of the opposed *YHB1*. Furthermore, a

full length 4.3 kb *SAP2-1* promoter deleted between -1.1 kb to -0.1 kb was still inducible in YCB-YE-BSA since expression of an *ecaFLP* reporter gene was not affected (Lermann, 2008, Wyzgol, 2005), albeit both repeat regions R1 and R2 were absent.

However, the *ecaFLP* reporter system might not be perfectly suited to such analysis since it provides only a yes/no answer of promoter activity and does not inform how strong a promoter is induced. Additionally, it is rather time consuming and also produced conflicting results. For example, when the 1.1 kb of proximal *SAP2-1* promoter sequences controlled activity no ecaFlp activity was determined but quantitative RT-PCR demonstrated increased transcript levels of the *ecaFLP* mRNA under the same conditions (Lermann, 2008). It should be noted that the tested 1.1 kb construct was fused to a distal *SAP2-1* promoter piece, i.e. the full 4.3 kb promoter was deleted between -3.5 kb and -1.1 kb. However, this distally l0.8 kb piece alone was unable to activate the *ecaFLP* reporter (Lermann, 2008).

In sum, these studies demonstrated that *SAP2-1* expression requires the proximal 2.5 kb of its promoter and the recent work showed that Stp1-HA bound to the region between -2.6 kb to -2.0 kb upstream of the *SAP2* start codon.

To overcome obstacles by the *ecaFLP* system and to verify and delimit important promoter regions, the deletion analysis of *SAP2-1* promoter was re-assessed and furthermore expanded to an analysis, for the first time, to *SAP2-2* using the detection of HA-tagged Sap2 in the supernatant.

2.2.2.1 Defining *SAP2* regulatory sequences

Prior to a comprehensive analysis, both Sap2 allele promoter sequences were determined. However, the complete sequence online available at the *Candida* genome database (CGD, www.candidagenome.org) unfortunately is a mixed sequence of both *SAP2* alleles and more than the reported polymorphisms (Forche *et al.*, 2004, Jones *et al.*, 2004) were present in the *SAP2* alleles from our reference wild type strain SC5314. It is noteworthy that besides the additional SNPs, all previously reported polymorphisms were also found in our *SAP2* alleles. Though, the C at position -1169 was not found in the SC5314 from our laboratory (all *SAP2* alleles contained a T at this position).

The *SAP2-1* sequence from plasmid pSAP2KS5 and the *SAP2-2* sequence from pSAP2KS4 were defined as reference sequences for both of our *SAP2* alleles, respectively (Appendix A2). To ensure consistency and traceability with respect to nucleotide positions (e.g. SNPs or deleted regions) a *SAP2* superalignment was created, where the sequences from both *SAP2* alleles

were merged. This *SAP2* superalignment contains all insertions from both alleles and served only for positional and regional purposes and represents no actual existing sequence (Appendix A2).

2.2.2.2 *SAP2* expression analysis

The presence of an HA-tagged Sap2 variant in the supernatant was analyzed by Western immunoblotting with an HA-specific antibody. This approach enabled the determination of the expression of the mature Sap2-HA protein in the supernatant.

All promoter constructs, controlling expression of tagged Sap2-HA, were integrated into *ACT1*-locus of the wild type strain SC5314 therefore leaving the endogenous *SAP2* alleles intact. This approach bypassed a possible impact on growth in YCB-BSA, which might become evident when endogenous *SAP2-2* promoter sequences were deleted. Furthermore, the induction of *SAP2* expression was also done in YCB-YE-BSA where the yeast extract provided additional low-molecular weight nitrogen sources and *SAP2* induction occurred more rapidly.

Each promoter construct was two times independently integrated into the wild type SC5314, resulting in two identical strains, termed A and B.

2.2.2.3 *SAP2-2* is induced earlier and better than *SAP2-1*

Both *SAP2* promoter alleles were analyzed for Sap2-HA expression under inducing conditions in YCB-YE-BSA. For this purpose Sap2-HA expression was controlled by either the full length 4.3 kb *SAP2-1* (in strains SCSAP2H5 A/B) or by the full length 4.3 kb *SAP2-1* promoter (in strains SCSAP2H3 A/B). Additionally Sap2-HA expression without any predicted Stp1-binding site was tested. Here, expression was controlled by a shorter, 2.0 kb, promoter region of both *SAP2* alleles (in strains SCSAP2H6 A/B and SCSAP2H4 A/B). As control Sap2-HA expression was compared to the levels from both full length 4.3 kb promoters, but in the endogenous *SAP2* locus (in strains SCSAP2H1 A, expressing Sap2-HA from the full *SAP2-1* promoter and SCSAP2H1 B, expressing Sap2-HA from the full *SAP2-2* promoter). For detailed cassette (pSAP2H3 – pSAP2H6) and strain constructions please see the following two sections (Table 2.3 and Table 2.4). Induction of Sap2-HA was determined during the first 5, 6, and 7 hours of growth in YCB-YE-BSA (Figure 2.10).

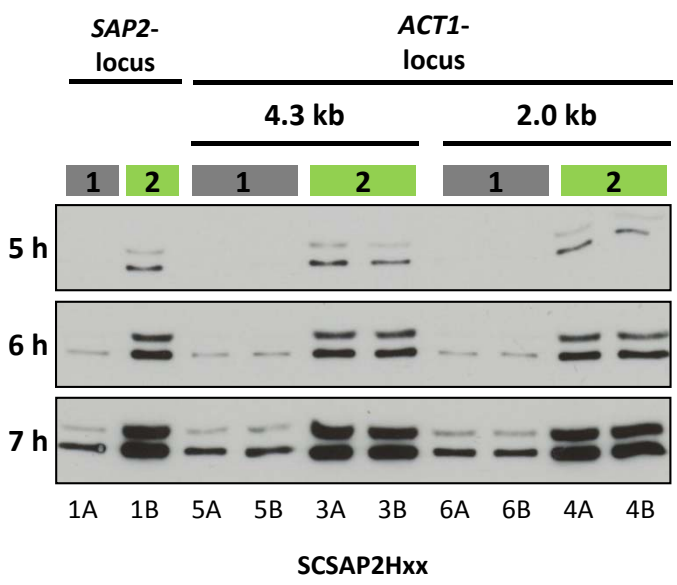

Figure 2.10: Different temporal Sap2-HA expression from both *SAP2* alleles. Presence of secreted Sap2-HA in the supernatant of cultures grown in inducing YCB-YE-BSA medium was determined. Sap2-HA expressed in the endogenous *SAP2*-locus or in the *ACT1* locus from both *SAP2* alleles (gray bar = *SAP2-1* and green bar = *SAP2-2*). Additionally, in the *ACT1* locus expression was controlled from two different promoter lengths (full 4.3 kb and 2.0 kb). Following strains were used: SCSAP2H1A/B, SCSAP2H3 A/B, SCSAP2H4 A/B, SCSAP2H5 A/B, SCSAP2H6 A/B with respective abbreviations at the bottom. YPD-overnight cultures were 1x washed with water and inoculated with a starting OD_{600}=0.2 into fresh YCB-YE-BSA medium and grown at 30°C. Sap2-HA expression from each culture at indicated time points was determined by Western immunoblotting with an anti-HA antibody.

First, no difference in Sap2-HA induction and expression was observed when comparing expression from the *ACT1*-locus on chromosome 1 with the endogenous *SAP2* locus on chromosome R (Figure 2.10; compare 1A with 5A/5B and 1B with 3A/3B). This confidently showed that the chromosomal location had no detectable influence on Sap2-HA expression. The size of the bottom band corresponds to the size of the predicted Sap2-HA variant Sap2-HA of approx. 46 kDa. However, the reason for the appearance of two bands is unknown, but might be explained by incomplete processing of tagged Sap2-HA.

Clear differences in Sap2-HA expression levels were prominent between both *SAP2* alleles during all tested time points. After 5 hours induction in YCB-YE-BSA only Sap2-HA expressed from the *SAP2-2* promoter was detectable in the supernatant. First after 6 hours Sap2-HA expression from the *SAP2-1* promoter was detected and the signals were weaker in comparison to the signals from *SAP2-2*. This strongly indicated an earlier and stronger induction from the *SAP2-2* promoter than from the *SAP2-1* promoter. However, these differences were only detectable at the earlier time points since BSA-induction for 24 hours resulted in very high Sap2-HA expression from both *SAP2* alleles (not shown). Surprisingly, when all identified Stp1-binding sites were absent and only 2.0 kb of each promoter controlled Sap2-HA expression no differences in induction and expression levels, compared to the full length 4.3 kb promoter, was apparent. This suggested an additional Stp1 binding site or that this particular deletion rendered *SAP2* expression Stp1-independent, presumably by an

additional transcriptional activator which binds to the 2.0 kb promoter (see next sections and discussion).

2.2.2.4 Construction of deleted *SAP2-1* promoters

For re-assessing the *SAP2-1* promoter deletion study the respective promoter constructs from the *ecaFLP* reporter study (Lermann, 2008) were re-used and adapted to control Sap2-HA expression. This resulted in a new set of plasmids, which harbored the identical internal *SAP2-1* promoter deletions tested by U. Lermann (Table 2.3). In addition, three new short promoter constructs were generated containing the proximal 1.0 kb, 0.8 kb, and 0.6 kb of *SAP2-1* promoter sequences. These short promoter fragments were amplified using pSAP2KS5 as template, and inserted into the vector according to the cloning strategy in Table 2.3.

Table 2.3: Plasmids and *C. albicans* strains containing Sap2-HA controlled by different *SAP2-1* promoters. Deleted regions, inserts and vectors used for the plasmid construction as well as resulting *C. albicans* mutants are listed.

Plasmid name	primer pair	inserts	vector	deleted region	*C. albicans* strains
pSAP2H5	-	ApaI-KpnI digested pSAP2KS5 and KpnI-PstI digested pSAP2H1	ApaI-PstI digested pGFP73	-	SCSAP2H5 A/B
pSAP2H6	-	ApaI-KpnI digested pSAP2H2 and KpnI-PstI digested pSAP2H1	ApaI-PstI digested pGFP73	-4.3 kb to -2.0 kb (-4334 to -2037)	SCSAP2H6 A/B
pSAP2H9	SAP2P29 / ACT38	ApaI-KpnI digested PCR-product and KpnI-PstI digested pSAP2H1	ApaI-PstI digested pGFP73	-4.3 kb to -1.0 kb (-4334 to -1034)	SCSAP2H9 A/B
pSAP2H10	SAP2P30 / ACT38	ApaI-KpnI digested PCR-product and KpnI-PstI digested pSAP2H1	ApaI-PstI digested pGFP73	-4.3 kb to -0.8 kb (-4334 to -759)	SCSAP2H10 A/B
pSAP2H12	SAP2P31 / ACT38	ApaI-HindIII digested PCR-product	ApaI-HindIII digested pSAP2H10	-4.3 kb to -0.6 kb (-4334 to -618)	SCSAP2H12 A/B
pSAP2H13	-	ApaI-EcoRV digested pSFL223	ApaI-EcoRV digested pSAP2H6	-3.5 kb to -1.1 kb (-3556 to -1091)	SCSAP2H13 A/B
pSAP2H14	-	ApaI-EcoRV digested pSFL224B	ApaI-EcoRV digested pSAP2H6	-2.5 kb to -1.1 kb (-2566 to -1091)	SCSAP2H14 A/B
pSAP2H15	-	ApaI-EcoRV digested pSFL225	ApaI-EcoRV digested pSAP2H6	-1.8 kb to -1.1 kb (-1824 to -1091)	SCSAP2H15 A/B
pSAP2H16	-	ApaI-EcoRV digested pSFL226	ApaI-EcoRV digested pSAP2H6	-2.6 kb to -1.8 kb (-2566 to -1824)	SCSAP2H16 A/B

Plasmid name	primer pair	inserts	vector	deleted region	*C. albicans* strains
pSAP2H17	-	ApaI-EcoRV digested pSFL227	ApaI-EcoRV digested pSAP2H6	-2.2 kb to -1.8 kb (-2186 to -1824)	SCSAP2H17 A/B
pSAP2H18	-	ApaI-EcoRV digested pSFL228	ApaI-EcoRV digested pSAP2H6	-2.6 kb to -2.2 kb (-2566 to -2186)	SCSAP2H18 A/B

The KpnI-SacI fragment from each individual plasmid was used to transform two times independently the wild type strain SC5314. The resulting mutants were designated according to the introduced cassette (Table 2.3). Correct integration into the *ACT1* locus was verified via Southern hybridization of BglII-digested genomic DNA with *ACT1*-specific probes (Figure 2.11). With the 3'*ACT1* probe each correctly integrated cassette created a unique fragment, depending on the respective promoter deletion and whether the BglII-sites in the *SAP2-1* promoter were retained or not. Note that *SAP2-1* has a BglII-site at position -2439 upstream of the ATG^{start} which is not present in *SAP2-2*. A schematic overview of the cassette integration and respective Southern blots, summarizing all constructed *SAP2-1* promoter reporter strains, are shown in Figure 2.11.

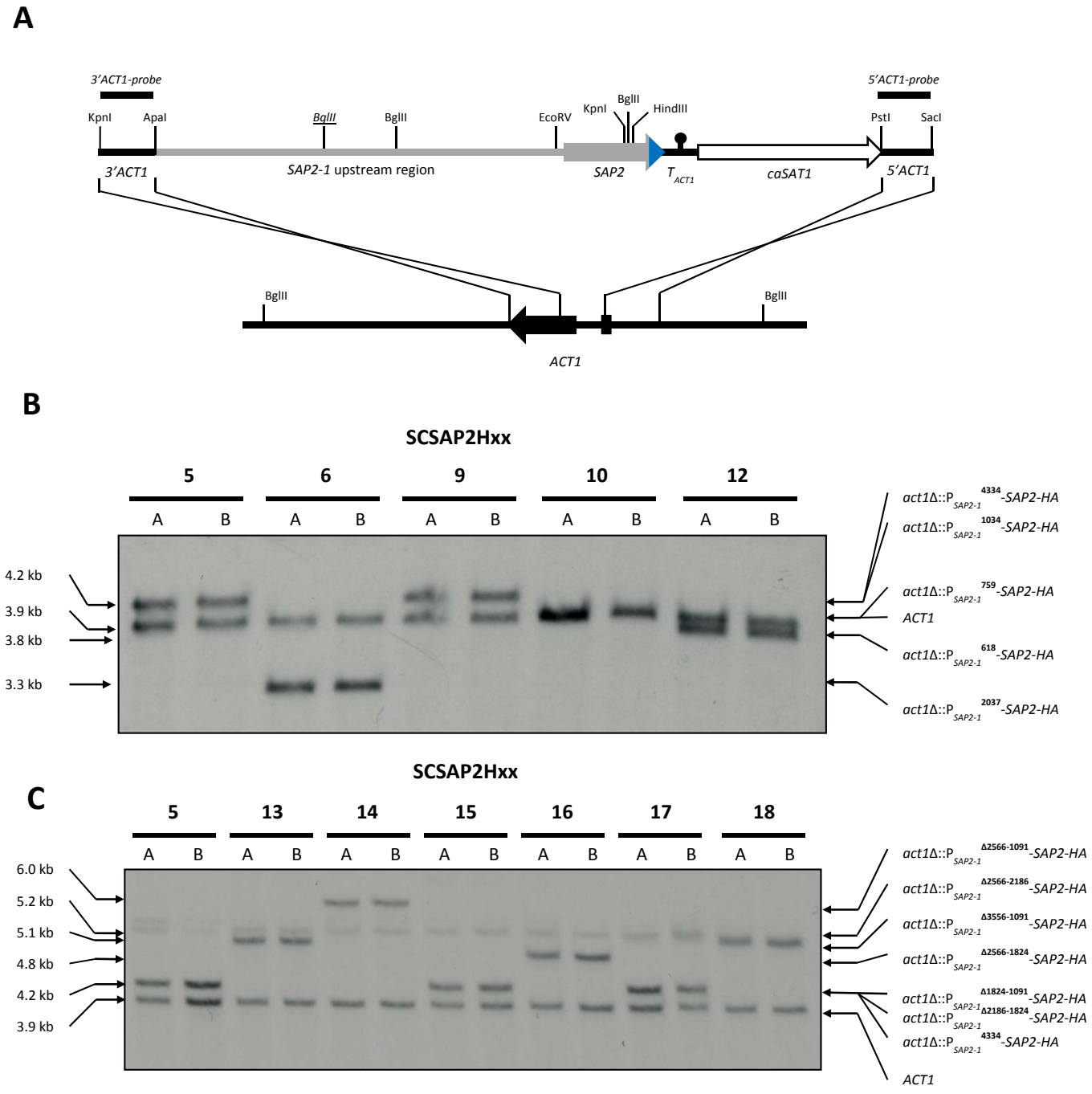

Figure 2.11: Integration of the different *SAP2-1* promoter constructs into the *ACT1* locus of the wild type SC5314. (A) Schematic drawing illustrating the integration of the KpnI-SacI fragment exemplarily for pSAP2H5, harboring the complete *SAP2-1* promoter sequence. *SAP2-1* sequences are colored in gray and *ACT1* sequences in black. The filled arrow depicts the *SAP2* gene, the blue triangle the HA-tag and the unfilled arrow the ca*SAT1* selection marker. The black bar and circle symbolizes the transcription termination sequence of *ACT1* (T_{ACT1}). Relevant restriction sites are indicated with the BglII-site only present in *SAP2-1* underlined and in italics. The lines indicate homologous regions where a cross-over can occur while integrating the cassette. (B and C) Analysis of BglII-digested genomic DNA from two independently constructed *SAP2*-HA reporter strains (SCSAP2Hxx) with the 3'*ACT1*-specific probe. The numbers at the top abbreviate the *SAP2*-HA reporter strains listed in Table 2.3. Identities and size of the hybridizing fragments are indicated in each case.

2.2.2.5 Construction deleted *SAP2-2* promoters

For the first time the *SAP2-2* allele was subjected to a detailed promoter analysis and therefore deleted promoter constructs were generated in a similar fashion as for *SAP2-1,* previously. Due to the cloning strategy (usage of the KpnI site at position +830) all *SAP2-2* ORFs contained Thymidine at position +1179, a nucleotide otherwise only present in *SAP2-1*. Since this exchange is silent, resulting in no amino acid sequence alteration, it consequently did not affect the mature protein. As template for PCR amplification served the *SAP2-2* sequence containing pSAP2KS4. Respective plasmids harboring differential shortened *SAP2-2* promoters are listed in Table 2.4. For the generation of the set of internal deleted *SAP2-2* promoters the cloning strategy from the *ecaFLP* reporter study (Lermann, 2008) was largely adopted by using the identical primer pairs, but *SAP2-2* sequences from pSAP2KS4 as template. Additionally, further internal deletions were generated for certain promoter regions. A detailed description is provided in Table 2.5, but in general two amplified promoter fragments were joined together at their introduced XhoI-sites and cloned into pSAP3H3.

Table 2.4: Plasmids and *C. albicans* strains containing Sap2-HA controlled by differently shortened *SAP2-2* promoters. Deleted regions, inserts and vectors used for the plasmid construction as well as resulting *C. albicans* mutants are listed.

Plasmid name	primer pair	inserts	vector	deleted region	*Candida* strain
pSAP2H3	-	ApaI-KpnI digested pSAP2KS4 and KpnI-PstI digested pSAP2H1	ApaI-PstI digested pGFP73	-	SCSAP2H3 A/B
pSAP2H4	-	ApaI-KpnI digested pSAP2KS3 and KpnI-PstI digested pSAP2H1	ApaI-PstI digested pGFP73	-4.3 kb to -2.0 kb (-4334 to -2037)	SCSAP2H4 A/B
pSAP2H7	SAP2P29 and ACT38	ApaI-KpnI digested PCR-product and KpnI-PstI digested pSAP2H1	ApaI-PstI digested pGFP73	-4.3 kb to -1.0 kb (-4334 to -1034)	SCSAP2H7 A/B
pSAP2H8	SAP2P30 and ACT38	ApaI-KpnI digested PCR-product and KpnI-PstI digested pSAP2H1	ApaI-PstI digested pGFP73	-4.3 kb to -0.8 kb (-4334 to -759)	SCSAP2H8 A/B
pSAP2H11	SAP2P31 and ACT38	ApaI-HindIII digested PCR-product	ApaI-HindIII digested pSAP2H10	-4.3 kb to -0.6 kb (-4334 to -618)	SCSAP2H11 A/B

Table 2.5: Plasmids and *C. albicans* strains containing Sap2-HA controlled by differently internal deleted *SAP2-2* promoters. Deleted regions, inserts and vectors used for the plasmid construction as well as resulting *C. albicans* mutants are listed.

Plasmid name	Primers for region upstream of XhoI-site	Primers for region downstream of XhoI-site	vector	deleted region	*Candida* strain
pSAP2H19	ApaI-XbaI digested pSFL224A		ApaI-XbaI digested pSAP2H3	-2.6 kb to -1.1 kb (-2566 to -1091)	SCSAP2H19 A/B
pSAP2H20	SAP2P10/SAP2P17 ApaI-XhoI digested	SAP2P14/ACT38 XhoI-BglII digested	ApaI-BglII digested pSAP2H3	-1.8 kb to -1.1 kb (-1824 to -1091)	SCSAP2H20 A/B
pSAP2H21	SAP2P10/SAP2P15 ApaI-XhoI digested	SAP2P16/SAP2P26 XhoI-XbaI digested	ApaI-XbaI digested pSAP2H3	-2.6 kb to -1.8 kb (-2566 to -1824)	SCSAP2H21 A/B
pSAP2H22	SAP2P10/SAP2P25 ApaI-XhoI digested	SAP2P16/SAP2P26 XhoI-XbaI digested	ApaI-XbaI digested pSAP2H3	-2.2 kb to -1.8 kb (-2186 to -1824)	SCSAP2H22 A/B
pSAP2H23	SAP2P33/SAP2P15 SpeI-XhoI digested	SAP2P24/SAP2P26 XhoI-XbaI digested	SpeI-XbaI digested pSAP2H3	-2.6 kb to -2.2 kb (-2566 to -2186)	SCSAP2H23 A/B
pSAP2H24	SAP2P33/SAP2P17 SpeI-XhoI digested	SAP2P36/SAP2P26 XhoI-XbaI digested	SpeI-XbaI digested pSAP2H3	-1.8 kb to -1.5 kb (-1824 to -1454)	SCSAP2H24 A/B
pSAP2H25	SAP2P33/SAP2P35 SpeI-XhoI digested	SAP2P14/ACT38 XhoI-BglII digested	SpeI-BglII digested pSAP2H3	-1.5 kb to -1.1 kb (-1454 to -1091)	SCSAP2H25 A/B
pSAP2H26	SAP2P33/SAP2P15 SpeI-XhoI digested	SAP2P38/SAP2P26 XhoI-XbaI digested	SpeI-XbaI digested pSAP2H3	-2.6 kb to -2.4 kb (-2566 to -2390)	SCSAP2H26 A/B
pSAP2H27	SAP2P33/SAP2P37 SpeI-XhoI digested	SAP2P24/SAP2P26 XhoI-XbaI digested	SpeI-XbaI digested pSAP2H3	-2.4 kb to -2.2 kb (-2390 to -2186)	SCSAP2H27 A/B

The KpnI-SacI fragments from each individual plasmid listed in Table 2.4 and Table 2.5 were used to two times independently transform the wild type strain SC5314. Correct integration into the *ACT1* locus was identically verified as for *SAP2-1* promoter reporter strains, previously. The resulting mutants were also designated according to the introduced cassette. A schematic overview of cassette integration and respective Southern blots, summarizing all constructed *SAP2-2* promoter reporter strains, are shown in Figure 2.12.

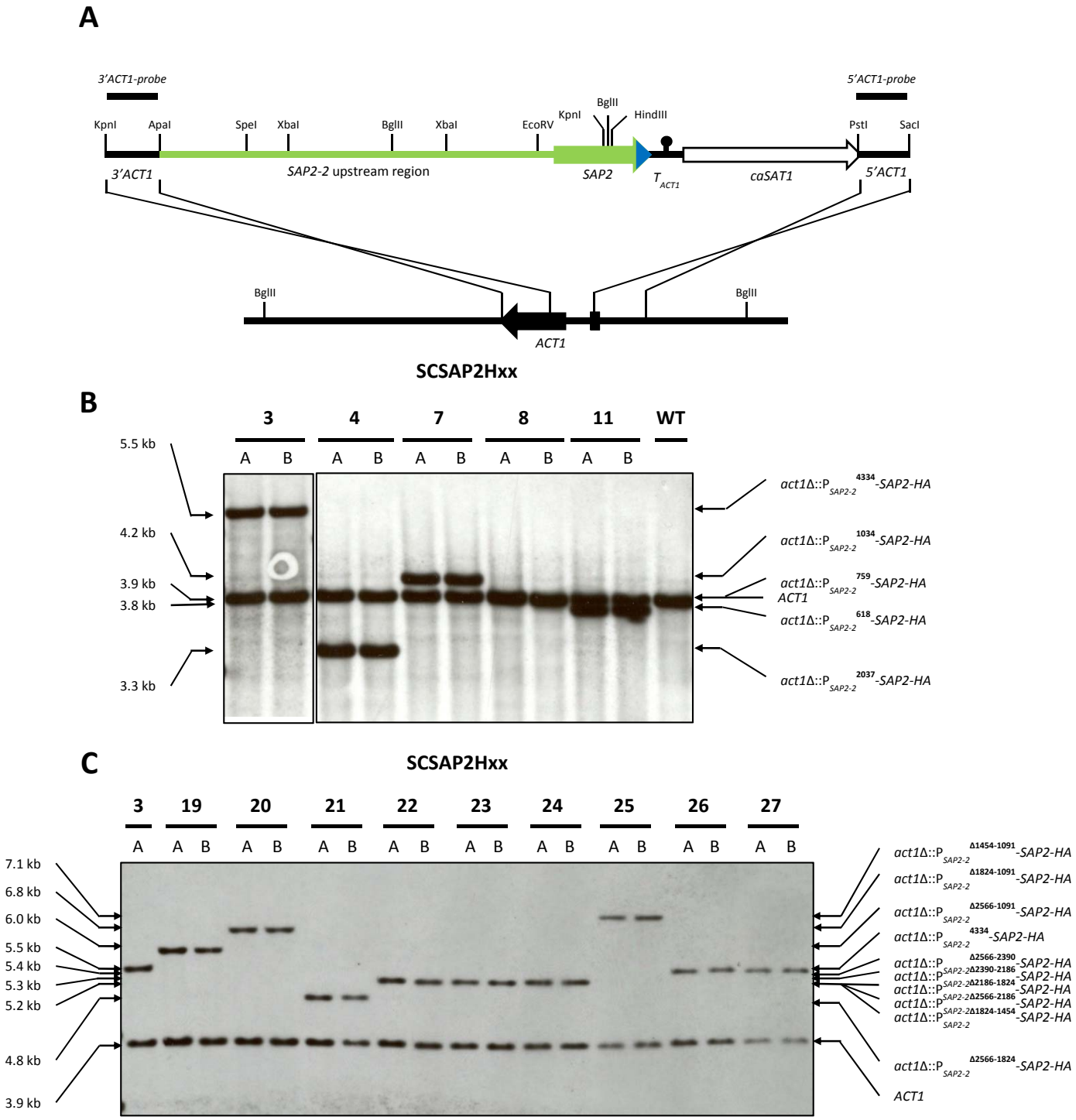

Figure 2.12: Integration of the different *SAP2-2* promoter constructs into the *ACT1* locus of the wild type SC5314. (A) Schematic drawing illustrating the integration of the KpnI-SacI fragment exemplarily for pSAP2H3, harboring the complete *SAP2-2* promoter sequences. *SAP2-2* sequences are colored in green and *ACT1* sequences in black. The filled arrow depicts the *SAP2* gene, the blue triangle the HA-tag and the unfilled arrow the ca*SAT1* selection marker. The black bar and circle symbolizes the transcription termination sequence of *ACT1* (T_{ACT1}). Relevant restriction sites are indicated. The lines indicate homologous regions where a cross-over can occur while integrating the cassette. (B and C) Analysis of BglII-digested genomic DNA from the wild type SC5314 (WT) and two independently constructed *SAP2*-HA reporter strains (SCSAP2Hxx) with the 3'*ACT1*-specific probe. The numbers at the top abbreviate the *SAP2*-HA reporter strains listed in Table 2.4 and Table 2.5. Identities and sizes of the hybridizing fragments are indicated in each case.

2.2.2.6 *SAP2* expression is controlled by distinct promoter elements

With these comprehensive sets of shortened and internal deleted promoter constructs for *SAP2-1* and *SAP2-2* the impact of different *cis*-acting regions on Sap2-HA expression was assessed. Therefore, the reporter strains were grown in Sap2 inducing medium, i.e. growth in the presence of BSA in YCB-(YE)-BSA, and the amount of secreted Sap2-HA was determined by analyzing the culture supernatant (Figure 2.13).

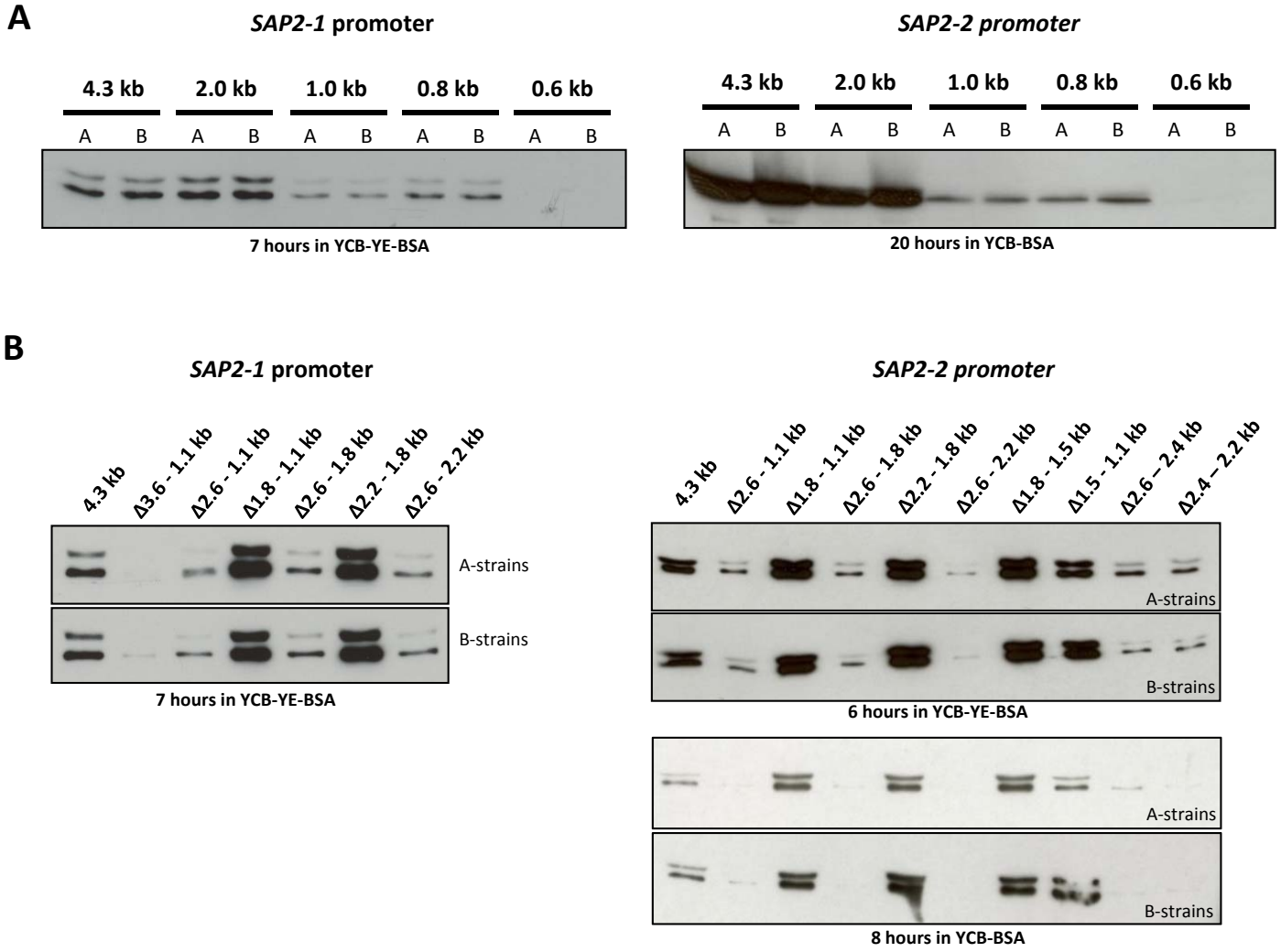

Figure 2.13: Sap2-HA expression from differentially deleted *SAP2* promoters. Strains listed in Table 2.3, Table 2.4, and Table 2.5 were used and their respective promoter length or internal deleted promoter regions are indicated. Expression of Sap2-HA was facilitated in the *ACT1* locus from differential (A) shortened or (B) internal deleted *SAP2-1* and *SAP2-2* promoters. Presence of secreted Sap2-HA in the supernatant of cultures grown in indicated media was determined. YPD-overnight cultures of each strain was washed with water and inoculated with a starting OD_{600}=0.2 into fresh YCB-(YE)-BSA medium and grown at 30°C. Sap2-expression from each culture at indicated time points was determined by SDS-PAGE and Western immunoblotting with an anti-HA antibody.

It is noteworthy that growth in YCB-YE-BSA was enhanced and Sap2-HA production occurred more rapidly than in YCB-BSA without yeast extract. Consequently longer incubation was required for *SAP2* induction in YCB-BSA medium.

All shortened *SAP2* promoter deletion reporter strains showed expression of Sap2-HA after induction by BSA with following exception: reporter strains, containing only the 0.6 kb promoter fragment of *SAP2*, did not express Sap2-HA to detectable levels (Figure 2.13 A). This indicated that first 0.6 kb of the *SAP2* promoter, which lacked the R1 repeat region, was not sufficient for *SAP2* expression. A longer *SAP2* promoter, comprising 0.8 kb or 1.0 kb of *SAP2* upstream sequences, enabled Sap2-HA expression, but not as strong as by the full length 4.3 kb promoters (Figure 2.13 A). Conclusively, the proximal 0.8 kb of the *SAP2* promoter, containing both repeats R1 and R2, was sufficient for a low *SAP2* expression and was designated low activity region LA1. However, full *SAP2* expression, as seen for the full length 4.3 kb promoter, required further distally located sequences.

Interestingly, when deleted for only 400 bp between -2.6 and -2.2 kb upstream of the *SAP2* ATG^{start}, then full Sap2-HA expression was drastically reduced in both *SAP2* alleles (see Δ2.6 – 2.2 in Figure 2.13 B). Consistently, all promoter constructs containing this region demonstrated full Sap2-HA induction. This strongly implied that this region was required for high *SAP2* expression and was therefore designated high activity region HA1. Stp1 is required to facilitate *SAP2* expression and, indeed, one of the Stp1-HA bound regions identified previously in this work (Figure 2.2 bottom) matched this region. This reasoned that Stp1 binding to the HA1 region is responsible high/full *SAP2* expression and the other two Stp1 binding events might control expression of the opposed *YHB1*. This is further supported by the previous finding that these other Stp1 binding sites alone cannot activate *SAP2* expression in the absence of the rest of the *SAP2-1* promoter (Lermann, 2008, Wyzgol, 2005).

A dissection made for the HA1 region in *SAP2-2*, i.e. Δ2.6 – 2.4 kb and Δ2.4 – 2.2 kb, could not delimit important sequences any further and both promoter constructs lost the ability to fully induce Sap2-HA expression (Figure 2.13 C). This demonstrated that only the complete HA1 region enabled high *SAP2* induction.

As observed previously (Figure 2.10), the 2.0 kb *SAP2* promoter retained full inducibility of Sap2-HA, although the Stp1-binding sites and region HA1 were absent, which suggested an alternative region that can also activate high *SAP2* expression. Evident from drastic reduction in Sap2-HA expression when only the 1.0 kb promoter controlled *SAP2* activity (Figure 2.13 A),

the sequences between -2.0 kb and -1.0 kb were designated high activity region HA2. Consistently, when both regions HA1 and HA2 were absent, like in the deleted promoter constructs Δ3.6 kb - 1.1 kb and Δ2.6 kb - 1.1 kb, the *SAP2* promoter was not highly inducible (Figure 2.13 B).

However, HA2 region was alone unable to induce high *SAP2* expression when in addition more distally located *SAP2* promoter sequences were present (e.g. Δ2.6 – 2.2 kb in Figure 2.13 B). This hinted that distal *SAP2* promoter sequences between -4.3 kb and -2.6 kb somehow inhibited full transcription from the HA2 region and were therefore designated inhibitory region IR1. Furthermore, the HA2 region can be almost completely deleted without affecting full *SAP2* inducibility, as long as region HA1 was present, like in Δ1.8 kb - 1.1 kb (Figure 2.13 B). One might argue that Sap2-HA expression from some internal deleted promoters was stronger than from the full length promoter, notably in strains carrying deletions between -2.2kb and -1.1 kb (Figure 2.13 B). However, quantification of Sap2-HA expression with an alternative detection method, an ELISA assay, refuted this observation, at least for the *SAP2-2* promoter (Figure 2.14).

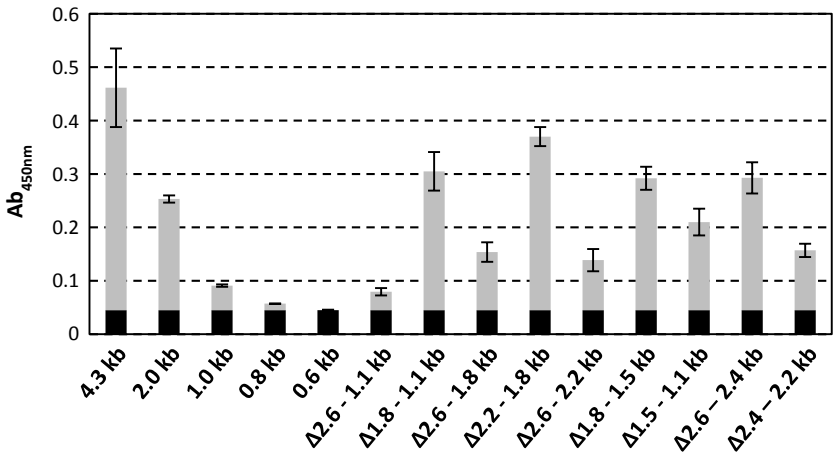

Figure 2.14: ELISA determination of Sap2-HA expression in the *ACT1* locus from differential shortened or internal deleted *SAP2-2* promoters. Each strain was inoculated from a 1x water washed YPD-overnight culture in fresh YCB-YE-BSA medium and grown at 30°C for 15 hours. The complete supernatant protein fraction was coated to the ELISA plate surface. Surface-coated Sap2-HA was detected using bound anti-HA-Peroxidase antibody catalyzed conversion of TMB. Absorbance values were determined at 450nm in an ELISA plate reader. Mean values and standard deviations from two technical replicates and combined values of respective A and B strains are given for each column. The black bars represent the background absorbance values from the parental wild type strains SC5314.

The independent determination of Sap2-HA expression by the ELISA overall confirmed the obtained results from the Western immunoblotting analysis (Figure 2.13). The variations for certain strains are likely to be caused by minimal differences in the experimental procedures. An overview summarizing all tested *SAP2* promoter constructs and their respective inducibility provides Figure 2.15.

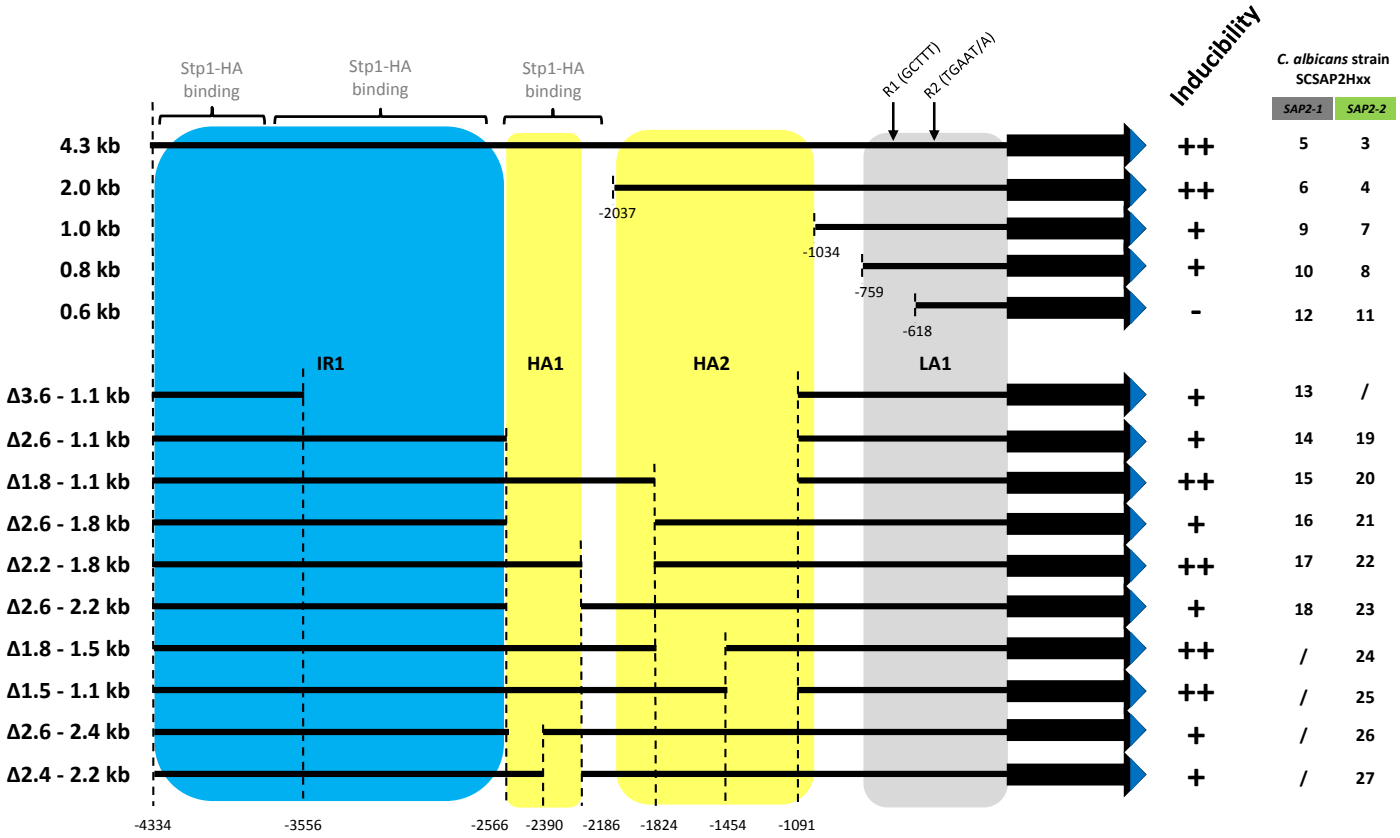

Figure 2.15: Overview and schematic illustration of all *SAP2* promoter constructs plus their determined (++) high, (+) low, or (-) uninducibility. *SAP2* sequences are colored in black and the filled arrow depicts the *SAP2* gene and the blue triangle the HA-tag. Indicated nucleotide positions of deleted regions are relative to the *SAP2* ATG^{start}. Binding regions of Stp1-HA, identified previously by ChIP-on-chip, are indicated. Characterized regulatory regions are colored as follows: low activity region LA1 (gray), high activaty regions HA1 and HA2 (yellow), and inhibitory region IR1 (blue). Strains (SCSAP2Hxx) are indicated with their respective abbreviations as bold numbers on the right side.

In sum, low *SAP2* expression requires the low activity region LA1, containing both repeats R1 and R2 and high *SAP2* transcription strongly depends on the Stp1-bound activation region LA1 between -2.6 kb and -2.2 kb upstream of the *SAP2* ATG^{start}. Additionally, an alternative activation region, termed HA2, can facilitate high *SAP2* expression without A1, but only in the absence of the inhibitory region IR1. Based on these results a model can be proposed of how Sap2 expression is regulated by its *cis*-acting sequences (Figure 2.16).

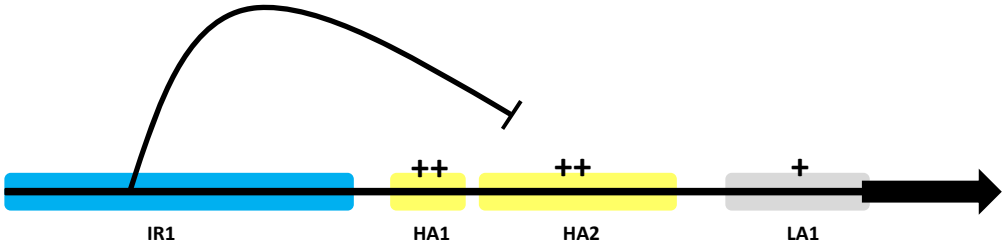

Figure 2.16: Proposed model of *SAP2* regulation by its *cis*-acting sequences. High activity regions HA1 and HA2 (yellow) are needed for (++) high *SAP2* induction. HA2 can only confer high *SAP2* induction in the absence of inhibitory region IR1 (blue). Low activity region LA1 (gray) confers (+) low induction of *SAP2* expression. Stp1 binds to HA1 in the Sap2 promoter.

Conclusively, the obtained results from the *SAP2* promoter analysis revealed different *cis*-acting regions that influence *SAP2* expression. Moreover, all tested *SAP2-2* promoter constructs retained their better and stronger inducibility in comparison to the *SAP2-1* promoter constructs. However, all constructs still contained the LA1 region, comprising both tandem repeats R1 and R2, which were demonstrated to cause the distinct allelic activation of *SAP2* (Staib *et al.*, 2002a). Thus, the identified distally located *cis*-acting regions equally influence S*AP2* allele expression, but based on the differential inducibility of both *SAP2* alleles, that relies on LA1 or the tandem repeats R1 and R2.

2.2.2.7 *SAP2* expression is induced independent of Stp1

The previous results strongly suggest Stp1-independent induction of *SAP2* expression. To test whether *SAP2* can still be expressed without Stp1 its expression was determined in a *stp1*Δ/Δ background. For this purpose the full 4.3 kb as well as the 2.0 kb promoter constructs of *SAP2-1* and *SAP2-2*, respectively, were integrated into SCSTP1M4A A/B resulting in strains SCΔ*stp1*SAP2H3 A/B, SCΔ*stp1*SAP2H4 A/B, SCΔ*stp1*SAP2H5 A/B, and SCΔ*stp1*SAP2H6 A/B. Strain construction and verification was done like previously. Due to impaired growth of the *stp1*Δ/Δ mutant in YCB-BSA, Stp1-indepented Sap2 induction was tested in YCB-YE-BSA, which contains additional low-molecular weight nitrogen sources (Figure 2.17).

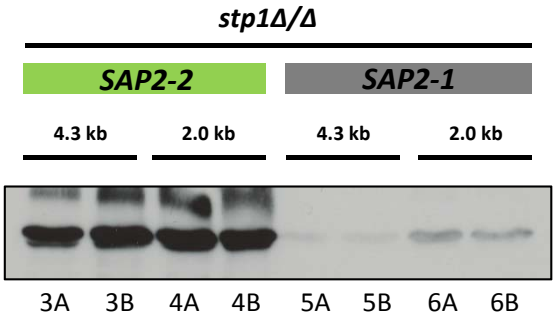

Figure 2.17: Stp1-independent Sap2-HA expression. Presence of secreted Sap2-HA in the supernatant of cultures grown in inducing YCB-YE-BSA medium was determined. Sap2-HA expressed from both *SAP2* alleles (gray bar = *SAP2-1* and green bar = *SAP2-2*) in the *ACT1* locus. Additionally, expression was controlled from two different promoter lengths (full 4.3 kb and 2.0 kb). Following strains were used: SCΔ*stp1*SAP2H3 A/B, SCΔ*stp1*SAP2H4 A/B, SCΔ*stp1*SAP2H5 A/B, and SCΔ*stp1*SAP2H6 A/B with respective abbreviations at the bottom. YPD-overnight cultures were 1x washed with water and inoculated with a starting OD_{600}=0.2 into fresh YCB-YE-BSA medium and grown at 30°C for 24 hours. Sap2-HA expression from each culture was determined by Western immunoblotting with an anti-HA antibody.

This result clearly showed that Sap2-HA expression was induced during prolonged growth in YCB-YE-BSA in a Stp1-independent manner, although extremely reduced in comparison to that in a wild type background (not shown). Similar to *SAP2* expression in the wild-type background no difference between the full 4.3 kb and 2.0 promoter was apparent in the *stp1*Δ/Δ background, likewise was the Sap2-HA expression markedly lower when controlled by *SAP2-1* sequences in comparison to SAP2-2.

Conclusively, a low *SAP2* expression was shown to be independent of Stp1, at least during growth in YCB-YE-BSA.

2.3 Transporter-mediated peptide uptake

The acquisition of proteins as source of cellular nitrogen requires uptake through specialized transporters of degradation products, which are produced by extracellular proteolysis. Two main transport systems, represented by the oligopeptide transporters (Opt1 – Opt8) and di-/tripeptide transporters (Ptr2 and Ptr22) serve as uptake system for the enormous variety of di-, tri-, and oligopeptides in *C. albicans.* Deletion mutants for multiple *opt* transporter genes are defective in the utilization of protein as nitrogen source, similar to deletion mutants which are defective for extracellular proteolysis, i.e. *sap2*Δ/Δ null mutants (Reuss & Morschhäuser, 2006).

Interestingly, the residual growth of the quintuple *opt1*Δ/Δ *opt2*Δ/Δ *opt3*Δ/Δ *opt4*Δ/Δ *opt5*Δ/Δ mutants was still somewhat better than that of *sap2*Δ/Δ mutants, suggesting less efficient amino acid or oligopeptide uptake by the retained Opt6 to Opt8 or by the di-/tripeptide transporters Ptr2 and Ptr22 (Reuss & Morschhäuser, 2006). However, the PTR system in *C. albicans* was dispensable for efficient oligopeptide uptake, evident from wild-type like growth of *ptr2*Δ/Δ *ptr22*Δ/Δ double deletion mutants in YCB-BSA (Hertlein, 2008). Unexpectedly, when the defined dipeptide RK or the tripeptide LWL served as sole nitrogen source the quintuple *opt1*Δ/Δ *opt2*Δ/Δ *opt3*Δ/Δ *opt4*Δ/Δ *opt5*Δ/Δ mutants were delayed in growth as compared to the wild type SC5314. This suggested a substantial contribution of one or more of the oligopeptide transporters in di-/tripeptide uptake (Hertlein, 2008). Consequently, impaired growth was only observed when in addition to the five *OPT* genes (*OPT1* to *OPT5*) both *PTR* genes (*PTR2* and *PTR22*) were deleted (Hertlein, 2008). Thus, the *opt1*Δ/Δ *opt2*Δ/Δ *opt3*Δ/Δ *opt4*Δ/Δ *opt5*Δ/Δ *ptr2*Δ/Δ *ptr22*Δ/Δ septuple mutants were impaired in peptide uptake.

To address whether indeed the *OPT* system can take up di- and tripeptides the contribution of individual transporters for their ability to support growth on distinct peptides was tested. For this purpose the individual transporters were constitutively expressed in the *opt1*Δ/Δ *opt2*Δ/Δ *opt3*Δ/Δ *opt4*Δ/Δ *opt5*Δ/Δ *ptr2*Δ/Δ *ptr22*Δ/Δ septuple mutant (OPT12345PTR222M4 A/B) background. Therefore, one copy of each individual transporter gene was reintegrated under the control of the strong and constitutively active *ADH1* promoter into the septuple mutants. For the seven transporters (Opt1 to Opt5 plus Ptr2 and Ptr22) respective mutant strains were generated, where each individual transporter then represented the only and

additionally overexpressed transporter. Each mutant strain was generated two times independently and denoted A and B.

2.3.1 Growth on amino acids as sole nitrogen source

During degradation of proteinaceous matter, like BSA, the small quantity of produced amino acids was not sufficient to support growth of the *opt1*Δ/Δ *opt2*Δ/Δ *opt3*Δ/Δ *opt4*Δ/Δ *opt5*Δ/Δ quintuple mutant (OPT12345MA A/B) as well as the *opt1*Δ/Δ *opt2*Δ/Δ *opt3*Δ/Δ *opt4*Δ/Δ *opt5*Δ/Δ *ptr2*Δ/Δ *ptr22*Δ/Δ septuple mutants (OPT12345PTR222M4 A/B) (Hertlein, 2008, Reuss & Morschhäuser, 2006). To test whether these strains may have generally lost the ability to utilize amino acids the growth on 20 standard L-amino acids as well as ornithine as sole nitrogen source was tested (Figure 2.18).

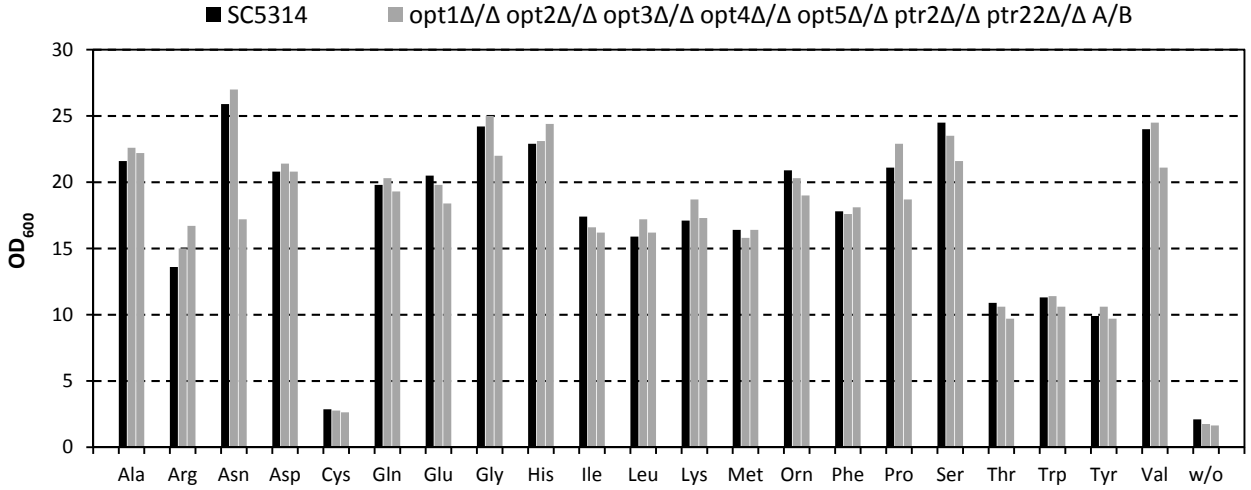

Figure 2.18: Growth on amino acids as sole nitrogen source. The wild type strain SC5314 (WT) and two independently constructed *opt1*Δ/Δ *opt2*Δ/Δ *opt3*Δ/Δ *opt4*Δ/Δ *opt5*Δ/Δ *ptr2*Δ/Δ *ptr22*Δ/Δ septuple mutants (OPT12345PTR222M4 A/B) were inoculated 1:100, after two water washes, from an YPD-overnight culture into fresh YCB-media supplement with 10 mM of the indicated amino acid. Cultures were grown c at 30°C for 24 hours and growth was determined by measuring the optical density (OD_{600}). Growth without any supplemented amino acid (w/o) was included as control.

All amino acids supported growth with a 10 mM concentration similarly in the wild type strain SC5314 as well as both septuple mutants (Figure 2.18). This demonstrates that lack of the peptide transporters Opt1 to Opt5 and Ptr2 and Ptr22 did not alter uptake and utilization of amino acids.

2.3.2 Contribution of different transporters to the growth with BSA as sole nitrogen source

To investigate the contribution of Opt1 to Opt5, Ptr2, and Ptr22 to the growth on BSA as sole nitrogen source the set of *C. albicans* mutants with the overexpressed transporter genes was analyzed (Figure 2.19). It is of note that forced overexpression from the *ADH1* promoter overcomes an unequal induction or various expression levels of individual transporters genes, albeit differential mRNA stability cannot be ruled out. Hence, growth were likely to be dependent on distinct substrate specificities and uptake efficiencies.

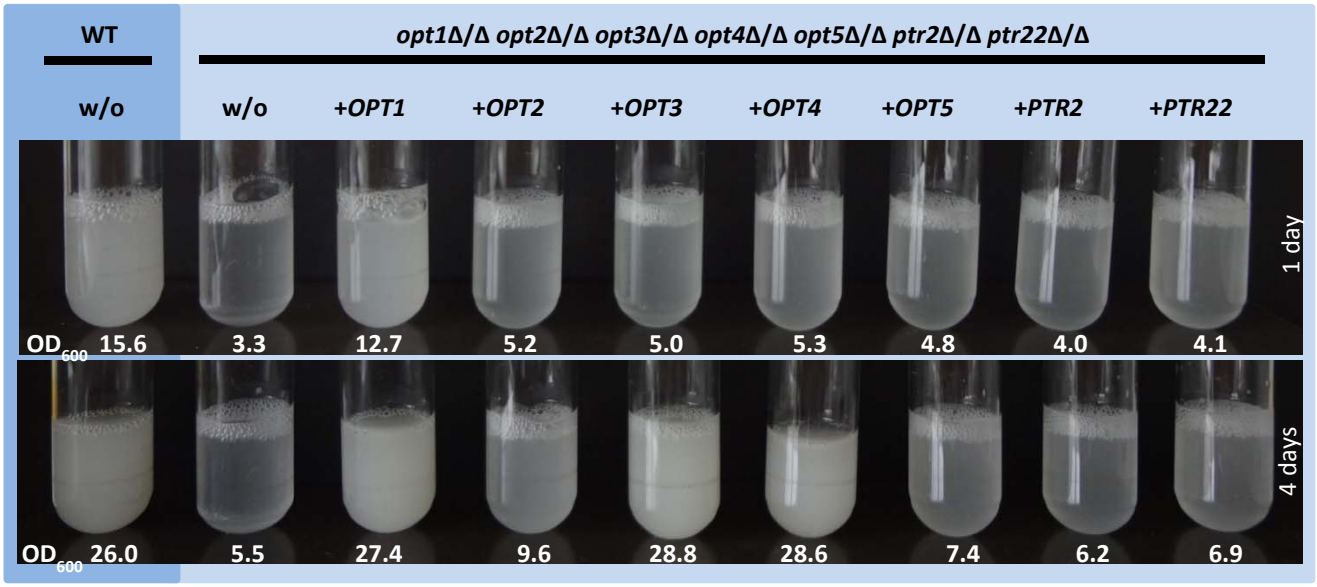

Figure 2.19: Growth on BSA as sole nitrogen source. Differential growth in YCB-BSA of the wild type SC5314 (WT) and the *opt1*Δ/Δ *opt2*Δ/Δ *opt3*Δ/Δ *opt4*Δ/Δ *opt5*Δ/Δ *ptr2*Δ/Δ *ptr22*Δ/Δ septuple mutant (w/o) plus their derivatives, which constitutively express individual peptide transporters from the *ADH1* promoter. Following mutant strains were used: septuple mutant (OPT12345PTR222M4A); septuple mutant expressing *OPT1* (OPT12345PTR222MOE1A); septuple mutant expressing *OPT2* (OPT12345PTR222MOE2A); septuple mutant expressing *OPT3* (OPT12345PTR222MOE3A); septuple mutant expressing *OPT4* (OPT12345PTR222MOE4A); septuple mutant expressing *OPT5* (OPT12345PTR222MOE5A); septuple mutant expressing *PTR2* (OPT12345PTR222MPE2A); septuple mutant expressing *PTR22* (OPT12345PTR222MPE22A). Strains were inoculated 1:100 from an YPD-overnight culture into fresh YCB-BSA media and grown constantly shaking at 30°C for several days. Growth was determined by measuring the optical densities (OD_{600}) and additionally photographing the cultures after 1 and 4 days of incubation. Note: Only the results from the A-strain series are shown and similar results were obtained with the independently constructed B-strain series. Additionally, independent repeat experiments demonstrated similar results.

While the wild type SC5314 efficiently grew, the *opt1*Δ/Δ *opt2*Δ/Δ *opt3*Δ/Δ *opt4*Δ/Δ *opt5*Δ/Δ *ptr2*Δ/Δ *ptr22*Δ/Δ septuple mutants failed to grow, with BSA as sole nitrogen source (Figure 2.19) even after prolonged incubation for 7 days (data not shown). Overexpression of individual oligopeptide transporter genes complemented the growth defect, albeit to various extents. E.g. overexpression of Opt1 restored robust growth already after 1 day, while overexpression of *OPT3* and *OPT4* only supported growth after 4 days (Figure 2.19). Opt2 conferred robust growth only after 7 days of incubation (data not shown), whereas *OPT5*

overexpression did not support robust growth at any analyzed time point. Conclusively, the oligopeptide transporters supported growth to various extents, implying different substrate specificities and uptake efficiencies. However, forced expression of either Ptr2 or Ptr22 did not rescue the growth defect, thereby validating that di-/tripeptide transporters did not mediate efficient uptake of peptides derived from Sap2-mediated BSA degradation and indicating that mainly oligopeptides were produced from BSA.

2.3.3 Contribution of different transporters to the growth with defined peptides as sole nitrogen source

To investigate individual substrate specificities the contribution of Opt1 to Opt5, Ptr2, and Ptr22 to support growth on defined di- and tripeptides as sole nitrogen source was assessed. For this purpose, the set of *C. albicans* mutants, with the overexpressed transporter genes, was grown in YCB-medium supplemented with defined di- and tripeptides as sole source for cellular nitrogen (Figure 2.20 and Figure 2.21).

Figure 2.20: Growth on different defined dipeptides as sole nitrogen source. Growth in YCB-medium, supplemented with indicated dipeptides, by the wild type SC5314 (WT) and *opt1*Δ/Δ *opt2*Δ/Δ *opt3*Δ/Δ *opt4*Δ/Δ *opt5*Δ/Δ *ptr2*Δ/Δ *ptr22*Δ/Δ septuple mutants (w/o) plus their derivatives, which constitutively express individual peptide transporters from the *ADH1* promoter. Following mutant strains were used: septuple mutants (OPT12345PTR222M4A/B); septuple mutants expressing *OPT1* (OPT12345PTR222MOE1A/B); septuple mutants expressing *OPT2* (OPT12345PTR222MOE2A/B); septuple mutants expressing *OPT3* (OPT12345PTR222MOE3A/B); septuple mutants expressing *OPT4* (OPT12345PTR222MOE4A/B); septuple mutants expressing *OPT5* (OPT12345PTR222MOE5A/B); septuple mutants expressing *PTR2* (OPT12345PTR222MPE2A/B); septuple mutants expressing *PTR22* (OPT12345PTR222MPE22A/B). Strains were inoculated 1:100 from an YPD-overnight culture into fresh YCB media containing 1 mg / ml of indicated dipeptides as sole nitrogen source and grown at 30°C. Growth was determined by measuring the optical densities (OD_{600}) at indicated time points. Note: Only the results from one experiment are shown and similar results were obtained in an independent repeat experiment.

→

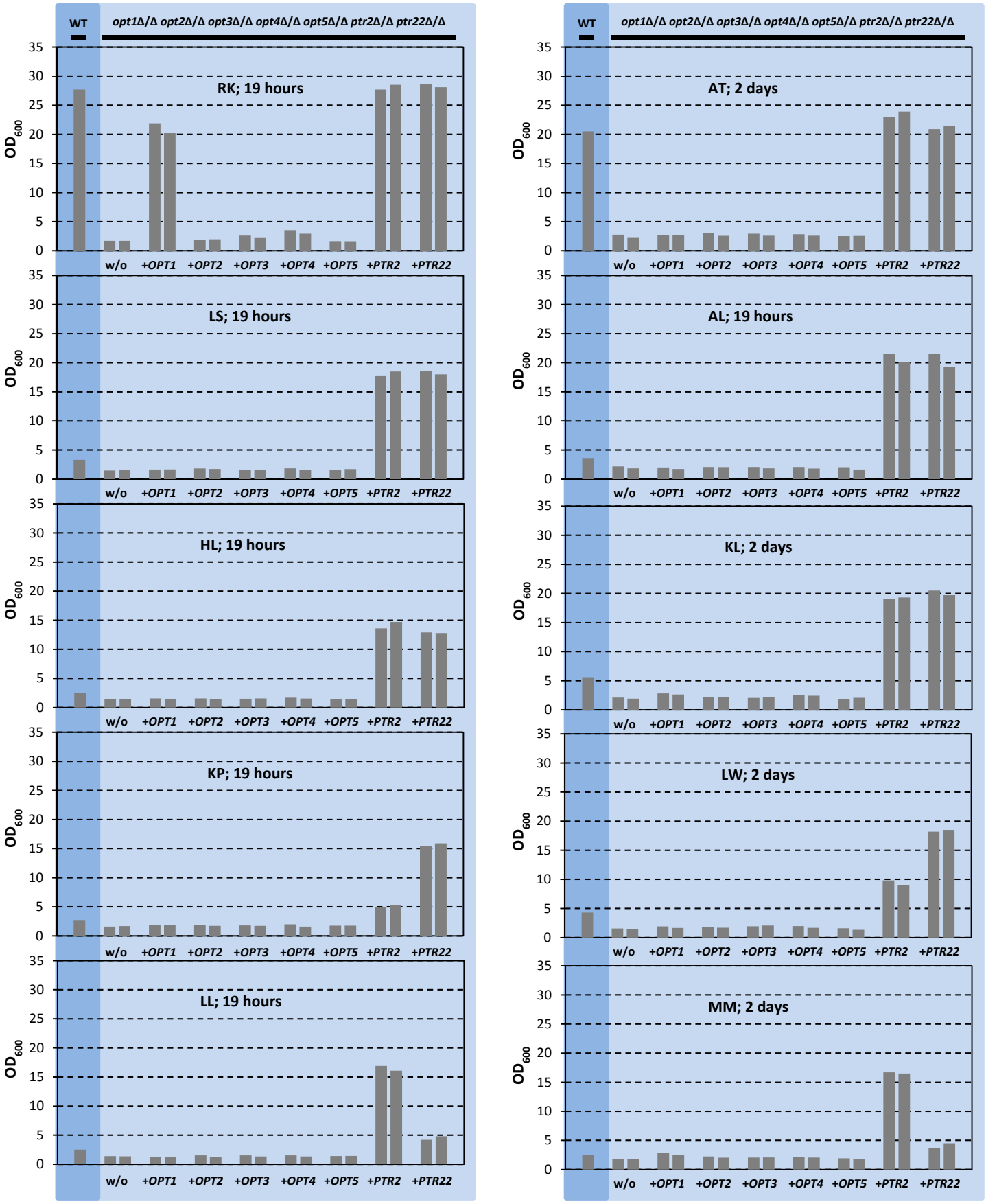
WT
opt1Δ/Δ opt2Δ/Δ opt3Δ/Δ opt4Δ/Δ opt5Δ/Δ ptr2Δ/Δ ptr22Δ/Δ
RK; 19 hours
LS; 19 hours
HL; 19 hours
KP; 19 hours
LL; 19 hours
AT; 2 days
AL; 19 hours
KL; 2 days
LW; 2 days
MM; 2 days
OD600
0
5
10
15
20
25
30
35
w/o
+OPT1
+OPT2
+OPT3
+OPT4
+OPT5
+PTR2
+PTR22

Expectably, the *opt1*Δ/Δ *opt2*Δ/Δ *opt3*Δ/Δ *opt4*Δ/Δ *opt5*Δ/Δ *ptr2*Δ/Δ *ptr22*Δ/Δ septuple mutants failed to grow on all tested defined di- and tripeptides (Figure 2.20 and Figure 2.21) and dipeptides almost exclusively supported growth in cells expressing *PTR2* and *PTR22* (Figure 2.20). Both di-/tripeptide transporters equally conferred growth on the dipeptides RK, KL, LS, HL, AT, and AL (and AI, not shown) but displayed also some different substrate preferences for certain dipeptides, like LW, LL, KP, and MM (Figure 2.20). Only forced expression of *PTR2* supported robust growth on LL and MM, while mutants overexpressing *PTR22* grew significantly better on LW and KP. Surprisingly, the oligopeptide transporter Opt1 also conferred growth, when overexpressed and the dipeptide RK (Arg-Lys) was the only source of nitrogen.

Interestingly, the wild type strain SC5314 showed impaired growth with most of the tested dipeptides as sole nitrogen source, whereas overexpression of *PTR2* or *PTR22* conferred robust growth with these dipeptides (Figure 2.20). This suggests that both di-/tripeptide transporters Ptr2 and Ptr22 were not sufficiently expressed in the wild type SC5314 under these conditions. Generally, all tested dipeptides could serve as sole source for cellular nitrogen, with KL, LW, and MM efficiently supporting growth only after longer incubation.

When the defined tripeptides LWL, AAP, and KFK served as sole nitrogen source the wild type strain SC5314 demonstrated robust growth (Figure 2.21), unlike the growth impairment on the other tested dipeptides (Figure 2.20). Cells overexpressing *PTR22* grew on all three tripeptides, but cells overexpressing *PTR2* grew only with AAP. Overexpression of *OPT1* enabled growth on all three tripeptides and besides Opt1 also Opt2, Opt3, and Opt4 conferred growth on KFK after prolonged incubation.

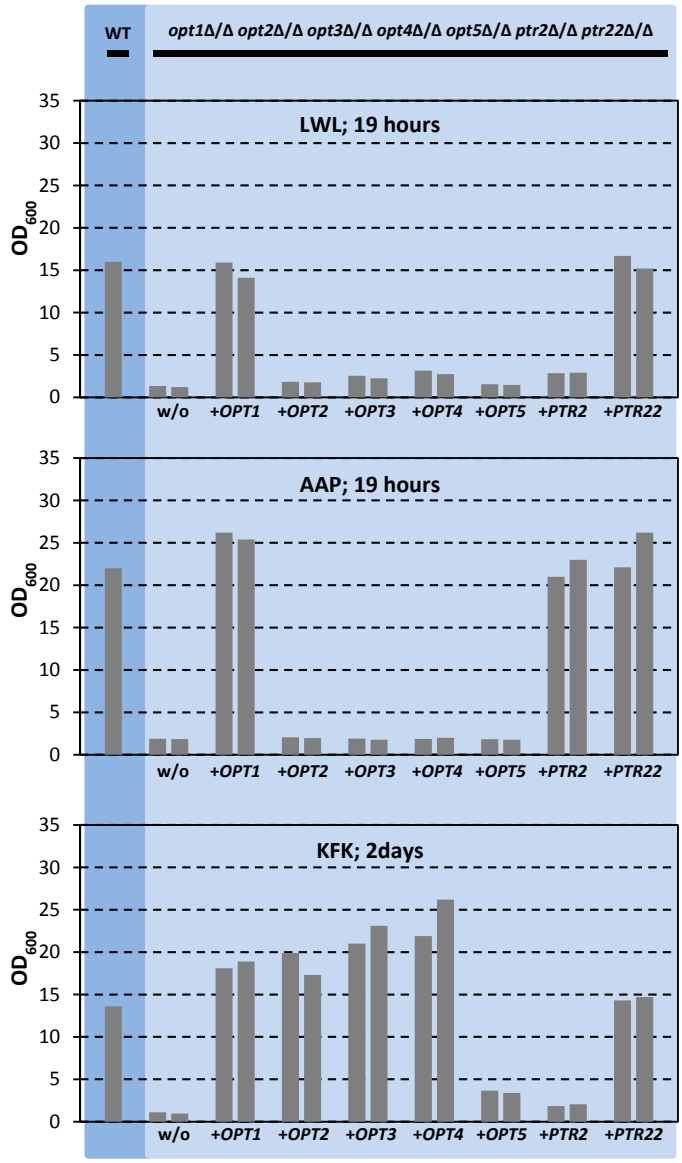

Figure 2.21: Growth on different defined tripeptides as sole nitrogen source. Growth in YCB-medium, supplemented with indicated dipeptides, by the wild type SC5314 (WT) and *opt1*Δ/Δ *opt2*Δ/Δ *opt3*Δ/Δ *opt4*Δ/Δ *opt5*Δ/Δ *ptr2*Δ/Δ *ptr22*Δ/Δ septuple mutants (w/o) plus their derivatives, which constitutively express individual peptide transporters from the *ADH1* promoter. Following mutant strains were used: septuple mutants (OPT12345PTR222M4A/B); septuple mutants expressing *OPT1* (OPT12345PTR222MOE1A/B); septuple mutants expressing *OPT2* (OPT12345PTR222MOE2A/B); septuple mutants expressing *OPT3* (OPT12345PTR222MOE3A/B); septuple mutants expressing *OPT4* (OPT12345PTR222MOE4A/B); septuple mutants expressing *OPT5* (OPT12345PTR222MOE5A/B); septuple mutants expressing *PTR2* (OPT12345PTR222MPE2A/B); septuple mutants expressing *PTR22* (OPT12345PTR222MPE22A/B). Strains were inoculated 1:100 from an YPD-overnight culture into fresh YCB media containing 1 mg / ml of indicated tripeptides as sole nitrogen source and grown at 30°C. Growth was determined by measuring the optical densities (OD_{600}) at indicated time points. Note: Only the results from one experiment are shown and similar results were obtained in an independent repeat experiment.

In summary, these results indicate that Ptr22, among both di-/tripeptide transporters, and Opt1, among the oligopeptide transporters, possessed a broader substrate spectrum. Furthermore, Opt1 appeared to be a highly versatile transporter, with an uptake capacity of peptides with various lengths (compare to (Lubkowitz *et al.*, 1997, Reuss & Morschhäuser, 2006), thus transporting oligopeptides as well as tripeptides and even a dipeptide.

2.3.4 Growth rate determination

The *opt1*Δ/Δ *opt2*Δ/Δ *opt3*Δ/Δ *opt4*Δ/Δ *opt5*Δ/Δ *ptr2*Δ/Δ *ptr22*Δ/Δ septuple mutants were exposed to massive stress during the multiple rounds of transformation that were necessary for their generation. This might have produced unintended and unspecific alteration in the genome, which was not unlikely as shown previously for the DSY459 mutant (see section 2.2.1). To exclude possible genomic changes affecting general growth of the septuple mutants the growth rate was determined in nutrient rich YPD and YNB-100mM NH_4^+ medium, which contained ammonium as sole nitrogen source. As described in material and methods both *opt1*Δ/Δ *opt2*Δ/Δ *opt3*Δ/Δ *opt4*Δ/Δ *opt5*Δ/Δ *ptr2*Δ/Δ *ptr22*Δ/Δ septuple mutants (OPT12345PTR222M4 A/B) were grown in both media and the doubling times were compared to those of the wild type strain SC5314 (Table 2.6). The doubling time of the SC5314-derivative SCADH1R1A was also determined, because this strain served as wild-type control in other experiments (see below).

Table 2.6: Doubling times of indicated strains in YPD and YNB-100mM NH_4^+. Overnight cultures in YPD or YNB-100mM NH_4^+ were diluted 1:1000 in fresh media and grown at 30°C in a 96-well microtiter plate. The measured optical densities from 10 min intervals and three independent cultures were used to calculate the mean doubling times. Statistical significance was determined with Mann-Whitney-U test and p-values <0.05 are indicated with asterisks.

Medium	Strain	Doubling time
YPD	SC5314	95.46 ±0.61 min
	SCADH1R1A	95.71 ±0.32 min
	OPT12345PTR222M4 A	95.04 ±0.07 min
	OPT12345PTR222M4 B	*97.35 ±0.44min
YNB-100mM NH_4^+	SC5314	134.51 ±1.48 min
	SCADH1R1A	131.75 ±1.11 min
	OPT12345PTR222M4 A	134.12 ±1.74 min
	OPT12345PTR222M4 B	*148.25 ±1.51min

The A-strain of the two independently constructed septuple mutants showed wild-type like doubling times in both media, whereas the B-strain differed by a significantly slower growth rate in both media (*p-values < 0.05). This suggested that during strain construction the B-strain of the *opt1*Δ/Δ *opt2*Δ/Δ *opt3*Δ/Δ *opt4*Δ/Δ *opt5*Δ/Δ *ptr2*Δ/Δ *ptr22*Δ/Δ septuple mutants (OPT12345PTR222M4 B) had acquired an unspecific general growth defect, not related to the deletion of the peptide transporter genes.

2.3.5 Impact of peptide-uptake deficiency on *in vitro* fitness

A deficiency in peptide uptake should not affect fitness under nutrient sufficient conditions, i.e. when proteins or peptides are not the sole nitrogen source. To test whether fitness was affected by the lack of seven peptide transporters an *in vitro* competitive fitness assay was performed. There, the test strain competes with the wild type, e.g. for nutrients, which allows the determination of relative fitness. So when the test strain exhibited wild type fitness then its initial proportion, within the mixture, does not change over time while competing with a wild type strain. Hence, the initial proportions remained and the ratio between the end and start point is around 1. Decreased fitness of a test strain does result in a decrease in its proportion, within the mixture, over time while competing with a wild type strain. Hence, the ratio between end and start is significantly below 1. The opposite is the case for increased fitness of a test strain. To discriminate the test strain from the wild type SC5314 in a mixed culture the RFP-labeled derivative of SC5314, denoted SCADH1R1A, was used instead of the unlabeled SC5314. Both strains, SC5314 and SCADH1R1A, share similar doubling times in nutrient rich YPD and ammonium rich YNB-100mM NH_4^+ medium (Table 2.6). The proportions of the strains within a mixed cultures were determined as described in materials and methods. To assess fitness during *in vitro* competition both *opt1*Δ/Δ *opt2*Δ/Δ *opt3*Δ/Δ *opt4*Δ/Δ *opt5*Δ/Δ *ptr2*Δ/Δ *ptr22*Δ/Δ septuple mutants were separately mixed 1:1 with the RFP-labeled SCADH1R1A and co-incubated for 24 hours in YPD and YNB-100mM NH_4^+ medium. As control also a 1:1 mixture with the wild type strain SC5314 was analyzed (Figure 2.22).

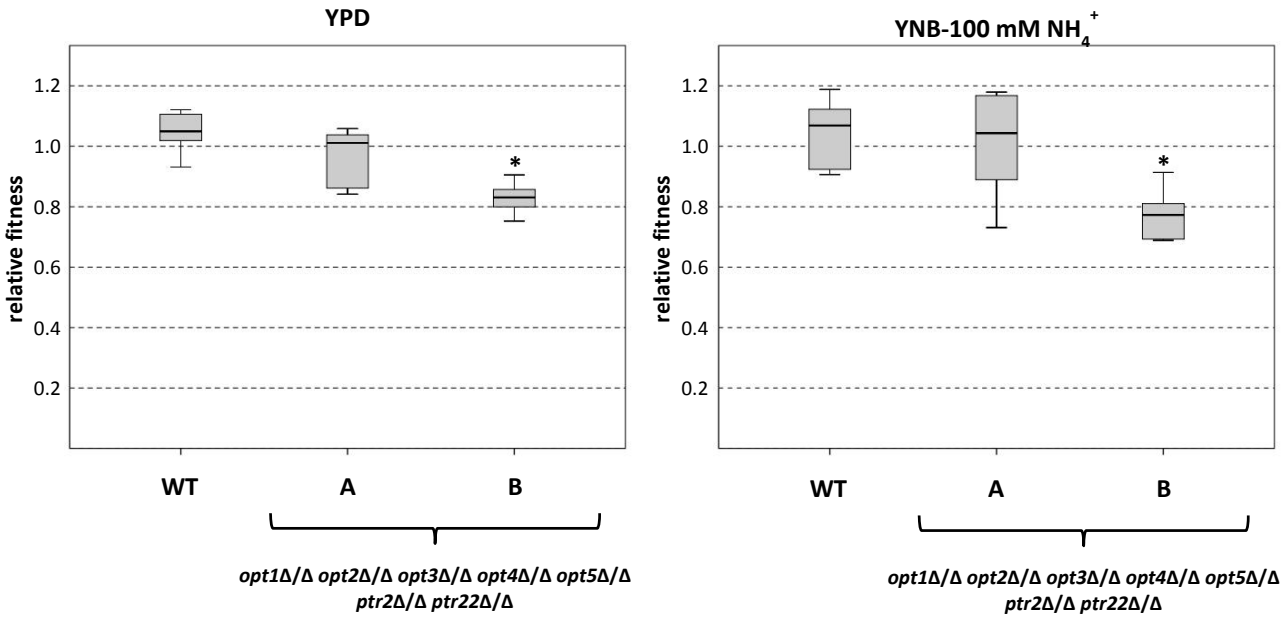

Figure 2.22: *In vitro* competitive fitness. Relative *in vitro* fitness of the wild type strain SC5314 (WT) and both *opt1*Δ/Δ *opt2*Δ/Δ *opt3*Δ/Δ *opt4*Δ/Δ *opt5*Δ/Δ *ptr2*Δ/Δ *ptr22*Δ/Δ septuple mutants A and B (OPT12345PTR222M4 A/B) in competition with the genetically labeled wild type derivative SCADH1R1A. Cells were precultured in both test media (YPD and YNB-100 mM NH_4^+), mixed in a 1:1 ratio with SCADH1R1A and inoculated with a starting OD_{600}=0.002 into fresh test medium. The ratio of the test strain in comparison to SCADH1R1A was determined at the beginning and after 24 hours of the co-incubation at 30°C. Medians (thick line), interquartile ranges (box) and standard deviations (whiskers) from six independent co-cultures for each test strain are shown. Significant differences from wild type SC5314 fitness determined with the Mann-Whitney-U test (p-value < 0.01) are marked with an asterisk.

BY comparing the ratios after 24 hours growth in both media wild-type fitness was determined for the wild type SC5314, of course, and also for the A-strain of the *opt1*Δ/Δ *opt2*Δ/Δ *opt3*Δ/Δ *opt4*Δ/Δ *opt5*Δ/Δ *ptr2*Δ/Δ *ptr22*Δ/Δ septuple mutants (Figure 2.22). Due to the general growth defect of the B-strain also a decreased *in vitro* fitness was apparent, demonstrated by significantly decreased proportions of unlabeled cells/cfus recovered after 24 hours of co-incubation (p-values < 0.05). Theses control experiments clearly showed that the B-strains had acquired a growth defect, unrelated to peptide-uptake deficiency, which significantly decreased *in vitro* fitness.

2.3.6 Impact of peptide-uptake deficiency on *in vivo* fitness

The role of the peptide- and oligopeptide-uptake capacity of *C. albicans* for an infection or the establishment within the host was not characterized so far. Proteins and their degradation products, peptides, are considered as abundant nitrogen source in the mammalian host. To investigate whether proteins or peptides are indeed an important nitrogen source for *C. albicans* during gut colonization the *in vivo* murine gut colonization model was used, which mimics the conditions present in the natural habitat of *C. albicans* in the human intestine (Ramírez-Zavala *et al.*, 2008, Sasse *et al.*, 2012, White *et al.*, 2007). Therefore, the *in vivo* competitive fitness of the peptide-uptake deficient *opt1*Δ/Δ *opt2*Δ/Δ *opt3*Δ/Δ *opt4*Δ/Δ *opt5*Δ/Δ *ptr2*Δ/Δ *ptr22*Δ/Δ septuple mutants in comparison to the wild type derivative SCADH1R1A was assessed. So if primarily proteins and peptides are utilized during gut colonization then the uptake-deficient mutants should exhibit a fitness defect when competing with SCADH1R1A for these nutrients. To assess *in vivo* fitness the same mixtures as previously for the *in vitro* fitness were tested, i.e. a 1:1 mixture of SCADH1R1A with both mutants as well as with the wild type strain SC5314. Prior to oral application of the mixtures the mice were treated with an antibiotic mix to prepare for *C. albicans* colonization and to decimate bacterial flora, which might disturb *C. albicans* colonization. It is noteworthy that the gastrointestinal tract of female BALB/c mice is naturally not colonized by *C. albicans,* but it mimics the natural habitat. During a time course of 7 days changes from the initially ratio at the beginning (inoculum) were determined for each day (Figure 2.23).

For the wild type control the ratio did not significantly change over the time course of seven days, indicating equal *in vivo* fitness of SC5314 and SCADH1R1A. The proportion of both peptide-uptake deficient *opt1*Δ/Δ *opt2*Δ/Δ *opt3*Δ/Δ *opt4*Δ/Δ *opt5*Δ/Δ *ptr2*Δ/Δ *ptr22*Δ/Δ septuple mutants also remained unchanged when competing with SCADH1R1A (Figure 2.23). One mouse (Mouse 9), infected with a mixture containing the A-strains died the day after infection and values were calculated from 4 instead of 5 mice in this case.

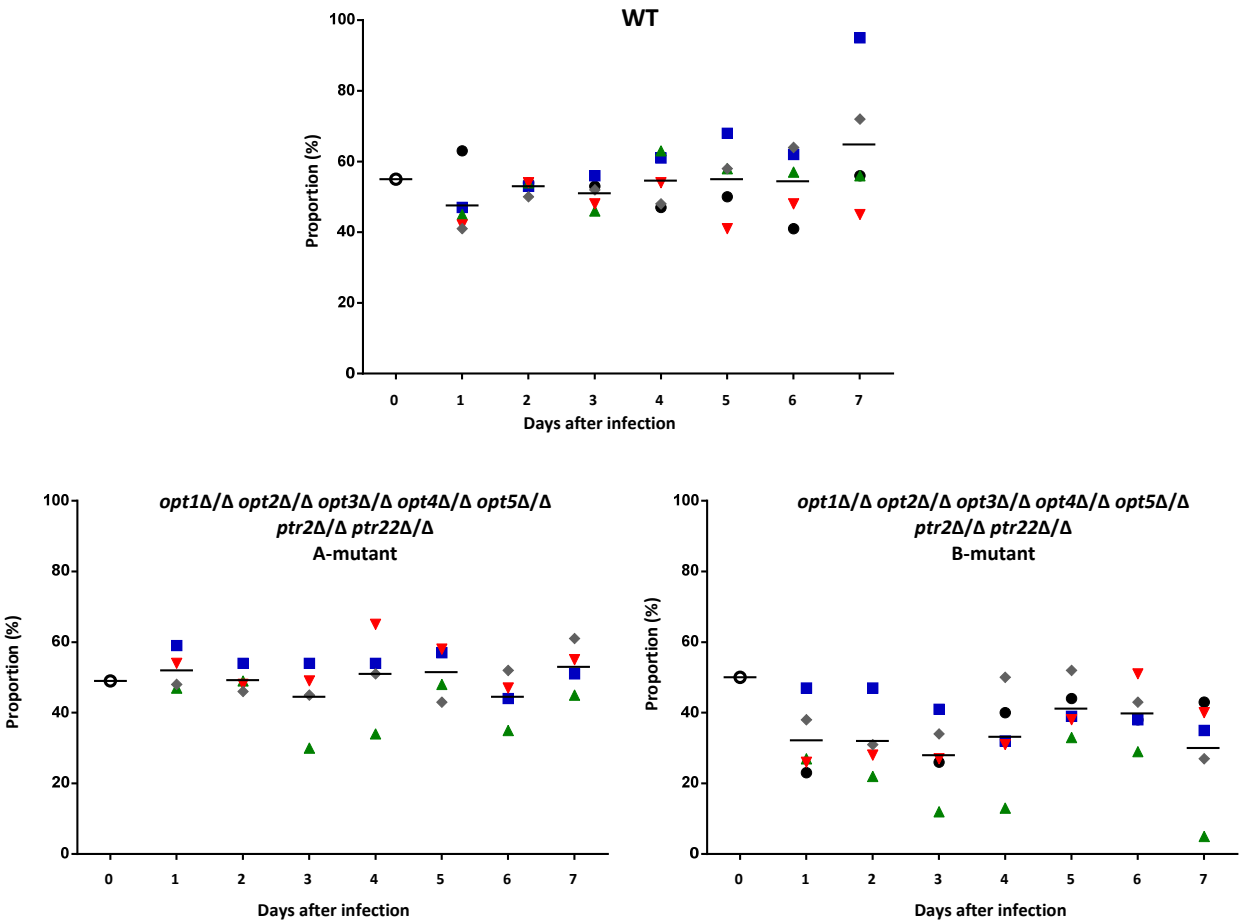

Figure 2.23: *In vivo* competitive fitness. Relative *in vivo* fitness of the wild type strain SC5314 (WT) and both *opt1*Δ/Δ *opt2*Δ/Δ *opt3*Δ/Δ *opt4*Δ/Δ *opt5*Δ/Δ *ptr2*Δ/Δ *ptr22*Δ/Δ septuple mutants A and B (OPT12345PTR222M4 A/B) in competition with the genetically labeled wild type derivative SCADH1R1A was assessed. Cells were pre-cultured in YPD medium and mixed in a 1:1 ratio with SCADH1R1A. Antibioticaly treated female BALB/c mice were orally infected with approx. $5x10^7$ cells of the respective mixtures. The ratio of the test strains in comparison to SCADH1R1A was determined before infection in the inoculum and during infection over a time course of 7 days by re-isolating cells from the feces as described in the methods section. A group of five mice was infected with each mixture and individual identities are illustrated by different colored symbols. One mice infected with the A-mutant mixture died after 1 day and was left out. Mean values for the test strain proportion within the mixture for each mice group were calculated from recovered cfus. For meaningful evaluation values derived from less than 30 recovered cfus were excluded. Statistical significance was calculated with the Friedmann test.

These results clearly demonstrated that lack of the peptide transporters Opt1 to Opt5 and Ptr2 and Ptr22 in *C. albicans* did not impact fitness in the mouse gut colonization model. It is also noteworthy that the general growth defect of the B-strain apparently did not affect the fitness in this model.

Taken together, although deficiency for the major oligopeptide transporters and both di-/tripeptide transporter impaired growth on proteins and peptides as sole nitrogen source *in vitro*, their absence had no influence on *in vivo* competitive fitness in a murine gut colonization model.

2.4 Control of the expression of virulence-associated traits by ammonium

For *C. albicans* and many other microorganisms the nitrogen source ammonium is the most favored one and it is preferentially used above all others. Availability of ammonium is one signal that drives the NCR response and thus controls filament formation and protease secretion. However, the way how the ammonium availability is sensed and actually elicits NCR is poorly understood. Sensing of ammonium availability could be achieved by direct external sensing or intracellular determination. A direct external sensing mechanism could be then excluded when uptake of ammonium into the cell is required for a NCR response. In order to discriminate between these possibilities the responses to extracellular ammonium was determined in uptake-deficient *C. albicans* mutants, where one or both of the ammonium permeases Mep1 and/or Mep2 were deleted. These two transporters represent the major uptake mechanism of free extracellular ammonium into the cell.

2.4.1 Various ammonium concentrations repress Sap2 expression to various degrees

A wide range of different external ammonium concentrations were reported to repress certain attributes and phenotypes in *C. albicans*. E.g. an external concentration of 100 mM NH_4^+ was shown to repress nitrogen starvation induced filamentation and concentrations between 10 and 30 mM were sufficient to support growth of a *mep1*Δ/Δ *mep2*Δ/Δ double mutant on agar plates (Biswas & Morschhäuser, 2005). The growth on BSA as sole nitrogen source strongly depends on the production of Sap2 enzymes. The expression from the *SAP2* promoter in inducing medium (YCB-YE-BSA) was shown to be repressed by the addition of 100 mM NH_4^+, which was consistent with the observed repression of BSA degradation by the same concentration (Dabas & Morschhäuser, 2008). However, which ammonium concentration is minimally required to fully repress BSA degradation under the experimental conditions used in the present work is unknown. In order to investigate that, Sap2 production and BSA degradation was determined by the wild type SC5314 in the presence of different external NH_4^+ concentrations (Figure 2.24).

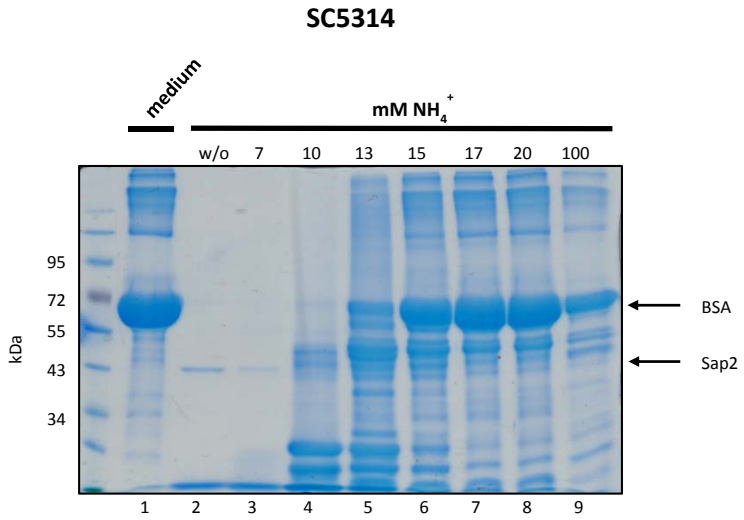

Figure 2.24: BSA-degradation and Sap2 expression with different NH_4 concentrations by the wild type SC5314. An YPD-overnight culture was inoculated 1:100 into fresh YCB-YE-BSA medium, indicated NH_4^+ concentrations were supplemented, and cultures were grown at 30°C for 24 hours. Proteins of the culture supernatants were analyzed by SDS-PAGE. Uninoculated YCB-YE-BSA medium was included as control. Lanes are numbered at the bottom and molecular sizes (kDa) of the protein marker are indicated at the left side.

After 24 hours BSA was completely degraded by the wild type SC5314 leaving no traces of degradation products in the supernatant (Figure 2.24 compare lane 1 and lane 2). Also a clearly stained band of the approx. 43 kDa Sap2 enzyme was detectable. Addition of 15 mM or higher concentrations of NH_4^+ prevented BSA degradation almost completely. Presence of 7 mM ammonium was not sufficient to repress BSA degradation although the slight less intense band of the Sap2 enzyme suggested less enzyme production (Figure 2.24 compare lanes 2 and 3). Presence of 10 or 13 mM ammonium only partially repressed BSA degradation, i.e. BSA was not degraded to full extent leaving many degradation products in the supernatant (Figure 2.24 lanes 4 and 5).

Conclusively, degradation of BSA and production of Sap2 by *C. albicans* was fully repressed by minimum 15 mM NH_4^+, but not repressed by 7 mM NH_4^+ after 24 hours of growth in YCB-YE-BSA. Intermediate BSA degradation was observed with intermediate (10 or 13 mM) NH_4^+ concentrations, indicating a gradual response to exterior NH_4^+ and not an all or none answer depending on a certain threshold.

2.4.2 Ammonium uptake is required to repress *SAP2* expression

Repression of BSA degradation and Sap2 expression strongly depend on the concentration of external applied ammonium. Whether ammonium is externally sensed or uptake was necessary to repress Sap2 expression could be simply tested in NH_4^+ uptake-deficient *C. albicans* mutants. Therefore, two independently constructed *C. albicans* mutants, lacking both *MEP* genes (*mep1*Δ/Δ *mep2*Δ/Δ double mutants SCMEP12M4 A/B) were analyzed for their Sap2 production and BSA degradation in the presence of repressing NH_4^+ concentrations in the exterior (Figure 2.25). As control the wild type SC5314 and the *mep* single deletion mutants were included.

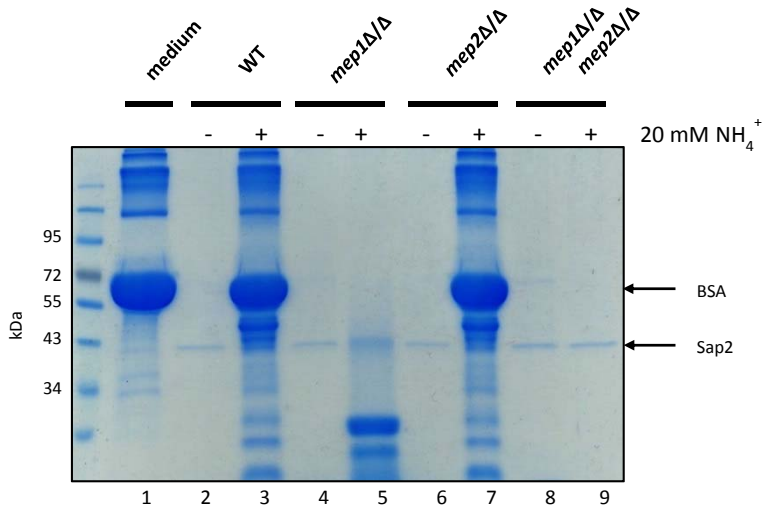

Figure 2.25: BSA-degradation and Sap2 expression by the wild type SC5314 (WT) and mutants lacking one or both *MEP* ammonium permeases. Following independently constructed mutants were used: SCMEP1M4 A/B (*mep1*Δ/Δ), SCMEP2M4 A/B (*mep2*Δ/Δ), SCMEP12M4 A/B (*mep1*Δ/Δ *mep2*Δ/Δ). Strains were inoculated 1:100 from an YPD-overnight culture into fresh YCB-YE-BSA media. As indicated, cultures were grown in the absence (-) or presence (+) of 20 mM NH_4^+ at 30°C for 24 hours. Proteins of the culture supernatants were analyzed by SDS-PAGE. Uninoculated YCB-YE-BSA medium was included as control. Note: Only the results from the A-strain series are shown and similar results were obtained with the independently constructed B-strain series. Lanes are numbered at the bottom and molecular sizes (kDa) of the protein marker are indicated at the left side.

The wild type SC5314 displayed high Sap2 production and full BSA degradation, which was completely repressed by the addition of 20 mM NH_4^+ (Figure 2.25 compare lane 2 and 3). In contrast, the mutants lacking both Mep transporters (*mep1*Δ/Δ *mep2*Δ/Δ double mutants) did not repress Sap2 expression with 20 mM NH_4^+ (Figure 2.25 lane 9), which resulted in full BSA degradation and Sap2 production. The inability of ammonium to repress Sap2 production in ammonium-uptake deficient *mep1*Δ/Δ *mep2*Δ/Δ double mutants suggests that the ammonium availability is determined intracellularily. Surprisingly, Sap2 expression and BSA degradation was only partially repressed by 20 mM NH_4^+ in the *mep1*Δ/Δ mutants, but fully repressed in *mep2*Δ/Δ mutants (Figure 2.25 compare lane 5 and 7). Presence of *MEP1*, but not *MEP2*, therefore seemed to be sufficient to fully repress Sap2 production and BSA degradation

by 20 mM NH_4^+. Mep2 was shown to be a less efficient transporter than Mep1, but still supports growth of *C. albicans* since Mep2 was induced at much higher levels than Mep1 under nitrogen starvation (Biswas & Morschhäuser, 2005). These differences reasoned that under the tested conditions simply low expression levels of *MEP2* caused the partial repression of BSA degradation by the *mep1*Δ/Δ single mutants. Indeed, low *MEP2* transcript levels with 20 mM NH_4^+ as sole nitrogen source were already observed by northern hybridization in wild type CAI4 cells grown in liquid minimal medium (Biswas & Morschhäuser, 2005).

Nevertheless, to test whether *MEP2* was induced under the tested condition its expression was determined in a *GFP* reporter strain. For this purpose the independently constructed SCMEP2G7 A/B *C. albicans* strains were analyzed, which harbored a functional Mep2-Gfp protein fusion under the control of the endogenous *MEP2* promoter (Dabas & Morschhäuser, 2007). Expression of *MEP2-GFP*, either controlled by the arbitrarily designated *MEP2-1* allele in the A-strain or by the *MEP2-2* allele in the B-strain, was tested (Figure 2.26). As control expression was tested in SLAD medium (YNB-0.1mM NH_4^+), known to induce *MEP2*.

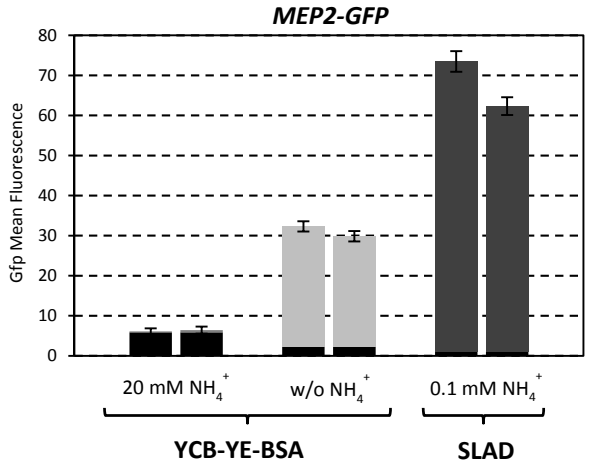

Figure 2.26: Expression of Gfp-tagged Mep2 fusion (*MEP2-GFP*) in different media. Two reporter strains (SCMEP2G7 A/B) were inoculated 1:100 from an YPD-overnight culture into indicated media and grown at 30°C for 7 hours. Fluorescence was quantified by flow cytometry and mean values plus standard deviations from three independent measurements are shown. The black bar in each column is the autofluorescence of the parental strain SC5314, which does not contain *GFP*.

Expression of *MEP2-GFP* was strongly induced in SLAD (YNB-0.1mM NH_4^+) medium and only half the induction was observed in the YCB-YE-BSA test medium without NH_4^+ (Figure 2.26). No *MEP2-GFP* expression above background level was detectable when 20 mM NH_4^+ was added to YCB-YE-BSA. This clearly showed that under the conditions used to repress Sap2 production *MEP2* was not efficiently induced. This explained the incomplete BSA degradation and partial Sap2 repression in the *mep1*Δ/Δ mutants, because the retained *MEP2* copies were

not expressed to mediate effective ammonium uptake needed to fully repress Sap2 production.

However, the partial repression in the *mep1*Δ/Δ mutant was only slightly enhanced when *MEP2* was constitutively expressed from the *ADH1* promoter (not shown). This indicated that even higher *MEP2* expression was required to sufficiently take up ammonium in order to result in full Sap2 repression.

One might argue that the *mep1*Δ/Δ *mep2*Δ/Δ double mutants generally lost the ability to repress Sap2 expression. In order to test that, Sap2 production in the *mep1*Δ/Δ *mep2*Δ/Δ double mutants was repressed by the alternative nitrogen sources glutamine, proline, and urea (Figure 2.27).

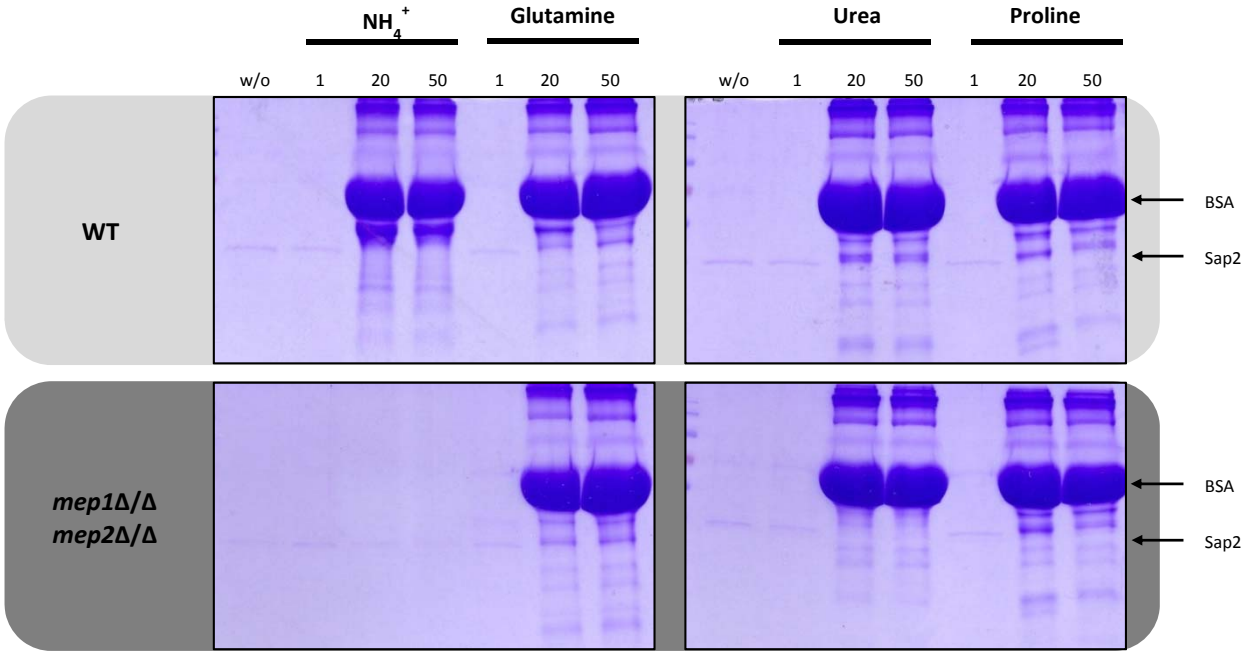

Figure 2.27: Repression of Sap2 production and BSA degradation by various concentrations of indicated alternative nitrogen sources. The wild type SC5314 (WT) and *mep1*Δ/Δ *mep2*Δ/Δ double mutants (SCMEP12M4 A/B) were inoculated 1:100 from an YPD-overnight culture into fresh YCB -BSA medium. Cultures were grown in the absence (w/o) or presence of 1 mM, 20 mM, or 50 mM of indicated alternative nitrogen sources at 30°C for 72 hours. Proteins of the culture supernatants were analyzed by SDS-PAGE. Note: Only the results from the A-strain series are shown and similar results were obtained with the independently constructed B-strain series.

Addition of glutamine, proline and urea similarly repressed Sap2 production and BSA degradation in the wild type SC5314 as well as the *mep1*Δ/Δ *mep2*Δ/Δ double mutants (Figure 2.27). This indicated that alternative nitrogen sources, other than ammonium, still repress Sap2 production in *mep1*Δ/Δ *mep2*Δ/Δ double mutants.

In sum, the inability of ammonium to repress Sap2 production in ammonium-uptake deficient *mep1*Δ/Δ *mep2*Δ/Δ double mutants suggests that its availability is rather determined intracellularily than by an external sensor.

2.4.3 Ammonium uptake is required to repress *OPT3* expression

Expression of oligopeptide transporters is co-regulated with the expression of secreted proteases since the produced degradation products require an appropriate uptake system. Also experimental evidence confirmed upregulation of *OPT1* and *OPT3* in medium with BSA as sole nitrogen source as well as co-regulation with Sap2 (Martínez & Ljungdahl, 2005, Reuss & Morschhäuser, 2006). In addition, the previous results from this study demonstrated that Stp1-HA bound to the promoters of *SAP2, OPT1, OPT2,* and *OPT3* under inducing conditions (YCB-YE-BSA), thus supporting co-regulation. In order to assess whether ammonium uptake is required to repress *OPT3* expression, the promoter activity was investigated in the various *mep*Δ/Δ backgrounds. Promoter activity was determined using the *GFP* reporter fusion from the plasmid pOPT3G22 (Reuss & Morschhäuser, 2006). The ApaI-SacI fragment from pOPT3G22 was two times independently introduced into the endogenous *OPT3*-locus in the *mep1*Δ/Δ *mep2*Δ/Δ double mutants as well as into the *mep*Δ/Δ single deletion mutants. Correct integration of the cassette into the *OPT3* locus was verified via Southern hybridization of SpeI-digested genomic DNA with *OPT3*-specific probes (not shown). The resulting mutants were designated SC*mep1*ΔOPT3G22 A/B, SC*mep2*ΔOPT3G22 A/B, and SC*mep12*ΔOPT3G22 A/B, where the reporter fusion was always integrated into the arbitrarily designated *OPT3-2* allele. As control served *OPT3* expression in the wild type background by using the reporter strains SCOPT3G22 A/B where GFP was either controlled by the *OPT3-1* allele in the A-strain or by the *OPT3-2* allele in the B-strain (Reuss & Morschhäuser, 2006). Expression of *OPT3* was finally tested in inducing YCB-YE-BSA medium in the absence or presence of 20 mM NH_4^+ (Figure 2.28).

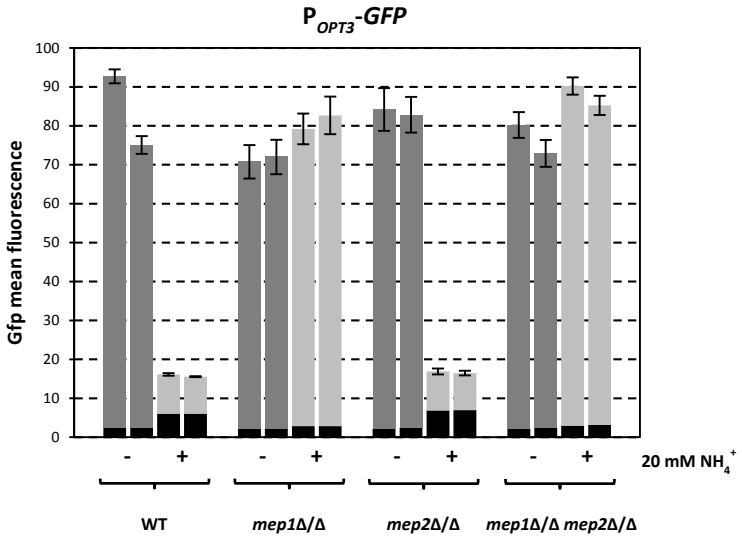

Figure 2.28: Repression of *OPT3*-promoter activity by 20 mM NH_4^+ in indicated mutant backgrounds. Gfp expression from the *OPT3*-promoter was determined in the wild type background and mutants lacking one or both Mep transporters. Following independently constructed reporter strains were used: SCOPT3G22 A/B (WT); SCΔ*mep1*OPT3G22 A/B (*mep1*Δ/Δ), SCΔ*mep2*OPT3G22 A/B (*mep2*Δ/Δ), SCΔ*mep12*OPT3G22 A/B (*mep1*Δ/Δ *mep2*Δ/Δ). Reporter strains were inoculated 1:100 from an YPD-overnight culture into inducing YCB-YE-BSA media in the absence (-) or presence (+) of 20 mM NH_4^+ and grown at 30°C for 7 hours. Gfp-fluorescence was quantified by flow cytometry and mean values plus standard deviations from three independent measurements are shown. The black bar in each column is the autofluorescence of the respective parental strains, which do not contain *GFP.*

OPT3 expression was strongly and similarly induced in all strains when grown in YCB-YE-BSA (Figure 2.28). The addition of 20 mM NH_4^+ repressed *OPT3* induction in the wild type background and in the *mep2*Δ/Δ background. In contrast, the double *mep1*Δ/Δ *mep2*Δ/Δ mutants showed no *OPT3* repression, despite the repressing 20 mM NH_4^+ concentration in the medium. Also did the *mep1*Δ/Δ single mutants not repress *OPT3* expression at 20 mM NH_4^+, which was consistent with the undetectable *MEP2* expression in YCB-YE-BSA + 20 mM NH_4^+ (Figure 2.26).

Conclusively, also the inability of ammonium to repress *OPT3* expression in ammonium-uptake deficient *mep1*Δ/Δ *mep2*Δ/Δ double mutants again suggests that the ammonium status is determined intracellularily and not by an external sensor.

2.4.4 Ammonium uptake is required to repress *DAL1* and *DUR3* expression

DAL1, which code for an allantoinase, and Dur3, recently shown to be the major urea transporter in *C. albicans* (Navarathna *et al.*, 2011), were upregulated under ammonium-limiting condition. This was shown by the of expression profiles of *C. albicans* strains compared under low (0.1 mM NH_4^+) versus high ammonium (76 mM NH_4^+) concentration (K. Biswas and N. Hauser, unpublished results).

To test whether repression of *DAL1* expression requires uptake of ammonium, the *DAL1* transcript level was determined in both *mep1*Δ/Δ *mep2*Δ/Δ double mutants (SCMEP12M4 A/B) in YNB-medium either containing low inducing 0.1 mM NH_4^+ (SLAD) or high repressive 20 mM NH_4^+ concentrations. For comparison *DAL1* transcript levels were also determined in the wild type SC5314 (Figure 2.29).

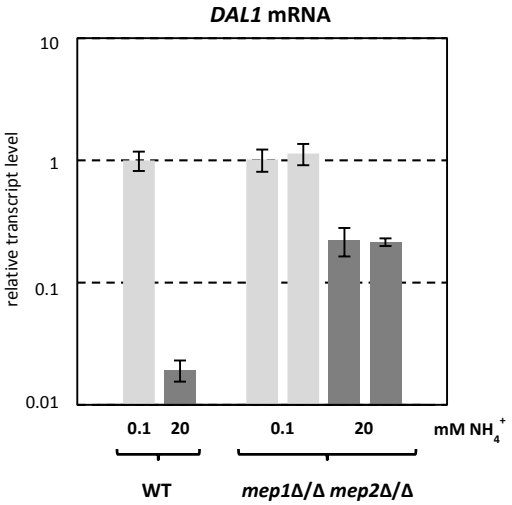

Figure 2.29: Expression of *DAL1* transcripts in the wild type SC5314 and *mep1*Δ/Δ *mep2*Δ/Δ double mutants. Dal1 transcript levels were determined in the wild type SC5314 (WT) and in two independently constructed *mep1*Δ/Δ *mep2*Δ/Δ mutants (SCMEP12M4 A/B), lacking both *MEP* ammonium permeases. An YPD-overnight culture of each strain was 3x washed with water and inoculated with a starting OD_{600}=0.2 into fresh YNB-medium. Cultures contained either low (0.1 mM) or high (20 mM) NH_4^+ concentrations and grown at 30°C for 7 hours. *DAL1* mRNA levels were determined by quantitative RT-PCR and relative *DAL1* transcript levels were calculated by the comparative cq method and plotted against those from the wild type strain SC5314 under inducing conditions (YNB-0.1 mM NH_4^+). Means and standard deviations from two independent experiments with duplicate measurements were shown in the graph.

With a low 0.1 mM NH_4^+ concentration a similar *DAL1* mRNA level was observed in all strains (Figure 2.29). The addition of 20 mM NH_4^+ concentration repressed *DAL1* transcription by approx. 50-fold in the wild type strain SC5314. In contrast, *DAL1* transcription was only 5-fold repressed in the *mep1*Δ/Δ *mep2*Δ/Δ double mutants.

To investigate whether ammonium uptake is also needed to repress *DUR3* expression, *DUR3* promoter activity was tested in both *mep1*Δ/Δ *mep2*Δ/Δ double mutants (SCMEP12M4 A/B). *DUR3*-promoter activity was determined using the *GFP* reporter fusion from the plasmid pDUR3G2. The ApaI-SacI fragment from pDUR3G2 was two times independently introduced into the endogenous *DUR3*-locus in the *mep1*Δ/Δ *mep2*Δ/Δ double mutants and the wild type SC5314. Correct integration of the cassette into the *DUR3* locus was verified via Southern hybridization of EcoRI-digested genomic DNA with *DUR3*-specific probes (not shown). The resulting mutants were designated SCDUR3G2 A/B and SC*mep12*ΔDUR3G2 A/B. The set of reporter strains was tested under inducing condition in YNB-1mM Urea for *DUR3* repression by external NH_4^+ (Figure 2.30).

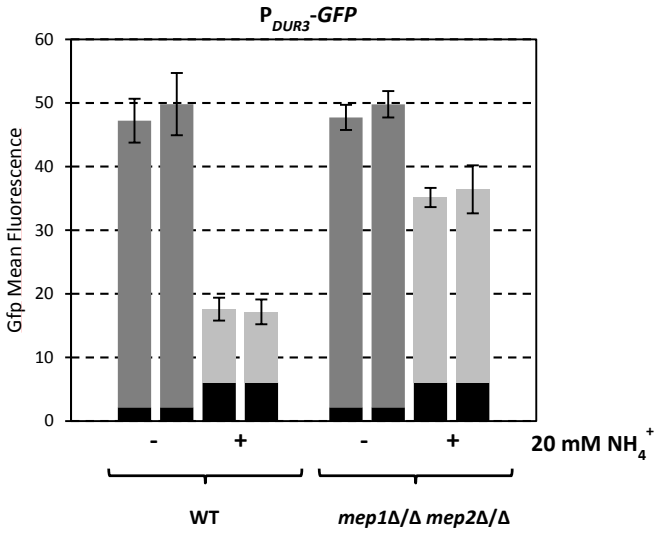

Figure 2.30: Expression from the *DUR3*-promoter in in the wild type background and mutants lacking both *MEP* permeases. Gfp expression from the *DUR3*-promoter was determined in the wild type background and *mep1*Δ/Δ*mep2*Δ/Δ double mutants. Following reporter strains were used: SCDUR3G2 A/B (WT) and SCΔ*mep12*DUR3G2 A/B (*mep1*Δ/Δ *mep2*Δ/Δ). Reporter strains were inoculated 1:100 from an YPD-overnight culture into inducing YNB-1mM Urea medium in the absence (-) or presence (+) of 20 mM NH_4^+ and grown at 30°C for 7 hours. Fluorescence was quantified by flow cytometry and mean values plus standard deviations from three independent measurements are shown. The black bar in each column is the autofluorescence of the wild type SC5314, which does not contain *GFP*.

Similar expression from the *DUR3*-promoter was observed in all strains when 1 mM Urea served as sole nitrogen source (Figure 2.30). The addition of 20 mM NH_4^+ repressed *DUR3* expression (approx. 4-fold) in the wild type background. Contrarily, only slight *DUR3* repression (approx. 1.5-fold) was observed in the ammonium-uptake deficient *mep1*Δ/Δ *mep2*Δ/Δ double mutants.

Collectively, these results suggest that the status of available ammonium is determined in the cell after uptake and not by an external sensor.

2.4.5 Ammonium uptake is required to repress arginine-induced filamentation

Nitrogen starvation is one environmental signal that induces filamentous growth in *C. albicans*. Nitrogen sufficiency, e.g. 10 mM NH_4^+, was demonstrated to repress filamentation induced by several poor nitrogen sources including urea, proline, histidine, and arginine (Biswas & Morschhäuser, 2005). Importantly, hyphal induction by most of these signals relied on the sensing and signaling function of the ammonium permease Mep2. So whether uptake was required to repress hyphal induction could only be tested, when induced by Mep2-independent signals. Otherwise absent filamentation resulted from the lack of the functional Mep2 permease. However, filamentation induced by the amino acid arginine was Mep2-independent and still inhibited by 10 mM NH_4^+ (Biswas & Morschhäuser, 2005). Conclusively, repression of nitrogen starvation induced filamentation by exterior ammonium can be investigated in mutants lacking *mep2*, when induced by arginine. In order to test repression of arginine-induced filamentation by NH_4^+ in both uptake-deficient *mep1*Δ/Δ *mep2*Δ/Δ double mutants they were propagated on agar plates containing 0.1 mM arginine in the presence or absence of an inhibiting 20 mM NH_4^+ concentration. For comparison the wild type SC5314 and the *mep1*Δ/Δ (SCMEP1M4 A/B) and *mep2*Δ/Δ (SCMEP2M4 A/B) single deletion mutants were included (Figure 2.31).

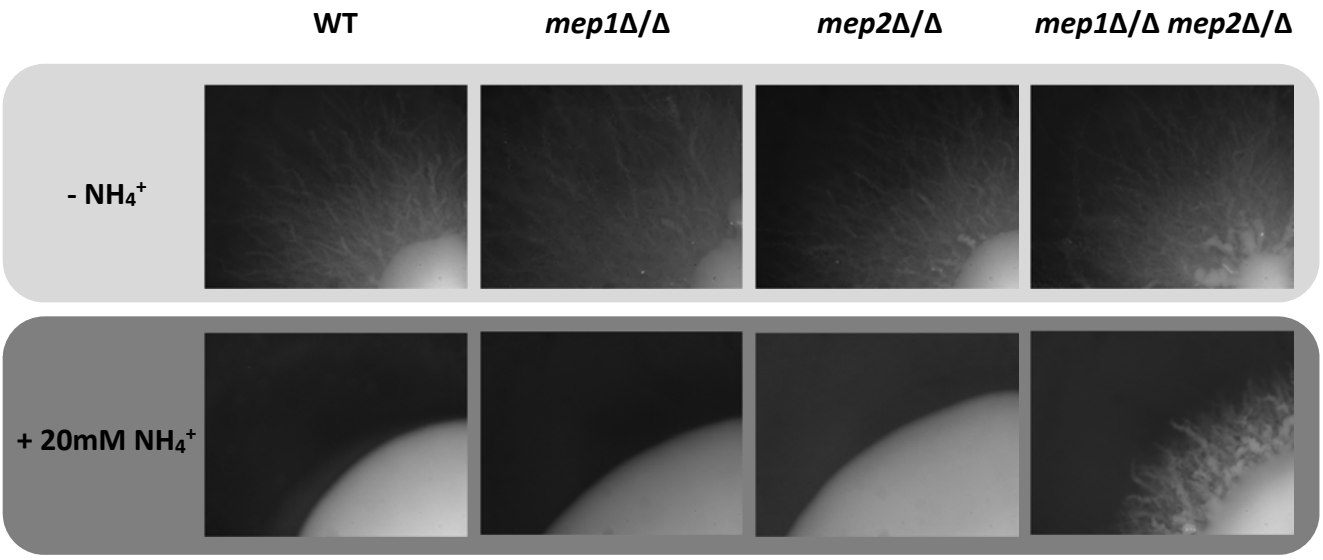

Figure 2.31: Arginine-induced filamentation of indicated strains. Hyphal formation on YNB-agar containing 0.1 mM arginine was determined for the wild type SC5314 (WT) and mutants lacking one or both Mep ammonium permeases. Following mutants were used: SCMEP1M4 A/B (*mep1*Δ/Δ), SCMEP2M4 A/B (*mep2*Δ/Δ), SCMEP12M4 A/B (*mep1*Δ/Δ *mep2*Δ/Δ). Cells from 100 µl of 1:10^{-6} diluted YPD-overnight cultures of each strain were plated on YNB-0.1mM arginine agar in the absence (-) or presence (+) of 20 mM NH_4^+ at 37°C for 7 days. Note: This experiment was performed with both sets of A- and B-strains, which behaved identically, but only the results with the A-strains are shown. Hyphal formation was documented by photographing the border of single colonies.

Filamentation was strongly and similarly induced in all strains on agar plates containing 0.1 mM arginine (Figure 2.31). Efficient repression by 20 mM NH_4^+ was observed in the wild type SC5314 as well as the in the *mep1*Δ/Δ and *mep2*Δ/Δ single mutants, suggesting uptake through either one of the Meps was sufficient to inhibit filamentation (Figure 2.31). In contrast, the *mep1*Δ/Δ *mep2*Δ/Δ double mutants did not repress arginine-induced filamentation by 20 mM NH_4^+, which resulted in continuous hyphal formation although an inhibiting ammonium concentration was present.

In sum, these results convincingly demonstrated that *C. albicans* did not sense availability of the preferred nitrogen source by an external sensor. Instead, to mediate NCR and control protease secretion, gene expression, and filamentation by NH_4^+, intracellular determination after uptake is required.

3 Discussion

3.1 Stp1, a transcriptional regulator involved in protein utilization and beyond

Unquestionably, a highly developed and flexible adaption to available nutrients is mandatory for *C. albicans* to survive and thrive within the human host. Interestingly, starvation for nutrients, like nitrogen, is tightly linked to the expression of virulence-associated traits. For example, the secreted aspartic proteases are required to use proteins as nitrogen source, but are also involved in tissue invasion and escape from attacks by the immune system. Moreover, nitrogen starvation is one signal that induces the formation of hyphae, a key attribute in *C. albicans* pathogenicity. The restricted availability of good nitrogen sources in certain host niches might therefore promote expression of virulence traits, which may represents a prerequisite for the commensal-to-pathogen switch in *C. albicans*. Proteins are a highly abundant nitrogen source in the host, but for their usage as source of cellular nitrogen extracellular degradation and uptake via specific peptide transporters is required. Expression of both traits is mediated by the transcriptional regulator Stp1 and consequently a *stp1*Δ/Δ null mutant was unable to grow on BSA as sole nitrogen source *in vitro* (Dabas & Morschhäuser, 2008, Martínez & Ljungdahl, 2005).

Although the role of Stp1 in the acquisition of proteins as nutrient is known only a small subset of Stp1- dependent genes have been identified. However, it is unclear whether Stp1 regulates their expression directly and which other genes are target of Stp1. To shed light on this a global binding profiling of Stp1 was performed in collaboration with the laboratory of Prof. Dr. Martine in the present work. For this purpose a functional variant of Stp1 was generated, which contained a HA-tag at its C-terminus. The HA-tag is commonly used for ChIP-on-chip analysis and its fusion to transcriptional regulators usually leaves properties or stability unaltered so that the HA-tagged version is likely to bind like the wild type variant. However, C-terminal fusion of an HA-tag to Mrr1 and Upc2, two regulators from the Zn-Cluster transcription factor family, were shown to result in hyperactive variants (Schubert *et al.*, 2011, Znaidi *et al.*, 2008). Nevertheless, the wild-type like growth of the *stp1*Δ/Δ mutant containing one copy of the Stp1-HA variant (Figure 2.1) clearly demonstrated that Stp1-HA was functional

and probably unaltered. The global Stp1 binding profile was determined during growth in YCB-YE-BSA, which contained BSA as well as other low-molecular weight nitrogen sources. Although under these conditions Stp1 function was dispensable for growth, demonstrated by wild-type like growth of *stp1*Δ/Δ null mutants, *STP1* expression was readily induced (Dabas & Morschhäuser, 2008). Consequently, Stp1 was likely to be active, which is additionally supported by the expression of the known Stp1 targets genes *SAP2* and *OPT3* in YCB-YE-BSA. The obtained global binding profile verified the known Stp1-dependent genes *SAP2*, *OPT1*, *OPT3*, and *PTR2* as direct Stp1 targets and thus validated the reliability of the data set.

However, from the analysis of Stp1-targets ORFs with Stp1-HA binding events downstream or within ORFs were excluded, since a classical transcriptional regulator acts through binding to upstream promoter sequences. This does not exclude that the omitted ORFs might be nonetheless regulated by Stp1 in one or the other way. For example, binding of the transcriptional regulator Cap1 was found within ORFs, which was even further increased when Cap1 was hyperactive (Znaidi *et al.*, 2009). It was therefore proposed that association of Cap1 with the transcription machinery during transcription was causing the ORF localization of Cap1 binding. Alternatively, association with chromatin-associated proteins might result in ORF binding or to regions were no obvious ORFs are annotated. Such binding events can also control the expression of non-coding small RNAs. In addition, binding events downstream of ORFs might also influence gene expression through transcriptional interference, which was described in *S. cerevisiae* and other fungi. In such scenario gene expression is blocked by simultaneous transcription from the opposite strand that interferes with the regular transcription from the conventional start site (Donaldson & Saville, 2012). Although 40% of *C. albicans* genes were predicted to be controlled by such natural antisense transcript mechanisms this type of gene regulation is so far only sparsely investigated in fungi and may represent special cases (Donaldson & Saville, 2012). Hence, only ORFs with ordinary binding of Stp1-HA to the promoter were considered in the present study as Stp1 target genes. Regular promoter sequences encompass the direct upstream located 500 – 1000 basepairs of the target gene, but also way longer promoter sequences have been reported, e.g. Efg1 bound to the complete 10 kb sequences of its own promoter (Lassak *et al.*, 2011). Most of the Stp1-HA binding events were located in the direct upstream located 1 kb of the target gene and only a minor fraction (9%) were situated over 2 kb apart the ATG^{start}. Overall, the genome wide binding profile revealed 610 ORFs as Stp1 targets and confirmed the involvement of Stp1 in

acquisition of nitrogenous compound, esp. proteins, peptides and amino acids. Stp1 has redundant functions with Stp2, the major regulator controlling expression of amino acid permeases, and their DNA binding domains share 74% similarities. Both control the expression of *PTR2* and *OPT3*, but only hyperactive Stp2 was shown to upregulate genes encoding amino acid permeases, e.g. *CAN1, GAP1, GAP2* (Martínez & Ljungdahl, 2005). However, Stp1-HA targets, identified in the preset study, were also enriched for genes encoding amino acid permease (*GAP1, CAN2, AGP1*, …) during growth in YCB-YE-BSA, suggesting regulation of amino acid uptake also by Stp1. Especially, Gap1 expression was considered as solely Stp2-dependent, because hyperactive Stp1 was unable to increase Gap1 transcript levels in a *csh3*Δ/Δ mutant background (Martínez & Ljungdahl, 2005). However, Stp1 might contribute to Stp2-dependent *GAP1* expression to a minor extent or differential growth conditions (SD medium versus YCB-BSA-BSA) might require differential needs by the two redundant factors. Stp1 trans-activates also a set of genes distinct from that of Stp2, as shown by impaired growth of the *stp2*Δ/Δ mutant, but not the *stp1*Δ/Δ mutant, in the presence of a branched-chain amino acids biosynthesis inhibitor (Martínez & Ljungdahl, 2005). Furthermore, *stp2*Δ/Δ mutants, but not *stp1*Δ/Δ mutants, showed severe growth defects *in vitro*, although only weak during growth on YPD or MM agar (Homann *et al.*, 2009, Pérez *et al.*, 2013). Overall, function and target genes of Stp1 and Stp2 in *C. albicans* are distinct, but they also overlap.

Interestingly, a recent study by Davis and co-workers showed reduced virulence of a *C. albicans stp1*Δ/Δ mutant, but not a *stp2*Δ/Δ mutant, during infection of the model host *Drosophila melanogaster* (Davis *et al.*, 2011). This was somewhat surprising since the *stp2*Δ/Δ mutant was severely deficient in growth under many laboratory conditions (see above), but still demonstrated wild-type like virulence. Furthermore, the concentration of free amino acids, circulating in the *Drosophila* hemolymph (Piyankarage *et al.*, 2010), was thought to diminish Stp1 function due to repression of *STP1* transcription. Because of the observed reduced tissue damage by the *stp1*Δ/Δ null mutant the authors reasoned that inability to express Sap2 was primarily causing reduced virulence. According to the identified Stp1 targets in the present study, the attenuated virulence of the *stp1*Δ/Δ mutant might be additionally caused by impaired expression of genes that are required for an appropriate stress response. For example, inability to properly express Hsp90, the prime Hsp which regulates morphogenesis, biofilm formation, drug resistance, and virulence or to express Hsp104, which is required for proper biofilm formation and for virulence in a *C. elegans* infection model

(Mayer *et al.*, 2013). Additionally, virulence may be attenuated due to absent expression of the small Hsp21, which is crucial to regulate intracellular levels of the 'molecular chaperone' trehalose and is strongly required for full virulence in a murine systemic infection model (Mayer *et al.*, 2013). Furthermore, if Stp1 is required to adapt to oxidative stress, due to the control of ROS neutralizing enzymes like Cat1, Yhb1, and Sod1 it possibly affects the virulence of the *stp1*Δ/Δ null mutant In addition, Stp1 might influence adherence behavior through its targets Mp65, Flo1, Mnt2, and Ecm33 or the general involvement in the adaption to nutrient availability may also contribute to fitness and virulence of *C. albicans* in the host.

The fact that over 40 transcriptional regulators were identified as Stp1 targets might place Stp1 in a more central position within the regulatory circuits governing *C. albicans* pathogenicity. Although, Stp1 is probably not a master regulator, it might still have an important role in fine tuning the expression of regulators in hyphal development (Efg1. Flo8, Nrg1, Gln3), or adherence and biofilm formation (Bcr1, Efg1, Tye7, Fcr3, Ahr1, Zcf21 and Try3) (Finkel *et al.*, 2012, Fox & Nobile, 2012). Conceivably, Stp1 may also function in order to integrate nitrogen availability signals into the expression of virulence-associated traits as pathway-specific regulator, apart from the global regulators Gat1 and Gln3.

Interestingly, a recent study identified a tightly interconnected transcriptional regulatory circuit, consisting of the transcriptional regulators, Hms1, Tye7, Zcf21, and Rgt1/3, which controls *C. albicans* commensalism and pathogenicity (Pérez *et al.*, 2013). The present study showed that Hms1, Tye7, Zcf21 and Rgt1 were also Stp1 targets, suggesting an involvement and participation in this regulatory circuit. This is further supported as Stp1 was also identified as target of Tye7 and Zcf21. Additionally, Stp1 bound to the promoters of *GAL10, NCE102, DFI1*, and *HAP41* the main effectors controlled by this interconnected transcriptional circuit and all four effectors were important for GI colonization or systemic infection (Pérez *et al.*, 2013).

Determination of genome wide binding sites of a transcriptional regulator allowed the identification of a consensus binding sequence for this factor. Previous studies already identified two binding sites for the CaStp2 ortholog in *S. cerevisiae*, ScStp2, which shares 41 % similarity to CaStp1 and even 78 % within the DNA-binding domain (Martínez & Ljungdahl, 2005). The 5'-CGGCTC-3' hexamer was identified by an *in vitro BAP3*-promotor analysis (de Boer *et al.*, 2000) and the 5'-GCGCCGCA-3' sequences was identified by using custom-designed universal protein-binding microarrays, which contained double-stranded

oligonucleotides, covering all possible contiguous 8-mer as well as gapped 8-mers (Zhu *et al.*, 2009). However, an approach to identify a binding motif for Stp1 from *C. albicans* with the extracted binding sequences from the ChIP-on-chip data in this study gave no conclusive results. The obtained motifs differed greatly depending on the respective algorithm used or were not significantly overrepresented, in comparison to a random set of sequences. Nevertheless, two different algorithms revealed a short CGG triplet as possible motif. Interestingly, CGG-triplets were also identified as major binding elements for Zn-Cluster transcription factors in fungi (MacPherson *et al.*, 2006). E.g. CGG-triplets are important for Tac1-mediated expression from the *CDR2*-promoter (Coste *et al.*, 2004), although all CGG triplets can be deleted in the *TAC1*-promoter without diminishing autoregulation by Tac1 (F. Louhichi, personal communication). However, whether CGG-triplets were also responsible for Stp1 binding to target sequences remains to be determined.

In sum, the identified Stp1 targets suggest a role for Stp1 in *C. albicans* that goes beyond nitrogen acquisition from proteins and Sap2 expression and reasonably extents the involvement to stress response, general nutrient adaption, and pathogenesis. Although new targets for Stp1 were identified the present work focused on Sap2, a prime example of a nitrogen-regulated virulence attribute, and other target genes, involved in the acquisition of proteins as nitrogen source.

3.2 Only *SAP2* is required for growth with BSA as sole nitrogen source and its expression is controlled by distinct *cis*-regulatory sequences

Within the concept of nitrogen-regulated pathogenesis, the major secreted aspartic protease Sap2 is as excellent example that combines nitrogen acquisition with virulence. It was therefore subjected in the present work to a detailed analysis to gain insight into its regulation. Under routine laboratory conditions Sap2 was crucial to support growth with BSA as sole nitrogen source. However, also Sap4 to Sap6 have been proposed to contribute to this growth, which was hypothesized on a growth defect with BSA by the *sap4*Δ/Δ *sap5*Δ/Δ *sap6*Δ/Δ mutant DSY459 (Sanglard *et al.*, 1997). On the contrary, the *sap4*Δ/Δ *sap5*Δ/Δ *sap6*Δ/Δ mutants SAP456MS4 A/B grew like the wild type SC5314, which contradicted this hypothesis. A comprehensive elucidation in the present study unambiguously proved that unintended loss of the *SAP2-2* allele in DSY459 was causing the growth defect and not deletion for *sap4* to

sap6. Furthermore, strain DSY459 became homozygous not only for *SAP2-1*, but also for the whole chromosome R. Since DSY459 was used to assess the involvement of the three *SAP4* to *SAP6* genes for *C. albicans* virulence in many infection models, this finding weakened the credibility of obtained results. Although lack of *SAP2-2* alone probably did not affect virulence, homozygosity for the complete chromosome R might have a stronger impact, which must be considered when interpreting results obtained with this mutant.

The genomic plasticity of *C. albicans* is proposed to represent means of adaption (Selmecki *et al.*, 2010), and it thus can also produce unintended genomic changes in laboratory mutant strains. Especially as consequence of certain stresses, e.g. antimycotic pressure, genomic alterations were frequently observed. Prominent examples for this phenomenon are drug resistance mutations, which are spontaneously acquired in one allele, and become homozygous in order to increase drug resistance through higher gene dosage. Such LOH events were reported for fluconazole resistant *C. albicans* strains, which became drug resistant due to mutations in *ERG11, TAC1, MRR1* , and *UPC2* (Morschhäuser, 2010a). Even while routinely maintaining strains in the laboratory LOH events can occur, as reported for some stocks of strain CAI8. They became homozygous for the MTL locus, which enabled them to switch to the opaque phase, unlike the “reference” CAI8 (Park & Morschhäuser, 2005). In sum, the genomic flexibility of *C. albicans* can produce striking phenotypic differences between theoretically identical strains.

To date it is not feasible to completely rule out that such unintended genomic alteration affect the phenotype of a generated mutant strain. Also exerted stress during mutants construction, e.g. by electroporation, enhances the occurrence of aneuploidies and LOH events (Arbour *et al.*, 2009). Nowadays, comparative genome hybridization and genome wide SNP analysis are potent tools to discover LOH events and aneuploidies (Selmecki *et al.*, 2010), but their application is expensive and restricted to laboratories with the respective expertise. Maybe, the exponentially fast evolving sequencing capacity will make whole genome sequencing affordable in the future. Nevertheless, construction of independent mutants, carrying the same deletion(s), and complementation of mutant phenotypes, by adding back the deleted gene(s), are important controls. In addition, genomic changes can be checked for individual chromosomal loci, which are prone for alterations. For example, chromosome 5 and its left arm (Chr5l) were demonstrated to vary in copy number during antimycotic pressure (Selmecki *et al.*, 2006, Selmecki *et al.*, 2008). Also homozygosity for chromosome R or the *SAP2* locus in

SC5314 derivatives was repeatedly reported and also occurred in strains from our laboratory (Forche *et al.*, 2009b, Legrand *et al.*, 2008, Neuhäuser *et al.*, 2011, Staib *et al.*, 2002b). Especially, unintended aneuploidies for chromosomes can have dramatic effects on the phenotype and thus lead to erroneous interpretation of obtained results. For example, *C. albicans* strains which were trisomic for chromosome 1 exhibited absent virulence in a mouse model of systemic infection, unlike closely related strains that were disomic for chromosome 1 (Chen *et al.*, 2004).

Most small-scale allelic differences leave function and regulation for genes unaffected and stay, therefore, unrecognized. Only some examples have been investigated were small-scale allelic differences strongly affect gene expression or function. Prominent examples are the differential regulation of *SAP2* (see below) or *HWP1*, a gene encoding the major *C. albicans* cell wall protein (Padovan *et al.*, 2009). A novel *HWP1* allele, not present in the reference strain SC5314, was isolated from a clinical *C. albicans* strains with defective hyphal growth and biofilm formation. Decreased *HWP1* expression was observed in strains either homozygous or heterozygous for the novel *HWP1* allele during hyphal growth and biofilm formation. Interestingly, the novel *HWP1* allele was not induced in biofilms and homozygosity for the novel *HWP1* allele reduced hyphal growth and biofilm formation *in vitro* (Padovan *et al.*, 2009).

Conclusively, the high genomic flexibility of *C. albicans* combined with the knowledge of aneuploidies, alteration-vulnerable genomic regions and allele-specific differential regulation might alert researches that undesired genomic changes can sometimes easily affect a mutant phenotype. Consequently, appropriate control measures are mandatory to reliably determine characteristics and phenotypes of genetically engineered and modified *C. albicans* mutant strains.

Coming back to nitrogen-regulated pathogenesis, the way how *SAP2* expression is controlled by its *cis*-acting elements is currently not well understood. Moreover, the *SAP2* regulation becomes especially interesting since these alleles are one of the best known examples of allelic heterogeneity in *C. albicans*. Thereby, the *SAP2-2* is more easily activated than *SAP2-1* and only *SAP2-2* is basally transcribed (Staib *et al.*, 2002a). Recalling the *SAP2* activation model this basal activity leads to basal Sap2 proteolytic activity in the exterior, providing inducing amino acids from protein degradation, which then activate the SPS-sensor and consequently Stp1 (Figure 1.6). Active Stp1 then mediates full *SAP2* expression from both *SAP2* alleles. Thus,

basal *SAP2-2* activity is crucial to provide the inducers in order to highly induce *SAP2* expression.

The present work clearly delimited the promoter region responsible for the differential induction of the *SAP2* alleles and showed that distinct sequences in the proximal 1.2 kb promoter, comprising the low activity region LA1 (see below) as well as the repeats R1 and R2, determined the differential induction. This was evident from a growth defect in YCB-BSA of a SC5314-transformant that contained the complete *SAP2-2* promoter except for the proximal 1.2 kb, which have been replaced by *SAP2-1* sequences (Figure 2.9 SC5314-transformant B1). Thus, *SAP2-2* lost its basal activity by replacing this proximal 1.2 kb of *SAP2-2* with *SAP2-1* sequences. On the other hand, the *SAP2-1* promoter gained basal activity by replacing this region with *SAP2-2* sequences (Figure 2.6 DSY459-transformant A3). However, the fact that most of this 1.2 kb region can be absent without impaired *SAP2* activation in YCB-YE-BSA suggested that this region is not a prerequisite for *SAP2* expression *per se* (Lermann, 2008). Probably, this part solely mediates a low activity (through LA1, but see below), but became dispensable once the active Stp1 initiates full/high *SAP2* expression. There is strong evidence that both tandem repeats R1 and R2 account for the differential *SAP2* induction (Staib *et al.*, 2002a). Staib and colleagues demonstrated low *SAP2* promoter activity, when the expression was controlled by artificial repeat number variations (e.g. 4xR1 + 5xR2 or 5xR1 + 6xR2), with the *caFLP* reporter system during a systemic infection of mice. However, these artificial repeat combinations retained their high inducibility *in vitro* so that the authors suggested a differential Sap2 activation between *in vivo* and *in vitro* signals. In the yeast *S. cerevisiae* tandem repeat number variations are implicated with expression divergence (Tirosh *et al.*, 2009). For example, the number of tandem repeats mediated changes in the expression of the Sc*SDT1* gene that also matched differences in growth (Vinces *et al.*, 2009). The authors of this study further provide evidence that neither altered spacing nor variations in transcriptional binding sites alone were sufficient to explain the effects of repeat number variation on expression. Rather tandem repeat sequences directly affected local chromatin structure, especially AT-rich repeats, thereby fostering nucleosome-free DNA regions and promoting transcriptional activation. Additionally, gene expression mediated by such repeat-containing promoters showed enhanced responsiveness to changes in the environment (Vinces *et al.*, 2009). Transferring this to the regulation of *SAP2* proposes a scenario in which the repeat combination in *SAP2-2* had evolved to make this allele prone to an easier access of

transcriptional regulators or the transcriptional machinery. Hence, the *SAP2-2* allele is basally transcribed and more easily and strongly activated than *SAP2-1*. Likewise the contrary might be the case and the *SAP2-1* allele lost this ability in order to fine tune the induction of this secreted protease.

Additionally, the present analysis of *SAP2-1* and *SAP2-2* revealed four promoter sequences that were important in mediating general *SAP2* expression (Figure 2.16). All the identified *cis*-acting elements similarly influenced *SAP2* expression in both alleles but based on their differential inducibility, i.e. the *SAP2-2* allele always retained its higher inducibility compared to *SAP2-1*. One identified region, comprising the proximal 0.8 kb of the promoter, was designated low activity region LA1 because it enabled low, but not high, Sap2 induction. For high Sap2 induction either high activity region HA1 (located between -2.6 kb and -2.2 kb upstream of the ATG^{start}) or HA2 (located between -2.0 kb and -1.0 kb) were required. However, HA2 only enabled high induction, when the inhibitory region IR1 (located between -4.3 kb and -2.6 kb) was absent and HA1, contrarily, acted independent of IR1. Whether LA1 was required for HA1 and/or HA2 to highly induce Sap2 expression was not directly tested, though, several *SAP2-1* promoter constructs containing HA1 and HA2, but lacking LA1 demonstrated inducibility of an *ecaFLP* reporter gene (Lermann, 2008). This indicates that expression from HA1 and HA2 did not rely on LA1 and consequently Sap2 expression was only then abolished, when all three regions were absent (Lermann, 2008) (Figure 2.13). Moreover, the identification of an inhibitory region is supported by incomplete suppression of *SAP2* promoter activity (i.e. leaky *SAP2* promoter activity), when controlled by a truncated/shorter promoter in non-inducing YPD medium (J. Morschhäuser; personal communication). There, expression of eca*FLP* was not completely repressed leading to subtle leaky Flp recombinase activity and MPA^R marker excision in some *C. albicans* strains, although no inducing BSA was present.

Gene expression is usually controlled by an interplay of different promoter elements rather than by one defined sequence. In *C. albicans*, for example, various distinct *cis*-acting elements were identified in the promoter of *MDR1*, encoding a multi-drug efflux pump. In the *MDR1* promoter a H_2O_2-responsive element (HRE) and a benomyl-responsive element (BRE) were identified (Harry *et al.*, 2005, Hiller *et al.*, 2006). However, in these studies also other regions were found to be required for benomyl-induced *MDR1* expression, indicating a strong dependence on the experimental induction conditions used in the different studies.

Additionally, a third region was responsible for *MDR1* overexpression in clinical isolates, but only when one of the two other activating regions was deleted (Hiller *et al.*, 2006).

Although binding motifs of the ortholog ScStp2 in *S. cerevisiae* have been identified the present work failed to determine a binding motif of CaStp1. However, two slightly distinct variations from the ScStp2 motif 5'-CGGCTC-3' (de Boer *et al.*, 2000) were identified in the *SAP2* promoter: the sequence 5'-CcGCTC-3', located between -2401 and -2336 and 5'-CGGCaC-3', located between -2295 and -2290 upstream of the ATG^{start}. The location of these two sites matched the identified Stp1-binding region and the characterized high activity region HA1 (Figure 2.16). Anyway, final proof of Stp1 binding to this sequence can only be obtained by analyzing the direct interaction of Stp1 and DNA-fragments containing the respective sequences, e.g. by EMSA (electrophoretic mobility shift assay).

The fact that only the HA1 region contains the Stp1 binding motifs and Stp1-HA bound to HA1 during growth in YCB-YE-BSA strongly implies that Stp1 controls *SAP2* expression mainly through binding to HA1. It also indicates that Stp1 might be dispensable for high *SAP2* induction through HA2 and for low induction through LA1, at least in YCB-YE-BSA.

However, the pivotal requirement of Stp1 for Sap2 expression suggests alternative binding to the Sap2 promoter, where Stp1 may also bind to the HA2 and LA1 regions in order to induce Sap2 expression. Stp1-HA binding to such sequences could have been undetectable by ChIP-on-chip due to low affinity binding or Stp1 binds only in the absence of certain regions to this sequences. Nevertheless, if Stp1 activates Sap2 expression via binding to LA1 it appears less effective and less efficient and activation via binding to HA2 requires absence of IR1. Alternatively, Stp1 may also activate *SAP2* expression via an intermediate regulator, which is supported by the fact that many other transcriptional regulators were among the Stp1 targets found by the genome wide binding study (Table 2.1 and Appendix A1). This would also explain that absence of the primary Stp1 binding site in HA1 did not abolished induction, since the intermediate factor still induces Sap2 expression, although less efficiently. In such scenario Stp1 directly and indirectly, via an intermediate transcriptional regulator, induces Sap2 expression. Consequently, deletion of *stp1* abolished Sap2 induction by Stp1 itself and by the intermediate regulator. Preliminary experiments failed to identify such an intermediate regulator (not shown). Within this trial 24 candidate genes were investigated, whether their overexpression can restore the growth of the *stp1*Δ/Δ null mutant in YCB-BSA. This approach was based on the TET-ON system (Weyler & Morschhäuser, 2012), were individual genes can

be overexpressed by the addition of the inducer doxycycline, or artificial activation of zinc-cluster transcription factors by C-terminal fusion of a Gal4-activation domain (Laboratory Morschhäuser; unpublished results). None of these candidate genes (*MDM34, STP1, EFG1, BCR1, MIG1, GCN4, AHR1, CBF1, TYE7, ZCF3, SFU1, TCC1, SSN6, GLN3, STP2, STP4, CTA4, RGT1, ZCF21, ZCF31, RPN4, NRG1, INO2,* and *ZCF2*), except for *STP1* itself, restored growth of the *stp1*Δ/Δ null mutant in YCB-BSA, when overexpressed or artificial activated. This showed that at least the 24 candidates were not able to induce Sap2 expression in a Stp1-independent manner and Stp1 is the major activator of Sap2 expression.

In order to show whether *SAP2* indeed can be expressed in a Stp1-independent manner its induction was tested in a *stp1*Δ/Δ background. The obtained results clearly demonstrated Stp1-indepented Sap2 expression during prolonged growth in YCB-YE-BSA, although extremely reduced (Figure 2.17). In this particular strains the *SAP2* promoter was not located at its endogenous genomic locus (but in the *ACT1* locus on chromosome 1) which might influence the dependency on Stp1, albeit the expression in the *ACT1* locus tested in this work was similar to that from the endogenous *SAP2* locus (Figure 2.10). On the other hand, *SAP2* expression might be differentially controlled with the additional nitrogen sources provided by the yeast extract, which might render *SAP2* induction, to a certain extent, Stp1-independent. Thus, an alternative activator of *SAP2* expression requires the presence of other low-molecular weight nitrogen sources to act Stp1-independent In line to this, identified Y.Chen *et al*. an additional regulator for *SAP2*, denoted *RSP1* (regulator of *SAP2* 1) (Chen *et al.*, 2008). Their work showed lower *SAP2* expression levels of a *C. albicans rsp1*Δ/Δ mutant and the mutant phenotype resembled that of a *sap2*Δ/Δ null mutant.

Similarly, induction from the *UPC2*-promoter was controlled by Upc2-dependent and Upc2-independent promoter regions (Hoot *et al.*, 2010, Hoot *et al.*, 2008). Moreover, a complex regulation by different transcription factors was also described for the expression of the drug efflux pump gene *MDR1*, e.g. by Mrr1, Cap1, Upc2, and Mcm1 (Mogavero *et al.*, 2011, Morschhäuser, 2010a, Schubert *et al.*, 2011)

In sum, the recent work delimited the promoter sequences responsible for the differential induction of the *SAP2* alleles to the proximal 1.2 kb region. Moreover, Sap2 expression is not controlled by one single defined *cis*-regulatory sequence, but rather by a complex interplay of multiple promoter sequences. Although Stp1 is the main regulator for Sap2 expression the present work demonstrated Stp1-independent induction of Sap2.

3.3 Utilization of proteins and peptides are not required for *C. albicans* gut colonization

To utilize proteins as source for cellular nitrogen their extracellular proteolytic degradation alone is not sufficient. Hence, the degradation products must be taken up by specialized transporters. *C. albicans* has two families of transporters, which possess the capacity to take up a great variety of di-, tri-, and oligopeptides. The *OPT* gene family encodes for eight distinct Opt transporters, that are considered to take up tetra- and pentapeptides. On the other hand, the *PTR* gene family has only two members and is considered to take up di- and tripeptides (Hauser *et al.*, 2001). The first evidence that a eukaryotic transporter facilitates peptide uptake was found by the restored dipeptide-growth of a peptide-uptake deficient *S. cerevisiae* mutant, when complemented with *ScPTR2* (Perry *et al.*, 1994). Similarly, the peptide transporters *CaPTR2* and *CaOPT1* from *C. albicans* were identified as *CaPTR2* restored growth of *S. cerevisiae ptr2*Δ mutant on a dipeptide (Basrai *et al.*, 1995), or as *CaOPT1* enabled growth on an otherwise non-utilized tetrapeptide and conferred sensitivity to toxic ethionine-based tetra- and pentapeptides (Lubkowitz *et al.*, 1997). That the substrate spectrum of the *OPT* system differed markedly from the *PTR* system was further supported by the investigation of other *OPT* genes from *Arabidopsis thalania* in the *S. cerevisiae ptr2*Δ mutant (Koh *et al.*, 2002). None of the heterologous expressed At*OPT* genes restored the growth defect on the tested di-and tripeptides, suggesting that Opts transport peptides longer than three residues. Indeed, Opts were shown to take up oligopeptides longer than 4 amino acids (Pike *et al.*, 2009, Reuss & Morschhäuser, 2006). Thereby, *C. albicans* Opts transported peptides with 8 amino acids and *A. thalania* Opt6 even peptide-based signal molecules with 13 amino acids. Moreover, the antimicrobial peptide Histatin-5, a 24-amino acid peptide, was demonstrated to be a substrate of the two polyamine transporters Dur3 and Dur31. There, Histatin-5 was shown to compete with the uptake of spermidine by these transporters and Histatin-5 resistance of *C. glabrata* was reversed by heterologous expression of Ca*DUR3* and Ca*DUR31* (Kumar *et al.*, 2011, Tati *et al.*, 2013). On the other side, tripeptide transport activity was also reported for CaOpt1 and the Opt transporter Isp4 from *Schizosacharomyces pombe*. In these studies uptake of a tetrapeptide (KLGL) was competitively inhibited, although not completely, by a tripeptide (KLG) (Lubkowitz *et al.*, 1998, Lubkowitz *et al.*, 1997).

The present study clearly demonstrated uptake of tripeptides by the *OPT* system in *C. albicans*. Several Opts (Opt1 to Opt4) mediated uptake of the tripeptide KFK and Opt1 additionally of LWL and AAP (Figure 2.21). Surprisingly, Opt1 also transported a dipeptide (RK), a feature not yet reported for oligopeptide transporters (Figure 2.20). Consequently, Opt1 appears to be the general Opt transporter, which has a broader substrate spectrum compared to the other Opts. Similarly, OptB from *A. fumigatus* demonstrated a higher substrate range than the other four tested Opts, indicating that OptB may is the general oligopeptide transporter in this fungus (Hartmann *et al.*, 2011). The fact that there is only one general Opt transporter in *C. albicans* and *A. fumigatus* reasoned that the whole *OPT* gene family had evolved out of this general *OPT* by gene duplication. The gene duplicates then diverged from this *OPT* gene in order to enlarged the substrate spectrum for the *OPT* system as means of adaption to available nitrogen sources.

It is noteworthy that ordinary deletion for individual peptide transporters would not have revealed the substrate spectrum identified in the present work. For example, *opt1*Δ/Δ null mutants are expected to grow on all tested defined peptides since peptides were taken up by the retained *PTR* system or other Opt transporters. Furthermore, the tripeptide LWL was identified as substrate for Ptr22 (Figure 2.21 top), which could not have been concluded from the phenotype of *ptr22*Δ/Δ null mutants, because these mutants demonstrated wild-type like growth on LWL (Hertlein, 2008), reasonably due to the uptake through Opt1. Additionally, individual transporters might not be sufficiently expressed, so that the respective null mutant phenotype would resemble the phenotype of a wild type, which simply does not express the transporter. Indeed, expression of *PTR2, OPT1,* and *OPT3* was shown to be controlled by the SPS-sensor and requires induction by extracellular amino acids (Martínez & Ljungdahl, 2005). Additionally, in *S. cerevisiae* the expression of the di-/tripeptide transporter gene Sc*PTR2* is, besides activation by ScStp1, repressed by ScCup9 (Ljungdahl, 2009). Activity of ScCup9 is controlled by ubiquitination, which accelerates its degradation and therefore releases Sc*PTR2* repression. A complex signal transduction pathway underlies this process, including the SPS-sensor system and activation of an ubiquitin-conjugating protein complex by direct di-/tripeptide binding (Hwang & Varshavsky, 2008). The overexpression of individual peptide transporters in the peptide-uptake deficient *opt1*Δ/Δ *opt2*Δ/Δ *opt3*Δ/Δ *opt4*Δ/Δ *opt5*Δ/Δ *ptr2*Δ/Δ *ptr22*Δ/Δ septuple mutant background bypassed these obstacles. Although, it cannot

be excluded that the retained Opt6 to Opt8 transporters, which might exhibit a more specific substrate spectrum, support growth under certain conditions.

The deletion of five major Opts and both Ptrs had no influence on the utilization of amino acids (at 10 mM concentration), which enabled wild-type like growth in both septuple mutants (Figure 2.18). The inability to efficiently grow on cysteine is largely attributed to its toxicity at elevated concentrations (like the used 10 mM), assuming that cysteine is not primarily used as nitrogen source, albeit *C. albicans* exhibits tolerance. The active excretion of sulfite has recently been reported as a cysteine detoxification mechanism in *C. albicans* (Hennicke *et al.*, 2013). Moreover, *C. albicans* growth was less efficiently supported by threonine, tryptophane, and tyrosine, unlike the efficient growth of the baker's yeast with these amino acids. On the other hand, histidine and lysine efficiently supported growth of *C. albicans*, but not for *S. cerevisiae*, suggesting differential capabilities between these two species in the use amino acids (Homann *et al.*, 2005).

The di-and tripeptide transporters Ptr2 and Ptr22 mediated uptake of all tested di- and tripeptides. Thereby, Ptr22 appears to have a broader substrate spectrum than Ptr2, since it supported growth on LWL, KFK, and AAP, whereas Ptr2 only mediated growth on AAP (Figure 2.21). Interestingly, the wild type SC5314 did not grow efficiently on certain dipeptides, whereas the overexpression of *PTR2* or *PTR22* supported growth on these dipeptides. This suggested that *PTR2* and *PTR22* were not sufficiently expressed. Actually, the wild type SC5314 grew only then, when the peptides were substrates of Opt1, implying that *OPT1* was expressed under the tested conditions.

It is noteworthy that one of the *opt1*Δ/Δ *opt2*Δ/Δ *opt3*Δ/Δ *opt4*Δ/Δ *opt5*Δ/Δ *ptr2*Δ/Δ *ptr22*Δ/Δ septuple mutants had acquired a general growth defect, which was not related to the deletion of the transporter genes (Table 2.6). However, the independent construction of the same mutant revealed this discrepancy, underscoring the importance of such control measures. Interestingly, this growth defect was only obvious under certain conditions, like growth in YPD and YNB-100mM NH_4^+ (Table 2.6 and Figure 2.22), but not during growth on amino acids or in the *in vivo* competition experiment (Figure 2.18 and Figure 2.23). Also the derivatives of this mutant demonstrated no defects, when grown with defined peptides or BSA as sole nitrogen source (Figure 2.20 and Figure 2.21). Conclusively, the growth defect, albeit only apparent under certain conditions, of this B-strain and its derivatives must be considered while analyzing obtained results.

Given that *C. albicans* has evolved two large gene families in order to utilize proteins as nitrogen source, the *SAP* and the *OPT* gene family, reasonably suggests that proteins or peptides are an important nitrogen source for this fungus, at least in certain host niches.

The peptide-uptake deficient *opt1*Δ/Δ *opt2*Δ/Δ *opt3*Δ/Δ *opt4*Δ/Δ *opt5*Δ/Δ *ptr2*Δ/Δ *ptr22*Δ/Δ septuple mutants allowed the assessment, whether proteins or peptides were indeed an important *in vivo* nitrogen source for *C. albicans*. For this purpose the fitness of the septuple mutants was analyzed during the competitive colonization of the mouse gastrointestinal tract. So if protein and peptide utilization is important for gut colonization then the septuple mutants should have a defect. However, while competing with a wild-type like strain in the mouse gut the septuple mutants demonstrated no fitness defect and colonized the gut mucosae as efficiently as a wild-type like strain (Figure 2.23). This indicates that sufficient alternative nitrogen sources, other than proteins and peptides, are available in the mouse intestine to support growth of peptide-uptake deficient *C. albicans* mutants. Nevertheless, in other host niches *C. albicans* may require the utilization of proteins and peptides as nitrogen source. Therefore, the *in vivo* competitive fitness of the septuple mutants was also assessed in a mouse model of systemic infection. Unfortunately, the recovered cells from the infected kidneys did not allowed reliable determination of fitness (not shown).

That oligopeptide transport was dispensable for virulence in a mouse model of systemic infection was already shown by preliminary studies, where the *opt1*Δ/Δ *opt2*Δ/Δ *opt3*Δ/Δ *opt4*Δ/Δ *opt5*Δ/Δ quintuple mutants demonstrated no attenuated virulence. (K. Schröppel, personal communication with J. Morschhäuser). Similarly, an *A. fumigatus* mutant, deleted for the whole *OPT* gene family, exhibited unaltered virulence in a neutropenic mouse model of pulmonary aspergillosis (Hartmann *et al.*, 2011).

These results suggest that proteins and peptides may not be the main nitrogen source of *C. albicans*, at least in the intestine of the mouse. Indeed, recent results suggested that primarily amino acids may serve as nitrogen source during colonization and systemic infection in a mouse model (Pérez *et al.*, 2013). This was proposed due to observed impairment in gut colonization and reduced fitness during systemic infection in a mouse model by *C. albicans* mutants deleted for *rgt1*Δ/Δ or *rgt3*Δ/Δ. Both factor, Rgt1 and Rgt3, were implicated in nitrogen acquisition from amino acids since their targets, identified by ChIP-on-chip analysis, were enriched for genes encoding amino acid permeases, but not for peptide transporters (except for *PTR22*) or secreted aspartic proteases (except for *SAP9*). Additionally, Stp2, the

major regulator controlling amino acid permease expression, was a target of Rgt1 and Rgt3. The authors of this study also proposed that allantoate, a product of purine catabolism, may represent a valuable *in vivo* nitrogen source. However, it remains elusive what primary nitrogen source *C. albicans* encounters and actually utilizes during the colonization or infection within the host. Most likely does the nutritional versatility enables the fungus to use whatever nitrogen source is available and accessible, thereby not relying on particular prominent nitrogenous compounds. *C. albicans* probably utilizes simultaneously various nitrogen sources, as suggested for the assimilation of different carbon sources (Fleck *et al.*, 2011). Nevertheless, the intestine of the mouse is obviously different from the human intestine, primarily because *C. albicans* is a commensal in the human gut, but not in the mouse. Consequently, the nutritional situation in the human intestine might be completely different than in the mouse and also diet and age severely influence the nutrient composition. It is noteworthy, that the closely related *C. tropicalis* was recently found as commensal in the mouse gut microbiome (Iliev *et al.*, 2012).

Nevertheless, peptide and proteins must be an important nitrogen source for *C. albicans*, at least in certain host niches, otherwise two large gene families involved in protein and peptide utilization are unlikely to have evolved and maintained by this fungus.

3.4 Ammonium must be taken up to control the expression of virulence-associated traits

Whatever nitrogenous compounds are available during *C. albicans* colonization or infection their usage as nitrogen source requires the proper acquisition and metabolic adaption by the fungus. NCR is a major regulatory mechanism by which a preferred nitrogen source represses gene expression required for the utilization of alternative/secondary nitrogen sources. Once the preferred nitrogen source gets depleted the repression is relieved and alternative nitrogen sources can be utilized. Moreover, quality and quantity of nitrogen sources are closely linked to pathogenesis in *C. albicans*. For example, the secreted aspartic protease Sap2 is expressed when non-preferred proteins serve as nitrogen source and hyphal growth is induced under nitrogen limitation (Morschhäuser, 2011). Thus, a preferred nitrogen sources, esp. ammonium, not only represses the utilization of alternative nitrogen sources but is also

capable to repress nitrogen-starvation-induced virulence traits. However, it is not quite clear whether the availability of certain nitrogen sources is determined by the intracellular nitrogen status or if dedicated cell-wall attached sensor proteins recognize their presence in the environment. In *S. cerevisiae* three major types of membrane nutrient sensors have been described (Rubio-Texeira *et al.*, 2010), denoted GPCRs (G-protein coupled receptors), transporting and non-transporting transceptors. The best characterized nutrient-sensing GPCR is ScGpr1 from *S. cerevisiae.* It activates the PKA pathway in response to fermentable sugars (glucose or sucrose) in the extracellular space in order to control growth, metabolism, and stress resistance (Lemaire *et al.*, 2004). Interestingly, a *C. albicans* null mutant of *gpr1*, the homolog of ScGpr1, was defective in amino acid induced (proline and methionine) filamentation, suggesting that these amino acids may trigger hyphal morphogenesis through ligand-binding to CaGpr1 (Maidan *et al.*, 2005). Other nutrient sensors are former nutrient transporters, which have lost their transport capability, but possessed a sensing and signaling function. Examples thereto are the yeast glucose sensors ScSnf3 and ScRgt2 and the amino acid sensor ScSsy1. ScSsy1 and also the *C. albicans* homolog CaSsy1 are the membrane associated sensors in the SPS-complex, which induces the expression of amino acid permeases, but also the Sap2 protease in *C. albicans*, in response to micromolar concentrations of extracellular amino acids (Ljungdahl, 2009). The last type of nutrient sensors promotes cellular responses while transporting and sensing nutrients simultaneously. For example, the three general amino acid permeases Gap1, Gap2, and Gap3 function as transporter and sensor for extracellular amino acids in *C. albicans* (Kraidlova *et al.*, 2011). They were shown to induce trehalase, a PKA pathway target, in response to external amino acids during heterologous expression in *S. cerevisiae*. Furthermore, the ammonium permease Mep2 is required for nitrogen-starvation (esp. low NH_4^+ concentrations) induced hyphal growth in *C. albicans*, thereby strongly implying a sensing function of the extracellular ammonium status (Biswas & Morschhäuser, 2005). However, it is currently not clear whether active transport through Mep2 is mandatory for the signaling activity or not (see section 1.10 “Nitrogen regulation”). Nevertheless, the variety of membrane-associated nutrient sensors suggested that external nutrient sensing, besides the cell’s determination of the internal nutrient status, has an important role in induction and coordination of metabolism and cellular responses.

Ammonium, a preferred nitrogen source by *C. albicans*, suppresses not only NCR-responsive gene expression, but also virulence-associated traits like Sap2 secretion and the switch to filamentous growth on solid media induced by other nitrogen sources.

To distinguish, whether extracellular or intracellular ammonium availability regulates expression of virulence-traits, ammonium-uptake deficient *mep* mutants were investigated. While comparing the behavior of the *mep* mutants with the wild type SC5314 it became clear that ammonium uptake was required to repress Sap2 secretion, arginine-induced filamentation, and genes required to utilize alternative nitrogen sources (e.g. *OPT3, DUR3,* and *DAL1*).

Supported is this further by the finding that ammonium-uptake deficient *S. cerevisiae mep1*Δ*mep2*Δ*mep3*Δ and *npr1Δ* null mutants, similarly, demonstrated expression of NCR-sensitive genes (*DAL5*, *DAL7*, and *MEP2* in the *npr1Δ* null mutant), albeit a repressing ammonium concentration (20 mM) was externally applied (Feller *et al.*, 2006). The authors further showed NCR-mediated repression was restored by the introduction of a heterologous NH_4^+ uptake system (HcAmt1 from *Hebeloma cylindrosporum*) into the Sc*npr1Δ* mutant, thereby demonstrating that ammonium uptake into the cell is required to suppress expression of these genes. Additionally, elevated NH_4^+ concentrations (80 mM) also restored the repression in these ammonium-uptake deficient mutants, suggesting that passive diffusion of gaseous NH_3 or unspecific NH_4^+ uptake was sufficient to mediate NCR. However, this was not observed for the Sc*npr1Δ* mutant, when tested in more acidic YNB-medium, which presumably favors protonated NH_4^+ and subsequently decreases the amount of freely diffusible NH_3. Similarly, passive diffusion of NH_3 at elevated NH_4^+ concentrations (76 mM) was also considered to enable wild-type like growth of *C. albicans mep1*Δ/Δ *mep2*Δ/Δ double mutants, which did not grow on low ammonium concentrations (Biswas & Morschhäuser, 2005).

Surprisingly, the recent study showed that repression of *SAP2* and *OPT3* expression by high NH_4^+ concentration was reduced/absent also in the *mep1*Δ/Δ single mutants, which contained *MEP2* (Figure 2.25 and Figure 2.28). But this could be correlated to insufficient expression of *MEP2* under the test conditions, thereby practically resembling an ammonium-uptake deficient *mep* double mutant (Figure 2.26). However, the constitutive expression of *MEP2* from the *ADH1* promoter in the *mep1*Δ/Δ mutant background did not restore repression of Sap2 production to wild-type levels (not shown), suggesting that forced *MEP2* expression was still not sufficient to fully restore Sap2 repression. Consistently, although *MEP2* mRNA levels

were increased, when expressed from the *ADH1*-promoter, only low Mep2 protein levels were detected by fluorescence microscopy in a previous work (Biswas & Morschhäuser, 2005). Hence, forced *MEP2* expression from the *ADH1*-promoter in this work was not sufficient to fully restore growth of a *mep1*Δ/Δ *mep2*Δ/Δ mutant on low ammonium. The authors therefore suggested that translation of *MEP2* transcripts was relatively inefficient, when carrying the *ADH1* upstream region.

The fact that expression of *DAL1* and *DUR3* was still residually repressed by ammonium in the *mep1*Δ/Δ *mep2*Δ/Δ mutants reasoned that these genes might be highly sensitive to ammonium availability (Figure 2.29 and Figure 2.30). Thus, a marginal concentration of passively diffused NH_3 already suppressed their expression, although only subtle.

It seems unlikely that ammonium is directly sensed since, once inside the cytosol, it is rapidly incorporated into α-ketoglutarate or glutamate, thereby producing glutamate and glutamine, respectively (Figure 1.5). Additionally, there is strong evidence from *S. cerevisiae* that intracellular glutamine levels, i.e. the ratio of glutamine/glutamate, is the control measure for the cell's nitrogen status and therefore controls NCR (Magasanik, 2005, Zaman *et al.*, 2008). There are also hints that ScGln3 might act as glutamate sensor (Marini *et al.*, 1997).

Interestingly, the inhibition of filamentation in *C. albicans* might be specific for ammonium and not the cellular nitrogen status. Hence, in contrast to ammonium, a 10 mM concentration of glutamine did not repress filamentation on solid agar (Biswas & Morschhäuser, 2005) although glutamine itself is a good nitrogen and represses *SAP2* production and BSA degradation at an identical concentration (not shown). Similarly, did urea and proline repress *SAP2* production and BSA degradation (Figure 2.27), but not filamentation at similar concentrations (Biswas & Morschhäuser, 2005). Somewhat surprising did urea not repress filamentation at higher concentrations (not shown), although it shares the assimilation pathway with NH_4^+ and even produces two ammonia molecules, when degraded (Figure 1.5). But this probably result from simultaneous CO_2 production by urea-breakdown that facilitates nitrogen source independent CO_2-induced filamentation (Ghosh *et al.*, 2009). Likewise to urea does arginine induces filamentation by raising intracellular CO_2 levels. However, nitrogen source independent CO_2-induced filamentation by arginine is inhibited under ammonium-replete conditions, but this is probably not due to direct interference of ammonium with the CO_2-pathway, but rather caused by simple repression of arginine uptake due to NCR.

Several studies provided additional hints that repression of filamentation might be independent of the cellular nitrogen status and specific for ammonium. For example, only ammonium was shown to efficiently repress *MEP2* expression, contrarily to 10 mM glutamine, which showed robust *MEP2* transcript levels in northern blot analysis (K. Biswas, unpublished results). A similar concentration (0.1% Gln, corresponding to > 10 mM) also failed to abolish expression of a P_{MEP2}-lacZ reporter fusion in *S. cerevisiae* (Marini *et al.*, 1997). Expression of *MEP2* for filamentation is thus important since Mep2 expression levels directly correlate with the filamentous growth, i.e. higher Mep2 levels resulted in increased filamentation (Biswas & Morschhäuser, 2005, Dabas & Morschhäuser, 2007). So if repression of filamentation is specific to ammonium, then only ammonium might repress Mep2 expression, while other nitrogen-replete conditions cannot efficiently downregulate Mep2 and consequently its hyphae inducing signaling activity. Alternatively, at elevated amino acid concentrations, were *MEP2* is repressed, the amino acids itself induce filamentation by different means, e.g. through CaGpr1 as demonstrated for proline and methionine (see above). Methionine can also induce hyphal formation in the presence of a high ammonium concentration (Maidan *et al.*, 2005). However, ammonium was also shown to repress filamentation in a Mep2-independent fashion, e.g. in a *mep2*Δ/Δ single mutant, when Ras1 or Gpa2 were dominant-active (Figure 1.3) (Biswas & Morschhäuser, 2005).

In conclusion, the way how *C. albicans* recognizes intracellular ammonium in order to repress filamentation stays unclear, but suppression of hyphae formation under ammonium-replete conditions is probably different from monitoring the cellular nitrogen status.

Lastly, whether ammonium or ammonia indeed is an available nitrogen source for *C. albicans* in the host remains elusive. However, there is a model proposing an interspecies flow of carbon and nitrogen between *Bacteroidetes* and *Firmicutes* (e.g. *Clostridium* spp.), the two dominant gut phyla (Fischbach & Sonnenburg, 2011). This was proposed as some bacterial strains are thought to depend on ammonia, since they cannot use free amino acids, peptides, nitrate, or urea as nitrogen source. Within this model *Firmicutes* assimilate peptides, amino acids, and urea, e.g. derived from diet, under the production and excretion of ammonia. The excreted ammonia, in turn, serves as nitrogen source for NH_3-dependent *Bacteriodes*. Supported is this by increased feces` content of urea, a main source of ammonia, when disturbing the microbial gut flora of rodents and humans by antibiotic treatment. Thus, disbalance decreases urease-mediated breakdown, thereby raising urea levels, by bacterial

strains. Possibly, the host might also secrete ammonium into the gut lumen in order to regulate growth of NH_3-dependent *Bacteriodes*. However, ammonium is toxic to mammalian cells and free ammonium is probably only transiently available and at very low concentrations. In a highly speculative scenario, certain *C. albicans* pathogenicity attributes might be suppressed by the transient ammonium levels in the microbial community in the gut. Hence, disturbance of the gut flora would create an ammonium-deplete situation, were certain virulence-traits become derepressed, supporting the commensal-to-pathogen switch.

In conclusion, the present work clearly demonstrated that ammonium has to be taken up to mediate NCR and to repress the expression of virulence-associated traits.

4 Material and Methods

4.1 Material

4.1.1 Growth media and agar

Table 4.1: Basic composition and supplements of growth media and agar used in this study

Growth media and agar	Basic composition	Supplemented substances
LB (Lysogeny broth)	1 % Peptone 0.5 % Yeast Extract 0.5 % NaCl (1.5 % Agar)	100 µg/ml ampicillin
YPD (yeast peptone dextrose)	2 % Peptone 1 % Yeast Extract 2 % Glucose (1.5 % Agar)	100, or 200 µg/ml Nourseothricin
YNB (yeast nitrogen base)	0.17 % YNB w/o amino acids and ammonium sulfate 2 % Glucose (2 % Agar)	0.05 to 50 mM ammonium sulfate 100 µM L-Arginine 1 mM Urea
YCB(-YE)-BSA (yeast carbon base)	1.17 % YCB 0.4 % BSA (0.2 % Yeast extract) pH 4.0 / pH 5.0	0.05 to 50 mM ammonium sulfate 1 mg/ml peptides 10 mM amino acids

4.1.2 General solutions

Table 4.2: Generals solutions with their basic composition and supplements

Solution	Composition
10xPBS (phosphate buffered saline)	38 mM KH_2PO_4 + 162 mM Na_2HPO_4 + 750 mM NaCl, pH7.4
10xTBS (tris buffered saline)	200 mM Tris-HCl pH 7.5 + 1.5 M NaCl
50xTAE	2 M Tris-Base + 1M actic acid + 0.05 M EDTA pH 8.0
5X DNA Loading dye	25 mM Tris-HCl pH 7.0 + 25% Glycerol + 150 mM EDTA pH 8.0 + 0.05% bromo phenol blue
10X TE	100 mM Tris-HCl pH 7.5 + 10 mM EDTA pH 7.5
Breaking Buffer for genomic DNA isolation	100 mM NaCl + 10 mM Tris-Cl pH 8.0 + 1 mM EDTA + 1% SDS + 2% Triton-X-100
20X SSC	3 M NaCl + 0.3 M tri-sodium citrate dihydrate
Southern Solution A	0.25 N HCl
Southern Solution B	1.5 M NaCl + 0.5 N NaOH
Southern Solution C	1.5 M NaCl, + 0.5 M Tris-Cl pH 7.5
Urea wash buffer	6 M Urea + 0.4% SDS + 0.5x SSC
Breaking Buffer for protein extraction	200 mM NaCl + 100 mM Tris-Cl + 20% glycerin + 5 mM EDTA pH 7.5 Freshly added: + 0.1 % β-Mercaptoethanol + 1xPIM (Protease Inhibitor Mix)
3xLämmli Loading Dye	240 mM Tris-Cl + 30% glycerin + 16% β-Mercaptoethanol + 6% SDS + 0.002% bromo phenol blue

Solution	Composition
10 x Running buffer for protein gels	2 M glycine + 250 mM Trisbase + 1% SDS
TES solution	10 mM Tris-Cl pH 7.5 + 10 mM EDTA + 0.5% SDS
DEPC-treated water	0.1% DEPC added and incubated overnight at 37°C and autoclaved
Lysis buffer (ChIP-on-chip)	50 mM HEPES-KOH pH 7.5 + 140 mM NaCl + 1 mM EDTA + 1% Triton X-100 + 0.1% Na-Deoxycholat Freshly added: + PIM (1 mM Phenylmethylsulfonyluorid, 1mM Benzamidin, 10 g/ml Aprotinin, 1 g/ml Leupeptin, 1 g/ml Pepstatin)
Wash buffer (ChIP-on-chip)	250 mM LiCl + 10 mM Tris-HCl pH 8.0 + 0.5% NP-40 + 0.5% Na-Deoxycholat + 1 mM EDTA pH 8.0
PBS-X% BSA	1x PBS + 0.1% / 0.5% BSA
PBST	1x PBS + 0.1% Tween 20
TE/SDS	1x TE + 1% SDS
phosphate wash buffer (ChIP-on-chip)	80% ethanol + 5 mM KH_2PO_4 pH 8.5

4.1.3 Enzymes and chemicals

Table 4.3: Enzymes and chemicals used in this study and their respective supplier

Enzymes and chemicals	Supplier / company
L-amino acids (Ala, Arg, Asn, Cys, Gln, Glu, His, Ile, Leu, Lys, Met, Orn, Phe, Pro, Ser, Thr, Trp, Tyr, Val)	Roth
2-propanole	Roth
30% Acrylamid mix solution	Roth / Applichem
aa-dUTP (5-(3-aminoallyl)-2'deoxyuridine-5'-triphosphate)	Sigma Aldrich
Acetic acid	Applichem
Agarose	Peqlab
Ammonium persulfate	Roth
Ampicillin	Roth
Bovine serum albumin (BSA) Fraction V	Gebru
Bromo phenol blue	AppliChem
Calcium chloride	Roth
Chloramphenicol	Roth
Chloroform	Merck
Coomassie Brilliant Blue R250	Serva
Cy5/Cy3 monoreactive dye packs	Amersham Biosciences
Difco Agar	BD
Dipeptides (AI, AL, AT, HL, KL, KP, LL, LS, LW, MM, RK)	Bachem
Disodium carbonate	Sigma Aldrich
DNA ladder 1 kb	Invitrogen
DNase I and DNase buffer	New England Biolabs
dNTPs	Fermentas / Sigma Aldrich
DTT (Dithiothretiole)	Roth
ECL "Enhanced chemiluminescence" Kit	Amersham Biosciences
EDTA	Roth
Ethanol	Roth
Ethidium bromide	Applichem
Formaldehyde	Roth

Enzymes and chemicals	Supplier / company
GelCode Blue Stain	ThermoScientific
Gentamycin sulfate salt	Sigma Aldrich
Glass beads	Roth
Glucose	Roth
Glycerin	Roth
Glycine	Roth
Glycogen	Roche
Hydrochloric acid	Roth
iQ™ SYBR® Green Supermix	Biorad
Isoamyl ethanol	Roth
Lithium acetate	AppliChem
Methanol	Roth
Microseal 96-Well PCR Plates, Skirted, low profile, white	Biorad
Microseal® 'B' Adhesive Seals	Biorad
Milk powder	Roth
Monoclonal rat anti-HA Antibody (3F10)	Roche
Monoclonal rat anti-HA Peroxidase (3F10)	Roche
Nourseothricin	Werner Bioagents
Nucleotides (dNTPs)	New England Biolabs
PageRuler™ Prestained Protein Ladder	Fermentas
Paq5000 DNA Polymerase	Agilent Technologies
PCI (Phenol/Chloroform/Isoamylalcohol)	Roth / Sigma Aldrich
Peptone / Tryptone	Roth
Pfu DNA Polymerase	Fermentas
Phusion High-Fidelity DNA polymerase	Finnzymes
Potassium phosphate	Sigma Aldrich
Protease Inhibitor Mix (PIM) cOmplete EDTA-free tablets	Roche
Proteinase K	Gibco
Quant-iT™ Picogreen dsDNA reagent	Invitrogen
Restriction enzymes (ApaI, BamHI, BglII, ClaI, EcoRI, EcRV, HindIII, KasI, KpnI, NarI, NdeI, NsiI, PstI, SacI, SacII, SalI, SpeI, XbaI, XhoI)	New England Biolabs
RNase A	
RNase Inhibitor, Murine	New England Biolabs
Sodium acetate	Roth / Sigma Aldrich
Sodium chloride	Roth
Sodium citrate	Roth
Sodium dodecylsulfate (SDS)	Roth
Sodium hydroxide	Roth
Sorbitol	Roth
SuperScript® III First-Strand Synthesis System	Invitrogen
T4 DNA Ligase	New England Biolabs / Invitrogen
T4 DNA Polymerase	New England Biolabs
Taq DNA Polymerase	New England Biolabs / Invitrogen
TEMED	Roth
Tetracycline-hydrochloride	Roth
TMB (3,3',5,5'-tetramethylbenzidine)	Thermo Scientific
Tripeptides (AAP, KFK, LWL)	Bachem

Enzymes and chemicals	Supplier / company
Tris-base	Roth
Tri-sodium citrate-dihydrate	Roth
Tween 20	Applichem
Urea	Roth
Yeast Carbon Base (YCB)	BD
Yeast extract (Bacto Yeast Extract)	BD
Yeast Nitrogen Base (YNB) w/o amino acids and ammonium sulfate	BD
β-mercaptoethanol	Applichem

4.1.4 Oligonucleotides

Oligonucleotides used for PCR reactions and sequencing were obtained from the company Eurofins MWG Operon as salt-free lyophilized powder and rehydrated with water.

Table 4.4: Oligonucleotides used in this study. Introduced restriction sites are underlined.

Name	5' → 3' sequence
Oligo 1	gcg gtg acc cgg gag atc tga att c
Oligo 2	gaa ttc aga tc
1007-1	ata tgt cga caa tgg tgt taa ttg tag ttg atg tac
1007-2	ata tag atc tta ctc tga aag tcc ttc gtc ttc ttc
ACT1RT	agt gtg aca tgg atg tta gaa aag aat tat acg g
ACT2RT	aca gag tat ttt ctt tct ggt gga gca
ACT38	ata tgg gcc ctg cag aca ttt tat gat gga atg aat ggg
BOI2-1	cca aaa aca ttt act caa tta ata acc a
BOI2-2	act agt gat act tgc ata ttg gga att t
CRZ2-1long	gtt aat cat tat ctc gag aat gtt atc aac cat gtc taa ttt gcc
CRZ2-2long	gtt aat cat tat aga tct att tat tag att gta ata att ttt taa
DAL1RTfor	caa gcc gtt ggc aca cac gc
DAL1RTrev	tcg gcg ttc tcc tgt tgc gc
EFB1A	aat gaa cga aat ctt ggc tga c
EFB1B	cat ctt ctt caa cag cag ctt g
FGR32-1	gat gca ttt gca gat tta att tca atc t
FGR32-2	caa gat cta att ttg tct tca atc ttg t
SAP2ex2	acc ccg gat cct tag gtc aag gca gaa ata ctg gaa gc
SAP2P1	ttg ttg ggc ccg ttg tca att tat ggg ccg atc tg
SAP2P2	cat tgg atc ctg gtg atg ttt agt ggg ttg ttg
SAP2P3	tta acc aat gac atc aga aat aga aag acg cc
SAP2P4	cgc acg cgt gaa tta ttg gta cta gaa agg
SAP2P5	ata tag ggc ccg cat ttg aat aaa cgg cat c
SAP2P6	caa taa aca tct aga aag aaa agg gta c
SAP2P7	ggg gtc tag aaa gtg aaa cgg gta ata ttg
SAP2P8	ata atc tag aaa agt tca agg tgt tta atg c
SAP2P9	gtt ctt aat ctg ttc aga tct aga att tca aaa aaa aga ata g
SAP2P10	tgg tgg gcc cgc tga tgc tcc ccg acg g
SAP2P12	ctc tac agt tgg act cat atg gc
SAP2P13	ggc tgg gga acg atc gta att ctg tag tga agc c
SAP2P14	act ttg act tct cga gtt ttt gcc agc

Name	5' → 3' sequence
SAP2P15	ggc ttt aaa tta ctc gag aaa ata tgg tta cgg c
SAP2P16	gca ttc aaa tta cct cga gca tta tta ttg tc
SAP2P17	gac aat aat aat gct cga ggt aat ttg aat gc
SAP2P18	gct cta tag ggc gtt gct ggg cat gtg gtg ggg c
SAP2P19	cca ata cgg tga caa caa caa tag att tcc gat ag
SAP2P20	gtg gta caa aac tta caa aca ata att atg aga ac
SAP2P21	gaa gaa gaa caa tag atc ttt caa ctc taa ctc
SAP2P22	cca tct aat ttc ttc ata cgg tcg ttc aat tc
SAP2P23	gca tgt aca tgt ctt tga ccg cct gaa tct cg
SAP2P24	cct caa taa aat ctc gag caa gaa ttg cgc
SAP2P25	gcg caa ttc ttg ctc gag att tta ttg agg
SAP2P26	aca ttt gat gtg agt gtg tca aaa taa tgt gtc
SAP2P29	ttc ggg ccc ctt gga act ttg act tta
SAP2P30	gaa acg ggc ccg gca cca caa aac aca
SAP2P33	aga agg gcc cta att aaa att act aat gat gt
SAP2P35	ttg ttg ttt caa tat ata act cga gct act tca
SAP2P36	agt agc tcg agt tat ata ttg aaa caa caa
SAP2P37	tct gtt act cga gag aaa gag cgg tat
SAP2P38	ctt tct ctc gag taa cag aaa ctc tta tc
STP1-5	atg aaa aga taa ggg ccc atg gaa agc c
STP1-6	agt tat agt cga cgt tct tta ata tg
STP1-7	ata tat cct gca ggt gta aag gc
STP1-8	taa tga aga gct cga acc tga acg
STP1-10	cta agg atc cat cta gta ata gat tg
TRK1-1	tgt tag act tta cta ctt tga gcg tca t
TRK1-2	tga gat atc act ggt ttc aga atc tat c
ZCF11-1	ata tgt cga caa tga aga tta aac agg aaa aca taa caa
ZCF11-2	ata tag atc tca tag tat tgg taa aaa gtt ccc cac

4.1.5 Plasmids and *C. albicans* mutants

All indicated positions were assigned respective to the nucleotide residue upstream of the cleavage site of the respective restriction enzyme.

Following abbreviations are used in the description:

(e)ca*FLP*: (enhanced) *C. albicans*-adapted *FLP* gene encoding the site specific recombinase Flp

ca*SAT1*: *C. albicans*-adapted nourseothricin resistance marker (dominant selection marker)

FRT: (Flp-recognition target) minimal recombination target sites of the Flp recombinase

GFP: Green fluorescent protein gene

XORF: open reading frame of the gene (X)

3xHA: HA-tag (human influenza hemaglutinin) with the amino acid sequence YPYDVPDYA

P_X: promoter of the gene (X)

5'X: upstream region of the gene (X)

3'X: downstream region of the gene (X)

ACT1T: Transcription termination sequence of the *ACT1* gene;

URA3: Orotidine-5'-phosphate decarboxylase gene,

Imm434: immunity region of λimm434

hisG: bacterial hisG sequences for spontaneous recombination

4.1.5.1 Plasmids

For bacterial cloning experiments *Escherichia coli* K12: *E. coli* strain DH5α (F-, endA1, hsdR17 [rk-, mk-], supE44, thi-1, recA1, gyrA96, relA1, Δ[argF-lac]U169, λ-, ϕ80dlacZΔM15) (Bethesda Research Laboratories, 1986) was used. All plasmids used in this study were based on the vector pBluescript KS II + (Stratagene, Heidelberg, Germany) and were listed in table

Table 4.5: Plasmids used in this study

Name	Genotype and description	Reference
Plasmids containing HA-tagged Stp1 and their respective donor plasmids		
pSTP1H1	[*STP1ORF-3xHA-ACT1T-caSAT1-FRT-3'STP1*] HA-tagged STP1	This study
pGAT1H1	[*GAT1ORF-3xHA-ACT1T-caSAT1-FRT-3'GAT1*] used to construct pSTP1H1	Laboratory Morschhäuser
pSTP1PG2	[*5'STP2-GFP-ACT1T-caSAT1*-3'*STP1*] used to construct pSTP1H1	(Dabas & Morschhäuser, 2008)
Plasmids containing both *SAP2* alleles and their respective donor plasmids		
pSAP2ex5	Used to construct pSAP2KS4	Laboratory Morschhäuser
pSAP2KS3	[$P_{SAP2\text{-}2}^{2037}$-*SAP2-2ORF-ACT1T-FRT-*P_{MAL2}-*caFLP-ACT1T-caSAT1-FRT-3'SAP2*] promoter contains 2037 bp upstream of *SAP2-2* ORF	(Lermann, 2008)
pSAP2KS4	[*PSAP2-2-SAP2-2ORF-3xHA-ACT1T-caSAT1*] promoter contains 4334 bp upstream of *SAP2-2* ORF	This study
pSAP2KS5	[*PSAP2-1-SAP2-1ORF-3xHA-ACT1T-caSAT1*] promoter contains 4334 bp upstream of *SAP2-1* ORF	This study
Plasmids containing *SAP2-HA* under control of differential shortened and internal deleted *SAP2* promotors and their respective donor plasmids		
pGFP73	[3'*ACT1-GFPORF-ACT1T-caSAT1*-5'*ACT1*] used to construct pSAP2H3	Laboratory Morschhäuser
pSAP2H1	[$P_{SAP2\text{-}1}^{293}$-*SAP2-1ORF-3xHA-ACT1T-caSAT1-3'SAP2*] used to construct pSAP2KS4, pSAP2KS5 and pSAP2Hxx	Laboratory Morschhäuser
pSAP2H2	[$P_{SAP2\text{-}1}^{2037}$-*SAP2-1ORF-3xHA-ACT1T-caSAT1-3'SAP2*] used to construct pSAP2H3 and pSAP2H6	Laboratory Morschhäuser
pSAP2H3	[3'*ACT1-*$P_{SAP2\text{-}2}^{4334}$-*SAP2-2ORF-3xHA-ACT1T-caSAT1*-5'*ACT1*] promoter contains 4334 bp upstream of *SAP2-2* ORF	This study
pSAP2H4	[3'*ACT1-*$P_{SAP2\text{-}2}^{2037}$-*SAP2-2ORF-3xHA-ACT1T-caSAT1*-5'*ACT1*] promotor contains 2037 bp upstream of *SAP2-2* ORF	This study
pSAP2H5	[3'*ACT1-*$P_{SAP2\text{-}1}^{4334}$-*SAP2-1ORF-3xHA-ACT1T-caSAT1*-5'*ACT1*] promoter contains 4334 bp upstream of *SAP2-1* ORF	This study
pSAP2H6	[3'*ACT1-*$P_{SAP2\text{-}1}^{2037}$-*SAP2-1ORF-3xHA-ACT1T-caSAT1*-5'*ACT1*] promoter contains 2037 bp upstream of *SAP2-1* ORF	This study

Name	Genotype and description	Reference
pSAP2H7	[3'*ACT1*-$P_{SAP2\text{-}2}^{1034}$-*SAP2-2ORF-3xHA-ACT1T-caSAT1*-5'*ACT1*] promoter contains 1034 bp upstream of *SAP2-2* ORF	This study
pSAP2H8	[3'*ACT1*-$P_{SAP2\text{-}2}^{759}$-*SAP2-2ORF-3xHA-ACT1T-caSAT1*-5'*ACT1*] promoter contains 759 bp upstream of *SAP2-2* ORF	This study
pSAP2H9	[3'*ACT1*-$P_{SAP2\text{-}1}^{1034}$-*SAP2-1ORF-3xHA-ACT1T-caSAT1*-5'*ACT1*] promoter contains 1034 bp upstream of *SAP2-1* ORF	This study
pSAP2H10	[3'*ACT1*-$P_{SAP2\text{-}1}^{759}$-*SAP2-1ORF-3xHA-ACT1T-caSAT1*-5'*ACT1*] promoter contains 759 bp upstream of *SAP2-1* ORF	This study
pSAP2H11	[3'*ACT1*-$P_{SAP2\text{-}2}^{618}$-*SAP2-2ORF-3xHA-ACT1T-caSAT1*-5'*ACT1*] promoter contains 618 bp upstream of *SAP2-2* ORF	This study
pSAP2H12	[3'*ACT1*-$P_{SAP2\text{-}1}^{618}$-*SAP2-1ORF-3xHA-ACT1T-caSAT1*-5'*ACT1*] promoter contains 759 bp upstream of *SAP2-1* ORF	This study
pSAP2H13	[3'*ACT1*-$P_{SAP2\text{-}1}^{\Delta 3556\text{-}1091}$-*SAP2-1ORF-3xHA-ACT1T-caSAT1*-5'*ACT1*] contains *SAP2-1* promoter with deletion between -3556 and -1091 bp upstream of *SAP2-1* ORF	This study
pSAP2H14	[3'*ACT1*-$P_{SAP2\text{-}1}^{\Delta 2566\text{-}1091}$-*SAP2-1ORF-3xHA-ACT1T-caSAT1*-5'*ACT1*] contains *SAP2-1* promoter with deletion between -2566 and -1091 bp upstream of *SAP2-1* ORF	This study
pSAP2H15	[3'*ACT1*-$P_{SAP2\text{-}1}^{\Delta 1824\text{-}1091}$-*SAP2-1ORF-3xHA-ACT1T-caSAT1*-5'*ACT1*] contains *SAP2-1* promoter with deletion between -1824 and -1091 bp upstream of *SAP2-1* ORF	This study
pSAP2H16	[3'*ACT1*-$P_{SAP2\text{-}1}^{\Delta 2566\text{-}1824}$-*SAP2-1ORF-3xHA-ACT1T-caSAT1*-5'*ACT1*] contains *SAP2-1* promoter with deletion between -2566 and -1824 bp upstream of *SAP2-1* ORF	This study
pSAP2H17	[3'*ACT1*-$P_{SAP2\text{-}1}^{\Delta 2186\text{-}1824}$-*SAP2-1ORF-3xHA-ACT1T-caSAT1*-5'*ACT1*] contains *SAP2-1* promoter with deletion between -2186 and -1824 bp upstream of *SAP2-1* ORF	This study
pSAP2H18	[3'*ACT1*-$P_{SAP2\text{-}1}^{\Delta 2566\text{-}2186}$-*SAP2-1ORF-3xHA-ACT1T-caSAT1*-5'*ACT1*] contains *SAP2-1* promoter with deletion between -2566 and -2186 bp upstream of *SAP2-1* ORF	This study
pSAP2H19	[3'*ACT1*-$P_{SAP2\text{-}2}^{\Delta 2566\text{-}1091}$-*SAP2-2ORF-3xHA-ACT1T-caSAT1*-5'*ACT1*] contains *SAP2-2* promoter with deletion between -2566 and -1091 bp upstream of *SAP2-2* ORF	This study
pSAP2H20	[3'*ACT1*-$P_{SAP2\text{-}2}^{\Delta 1824\text{-}1091}$-*SAP2-2ORF-3xHA-ACT1T-caSAT1*-5'*ACT1*] contains *SAP2-2* promoter with deletion between -1824 and -1091 bp upstream of *SAP2-2* ORF	This study
pSAP2H21	[3'*ACT1*-$P_{SAP2\text{-}2}^{\Delta 2566\text{-}1824}$-*SAP2-2ORF-3xHA-ACT1T-caSAT1*-5'*ACT1*] contains *SAP2-2* promoter with deletion between -2566 and -1824 bp upstream of *SAP2-2* ORF	This study
pSAP2H22	[3'*ACT1*-$P_{SAP2\text{-}2}^{\Delta 2186\text{-}1824}$-*SAP2-2ORF-3xHA-ACT1T-caSAT1*-5'*ACT1*] contains *SAP2-2* promoter with deletion between -2186 and -1824 bp upstream of *SAP2-2* ORF	This study
pSAP2H23	[3'*ACT1*-$P_{SAP2\text{-}2}^{\Delta 2566\text{-}2186}$-*SAP2-2ORF-3xHA-ACT1T-caSAT1*-5'*ACT1*] contains *SAP2-2* promoter with deletion between -2566 and -2186 bp upstream of *SAP2-2* ORF	This study
pSAP2H24	[3'*ACT1*-$P_{SAP2\text{-}2}^{\Delta 1824\text{-}1454}$-*SAP2-2ORF-3xHA-ACT1T-caSAT1*-5'*ACT1*] contains *SAP2-2* promoter with deletion between -1824 and -1454 bp upstream of *SAP2-2* ORF	This study

Name	Genotype and description	Reference
pSAP2H25	[3'*ACT1*-$P_{SAP2\text{-}2}^{\Delta 1454\text{-}1091}$-*SAP2-2ORF-3xHA-ACT1T-caSAT1*-5'*ACT1*] contains *SAP2-2* promoter with deletion between -1454 and -1091 bp upstream of *SAP2-2* ORF	This study
pSAP2H26	[3'*ACT1*-$P_{SAP2\text{-}2}^{\Delta 2566\text{-}2390}$-*SAP2-2ORF-3xHA-ACT1T-caSAT1*-5'*ACT1*] contains *SAP2-2* promoter with deletion between -2566 and -2390 bp upstream of *SAP2-2* ORF	This study
pSAP2H27	[3'*ACT1*-$P_{SAP2\text{-}2}^{\Delta 2390\text{-}2186}$-*SAP2-2ORF-3xHA-ACT1T-caSAT1*-5'*ACT1*] contains *SAP2-2* promoter with deletion between -2390 and -2186 bp upstream of *SAP2-2* ORF	This study
pSFL223	[$P_{SAP2\text{-}1}^{\Delta 3556\text{-}1091}$-*ecaFLP-ACT1T-URA3-3'SAP2*] used to construct pSAP2H13	(Lermann, 2008)
pSFL224A	[$P_{SAP2\text{-}2}^{\Delta 2566\text{-}1091}$-*ecaFLP-ACT1T-URA3-3'SAP2*] used to construct pSAP2H14	(Lermann, 2008)
pSFL224B	[$P_{SAP2\text{-}1}^{\Delta 2566\text{-}1091}$-*ecaFLP-ACT1T-URA3-3'SAP2*] used to construct pSAP2H14	(Lermann, 2008)
pSFL225	[$P_{SAP2\text{-}1}^{\Delta 1824\text{-}1091}$-*ecaFLP-ACT1T-URA3-3'SAP2*] used to construct pSAP2H15	(Lermann, 2008)
pSFL226	[$P_{SAP2\text{-}1}^{\Delta 2566\text{-}1824}$-*ecaFLP-ACT1T-URA3-3'SAP2*] used to construct pSAP2H16	(Lermann, 2008)
pSFL227	[$P_{SAP2\text{-}1}^{\Delta 2186\text{-}1824}$-*ecaFLP-ACT1T-URA3-3'SAP2*] used to construct pSAP2H17	(Lermann, 2008)
pSFL228	[$P_{SAP2\text{-}1}^{\Delta 2566\text{-}2186}$-*ecaFLP-ACT1T-URA3-3'SAP2*] used to construct pSAP2H18	(Lermann, 2008)
Plasmids containing *GFP* reporter fusions of *OPT3* and *DUR3*		
pOPT3G22	[*5'OPT3-GFP-ACT1T-caSAT1*-3'*OPT3*] contains *GFP* under control of the *OPT3* promoter	(Reuss & Morschhäuser, 2006)
pDUR3G2	[*5'DUR3-GFP-ACT1T-caSAT1*-3'*DUR3*] contains *GFP* under control of the *DUR3* promoter	Laboratory Morschhäuser

4.1.5.2 *C. albicans* strains

All *C. albicans* strains used in this study are summarized in Table 4.6. The genetic background for all mutant strains was the wild type SC5314 (Gillum *et al.*, 1984), if not indicated otherwise. Note that according to the laboratory quality standards each mutant was generated two times in an independent fashion as indicated with the suffix A or B.

Table 4.6: *C. albicans* strains used in this study

Name	Genotype and description	Reference
SC5314	*Candida albicans* wild-type strain	(Gillum *et al.*, 1984)
Strains expressing Stp1-HA and its parental strains		
STP1M4 A/B	[*stp1*Δ::*FRT*/*stp1*Δ::*FRT*] homozygous *stp1* null mutants	Laboratory Morschhäuser
***stp1*ΔSTP1H1 A/B**	[*stp1*Δ::*FRT*/*stp1*Δ:: P_{STP1}-*STP1-3xHA*] homozygous *stp1* null mutant with 3xHA-tagged *STP1* under control of its own promoter	This study
***sap* single and multiple deletion strains**		
DSY459	[*ura3*Δ::*imm434*/*ura3*Δ::*imm434* *sap4*Δ::*hisG*/ *sap4*Δ::*hisG* *sap5*Δ::*hisG*/ *sap5*Δ::*hisG-URA3-hisG* *sap6*Δ::*hisG*/ *sap6*Δ::*hisG*] triple *sap4 sap5 sap6* deletion mutant derived from CAI4	(Sanglard *et al.*, 1997)
SAP456MS4 A/B	[*sap4*Δ::*FRT*/*sap4*Δ::*FRT* *sap5*Δ::*FRT*/*sap5*Δ::*FRT* *sap6*Δ::*FRT*/*sap6*Δ::*FRT*] triple *sap4 sap5 sap6* deletion mutant derived from SC5314	(Lermann & Morschhäuser, 2008)
SAP2MS2 A	[*sap2-1*Δ::*FRT*/*SAP2-2*] heterozygous *sap2* mutant, deleted for the *sap2-1* allele	(Staib *et al.*, 2008)
SAP2MS2 B	[*SAP2-1*/*sap2-2*Δ::*FRT*] heterozygous *sap2* mutant, deleted for the *sap2-2* allele	(Staib *et al.*, 2008)
SAP2MS4 A/B	[*sap2-1*Δ::*FRT*/*sap2-2*Δ::*FRT*] homozygous *sap2* null mutants	(Staib *et al.*, 2008)
Strains used to assess the effects of LOH in the *SAP2* locus		
YJB10698	[*gal1*::*URA3*/*gal1*::*URA3*] Strain homozygous for chromosome R (harboring only the *SAP2-1* allele)	(Legrand *et al.*, 2008)
DSY459-transformants A1-A6/B1-B6	[*ura3*Δ::*imm434*/*ura3*Δ::*imm434* *sap4*Δ::*hisG*/ *sap4*Δ::*hisG* *sap5*Δ::*hisG*/ *sap5*Δ::*hisG-URA3-hisG* *sap6*Δ::*hisG*/ *sap6*Δ::*hisG* *sap2-1*Δ::*FRT*/*sap2-1*Δ::*SAP2-2-caSAT1*] triple *sap4*Δ *sap5*Δ *sap6*Δ deletion mutants with differently reintroduced *SAP2-2* sequences	This study

Name	Genotype and description	Reference
SC5314-transformants A1-A6/B1-B6	[*SAP2*/*sap2*Δ::*SAP2-1-caSAT1*] SC5314 mutants with differently replaced *SAP2* sequences	This study
Strains expressing Sap2-HA from distinct deleted promoters		
SCSAP2H1 A	[*sap2-1*Δ::*SAP2-HA-caSAT1*/*SAP2-2*] Contains Sap2-HA in the endogenous *SAP2-1* locus	Laboratory Morschhäuser
SCSAP2H1 B	[*SAP2-1*/*sap2-2*Δ::*SAP2-HA-caSAT1*] Contains Sap2-HA in the endogenous *SAP2-2* locus	Laboratory Morschhäuser
SCSAP2H3 A/B	[*ACT1*/*act1*Δ::P_{SAP2-2}^{4334}-*SAP2-HA-caSAT1*] Contain Sap2-HA in the *ACT1* locus controlled by a full length 4334 bp P_{SAP2-2} promoter	This study
SCSAP2H4 A/B	[*ACT1*/*act1*Δ::P_{SAP2-2}^{2037}-*SAP2-HA-caSAT1*] Contain Sap2-HA in the *ACT1* locus controlled by a 2037 bp P_{SAP2-2} promoter	This study
SCSAP2H5 A/B	[*ACT1*/*act1*Δ::P_{SAP2-1}^{4334}-*SAP2-HA-caSAT1*] Contain Sap2-HA in the *ACT1* locus controlled by a full length 4334 bp P_{SAP2-1} promoter	This study
SCSAP2H6 A/B	[*ACT1*/*act1*Δ::P_{SAP2-1}^{2037}-*SAP2-HA-caSAT1*] Contain Sap2-HA in the *ACT1* locus controlled by a 2037 bp P_{SAP2-1} promoter	This study
SCSAP2H7 A/B	[*ACT1*/*act1*Δ::P_{SAP2-2}^{1034}-*SAP2-HA-caSAT1*] Contain Sap2-HA in the *ACT1* locus controlled by a 1034 bp P_{SAP2-2} promoter	This study
SCSAP2H8 A/B	[*ACT1*/*act1*Δ::P_{SAP2-2}^{759}-*SAP2-HA-caSAT1*] Contain Sap2-HA in the *ACT1* locus controlled by a 759 bp P_{SAP2-2} promoter	This study
SCSAP2H9 A/B	[*ACT1*/*act1*Δ::P_{SAP2-1}^{1034}-*SAP2-HA-caSAT1*] Contain Sap2-HA in the *ACT1* locus controlled by a 1034 bp P_{SAP2-1} promoter	This study
SCSAP2H10 A/B	[*ACT1*/*act1*Δ::P_{SAP2-1}^{759}-*SAP2-HA-caSAT1*] Contain Sap2-HA in the *ACT1* locus controlled by a 759 bp P_{SAP2-1} promoter	This study
SCSAP2H11 A/B	[*ACT1*/*act1*Δ::P_{SAP2-2}^{618}-*SAP2-HA-caSAT1*] Contain Sap2-HA in the *ACT1* locus controlled by a 618 bp P_{SAP2-2} promoter	This study
SCSAP2H12 A/B	[*ACT1*/*act1*Δ::P_{SAP2-1}^{618}-*SAP2-HA-caSAT1*] Contain Sap2-HA in the *ACT1* locus controlled by a 618 bp P_{SAP2-1} promoter	This study
SCSAP2H13 A/B	[*ACT1*/*act1*Δ::$P_{SAP2-1}^{\Delta 3556-1091}$-*SAP2-HA-caSAT1*] Contain Sap2-HA in the *ACT1* locus controlled by a P_{SAP2-1} promoter with deletion between -3556 and -1091	This study
SCSAP2H14 A/B	[*ACT1*/*act1*Δ::$P_{SAP2-1}^{\Delta 2566-1091}$-*SAP2-HA-caSAT1*] Contain Sap2-HA in the *ACT1* locus controlled by a P_{SAP2-1} promoter with deletion between -2566 and -1091	This study
SCSAP2H15 A/B	[*ACT1*/*act1*Δ::$P_{SAP2-1}^{\Delta 1824-1091}$-*SAP2-HA-caSAT1*] Contain Sap2-HA in the *ACT1* locus controlled by a P_{SAP2-1} promoter with deletion between -1824 and -1091	This study

Name	Genotype and description	Reference
SCSAP2H16 A/B	[*ACT1*/*act1*Δ::$P_{SAP2\text{-}1}^{\Delta 2566\text{-}1824}$-*SAP2-HA-caSAT1*] Contain Sap2-HA in the *ACT1* locus controlled by a $P_{SAP2\text{-}1}$ promoter with deletion between -2566 and -1824	This study
SCSAP2H17 A/B	[*ACT1*/*act1*Δ::$P_{SAP2\text{-}1}^{\Delta 2186\text{-}1824}$-*SAP2-HA-caSAT1*] Contain Sap2-HA in the *ACT1* locus controlled by a $P_{SAP2\text{-}1}$ promoter with deletion between -2186 and -1824	This study
SCSAP2H18 A/B	[*ACT1*/*act1*Δ::$P_{SAP2\text{-}1}^{\Delta 2566\text{-}2186}$-*SAP2-HA-caSAT1*] Contain Sap2-HA in the *ACT1* locus controlled by a $P_{SAP2\text{-}1}$ promoter with deletion between -2566 and -2186	This study
SCSAP2H19 A/B	[*ACT1*/*act1*Δ::$P_{SAP2\text{-}2}^{\Delta 2566\text{-}1091}$-*SAP2-HA-caSAT1*] Contain Sap2-HA in the *ACT1* locus controlled by a $P_{SAP2\text{-}2}$ promoter with deletion between -2566 and -1091	This study
SCSAP2H20 A/B	[*ACT1*/*act1*Δ::$P_{SAP2\text{-}2}^{\Delta 1824\text{-}1091}$-*SAP2-HA-caSAT1*] Contain Sap2-HA in the *ACT1* locus controlled by a $P_{SAP2\text{-}2}$ promoter with deletion between -1824 and -1091	This study
SCSAP2H21 A/B	[*ACT1*/*act1*Δ::$P_{SAP2\text{-}2}^{\Delta 2566\text{-}1824}$-*SAP2-HA-caSAT1*] Contain Sap2-HA in the *ACT1* locus controlled by a $P_{SAP2\text{-}2}$ promoter with deletion between -2566 and -1824	This study
SCSAP2H22 A/B	[*ACT1*/*act1*Δ::$P_{SAP2\text{-}2}^{\Delta 2186\text{-}1824}$-*SAP2-HA-caSAT1*] Contain Sap2-HA in the *ACT1* locus controlled by a $P_{SAP2\text{-}2}$ promoter with deletion between -2186 and -1824	This study
SCSAP2H23 A/B	[*ACT1*/*act1*Δ::$P_{SAP2\text{-}2}^{\Delta 2566\text{-}2186}$-*SAP2-HA-caSAT1*] Contain Sap2-HA in the *ACT1* locus controlled by a $P_{SAP2\text{-}2}$ promoter with deletion between -2566 and -2186	This study
SCSAP2H24 A/B	[*ACT1*/*act1*Δ::$P_{SAP2\text{-}2}^{\Delta 1824\text{-}1454}$-*SAP2-HA-caSAT1*] Contain Sap2-HA in the *ACT1* locus controlled by a $P_{SAP2\text{-}2}$ promoter with deletion between -1824 and -1454	This study
SCSAP2H25 A/B	[*ACT1*/*act1*Δ::$P_{SAP2\text{-}2}^{\Delta 1454\text{-}1091}$-*SAP2-HA-caSAT1*] Contain Sap2-HA in the *ACT1* locus controlled by a $P_{SAP2\text{-}2}$ promoter with deletion between -1454 and -1091	This study
SCSAP2H26 A/B	*ACT1*/*act1*Δ::$P_{SAP2\text{-}2}^{\Delta 2566\text{-}2390}$-*SAP2-HA-caSAT1*] Contain Sap2-HA in the *ACT1* locus controlled by a $P_{SAP2\text{-}2}$ promoter with deletion between -2566 and -2390	This study
SCSAP2H27 A/B	*ACT1*/*act1*Δ::$P_{SAP2\text{-}2}^{\Delta 2390\text{-}2186}$-*SAP2-HA-caSAT1*] Contain Sap2-HA in the *ACT1* locus controlled by a $P_{SAP2\text{-}2}$ promoter with deletion between -2390 and -2186	This study
Strains expressing Sap2-HA in the *stp1*Δ/Δ background		
SCΔ*stp1*SAP2H3 A/B	[*stp1*Δ::*FRT*/*stp1*Δ::*FRT* *ACT1*/*act1*Δ::$P_{SAP2\text{-}2}^{4334}$-*SAP2-HA-caSAT1*] Contain Sap2-HA in the *ACT1* locus controlled by a full length 4334 bp $P_{SAP2\text{-}2}$ promoter	This study
SCΔ*stp1*SAP2H4 A/B	[*stp1*Δ::*FRT*/*stp1*Δ::*FRT* *ACT1*/*act1*Δ::$P_{SAP2\text{-}2}^{2037}$-*SAP2-HA-caSAT1*] Contain Sap2-HA in the *ACT1* locus controlled by a 2037 bp $P_{SAP2\text{-}2}$ promoter	This study
SCΔ*stp1*SAP2H5 A/B	[*stp1*Δ::*FRT*/*stp1*Δ::*FRT* *ACT1*/*act1*Δ::$P_{SAP2\text{-}1}^{4334}$-*SAP2-HA-caSAT1*] Contain Sap2-HA in the *ACT1* locus controlled by a full length 4334 bp $P_{SAP2\text{-}1}$ promoter	This study

Name	Genotype and description	Reference
SCΔ*stp1*SAP2H6 A/B	[*stp1*Δ::*FRT*/*stp1*Δ::*FRT* *ACT1*/*act1*Δ::$P_{SAP2\text{-}1}^{2037}$-*SAP2-HA-caSAT1*] Contain Sap2-HA in the *ACT1* locus controlled by a 2037 bp $P_{SAP2\text{-}1}$ promoter	This study
***mep* deletion mutants**		
SCMEP1M4 A/B	[*mep1-1Δ::FRT*/*mep1-2Δ::FRT*] homozygous *mep1* null mutants	Laboratory Morschhäuser
SCMEP2M4 A/B	[*mep2-1Δ::FRT*/*mep2-2Δ::FRT*] homozygous *mep2* null mutants	(Dabas & Morschhäuser , 2007)
SCMEP12M4 A/B	[*mep1-1Δ::FRT*/*mep1-2Δ::FRT* *mep2-1Δ::FRT*/*mep2-2Δ::FRT*] homozygous *mep1* and *mep2* double null mutants	(Neuhäuser *et al.*, 2011)
***MEP2-GFP* reporter strains**		
SCMEP2G7 A	[*mep2-1Δ::*$P_{MEP2\text{-}1}$*-MEP2-GFP*/*MEP2-2*] homozygous *mep1* null mutants with *MEP2-GFP* Fusion under control of the *MEP2-1*-Promoter	(Dabas & Morschhäuser , 2007)
SCMEP2G7 B	[*MEP2-1*/*mep2-2Δ::*$P_{MEP2\text{-}2}$*-MEP2-GFP*] homozygous *mep1* null mutants with *MEP2-GFP* Fusion under control of the *MEP2-2*-Promoter	(Dabas & Morschhäuser , 2007)
***OPT3*-promoter reporter strains**		
SCOPT3G22 A	[*opt3-1*Δ::$P_{OPT3\text{-}2}$*-GFP /OPT3-2*] SC5314 with *GFP* under control of the *OPT3-1* Promoter	(Reuss & Morschhäuser , 2006)
SCOPT3G22 B	[*OPT3-1/opt3-2*Δ::$P_{OPT3\text{-}2}$*-GFP*] SC5314 with *GFP* under control of the *OPT3-2* Promoter	(Reuss & Morschhäuser , 2006)
SC*Δmep1*OPT3G22 A/B	[*mep1-1Δ::FRT*/*mep1-2Δ::FRT* *OPT3-1/opt3-2*Δ::$P_{OPT3\text{-}2}$*-GFP*] homozygous *mep1* null mutants with *GFP* under control of the *OPT3-2* Promoter	This study
SC*Δmep2*OPT3G22 A/B	[*mep2-1Δ::FRT*/*mep2-2Δ::FRT* *OPT3-1/opt3-2*Δ::$P_{OPT3\text{-}2}$*-GFP*] homozygous *mep2* null mutants with *GFP* under control of the *OPT3-2* Promoter	This study
SC*Δmep12*OPT3G22 A/B	[*mep1-1Δ::FRT*/*mep1-2Δ::FRT* *mep2-1Δ::FRT*/*mep2-2Δ::FRT* *OPT3-1/opt3-2*Δ::$P_{OPT3\text{-}2}$*-GFP*] homozygous *mep1* and *mep2* double null mutants with *GFP* under control of the *OPT3-2* Promoter	This study
***DUR3*-promoter reporter strains**		
SCDUR3G2 A/B	[*DUR3*Δ::*FRT*/*dur3*Δ::P_{DUR3}*-GFP*] SC5314 with *GFP* under control of the *DUR3* Promoter	This study
SC*Δmep12*DUR3G2 A/B	[*mep1-1Δ::FRT*/*mep1-2Δ::FRT* *mep2-1Δ::FRT*/*mep2-2Δ::FRT* *DUR3*Δ::*FRT*/*dur3*Δ::P_{DUR3}*-GFP*] homozygous *mep1* and *mep2* double null mutants with *GFP* under control of the *DUR3* Promoter	This study

Name	Genotype and description	Reference
***RFP*-labeled wild type strain**		
SCADH1R1A	[*ADH1/adh1*Δ::P_{ADH1}-*RFP-caSAT1*] *Candida albicans* wild type strain marked with *RFP* and the *caSAT1* marker	(Sasse *et al.*, 2012)
***opt* and *ptr* septuple deletion mutants and *OPT* and *PTR* overexpressing strains**		
OPT12345PTR222M4 A/B	[*opt1-1*Δ::*FRT*/*opt1-2*Δ::*FRT* *opt23-1*Δ::*FRT*/*opt23-1*Δ::*FRT* *opt4-1*Δ::*FRT*/*opt4-2*Δ::*FRT* *opt5-1*Δ::*FRT*/*opt5-2*Δ::*FRT* *ptr2-1*Δ::*FRT*/ptr2-*2*Δ::*FRT* *ptr22-1*Δ::*FRT*/ptr22-*2*Δ::*FRT*] homozygous null mutants for *opt1, opt2, opt3, opt4, opt5, ptr2,* and *ptr22*	Laboratory Morschhäuser
OPT12345PTR222MOE1 A/B	[*opt1-1*Δ::*FRT*/*opt1-2*Δ::*FRT* *opt23-1*Δ::*FRT*/*opt23-1*Δ::*FRT* *opt4-1*Δ::*FRT*/*opt4-2*Δ::*FRT* *opt5-1*Δ::*FRT*/*opt5-2*Δ::*FRT* *ptr2-1*Δ::*FRT*/ptr2-*2*Δ::*FRT* *ptr22-1*Δ::*FRT*/ptr22-*2*Δ::*FRT* *ADH1/adh1*Δ::P_{ADH1}-*OPT1*] homozygous null mutants for *opt1, opt2, opt3, opt4, opt5, ptr2,* and *ptr22* with *OPT1* expressed from *ADH1*-Promoter	Laboratory Morschhäuser
OPT12345PTR222MOE2 A/B	[*opt1-1*Δ::*FRT*/*opt1-2*Δ::*FRT* *opt23-1*Δ::*FRT*/*opt23-1*Δ::*FRT* *opt4-1*Δ::*FRT*/*opt4-2*Δ::*FRT* *opt5-1*Δ::*FRT*/*opt5-2*Δ::*FRT* *ptr2-1*Δ::*FRT*/ptr2-*2*Δ::*FRT* *ptr22-1*Δ::*FRT*/ptr22-*2*Δ::*FRT* *ADH1/adh1*Δ::P_{ADH1}-*OPT2*] homozygous null mutants for *opt1, opt2, opt3, opt4, opt5, ptr2,* and *ptr22* with *OPT2* expressed from *ADH1*-Promoter	Laboratory Morschhäuser
OPT12345PTR222MOE3 A/B	[*opt1-1*Δ::*FRT*/*opt1-2*Δ::*FRT* *opt23-1*Δ::*FRT*/*opt23-1*Δ::*FRT* *opt4-1*Δ::*FRT*/*opt4-2*Δ::*FRT* *opt5-1*Δ::*FRT*/*opt5-2*Δ::*FRT* *ptr2-1*Δ::*FRT*/ptr2-*2*Δ::*FRT* *ptr22-1*Δ::*FRT*/ptr22-*2*Δ::*FRT* *ADH1/adh1*Δ::P_{ADH1}-*OPT3*] homozygous null mutants for *opt1, opt2, opt3, opt4, opt5, ptr2,* and *ptr22* with *OPT3* expressed from *ADH1*-Promoter	Laboratory Morschhäuser

Name	Genotype and description	Reference
OPT12345PTR222MOE4 A/B	[*opt1-1*Δ::*FRT*/*opt1-2*Δ::*FRT* *opt23-1*Δ::*FRT*/*opt23-1*Δ::*FRT* *opt4-1*Δ::*FRT*/*opt4-2*Δ::*FRT* *opt5-1*Δ::*FRT*/*opt5-2*Δ::*FRT* *ptr2-1*Δ::*FRT*/ptr2-*2*Δ::*FRT* *ptr22-1*Δ::*FRT*/ptr22-*2*Δ::*FRT* *ADH1/adh1*Δ::P_{ADH1}-*OPT4*] homozygous null mutants for *opt1, opt2, opt3, opt4, opt5, ptr2,* and *ptr22* with *OPT4* expressed from *ADH1*-Promoter	Laboratory Morschhäuser
OPT12345PTR222MOE5 A/B	[*opt1-1*Δ::*FRT*/*opt1-2*Δ::*FRT* *opt23-1*Δ::*FRT*/*opt23-1*Δ::*FRT* *opt4-1*Δ::*FRT*/*opt4-2*Δ::*FRT* *opt5-1*Δ::*FRT*/*opt5-2*Δ::*FRT* *ptr2-1*Δ::*FRT*/ptr2-*2*Δ::*FRT* *ptr22-1*Δ::*FRT*/ptr22-*2*Δ::*FRT* *ADH1/adh1*Δ::P_{ADH1}-*OPT5*] homozygous null mutants for *opt1, opt2, opt3, opt4, opt5, ptr2,* and *ptr22* with *OPT5* expressed from *ADH1*-Promoter	Laboratory Morschhäuser
OPT12345PTR222MPE2 A/B	[*opt1-1*Δ::*FRT*/*opt1-2*Δ::*FRT* *opt23-1*Δ::*FRT*/*opt23-1*Δ::*FRT* *opt4-1*Δ::*FRT*/*opt4-2*Δ::*FRT* *opt5-1*Δ::*FRT*/*opt5-2*Δ::*FRT* *ptr2-1*Δ::*FRT*/ptr2-*2*Δ::*FRT* *ptr22-1*Δ::*FRT*/ptr22-*2*Δ::*FRT* *ADH1/adh1*Δ::P_{ADH1}-*PTR2*] homozygous null mutants for *opt1, opt2, opt3, opt4, opt5, ptr2,* and *ptr22* with *PTR2* expressed from *ADH1*-Promoter	Laboratory Morschhäuser
OPT12345PTR222MPE22 A/B	[*opt1-1*Δ::*FRT*/*opt1-2*Δ::*FRT* *opt23-1*Δ::*FRT*/*opt23-1*Δ::*FRT* *opt4-1*Δ::*FRT*/*opt4-2*Δ::*FRT* *opt5-1*Δ::*FRT*/*opt5-2*Δ::*FRT* *ptr2-1*Δ::*FRT*/ptr2-*2*Δ::*FRT* *ptr22-1*Δ::*FRT*/ptr22-*2*Δ::*FRT* *ADH1/adh1*Δ::P_{ADH1}-*PTR22*] homozygous null mutants for *opt1, opt2, opt3, opt4, opt5, ptr2,* and *ptr22* with *PTR22* expressed from *ADH1*-Promoter	Laboratory Morschhäuser

4.2 Methods

4.2.1 Growth of *Escherischa coli* strains

E.coli was routinely grown in LB-Medium or on solid LB-Agar at 37°C. For the selection of plasmid carrying transformants 100 µg/ml ampicilline was added to the agar or medium. Liquid media was constantly shaken at 230 rpm in a 37°C incubator.

4.2.2 Growth of *Candida albicans* strains

All *C. albicans* strains used in this study were stored as frozen stocks with 15% glycerol at -80°C and routinely grown in YPD-Medium or on solid YPD-Agar at 30°C. To select for transformants, using the *SAT1*-resistance marker, a 200 µg/ml concentration of nourseothricin was supplemented to the agar.

To test growth on bovine serum albumin (BSA) YCB medium, pH = 4, and growth on di-/tripeptides and L-amino acids as sole nitrogen source YCB-medium, pH = 5, was used. Induction by BSA was tested in YCB medium, pH = 4 (pH optimum for Sap2 protease), supplemented either with or without yeast extract (YE). To test repression by a preferred nitrogen source various concentrations of ammonium sulfate or amino acids were added to YCB-YE-BSA medium. YNB-media was used to test growth on and induction/repression by various ammonium concentrations as well as induction by 1 mM urea.

4.2.3 DNA manipulation and strain construction

4.2.3.1 Agarose gel electrophoresis and visualization of DNA-fragments

Agarose gel electrophoresis was routinely used to visualize the presence and the size of DNA-fragments. For most purposes 1% gels and 1X TAE buffer (prepared from 50X Stock) was used. DNA was loaded on the gel in 1X Loading dye buffer and separated by electrophoresis. The fragments were afterwards analyzed using UV-light after staining of the agarose gel in an ethidium bromide bath (10 mg/ml in water). Photographs were taken using a geldocumentation system. The sizes of the fragments were estimated by measuring the relative mobility of the bands in comparison to markers of known molecular size.

4.2.3.2 PCR (Polymerase chain reaction)

PCR was used to amplify DNA-fragments from plasmids or genomic DNA of *C. albicans* strains. The PCR mixtures and the PCR-cycles were prepared/adjusted following the manufacturer's instructions of the respective DNA-Polymerase used (e.g. Phusion, TAQ, PAQ, Pfu). The elongation time was adapted according to the particular DNA-fragment (average speed approx. 2 kb in 1 minute). The success of the PCR and the correct size of the PCR product were afterwards determined using agarose gel electrophoresis. The PCR product was then purified using the Machery and Nagel Nucleic Extraction Kit by following the manufacturer's instructions and finally stored at -20°C until further use.

4.2.3.3 Digestion and purification of DNA fragments

An appropriate amount of DNA was digested with restriction enzymes from NEB (New England Biolabs) following the manufacturer's instructions. After complete digestion the DNA-fragments were separated using gel electrophoresis. DNA-Fragments used for plasmid construction were visualized under low-intensity UV-light and excised from the agarose gel. The excised DNA-fragments were afterwards purified using the Machery and Nagel Nucleic Extraction Kit by following the manufacturer's instructions and finally stored at -20°C until further use.

4.2.3.4 Plasmid construction

All plasmids used in this study were based on the vector pBluescript KS II + (Stratagene). Properly digested and purified DNA fragments and identical digested plasmid vector were ligated together to produce autonomously replicating plasmids. The ligation mix contained 1X Ligation buffer and 1 unit T4 DNA Ligase. In general the fragments were mixed in the ratio 1:5, vector to insert fragment, respectively. The ligation was done for 2-4 hours at room temperature or, for ligation of multiple inserts into one vector, overnight at 15°C. The ligation mix was then directly used to transform competent *E. coli* cells.

4.2.3.5 Preparation of competent *E. coli* cells

Competent *E. coli* cells were prepared with the calcium chloride method. A single colony of *E. coli* DH5α was inoculated in 10 ml LB medium and grown at 37°C with constant agitation for 16-18 hours. The culture was then inoculated in 1:100 dilution in 50 ml fresh LB medium and constantly shaken at 37°C for 3-4 hours (to OD_{600}=0.7-0.9). The culture was transferred to chilled 50 ml tubes and pelleted at 3,000 rpm for 10 min at 4°C in a centrifuge. The supernatant was discarded and the cell pellet was resuspended in 20 ml ice cold 100 mM calcium chloride. This cell mix was then chilled on ice for 30 minutes and centrifuged at 4,000 rpm for 10 minutes at 4°C. After gentle resuspension of the pellet in 2.5 ml of 100 mM calcium chloride 86% glycerol was added to a final concentration of 15% (v/v). Aliquotes of 200 µl competent cells were made and stored at -80°C for later use.

4.2.3.6 Transformation of competent *E. coli* cells

For each transformation a frozen aliquot of competent *E. coli* cells was carefully thawed on ice. The ligation mixture (20 µl) was directly added to 200 µl competent *E. coli* cells and chilled for 30 minutes on ice. The cells were subjected to heat shock at 42°C for 90 seconds and then chilled on ice for 5 minutes. After adding 1 ml LB medium the cells were grown with constant agitation for 1h at 37°C. Finally, the cells were spread on LB-ampicillin selection plate. The plates were incubated at 37°C until colonies appeared (usually overnight).

4.2.3.7 Isolation of *E. coli* plasmid DNA

For the small scale isolation of plasmid DNA a single *E. coli* colony was inoculated in 3 ml LB-Ampicillin for an overnight culture. The cells were harvested and isolation with purification was done using the Machery and Nagel Plasmid Isolation Kit by following the manufacturer's instructions. In replacement for the elution buffer water was used and the plasmid DNA was finally stored at -20°C until further use.

The success of the ligation was checked by digestion of the isolated plasmid DNA with appropriate enzymes followed by gel electrophoresis and UV-light visualization. The pattern and size of the fragments served to validate the correctness of the plasmid. Plasmids based on PCR-products were further send for sequencing to exclude PCR errors.

4.2.3.8 Sequencing

Plasmids and PCR products were sent to Seqlab (Sequence laboratories Göttingen, Germany) and afterwards analyzed using web-based sequence analysis tools (e.g. BLAST option on candidagenome.org)

4.2.3.9 Transformation of *Candida albicans*

Transformation of *C. albicans* cells was achieved using the lithium acetate method (Sanglard *et al.*, 1996) and electroporation (De Backer *et al.*, 1999) based on the protocol described by Köhler *et al.* (Köhler *et al.*, 1997) and the *SAT1* marker described by Reuss *et al.* (Reuss *et al.*, 2004, Sasse & Morschhäuser, 2012). An overnight culture from a single colony of the strain, to be transformed, was prepared. Cells present in 0.5 µl of this preculture were transferred into 50 ml fresh YPD medium and grown overnight to reach mid log phase. Cells were collected by centrifugation for 5 minutes at 4000 rpm at 4°C. The pellet was suspended in 8 ml sterile water, 1 ml 1M lithium acetate and 1 ml 10X TE buffer pH 7.5. The suspension was then incubated in a rotary shaker for 60 minutes at 30°C. After addition of 250 µl 1 M dithiothreitol (DTT) the suspension was further shaken at 30°C for 15 minutes. After addition of 40 ml of sterile water the cells were collected by centrifugation for 5 minutes at 4000 rpm at 4°C. The cell pellet was then sequentially washed in 25 ml ice cold water and 5 ml ice cold 1 M sorbitol. The supernatant was afterwards discarded and the washed cell pellet was resuspended in the residual sorbitol and kept on ice. 40 µl of, now competent, cells were transferred to a cooled 0.2 cm electroporation cuvette (Peqlab) and 5 µl of linear DNA fragments. Electroporation was carried out at 1.8 kV using an electroporator (Equibio). The cuvette with electroporated cells was chilled on ice for 2 minutes. After addition of 1 ml fresh YPD medium the electroporated cells were transferred to a 2 ml cap and incubated at 30°C with constant agitation for 4 hours. During this time the successfully transformed cells, now harboring the *SAT1* gene, were able establish the resistance against nourseothricin. Selection took place after plating out the transformed cells on YPD agar plates containing 200 µg/ml nourseothricin. After 2 days at 30°C only cells containing the *SAT1* gene formed colonies and were picked for further analysis.

4.2.3.10 Isolation of genomic DNA from *C. albicans*

An overnight culture, inoculated from a single colony, was done in 5 ml YPD medium. Cells were collected by centrifugation at 4000 rpm for 5 minutes. The cell pellet was washed with 1 ml water and centrifuged again at 4000 rpm for 2 minutes. Washed cells were resupended in 200 µl Breaking buffer for genomic DNA and transferred to 200 µl glass beads (diameter: 0.25-0.5 mm) in a new 1.5 ml screw cap tube. To eradicate proteins 200 µl of phenol/chloroform/isoamylalcohol (25/24/1) was added. Mechanical breakage of the cells was done by vortexing at maximum speed for at least 5 minutes. After addition of 200 µl 1xTE, vortexing was continued for at least 5 minutes. Afterwards the mixture was centrifuged at 13,000 rpm for 5 minutes. The aqueous top phase was decanted to a new tube. DNA was precipitated by the addition of 1 ml ice cold pure ethanol. The precipitates were centrifuged at maximum speed for 3 minutes and the supernatant was discarded. The DNA pellet was washed with ice cold 70% ethanol and again centrifuged at maximum speed for 3 minutes. The supernatant was completely removed and the DNA pellet was dried at 50°C for approx. 10-15 minutes. The DNA was resolved in 50 µl 1xTE with 0.6 mg/ml RNase A (3 µl of 10 mg/ml stock) by vigorous shaking at 50°C until pellet was completely in solution. The extracted genomic DNA was finally stored at -20°C until further use.

4.2.3.11 Southern DNA transfer and hybridization

To guarantee correct genetic manipulation of *Candida albicans* the isolated genomic DNA was transferred to a nylon membrane using the Southern DNA transfer method. Therefore, approx. 10 µg of genomic DNA was digested with an appropriate restriction enzyme overnight. Afterwards the digested DNA was separated using a 1% agarose gel. Prior to the transfer a Nylon Membrane of appropriate size was moistened in water, followed by a 5 minute wash in 20xSSC. The digested DNA-containing gel was then put on the so prepared nylon membrane an incorporated into a vacuum blotter. The vacuum pump pressure was set to approx. 50 mbar. For depurination of the DNA the gel was first covered with Southern solution A for 15 minutes. Then this solution was replaced by Southern solution B to denaturate the DNA. As third, solution B was replaced by Southern solution C to neutralize the previous treatments. The actual transfer was then accomplished by covering the gel with 20xSSC for 90 minutes. After the transfer, vacuum was switched off and the blotting apparatus was dissembled. The nylon membrane was then denaturated in 0.4 M NaOH for 30 seconds followed by the

neutralization with 0.2 M Tris pH 7.5 for 30 seconds. After complete drying on Whatman paper the DNA fragments were crosslinked to the nylon membrane with UV-light. This was done using the auto crosslink setting of the Stratalinker 1800 (Stratagene). The so treated nylon membrane was now ready for hybridization with a specific DNA probe using the Amersham ECL "Enhanced chemiluminescence" Kit by following the manufacturer's instructions. Final exposition to a detection film was adapted to the signal intensity.

4.2.4 Expression reporter assays

4.2.4.1 Quantitative real time PCR

RNA-extraction with "Hot Phenol" and Qiagen RNeasy Kit

The cells were collected by centrifugation at 3000 rpm for 4 minutes and 4°C. After discarding the supernatant the cells were shock-freezed in liquid nitrogen and stored at -80°C until further use. The cell pellet was resuspended in 1 ml ice cold DEPC-treated water and transferred to a clean RNAse-free 2 ml tube. After a short spin of 10 seconds at 4°C the supernatant was removed and the cell pellet was resuspended in 400 µl TES solution. RNA was extracted using the "Hot-Phenol" method (Ausubel, 1989) and 400 µl of acid phenol was added. The suspension was vigorously vortexed for 10 seconds and incubated for 1 hour at 65°C with occasional, brief vortexing. Afterwards the suspension was chilled on ice for 5 minutes and the phases were separated by centrifugation at top speed for 5 minutes and 4°C. The aqueous (top) phase was transferred to a new tube and 1 volume of RLT buffer (provided by RNeasy Kit, Qiagen) and 1 volume of pure ethanol were added. After each addition the suspension was mixed well. The proceeding steps were done using the Qiagen RNeasy Kit by following the manufacturer's instructions. The obtained RNA was stored in 50 µl RNase-free water at -80°C until further use.

DNase treatment

To eliminate remaining traces of DNA, the extracted RNA was treated with DNase I. Therefore, 1 µl of RNase Inhibitor, 3 µl of 10X DNase buffer and 1 µl of of DNase I were added to 30 µl of extracted RNA. DNA digestion took place during 10 minutes incubation at 37°C. To prevent RNA-degradation during the next steps 0.3 µl DEPC-treated 0.5 M EDTA (for final concentration of 5 mM) was added. DNase I was inactivated by incubation at 75°C for 10

minutes. Finally the DNA-free RNA was centrifuged at top speed for 1 minute and transferred into a new tube and stored at -80°C until further use.

To check for remaining traces of DNA a PCR was performed using the primer pair EFB1A/EFB1B that bind outside the *EFB1* intron and yield a PCR product of approx. 800 bp from genomic DNA. In all the RNA samples no amplification should occur.

To obey the MIQE guidelines (Bustin *et al.*, 2009), the minimum information for publication of quantitative real-time PCR experiments, RNA purity and integrity was determined before proceeding with the next steps.

RNA purity, with respect to protein contamination was assessed spectrophotometrically by measuring the $OD_{260/280}$ ratio in a neutral pH (10 mM Tris, pH 7). A ratio between 1.8 and 2.0 served as indicator for good RNA purity, which was devoid of phenol and protein contamination. In addition the $OD_{260/280}$ ratio should be close to 2.0 and not under 1.0, which clearly indicates contaminations. Within the same measurement also the RNA concentration was determined from the absorbance values at 280 nm, usually between 100 – 3000 ng/µl.

RNA integrity, with respect to degradation, was assessed using traditional electrophoresis on a 1% agarose gel, followed by EtBr staining and visualization with UV-light. Intact RNA gave two sharp bands representing the large and small subunit ribosomal RNAs. Thereby the large band should have twice the intensity of the smaller band.

Convertion to cDNA

Prior to quantitative real time PCR the obtained RNA was converted into cDNA using the SuperScript® III First-Strand Synthesis SuperMix (Invitrogen) by following the manufacturer's instructions. Production of cDNA was afterwards checked using again PCR with the primer pair EFB1A/ EFB1B. Here, the correctly produced cDNA should give a band of an *EFB1* amplicon, lacking the intron, with the size of approx. 550 bp. A PCR product from genomic DNA with approx. 800 bp size served as control.

Primer Design

For reliable and reproducible qRT-PCR results the design of primers is a critical point. Therefore, the Primer3 tool (http://www.ncbi.nlm.nih.gov/tools/primer-blast/) was used to design oligonucleotides that give optimal amplicon size (150 to 250 nucleotides) by comparable annealing and melting temperatures (60±3°C). These primers were prior to quantitative real time PCR tested for their efficiency. The amplification efficiency of the *DAL1* primer pair (DAL1RTfor/DAL1RTrev) was determined as 90% and was identical to the efficiency

of the control reference primer pair for the housekeeping gene *ACT1* (ACT1RT/ ACT2RT) and therefore considered as suitable. The purpose of a housekeeping gene is to serve as control to adjust different transcript levels in all individual RNA isolations, since it is considered as not regulated and therefore at equal transcript level under each condition.

Quantitative real time PCR

The actual quantitative real time PCR reaction was performed, using the CFX96™ Real-Time PCR Detection System (C1000™ thermal cycler, Biorad), in a 25 µl reaction, consisting of 12.5 µl iQ™ SYBR® Green Supermix (Biorad) and 12.5 µl cDNA-primer Mix, containing 1:100 diluted cDNA with à 625 nM forward and reverse primer (ACT1RT/ ACT2RT or DAL1RTfor/DAL1RTrev). The reaction took place in Microseal 96-Well PCR Plates covered with Microseal® 'B' Adhesive Seals and the reaction cycles were as follows: After initial denaturation for 10 minutes at 95°C 45 cycles of a 2-step amplification protocol was ensued, with 10 seconds denaturation at 95°C and 30 seconds at 60°C for primer annealing and amplification. As internal control also reactions with no template were included. During amplification the intercalating fluorescent dye SYBR Green I was permanently incorporated into double stranded DNA PCR products, giving quantifiable fluorescent intensities. SYBR green fluorescence served as direct measure to determine DNA abundance in real time by the detection system. As further control melt curves were generated, by ramping in 0.5°K steps from 65°C to 98°C. Here a clear and defined Melt peak indicated a single PCR product and ensures that no unspecific amplicons were disturbing the determination by the detection system. Each reaction was done as triplicates to avoid errors during pipetting. Two times independently total RNA was extracted followed by two times independently conversion to cDNA for each of the 2 biological replicates to give also technical replicates. The Biorad CFX Manager™ software (Version 1.6) calculated the quantification cycle (cq) values, which are defined as the reaction cycle where a defined threshold was reached. The more initial cDNA was present the earlier the threshold was reached, resulting in a low cq value. Less initial cDNA needed more reaction cycles to reach the threshold, resulting in a high cq value. The differences in the cq values (Δcq) served to calculate the differences in initial cDNA abundance and consequently initial mRNA transcript abundance in the samples. The obtained Δcq values were used to calculate means and standard deviations of the final relative expression values using the comparative cq value calculations.

4.2.4.2 Flow cytometry

Flow cytometry was used to determine gene expression in *C. albicans* under different experimental condition with the green fluorescent protein (Gfp) as reporter. Therefore, cells of the respective reporter strains were grown for indicated times in the various experimental media and suspended in 1x PBS. Flow cytometry was performed using the MACSQuant®Analyzer (Miltenyi Biotec) equipped with an argon laser emitting at 488 nm. Fluorescence was detected using the B1 fluorescence channel equipped with a 525 nm band-pass filter (bandwidth 50 nm). Twenty thousand cells were analyzed per sample and counted at a flow rate of approximately 500 cells per second. Fluorescence data were collected by using logarithmic amplifiers. The mean fluorescence (arbitrary values) was determined with MACSQuantify™ (Version 2.4, Miltenyi Biotec) software.

4.2.4.3 Raw protein extract isolation

To obtain complete raw protein extracts from *C. albicans* cells were grown in desired experimental medium to an OD_{600} between 0.5 and 1.0. Therfore, an YPD overnight culture was diluted 1:200 in 50 ml fresh test medium and grown constantly shaking at 30°C till OD_{600} was reached. Cells were collected by centrifugation and the pellet was shock-freezed with liquid nitrogen and stored at -80°C until further use. The cell pellet was two times washed in ice cold water and one time in B-buffer. Afterwards cells were resuspended in freshly prepared B+-buffer and transferred to 500 µl glass beads (diameter: 0.25-0.5 mm) in a new 1.5 ml screw cap tube. Mechanical breakage of the cells was done by vortexing at maximum speed for at least 5 minutes. After centrifugation at top speed at 4°C the supernatant, containing the raw proteins, was collected and stored at -20°C until further use.

4.2.4.4 SDS-PAGE

To visualize proteins 3xLämmli Loading Dye was added to the respective supernatant or raw protein extract and all proteins were denatured at 65°C for 5 minutes. The samples were loaded on a 10% SDS polyacrylamid gel (prepared following general preparation protocols) and then separated by a voltage driven electronic force.

To visualize all proteins the gel was stained with Coomassie or GelCode Blue Stain by following manufacturer's instructions and to detect HA-tagged proteins Western immunoblotting was ensued.

4.2.4.5 Western Blotting and antibody detection

For the detection of HA-tagged proteins the electrophoretic separated proteins were transferred to a nitrocellulose membrane. Therefore, the Wet-Blot Western system from Biorad was used by obeying the manufacturer's instructions. The Roche Anti-HA-Peroxidase, High Affinity (3F10), was used to detect the HA tag and consequently the coupled protein. This antibody unified the detecting peroxidase already with the HA-tag specific variable domain of the antibody, obviating the need for a secondary antibody. The blocking and washing steps of the nitrocellulose membrane were performed by following the manufacturer's instructions with minor changes. So was the blocking reagent in the blocking solution replaced by 5% milk powder and the specific antibody binding was usually done overnight at 4°C. After three washing steps detection of bound Anti-HA-Peroxidase was done using the Amersham ECL "Enhanced chemiluminescence" Kit by following the manufacturer's instructions. Final exposition to a detection film was adapted to the signal intensity.

4.2.4.6 Enzyme-linked immnunosorbent assay (ELISA)

For the detection and determination of various amounts of Sap2-HA proteins in the supernatant the enzyme-linked immnunosorbent assay (ELISA) was used. Strains were grown under desired test condition and 200 µl of the supernatant were, with gently agitation, incubated overnight at 4°C in a Nunc™ Amino™ Immobilizer 96 well plate (ThermoScientific). During this time the complete protein fraction of the supernatant was covalently linked to the well surface. After 3 washing steps with approx. 300 µl PBST the protein coated surface was incubated with PBS-0.1% BSA blocking solution for 2 hours at room temperature. To detect HA-tagged protein within the coated protein fraction a 1:500 dilution of Roche Anti-HA-Peroxidase, High Affinity (3F10), in 1xPBS-0.1% BSA blocking solution was used. Final colorimetric detection with TMB (3,3',5,5'-tetramethylbenzidine) substrate was done following manufacturer's instructions. There, the antibody-coupled peroxidase converted the TMB substrate into a blue intermediate, which was after addition of sulphuric acid further converted into a stable yellow complex. Depending on the amount of antibody bound to immobilized Sap2-HA molecules the amount of the yellow complex differed. These variations were then quantified in a Multiskan Ascent ELISA-reader (ThermoScientific) at 450 nm wavelength and analysed using the Ascent Software (Version 2.6).

4.2.5 Phenotypic assays

4.2.5.1 Growth rate determination

To determine the growth rates of *C. albicans* strains overnight cultures of the strains in the respective medium were diluted 1:1000 in 100 µl fresh medium in 96-well microtiter plates (Nunc; ThermoScientific) and grown at 30°C in an Infinite F200 PRO microplate reader (TECAN) with shaking at 280 rpm. The OD of the cultures were measured at 585 nm every 10 min from 4 replicates. The generation times and standard deviations in log phase were calculated from three independent cultures of each strain. The Mann-Whitney-U for not-normal distributed independent samples was used to compare growth rate differences for statistical significance.

4.2.5.2 *In vitro* competitive fitness assay

To evaluate effects of multiple deletions or comparable genomic changes on fitness of *C. albicans* mutant strains in comparison to the unaltered wild type strain SC5314, a competitive fitness assay *in vitro* was performed. To discriminate between the test strain and the wild type strain SC5314 in a mixed co-culture instead of SC5315 itself a derivative, the *RFP*-labeled strain SCADH1R1A, was used. Strains were grown overnight in the respective medium and mixed in a 1:1 ratio with SCADH1R1A in fresh medium at a starting OD_{600} of 0.002 and grown for 24 h at 30°C. Cells from each mixed culture at the beginning and at the end of the co-incubation were plated on YPD plates, by using an appropriate dilution, and grown for 2 days at 30°C. After some weeks of incubation at 4°C constitutively expression of *RFP* in the strain SCADH1R1A produced red colored colonies on agar plates. The percentage of red colonies (strain SCADH1R1A) and white colonies (test strain) was determined from agar plates with more than 30 colony forming units to give reliable results. The relative fitness of a strain was the ratio of its proportions in the co-culture at the end and beginning of the experiment. A value of 1 indicated wild-type fitness and values below or above 1 indicated decreased and increased fitness, respectively, compared to SCADH1R1A. The Mann-Whitney-U test for not-normal distributed independent samples was used to compare the relative fitness of the mutants with that of the wild-type strain SC5314.

4.2.5.3 *In vivo* competitive fitness assay

To assess effects of multiple deletions on *in vivo* fitness of *C. albicans* mutant strains in comparison to the unaltered wild type strain SC5314, a comparative fitness assay in a gastrointestinal (gut) colonization model was done. Therefore, female Balb/c mice were prepared for *C. albicans* colonization by feeding them with 1 mg/ml tetracycline, 2 mg/ml streptomycin, and 0.1 mg/ml gentamycin (in their drinking water), starting from day 4 prior to infection. *C. albicans* strains were grown overnight in YPD medium at 30°C, washed two times in phosphate-buffered saline (1xPBS), and adjusted to a density of 10^9 cells per ml. Each of the test strains and the wild type parent SC5314 was mixed in a 1:1 ratio with the *RFP*-labeled strain SCADH1R1A. Fifty microliters, containing approximately $5x10^7$ cells of the mixed suspensions, were orally applied to the mice (five mice per strain pair). After 24 h and on the following days, the feces of the mice were collected and homogenized in 0.5 ml sterile water. An appropriate dilution of the homogenizate was spread on YPD plates, supplemented with 50 µg/ml chloramphenicol to eradicate bacterial cells. The proportions of reference and test strains in the inoculum and in the populations recovered on each following day from the feces was identically determined as described for the *in vitro* competition experiments. Statistical significance for the repeated measures was calculated using the Friedmann test for K-related and not normally distributed values.

4.2.6 Genome-wide binding profiling (ChIP-on-chip)

A global view of binding sites of transcription factors to potentially regulated target genes can be provided by a genome-wide location analysis, also known as ChIP-on-chip analysis.
ChIP-on-chip combines protein-bound DNA isolation by chromatin immunoprecipitation with hybridization to a whole genome tiling array. This allowed the isolation and identification of DNA sequences occupied by specific DNA binding proteins in cells. In order to tag the protein of interest a HA-tag was used. The ChIP-on-chip was performed based on the protocol established by Liu *et al.* (Liu *et al.*, 2007) with some modifications.

Chromatin immunoprecipitation (ChIP)

The strain containing the HA-tagged version of the protein of interest was analyzed and as control served the untagged wild type strain SC5314. An YPD overnight culture was inoculated into the inducing media (YCB-YE-BSA) and grown at 30°C to an OD_{600} of 2.0, this relatively high OD_{600} ensured in this case proper expression of the tagged factor. Following the established protocol proteins and DNA were cross-linked using formaldehyde. Cross-linking was stopped by glycine addition and after several washing steps with TBS buffer cells were shock-frozen in liquid nitrogen. Total cell extracts were obtained by mechanical disruption using lysis buffer, glass beads and the mini-bead beater (Biospec products). Chromatin was shredded into soluble (400-500 bp) DNA fragments by sonication using the Sonic Dismembrator model 1000 sonicator (Fisher Scientific). HA-tagged proteins and cross-linked DNA was precipitated using the Roche rat Anti-HA-Antibody (3F10) coupled to Dynabeads® Sheep Anti-Rat IgG magnetic beads (Dynal Biotech). After several washing steps, which eradicated unspecific precipitates, the protein-DNA cross link was reversed at 65°C in TE-1%SDS and DNA was eluted. To obtain pure DNA the eluate was treated with proteinase K, and RNase A followed by PCI and ethanol precipitation. Quantity of obtained DNA fragments was determined using Picogreen mix (Quant-iT™ Picogreen dsDNA reagent) and by following manufacturer's instructions. The quantification with the *Envision* luminometer (Perkin-Elmer) should give concentrations between 0.01 and 0.1 ng/µl. Prior to amplification the DNA fragments were blunted using the T4 DNA Polymerase and ligated with the oligonucleotides oligo 1 and oligo 2 using the T4 DNA Ligase. DNA amplification was performed using only oligo 1 as primer and two DNA Polymerases (Taq and Pfu) and a mixture of all dNTPs plus aa-dUTP (aminoalyl-desoxyUTP). The Aminoallyl group served to couple the specific Cy-Dyes to the amplified DNA-fragments.

Amplified DNA was purified using the Qiaquick PCR purification kit (Qiagen) following manufacturer's instructions with minor modifications. The obtained DNA from the HA-tagged strain was labeled with Cy3 and as control the obtained DNA from the untagged wild type strain SC5314 was labeled with Cy5 by following manufacturer's instructions. It is noteworthy that due to the different chemical properties of Cy3 and Cy5 their incorporation has slightly distinct efficiencies, which might produce a minimal bias.

Whole genome tiling array hybridization

Both labeled DNA fragments were mixed (Cy3-labeled DNA from HA-tagged strain and Cy5-labeled DNA from SC5314) and hybridized to *C. albicans* whole genome tiling array (NimbleGen Systems Inc.) according to manufacturer's instructions. The individual signal intensities of Cy3 and Cy5 dyes on the array slides were scanned with GenePix 400B scanner (Molecular Devices) and processed with NimbleScan Software (NimbleGen Systems Inc; version 2.4). The output data was reported as general feature format (*.gff-files), where each Cy-Dye intensity for each independent replicate represented a single file. Using the Tilescope program (http://tilescope.gersteinlab.org/8080/mosaic/pipeline.html) (Zhang *et al.*, 2007) fluorescence intensities were normalized with the unspecific signals derived from SC5314 samples using following parameter settings: window size 400 bp; max. genomic distance 60 bp; min. length 120 bp. DNA regions enriched in the samples obtained from the HA-tagged strain will give higher Cy-Dye fluorescence intensities highlighting this region as bound by the HA-tagged factor. The data for all three independently created replicates were combined and peak finding was done using a threshold of ≥1.5 ($\log_2$ pseudomedian signal threshold) with a p-value cut off of ≤0.01. The data sets were uploaded to the *Candida albicans* Montréal Database (https://www.candida-montreal.ca) and bound regions were visualized on the web-based interactive Genome Browser platform. Open reading frames were manually assigned by analyzing each individual bound region and gathered in an Excel-file.

References

Albrecht, A., A. Felk, I. Pichova, J. R. Naglik, M. Schaller, P. de Groot, D. Maccallum, F. C. Odds, W. Schafer, F. Klis, M. Monod & B. Hube, (2006) **Glycosylphosphatidylinositol-anchored proteases of *Candida albicans* target proteins necessary for both cellular processes and host-pathogen interactions**. *The Journal of biological chemistry* 281: 688-694.

Aoki, W., N. Kitahara, N. Miura, H. Morisaka, Y. Yamamoto, K. Kuroda & M. Ueda, (2011) **Comprehensive characterization of secreted aspartic proteases encoded by a virulence gene family in *Candida albicans***. *Journal of biochemistry* 150: 431-438.

Arbour, M., E. Epp, H. Hogues, A. Sellam, C. Lacroix, J. Rauceo, A. Mitchell, M. Whiteway & A. Nantel, (2009) **Widespread occurrence of chromosomal aneuploidy following the routine production of *Candida albicans* mutants**. *FEMS yeast research* 9: 1070-1077.

Ausubel, F., *et al*, (1989) **Current protocols in molecular biology**. John Wiley & Sons, Inc., New York, NY.

Basrai, M. A., M. A. Lubkowitz, J. R. Perry, D. Miller, E. Krainer, F. Naider & J. M. Becker, (1995) **Cloning of a *Candida albicans* peptide transport gene**. *Microbiology* 141 (Pt 5): 1147-1156.

Bergmann, A., T. Hartmann, T. Cairns, E. M. Bignell & S. Krappmann, (2009) **A regulator of *Aspergillus fumigatus* extracellular proteolytic activity is dispensable for virulence**. *Infection and immunity* 77: 4041-4050.

Biswas, K. & J. Morschhäuser, (2005) **The Mep2p ammonium permease controls nitrogen starvation-induced filamentous growth in *Candida albicans***. *Molecular microbiology* 56: 649-669.

Boeckstaens, M., B. André & A. M. Marini, (2007) **The yeast ammonium transport protein Mep2 and its positive regulator, the Npr1 kinase, play an important role in normal and pseudohyphal growth on various nitrogen media through retrieval of excreted ammonium**. *Molecular microbiology* 64: 534-546.

Brand, A., D. M. MacCallum, A. J. Brown, N. A. Gow & F. C. Odds, (2004) **Ectopic expression of *URA3* can influence the virulence phenotypes and proteome of *Candida albicans* but can be overcome by targeted reintegration of *URA3* at the *RPS10* locus**. *Eukaryotic cell* 3: 900-909.

Brand, A. C. & D. M. MacCallum, (2012) **Host-Fungus Interactions Methods and Protocols**. *Methods in molecular biology* 845.

Broach, J. R., (2012) **Nutritional control of growth and development in yeast**. *Genetics* 192: 73-105.

Brown, G. D., D. W. Denning, N. A. Gow, S. M. Levitz, M. G. Netea & T. C. White, (2012a) **Hidden killers: human fungal infections**. *Science translational medicine* 4: 165rv113.

Brown, G. D., D. W. Denning & S. M. Levitz, (2012b) **Tackling human fungal infections**. *Science* 336: 647.

Bustin, S. A., V. Benes, J. A. Garson, J. Hellemans, J. Huggett, M. Kubista, R. Mueller, T. Nolan, M. W. Pfaffl, G. L. Shipley, J. Vandesompele & C. T. Wittwer, (2009) **The MIQE guidelines: minimum information for publication of quantitative real-time PCR experiments**. *Clinical chemistry* 55: 611-622.

Cai, H., M. Hauser, F. Naider & J. M. Becker, (2007) **Differential regulation and substrate preferences in two peptide transporters of *Saccharomyces cerevisiae***. *Eukaryotic cell* 6: 1805-1813.

Calderone, R. A. & C. J. Clancy, (2012) ***Candida* and *Candidiasis***. ASM Press, Washington, DC.

Calderone., G. L. a. R. A., (2008) **Heterozygosity and loss of heterozygosity in *Candida albicans***. In: Pathogenic Fungi: Insights in Molecular Biology. G. S.-B. a. R. A. Calderone (ed). Norfolk, United Kingdom: Caister Academic Press, pp. p. 43–72.

Carlson, J. M., A. Chakravarty, C. E. DeZiel & R. H. Gross, (2007) **SCOPE: a web server for practical *de novo* motif discovery**. *Nucleic acids research* 35: W259-264.

CDC, (2012) **Candidiasis**. http://www.cdc.gov/fungal/candidiasis/: U.S. Centers fo Disease Control and Prevention.

Chauhan, N., J. P. Latge & R. Calderone, (2006) **Signalling and oxidant adaptation in *Candida albicans* and *Aspergillus fumigatus***. *Nature reviews. Microbiology* 4: 435-444.

Chen, X., B. B. Magee, D. Dawson, P. T. Magee & C. A. Kumamoto, (2004) **Chromosome 1 trisomy compromises the virulence of *Candida albicans***. *Molecular microbiology* 51: 551-565.

Chen, Y., F. de Bernardis, S. Kauffman & T. B. Reynolds, (2008) **The *RSP1* gene regulates morphogenesis, secreted aspartyl protease transcritpion, and virulence in *Candida albicans***. *9th ASM Conference on Candida and Candidiasis* New York, USA.

Correia, A., U. Lermann, L. Teixeira, F. Cerca, S. Botelho, R. M. da Costa, P. Sampaio, F. Gartner, J. Morschhäuser, M. Vilanova & C. Pais, (2010) **Limited role of secreted aspartyl proteinases Sap1 to Sap6 in *Candida albicans* virulence and host immune response in murine hematogenously disseminated candidiasis**. *Infection and immunity* 78: 4839-4849.

Coste, A. T., M. Karababa, F. Ischer, J. Bille & D. Sanglard, (2004) ***TAC1*, transcriptional activator of *CDR* genes, is a new transcription factor involved in the regulation of *Candida albicans* ABC transporters *CDR1* and *CDR2***. *Eukaryotic cell* 3: 1639-1652.

Dabas, N. & J. Morschhäuser, (2007) **Control of ammonium permease expression and filamentous growth by the GATA transcription factors *GLN3* and *GAT1* in *Candida albicans***. *Eukaryotic cell* 6: 875-888.

Dabas, N. & J. Morschhäuser, (2008) **A transcription factor regulatory cascade controls secreted aspartic protease expression in *Candida albicans***. *Molecular microbiology* 69: 586-602.

Dabas, N., S. Schneider & J. Morschhäuser, (2009) **Mutational analysis of the *Candida albicans* ammonium permease Mep2p reveals residues required for ammonium transport and signaling**. *Eukaryotic cell* 8: 147-160.

Dalle, F., B. Wächtler, C. L'Ollivier, G. Holland, N. Bannert, D. Wilson, C. Labruere, A. Bonnin & B. Hube, (2010) **Cellular interactions of *Candida albicans* with human oral epithelial cells and enterocytes**. *Cellular microbiology* 12: 248-271.

Davis, M. M., F. J. Alvarez, K. Ryman, A. A. Holm, P. O. Ljungdahl & Y. Engström, (2011) **Wild-type *Drosophila melanogaster* as a model host to analyze nitrogen source dependent virulence of *Candida albicans***. *PloS one* 6: e27434.

De Backer, M. D., D. Maes, S. Vandoninck, M. Logghe, R. Contreras & W. H. Luyten, (1999) **Transformation of *Candida albicans* by electroporation**. *Yeast* 15: 1609-1618.

De Bernardis, F., S. Arancia, L. Morelli, B. Hube, D. Sanglard, W. Schafer & A. Cassone, (1999) **Evidence that members of the secretory aspartyl proteinase gene family, in particular *SAP2*, are virulence factors for *Candida vaginitis***. *The Journal of infectious diseases* 179: 201-208.

De Bernardis, F., M. Boccanera, D. Adriani, A. Girolamo & A. Cassone, (2002) **Intravaginal and intranasal immunizations are equally effective in inducing vaginal antibodies and conferring protection against vaginal candidiasis**. *Infection and immunity* 70: 2725-2729.

de Boer, M., P. S. Nielsen, J. P. Bebelman, H. Heerikhuizen, H. A. Andersen & R. J. Planta, (2000) **Stp1p, Stp2p and Abf1p are involved in regulation of expression of the amino acid transporter gene *BAP3* of *Saccharomyces cerevisiae***. *Nucleic acids research* 28: 974-981.

Desai, P. R., A. Thakur, D. Ganguli, S. Paul, J. Morschhäuser & A. K. Bachhawat, (2011) **Glutathione utilization by *Candida albicans* requires a functional glutathione degradation (DUG) pathway and *OPT7*, an unusual member of the oligopeptide transporter family**. *The Journal of biological chemistry* 286: 41183-41194.

Donaldson, M. E. & B. J. Saville, (2012) **Natural antisense transcripts in fungi**. *Molecular microbiology* 85: 405-417.

dos Santos, A. L., I. M. de Carvalho, B. A. da Silva, M. B. Portela, C. S. Alviano & R. M. de Araujo Soares, (2006) **Secretion of serine peptidase by a clinical strain of *Candida albicans*: influence of growth conditions and cleavage of human serum proteins and extracellular matrix components**. *FEMS immunology and medical microbiology* 46: 209-220.

Ene, I. V., A. K. Adya, S. Wehmeier, A. C. Brand, D. M. MacCallum, N. A. Gow & A. J. Brown, (2012) **Host carbon sources modulate cell wall architecture, drug resistance and virulence in a fungal pathogen**. *Cellular microbiology* 14: 1319-1335.

Ene, I. V., S. C. Cheng, M. G. Netea & A. J. Brown, (2013) **Growth of *Candida albicans* cells on the physiologically relevant carbon source lactate affects their recognition and phagocytosis by immune cells**. *Infection and immunity* 81: 238-248.

Falagas, M. E., N. Roussos & K. Z. Vardakas, (2010) **Relative frequency of albicans and the various non-*albicans Candida* spp among candidemia isolates from inpatients in various parts of the world: a systematic review**. *International journal of infectious diseases : IJID : official publication of the International Society for Infectious Diseases* 14: e954-966.

Fallon, K., K. Bausch, J. Noonan, E. Huguenel & P. Tamburini, (1997) **Role of aspartic proteases in disseminated *Candida albicans* infection in mice**. *Infection and immunity* 65: 551-556.

Felk, A., M. Kretschmar, A. Albrecht, M. Schaller, S. Beinhauer, T. Nichterlein, D. Sanglard, H. C. Korting, W. Schafer & B. Hube, (2002) ***Candida albicans* hyphal formation and the expression of the Efg1-regulated proteinases Sap4 to Sap6 are required for the invasion of parenchymal organs**. *Infection and immunity* 70: 3689-3700.

Feller, A., M. Boeckstaens, A. M. Marini & E. Dubois, (2006) **Transduction of the nitrogen signal activating Gln3-mediated transcription is independent of Npr1 kinase and Rsp5-Bul1/2 ubiquitin ligase in *Saccharomyces cerevisiae***. *The Journal of biological chemistry* 281: 28546-28554.

Finkel, J. S. & A. P. Mitchell, (2011) **Genetic control of *Candida albicans* biofilm development**. *Nature reviews. Microbiology* 9: 109-118.

Finkel, J. S., W. Xu, D. Huang, E. M. Hill, J. V. Desai, C. A. Woolford, J. E. Nett, H. Taff, C. T. Norice, D. R. Andes, F. Lanni & A. P. Mitchell, (2012) **Portrait of *Candida albicans* adherence regulators**. *PLoS pathogens* 8: e1002525.

Fischbach, M. A. & J. L. Sonnenburg, (2011) **Eating for two: how metabolism establishes interspecies interactions in the gut**. *Cell host & microbe* 10: 336-347.

Fleck, C. B., F. Schobel & M. Brock, (2011) **Nutrient acquisition by pathogenic fungi: nutrient availability, pathway regulation, and differences in substrate utilization**. *International journal of medical microbiology : IJMM* 301: 400-407.

Fonzi, W. A. & M. Y. Irwin, (1993) **Isogenic strain construction and gene mapping in *Candida albicans***. *Genetics* 134: 717-728.

Forche, A., P. T. Magee, B. B. Magee & G. May, (2004) **Genome-wide single-nucleotide polymorphism map for *Candida albicans***. *Eukaryotic cell* 3: 705-714.

Forche, A., P. T. Magee, A. Selmecki, J. Berman & G. May, (2009a) **Evolution in *Candida albicans* populations during a single passage through a mouse host**. *Genetics* 182: 799-811.

Forche, A., M. Steinbach & J. Berman, (2009b) **Efficient and rapid identification of *Candida albicans* allelic status using SNP-RFLP**. *FEMS yeast research* 9: 1061-1069.

Fox, E. P. & C. J. Nobile, (2012) **A sticky situation: Untangling the transcriptional network controlling biofilm development in *Candida albicans***. *Transcription* 3.

Gácser, A., F. Stehr, C. Kroger, L. Kredics, W. Schäfer & J. D. Nosanchuk, (2007) **Lipase 8 affects the pathogenesis of *Candida albicans***. *Infection and immunity* 75: 4710-4718.

Ghannoum, M. A. & L. B. Rice, (1999) **Antifungal agents: mode of action, mechanisms of resistance, and correlation of these mechanisms with bacterial resistance**. *Clinical microbiology reviews* 12: 501-517.

Ghosh, S., D. H. Navarathna, D. D. Roberts, J. T. Cooper, A. L. Atkin, T. M. Petro & K. W. Nickerson, (2009) **Arginine-induced germ tube formation in *Candida albicans* is essential for escape from murine macrophage line RAW 264.7**. *Infection and immunity* 77: 1596-1605.

Gillum, A. M., E. Y. Tsay & D. R. Kirsch, (1984) **Isolation of the *Candida albicans* gene for orotidine-5'-phosphate decarboxylase by complementation of *S. cerevisiae ura3* and *E. coli pyrF* mutations**. *Molecular & general genetics : MGG* 198: 179-182.

Gómez-Raja, J., E. Andaluz, B. Magee, R. Calderone & G. Larriba, (2008) **A single SNP, G929T (Gly310Val), determines the presence of a functional and a non-functional allele of *HIS4* in *Candida albicans* SC5314: detection of the non-functional allele in laboratory strains**. *Fungal genetics and biology : FG & B* 45: 527-541.

Gow, N. A., F. L. van de Veerdonk, A. J. Brown & M. G. Netea, (2012) ***Candida albicans*** **morphogenesis and host defence: discriminating invasion from colonization**. *Nature reviews. Microbiology* 10: 112-122.

Harry, J. B., B. G. Oliver, J. L. Song, P. M. Silver, J. T. Little, J. Choiniere & T. C. White, (2005) **Drug-induced regulation of the *MDR1* promoter in *Candida albicans***. *Antimicrobial agents and chemotherapy* 49: 2785-2792.

Hartmann, T., T. C. Cairns, P. Olbermann, J. Morschhäuser, E. M. Bignell & S. Krappmann, (2011) **Oligopeptide transport and regulation of extracellular proteolysis are required for growth of *Aspergillus fumigatus* on complex substrates but not for virulence**. *Molecular microbiology* 82: 917-935.

Hauser, M., V. Narita, A. M. Donhardt, F. Naider & J. M. Becker, (2001) **Multiplicity and regulation of genes encoding peptide transporters in *Saccharomyces cerevisiae***. *Molecular membrane biology* 18: 105-112.

Hennicke, F., M. Grumbt, U. Lermann, N. Ueberschaar, K. Palige, B. Bottcher, I. D. Jacobsen, C. Staib, J. Morschhäuser, M. Monod, B. Hube, C. Hertweck & P. Staib, (2013) **Factors supporting cysteine tolerance and sulfite production in *Candida albicans***. *Eukaryotic cell* 12: 604-613.

Hensel, M., H. N. Arst, Jr., A. Aufauvre-Brown & D. W. Holden, (1998) **The role of the *Aspergillus fumigatus* areA gene in invasive pulmonary aspergillosis**. *Molecular & general genetics : MGG* 258: 553-557.

Hertlein, T., (2008) **Funktionale Analyse von Peptidtransportern in *Candida albicans***. In: Insitute for Molecular Infection Biology. Univeristät Würzburg.

Hickman, M. A., G. Zeng, A. Forche, M. P. Hirakawa, D. Abbey, B. D. Harrison, Y. M. Wang, C. H. Su, R. J. Bennett, Y. Wang & J. Berman, (2013) **The 'obligate diploid' *Candida albicans* forms mating-competent haploids**. *Nature* 494: 55-59.

Hiller, D., S. Stahl & J. Morschhäuser, (2006) **Multiple cis-acting sequences mediate upregulation of the *MDR1* efflux pump in a fluconazole-resistant clinical *Candida albicans* isolate**. *Antimicrobial agents and chemotherapy* 50: 2300-2308.

Homann, O. R., H. Cai, J. M. Becker & S. L. Lindquist, (2005) **Harnessing natural diversity to probe metabolic pathways**. *PLoS genetics* 1: e80.

Homann, O. R., J. Dea, S. M. Noble & A. D. Johnson, (2009) **A phenotypic profile of the *Candida albicans* regulatory network**. *PLoS genetics* 5: e1000783.

Hoot, S. J., R. P. Brown, B. G. Oliver & T. C. White, (2010) **The *UPC2* promoter in *Candida albicans* contains two cis-acting elements that bind directly to Upc2p, resulting in transcriptional autoregulation**. *Eukaryotic cell* 9: 1354-1362.

Hoot, S. J., B. G. Oliver & T. C. White, (2008) ***Candida albicans UPC2*** **is transcriptionally induced in response to antifungal drugs and anaerobicity through Upc2p-dependent and -independent mechanisms**. *Microbiology* 154: 2748-2756.

Hornbach, A., A. Heyken, L. Schild, B. Hube, J. Loffler & O. Kurzai, (2009) **The glycosylphosphatidylinositol-anchored protease Sap9 modulates the interaction of *Candida albicans* with human neutrophils**. *Infection and immunity* 77: 5216-5224.

Hromatka, B. S., S. M. Noble & A. D. Johnson, (2005) **Transcriptional response of *Candida albicans* to nitric oxide and the role of the *YHB1* gene in nitrosative stress and virulence**. *Molecular biology of the cell* 16: 4814-4826.

Hube, B., D. Sanglard, F. C. Odds, D. Hess, M. Monod, W. Schafer, A. J. Brown & N. A. Gow, (1997) **Disruption of each of the secreted aspartyl proteinase genes *SAP1*, *SAP2*, and *SAP3* of *Candida albicans* attenuates virulence**. *Infection and immunity* 65: 3529-3538.

Hube, B., C. J. Turver, F. C. Odds, H. Eiffert, G. J. Boulnois, H. Kochel & R. Ruchel, (1991) **Sequence of the *Candida albicans* gene encoding the secretory aspartate proteinase**. *Journal of medical and veterinary mycology : bi-monthly publication of the International Society for Human and Animal Mycology* 29: 129-132.

Hwang, C. S. & A. Varshavsky, (2008) **Regulation of peptide import through phosphorylation of Ubr1, the ubiquitin ligase of the N-end rule pathway**. *Proceedings of the National Academy of Sciences of the United States of America* 105: 19188-19193.

Iliev, I. D., V. A. Funari, K. D. Taylor, Q. Nguyen, C. N. Reyes, S. P. Strom, J. Brown, C. A. Becker, P. R. Fleshner, M. Dubinsky, J. I. Rotter, H. L. Wang, D. P. McGovern, G. D. Brown & D. M. Underhill, (2012) **Interactions between commensal fungi and the C-type lectin receptor Dectin-1 influence colitis**. *Science* 336: 1314-1317.

Jackson, B. E., K. R. Wilhelmus & B. Hube, (2007) **The role of secreted aspartyl proteinases in Candida albicans keratitis**. *Investigative ophthalmology & visual science* 48: 3559-3565.

Jones, T., N. A. Federspiel, H. Chibana, J. Dungan, S. Kalman, B. B. Magee, G. Newport, Y. R. Thorstenson, N. Agabian, P. T. Magee, R. W. Davis & S. Scherer, (2004) **The diploid genome sequence of *Candida albicans***. *Proceedings of the National Academy of Sciences of the United States of America* 101: 7329-7334.

Kabir, M. A. & M. A. Hussain, (2009) **Human fungal pathogen *Candida albicans* in the postgenomic era: an overview**. *Expert review of anti-infective therapy* 7: 121-134.

Kaur, R., B. Ma & B. P. Cormack, (2007) **A family of glycosylphosphatidylinositol-linked aspartyl proteases is required for virulence of *Candida glabrata***. *Proceedings of the National Academy of Sciences of the United States of America* 104: 7628-7633.

Koh, S., A. M. Wiles, J. S. Sharp, F. R. Naider, J. M. Becker & G. Stacey, (2002) **An oligopeptide transporter gene family in *Arabidopsis***. *Plant physiology* 128: 21-29.

Köhler, G. A., T. C. White & N. Agabian, (1997) **Overexpression of a cloned *IMP* dehydrogenase gene of *Candida albicans* confers resistance to the specific inhibitor mycophenolic acid**. *Journal of bacteriology* 179: 2331-2338.

Kojic, E. M. & R. O. Darouiche, (2004) ***Candida* infections of medical devices**. *Clinical microbiology reviews* 17: 255-267.

Kraidlova, L., G. Van Zeebroeck, P. Van Dijck & H. Sychrová, (2011) **The *Candida albicans GAP* gene family encodes permeases involved in general and specific amino acid uptake and sensing**. *Eukaryotic cell* 10: 1219-1229.

Krappmann, S., E. M. Bignell, U. Reichard, T. Rogers, K. Haynes & G. H. Braus, (2004) **The Aspergillus fumigatus transcriptional activator CpcA contributes significantly to the virulence of this fungal pathogen**. *Molecular microbiology* 52: 785-799.

Kretschmar, M., B. Hube, T. Bertsch, D. Sanglard, R. Merker, M. Schroder, H. Hof & T. Nichterlein, (1999) **Germ tubes and proteinase activity contribute to virulence of *Candida albicans* in murine peritonitis**. *Infection and immunity* 67: 6637-6642.

Kumar, R., S. Chadha, D. Saraswat, J. S. Bajwa, R. A. Li, H. R. Conti & M. Edgerton, (2011) **Histatin 5 uptake by *Candida albicans* utilizes polyamine transporters Dur3 and Dur31 proteins**. *The Journal of biological chemistry* 286: 43748-43758.

Lass-Flörl, C., (2009) **The changing face of epidemiology of invasive fungal disease in Europe**. *Mycoses* 52: 197-205.

Lassak, T., E. Schneider, M. Bussmann, D. Kurtz, J. R. Manak, T. Srikantha, D. R. Soll & J. F. Ernst, (2011) **Target specificity of the *Candida albicans* Efg1 regulator**. *Molecular microbiology* 82: 602-618.

Lay, J., L. K. Henry, J. Clifford, Y. Koltin, C. E. Bulawa & J. M. Becker, (1998) **Altered expression of selectable marker *URA3* in gene-disrupted *Candida albicans* strains complicates interpretation of virulence studies**. *Infection and immunity* 66: 5301-5306.

Lee, I. R., E. W. Chow, C. A. Morrow, J. T. Djordjevic & J. A. Fraser, (2011) **Nitrogen metabolite repression of metabolism and virulence in the human fungal pathogen *Cryptococcus neoformans***. *Genetics* 188: 309-323.

Lee, I. R., C. A. Morrow & J. A. Fraser, (2013) **Nitrogen Regulation of Virulence in Clinically Prevalent Fungal Pathogens**. *FEMS microbiology letters*.

Legrand, M., A. Forche, A. Selmecki, C. Chan, D. T. Kirkpatrick & J. Berman, (2008) **Haplotype mapping of a diploid non-meiotic organism using existing and induced aneuploidies**. *PLoS genetics* 4: e1.

Lemaire, K., S. Van de Velde, P. Van Dijck & J. M. Thevelein, (2004) **Glucose and sucrose act as agonist and mannose as antagonist ligands of the G protein-coupled receptor Gpr1 in the yeast *Saccharomyces cerevisiae***. *Molecular cell* 16: 293-299.

Lermann, U., (2008) **Molekulare Untersuchungen zu Regulation und Funktion der sekretierten Aspartatproteasen von *Candida albicans***. University of Wuerzburg.

Lermann, U. & J. Morschhäuser, (2008) **Secreted aspartic proteases are not required for invasion of reconstituted human epithelia by *Candida albicans***. *Microbiology* 154: 3281-3295.

Liao, W. L., A. M. Ramón & W. A. Fonzi, (2008) ***GLN3* encodes a global regulator of nitrogen metabolism and virulence of *C. albicans***. *Fungal genetics and biology : FG & B* 45: 514-526.

Liao, Y., M. Chen, T. Hartmann, R. Y. Yang & W. Q. Liao, (2013) **Epidemiology of opportunistic invasive fungal infections in China: review of literature**. *Chinese medical journal* 126: 361-368.

Limjindaporn, T., R. A. Khalaf & W. A. Fonzi, (2003) **Nitrogen metabolism and virulence of *Candida albicans* require the GATA-type transcriptional activator encoded by *GAT1***. *Molecular microbiology* 50: 993-1004.

Liu, T. T., S. Znaidi, K. S. Barker, L. Xu, R. Homayouni, S. Saidane, J. Morschhäuser, A. Nantel, M. Raymond & P. D. Rogers, (2007) **Genome-wide expression and location analyses of the *Candida albicans* Tac1p regulon**. *Eukaryotic cell* 6: 2122-2138.

Ljungdahl, P. O., (2009) **Amino-acid-induced signalling via the SPS-sensing pathway in yeast**. *Biochemical Society transactions* 37: 242-247.

Ljungdahl, P. O. & B. Daignan-Fornier, (2012) **Regulation of amino acid, nucleotide, and phosphate metabolism in *Saccharomyces cerevisiae***. *Genetics* 190: 885-929.

Lorenz, M. C. & G. R. Fink, (2001) **The glyoxylate cycle is required for fungal virulence**. *Nature* 412: 83-86.

Lubkowitz, M. A., D. Barnes, M. Breslav, A. Burchfield, F. Naider & J. M. Becker, (1998) ***Schizosaccharomyces pombe isp4* encodes a transporter representing a novel family of oligopeptide transporters**. *Molecular microbiology* 28: 729-741.

Lubkowitz, M. A., L. Hauser, M. Breslav, F. Naider & J. M. Becker, (1997) **An oligopeptide transport gene from *Candida albicans***. *Microbiology* 143 (Pt 2): 387-396.

MacPherson, S., M. Larochelle & B. Turcotte, (2006) **A fungal family of transcriptional regulators: the zinc cluster proteins**. *Microbiology and molecular biology reviews : MMBR* 70: 583-604.

Magasanik, B., (2005) **The transduction of the nitrogen regulation signal in *Saccharomyces cerevisiae***. *Proceedings of the National Academy of Sciences of the United States of America* 102: 16537-16538.

Magasanik, B. & C. A. Kaiser, (2002) **Nitrogen regulation in *Saccharomyces cerevisiae***. *Gene* 290: 1-18.

Magee, P. T. & B. B. Magee, (2004) **Through a glass opaquely: the biological significance of mating in *Candida albicans***. *Current opinion in microbiology* 7: 661-665.

Maidan, M. M., L. De Rop, J. Serneels, S. Exler, S. Rupp, H. Tournu, J. M. Thevelein & P. Van Dijck, (2005) **The G protein-coupled receptor Gpr1 and the Galpha protein Gpa2 act through the cAMP-protein kinase A pathway to induce morphogenesis in *Candida albicans***. *Molecular biology of the cell* 16: 1971-1986.

Marini, A. M., S. Soussi-Boudekou, S. Vissers & B. Andre, (1997) **A family of ammonium transporters in *Saccharomyces cerevisiae***. *Molecular and cellular biology* 17: 4282-4293.

Martínez, P. & P. O. Ljungdahl, (2004) **An ER packaging chaperone determines the amino acid uptake capacity and virulence of *Candida albicans***. *Molecular microbiology* 51: 371-384.

Martínez, P. & P. O. Ljungdahl, (2005) **Divergence of Stp1 and Stp2 transcription factors in *Candida albicans* places virulence factors required for proper nutrient acquisition under amino acid control**. *Molecular and cellular biology* 25: 9435-9446.

Marzluf, G. A., (1997) **Genetic regulation of nitrogen metabolism in the fungi**. *Microbiology and molecular biology reviews : MMBR* 61: 17-32.

Massey, S. E., G. Moura, P. Beltrao, R. Almeida, J. R. Garey, M. F. Tuite & M. A. Santos, (2003) **Comparative evolutionary genomics unveils the molecular mechanism of reassignment of the CTG codon in *Candida* spp**. *Genome research* 13: 544-557.

Mayer, F. L., D. Wilson & B. Hube, (2013) ***Candida albicans* pathogenicity mechanisms**. *Virulence* 4: 119-128.

Meiller, T. F., B. Hube, L. Schild, M. E. Shirtliff, M. A. Scheper, R. Winkler, A. Ton & M. A. Jabra-Rizk, (2009) **A novel immune evasion strategy of *Candida albicans*: proteolytic cleavage of a salivary antimicrobial peptide**. *PloS one* 4: e5039.

Mogavero, S., A. Tavanti, S. Senesi, P. D. Rogers & J. Morschhäuser, (2011) **Differential requirement of the transcription factor Mcm1 for activation of the *Candida albicans* multidrug efflux pump *MDR1* by its regulators Mrr1 and Cap1**. *Antimicrobial agents and chemotherapy* 55: 2061-2066.

Moran, G. P., D. C. Coleman & D. J. Sullivan, (2011) **Comparative genomics and the evolution of pathogenicity in human pathogenic fungi**. *Eukaryotic cell* 10: 34-42.

Morschhäuser, J., (2010a) **Regulation of multidrug resistance in pathogenic fungi**. *Fungal genetics and biology : FG & B* 47: 94-106.

Morschhäuser, J., (2010b) **Regulation of white-opaque switching in *Candida albicans***. *Medical microbiology and immunology* 199: 165-172.

Morschhäuser, J., (2011) **Nitrogen regulation of morphogenesis and protease secretion in *Candida albicans***. *International journal of medical microbiology : IJMM* 301: 390-394.

Naglik, J. R., S. J. Challacombe & B. Hube, (2003) ***Candida albicans* secreted aspartyl proteinases in virulence and pathogenesis**. *Microbiology and molecular biology reviews : MMBR* 67: 400-428, table of contents.

Navarathna, D. H., A. Das, J. Morschhäuser, K. W. Nickerson & D. D. Roberts, (2011) **Dur3 is the major urea transporter in *Candida albicans* and is co-regulated with the urea amidolyase Dur1,2**. *Microbiology* 157: 270-279.

Neuhäuser, B., N. Dunkel, S. V. Satheesh & J. Morschhäuser, (2011) **Role of the Npr1 kinase in ammonium transport and signaling by the ammonium permease Mep2 in *Candida albicans***. *Eukaryotic cell* 10: 332-342.

Newport, G., A. Kuo, A. Flattery, C. Gill, J. J. Blake, M. B. Kurtz, G. K. Abruzzo & N. Agabian, (2003) **Inactivation of Kex2p diminishes the virulence of *Candida albicans***. *The Journal of biological chemistry* 278: 1713-1720.

Nucci, M. & E. Anaissie, (2001) **Revisiting the source of candidemia: skin or gut?** *Clinical infectious diseases : an official publication of the Infectious Diseases Society of America* 33: 1959-1967.

Ohama, T., T. Suzuki, M. Mori, S. Osawa, T. Ueda, K. Watanabe & T. Nakase, (1993) **Non-universal decoding of the leucine codon CUG in several *Candida* species**. *Nucleic acids research* 21: 4039-4045.

Padovan, A. C., G. M. Chaves, A. L. Colombo & M. R. Briones, (2009) **A novel allele of *HWP1*, isolated from a clinical strain of *Candida albicans* with defective hyphal growth and biofilm formation, has deletions of Gln/Pro and Ser/Thr repeats involved in cellular adhesion**. *Medical mycology : official publication of the International Society for Human and Animal Mycology* 47: 824-835.

Pappas, P. G., C. A. Kauffman, D. Andes, D. K. Benjamin, Jr., T. F. Calandra, J. E. Edwards, Jr., S. G. Filler, J. F. Fisher, B. J. Kullberg, L. Ostrosky-Zeichner, A. C. Reboli, J. H. Rex, T. J. Walsh, J. D. Sobel & A. Infectious Diseases Society of, (2009) **Clinical practice guidelines for the management of candidiasis: 2009 update by the Infectious Diseases Society of America**. *Clinical infectious diseases : an official publication of the Infectious Diseases Society of America* 48: 503-535.

Park, Y. N. & J. Morschhäuser, (2005) ***Candida albicans MTL*alpha *tup1*Delta mutants can reversibly switch to mating-competent, filamentous growth forms**. *Molecular microbiology* 58: 1288-1302.

Pérez, J. C., C. A. Kumamoto & A. D. Johnson, (2013) ***Candida albicans* Commensalism and Pathogenicity Are Intertwined Traits Directed by a Tightly Knit Transcriptional Regulatory Circuit**. *PLoS biology* 11: e1001510.

Perlroth, J., B. Choi & B. Spellberg, (2007) **Nosocomial fungal infections: epidemiology, diagnosis, and treatment**. *Medical mycology : official publication of the International Society for Human and Animal Mycology* 45: 321-346.

Perry, J. R., M. A. Basrai, H. Y. Steiner, F. Naider & J. M. Becker, (1994) **Isolation and characterization of a *Saccharomyces cerevisiae* peptide transport gene**. *Molecular and cellular biology* 14: 104-115.

Pfaller, M. A. & D. J. Diekema, (2007) **Epidemiology of invasive candidiasis: a persistent public health problem**. *Clinical microbiology reviews* 20: 133-163.

Pfaller, M. A. & D. J. Diekema, (2010) **Epidemiology of invasive mycoses in North America**. *Critical reviews in microbiology* 36: 1-53.

Pike, S., A. Patel, G. Stacey & W. Gassmann, (2009) ***Arabidopsis OPT6* is an oligopeptide transporter with exceptionally broad substrate specificity**. *Plant & cell physiology* 50: 1923-1932.

Piyankarage, S. C., H. Augustin, D. E. Featherstone & S. A. Shippy, (2010) **Hemolymph amino acid variations following behavioral and genetic changes in individual *Drosophila* larvae**. *Amino acids* 38: 779-788.

Puri, S., R. Kumar, S. Chadha, S. Tati, H. R. Conti, B. Hube, P. J. Cullen & M. Edgerton, (2012) **Secreted aspartic protease cleavage of *Candida albicans* Msb2 activates Cek1 MAPK signaling affecting biofilm formation and oropharyngeal candidiasis**. *PloS one* 7: e46020.

Rahman, D., M. Mistry, S. Thavaraj, S. J. Challacombe & J. R. Naglik, (2007) **Murine model of concurrent oral and vaginal *Candida albicans* colonization to study epithelial host-pathogen interactions**. *Microbes and infection / Institut Pasteur* 9: 615-622.

Ramírez-Zavala, B., O. Reuss, Y. N. Park, K. Ohlsen & J. Morschhäuser, (2008) **Environmental induction of white-opaque switching in *Candida albicans***. *PLoS pathogens* 4: e1000089.

Ramírez, M. A. & M. C. Lorenz, (2007) **Mutations in alternative carbon utilization pathways in *Candida albicans* attenuate virulence and confer pleiotropic phenotypes**. *Eukaryotic cell* 6: 280-290.

Remold, H., H. Fasold & F. Staib, (1968) **Purification and characterization of a proteolytic enzyme from *Candida albicans***. *Biochimica et biophysica acta* 167: 399-406.

Reuss, O. & J. Morschhäuser, (2006) **A family of oligopeptide transporters is required for growth of *Candida albicans* on proteins**. *Molecular microbiology* 60: 795-812.

Reuss, O., A. Vik, R. Kolter & J. Morschhäuser, (2004) **The *SAT1* flipper, an optimized tool for gene disruption in *Candida albicans***. *Gene* 341: 119-127.

Rubio-Texeira, M., G. Van Zeebroeck, K. Voordeckers & J. M. Thevelein, (2010) ***Saccharomyces cerevisiae* plasma membrane nutrient sensors and their role in PKA signaling**. *FEMS yeast research* 10: 134-149.

Ryan, O., R. S. Shapiro, C. F. Kurat, D. Mayhew, A. Baryshnikova, B. Chin, Z. Y. Lin, M. J. Cox, F. Vizeacoumar, D. Cheung, S. Bahr, K. Tsui, F. Tebbji, A. Sellam, F. Istel, T. Schwarzmüller, T. B. Reynolds, K. Kuchler, D. K. Gifford, M. Whiteway, G. Giaever, C. Nislow, M. Costanzo, A. C. Gingras, R. D. Mitra, B. Andrews, G. R. Fink, L. E. Cowen & C. Boone, (2012) **Global gene deletion analysis exploring yeast filamentous growth**. *Science* 337: 1353-1356.

Sanglard, D., B. Hube, M. Monod, F. C. Odds & N. A. Gow, (1997) **A triple deletion of the secreted aspartyl proteinase genes *SAP4*, *SAP5*, and *SAP6* of *Candida albicans* causes attenuated virulence**. *Infection and immunity* 65: 3539-3546.

Sanglard, D., F. Ischer, M. Monod & J. Bille, (1996) **Susceptibilities of *Candida albicans* multidrug transporter mutants to various antifungal agents and other metabolic inhibitors**. *Antimicrobial agents and chemotherapy* 40: 2300-2305.

Sasse, C., N. Dunkel, T. Schäfer, S. Schneider, F. Dierolf, K. Ohlsen & J. Morschhäuser, (2012) **The stepwise acquisition of fluconazole resistance mutations causes a gradual loss of fitness in *Candida albicans***. *Molecular microbiology* 86: 539-556.

Sasse, C., M. Hasenberg, M. Weyler, M. Gunzer & J. Morschhäuser, (2013) **White-opaque switching of *Candida albicans* allows immune evasion in an environment-dependent fashion**. *Eukaryotic cell* 12: 50-58.

Sasse, C. & J. Morschhäuser, (2012) **Gene deletion in *Candida albicans* wild-type strains using the *SAT1*-flipping strategy**. *Methods in molecular biology* 845: 3-17.

Schaller, M., M. Bein, H. C. Korting, S. Baur, G. Hamm, M. Monod, S. Beinhauer & B. Hube, (2003) **The secreted aspartyl proteinases Sap1 and Sap2 cause tissue damage in an *in vitro* model of**

vaginal candidiasis based on reconstituted human vaginal epithelium. *Infection and immunity* 71: 3227-3234.

Schaller, M., C. Borelli, H. C. Korting & B. Hube, (2005) **Hydrolytic enzymes as virulence factors of *Candida albicans***. *Mycoses* 48: 365-377.

Schild, L., A. Heyken, P. W. de Groot, E. Hiller, M. Mock, C. de Koster, U. Horn, S. Rupp & B. Hube, (2011) **Proteolytic cleavage of covalently linked cell wall proteins by *Candida albicans* Sap9 and Sap10**. *Eukaryotic cell* 10: 98-109.

Schubert, S., K. S. Barker, S. Znaidi, S. Schneider, F. Dierolf, N. Dunkel, M. Aid, G. Boucher, P. D. Rogers, M. Raymond & J. Morschhäuser, (2011) **Regulation of efflux pump expression and drug resistance by the transcription factors Mrr1, Upc2, and Cap1 in *Candida albicans***. *Antimicrobial agents and chemotherapy* 55: 2212-2223.

Selmecki, A., A. Forche & J. Berman, (2006) **Aneuploidy and isochromosome formation in drug-resistant *Candida albicans***. *Science* 313: 367-370.

Selmecki, A., A. Forche & J. Berman, (2010) **Genomic plasticity of the human fungal pathogen *Candida albicans***. *Eukaryotic cell* 9: 991-1008.

Selmecki, A., M. Gerami-Nejad, C. Paulson, A. Forche & J. Berman, (2008) **An isochromosome confers drug resistance *in vivo* by amplification of two genes, *ERG11* and *TAC1***. *Molecular microbiology* 68: 624-641.

Shapiro, R. S., N. Robbins & L. E. Cowen, (2011) **Regulatory circuitry governing fungal development, drug resistance, and disease**. *Microbiology and molecular biology reviews : MMBR* 75: 213-267.

Sherwood, R. K. & R. J. Bennett, (2009) **Fungal meiosis and parasexual reproduction--lessons from pathogenic yeast**. *Current opinion in microbiology* 12: 599-607.

Sobel, J. D., (2007) **Vulvovaginal candidosis**. *Lancet* 369: 1961-1971.

Soll, D. R., (2009) **Why does *Candida albicans* switch?** *FEMS yeast research* 9: 973-989.

Staab, J. F. & P. Sundstrom, (2003) ***URA3* as a selectable marker for disruption and virulence assessment of *Candida albicans* genes**. *Trends in microbiology* 11: 69-73.

Staib, F., (1965) **Serum-proteins as nitrogen source for yeastlike fungi**. *Sabouraudia* 4: 187-193.

Staib, F., (1969) **Proteolysis and pathogenicity of *Candida albicans* strains**. *Mycopathologia et mycologia applicata* 37: 345-348.

Staib, P., M. Kretschmar, T. Nichterlein, H. Hof & J. Morschhäuser, (2002a) **Host versus in vitro signals and intrastrain allelic differences in the expression of a *Candida albicans* virulence gene**. *Molecular microbiology* 44: 1351-1366.

Staib, P., M. Kretschmar, T. Nichterlein, H. Hof & J. Morschhäuser, (2002b) **Transcriptional regulators Cph1p and Efg1p mediate activation of the *Candida albicans* virulence gene *SAP5* during infection**. *Infection and immunity* 70: 921-927.

Staib, P., U. Lermann, J. Blass-Warmuth, B. Degel, R. Wurzner, M. Monod, T. Schirmeister & J. Morschhäuser, (2008) **Tetracycline-inducible expression of individual secreted aspartic proteases in *Candida albicans* allows isoenzyme-specific inhibitor screening**. *Antimicrobial agents and chemotherapy* 52: 146-156.

Staib, P. & J. Morschhäuser, (2007) **Chlamydospore formation in *Candida albicans* and *Candida dubliniensis*--an enigmatic developmental programme**. *Mycoses* 50: 1-12.

Sudbery, P., N. Gow & J. Berman, (2004) **The distinct morphogenic states of *Candida albicans***. *Trends in microbiology* 12: 317-324.

Sudbery, P. E., (2011) **Growth of *Candida albicans* hyphae**. *Nature reviews. Microbiology* 9: 737-748.

Szafranski-Schneider, E., M. Swidergall, F. Cottier, D. Tielker, E. Román, J. Pla & J. F. Ernst, (2012) **Msb2 shedding protects *Candida albicans* against antimicrobial peptides**. *PLoS pathogens* 8: e1002501.

Tati, S., W. S. Jang, R. Li, R. Kumar, S. Puri & M. Edgerton, (2013) **Histatin 5 Resistance of *Candida glabrata* Can Be Reversed by Insertion of *Candida albicans* Polyamine Transporter-Encoding Genes *DUR3* and *DUR31***. *PloS one* 8: e61480.

Thomas-Chollier, M., C. Herrmann, M. Defrance, O. Sand, D. Thieffry & J. van Helden, (2012) **RSAT peak-motifs: motif analysis in full-size ChIP-seq datasets**. *Nucleic acids research* 40: e31.

Thompson, D. S., P. L. Carlisle & D. Kadosh, (2011) **Coevolution of morphology and virulence in *Candida* species**. *Eukaryotic cell* 10: 1173-1182.

Tirosh, I., N. Barkai & K. J. Verstrepen, (2009) **Promoter architecture and the evolvability of gene expression**. *Journal of biology* 8: 95.

van het Hoog, M., T. J. Rast, M. Martchenko, S. Grindle, D. Dignard, H. Hogues, C. Cuomo, M. Berriman, S. Scherer, B. B. Magee, M. Whiteway, H. Chibana, A. Nantel & P. T. Magee, (2007) **Assembly of the *Candida albicans* genome into sixteen supercontigs aligned on the eight chromosomes**. *Genome biology* 8: R52.

Vilanova, M., L. Teixeira, I. Caramalho, E. Torrado, A. Marques, P. Madureira, A. Ribeiro, P. Ferreira, M. Gama & J. Demengeot, (2004) **Protection against systemic candidiasis in mice immunized with secreted aspartic proteinase 2**. *Immunology* 111: 334-342.

Vinces, M. D., M. Legendre, M. Caldara, M. Hagihara & K. J. Verstrepen, (2009) **Unstable tandem repeats in promoters confer transcriptional evolvability**. *Science* 324: 1213-1216.

Vylkova, S., A. J. Carman, H. A. Danhof, J. R. Collette, H. Zhou & M. C. Lorenz, (2011) **The fungal pathogen *Candida albicans* autoinduces hyphal morphogenesis by raising extracellular pH**. *mBio* 2: e00055-00011.

Wächtler, B., D. Wilson, K. Haedicke, F. Dalle & B. Hube, (2011) **From attachment to damage: defined genes of *Candida albicans* mediate adhesion, invasion and damage during interaction with oral epithelial cells**. *PloS one* 6: e17046.

Werner, H., (1966) **[Studies on the lipase activity in yeasts and yeast-like fungi]**. *Zentralblatt fur Bakteriologie, Parasitenkunde, Infektionskrankheiten und Hygiene. 1. Abt. Medizinisch-hygienische Bakteriologie, Virusforschung und Parasitologie. Originale* 200: 113-124.

Weyler, M. & J. Morschhäuser, (2012) **Tetracycline-inducible gene expression in *Candida albicans***. *Methods in molecular biology* 845: 201-210.

White, S. J., A. Rosenbach, P. Lephart, D. Nguyen, A. Benjamin, S. Tzipori, M. Whiteway, J. Mecsas & C. A. Kumamoto, (2007) **Self-regulation of *Candida albicans* population size during GI colonization**. *PLoS pathogens* 3: e184.

WHO, (2012) **WHO Global Report for Research on Infectious Diseases of Poverty**. Geneva, Switzerland: WHO.

Wyzgol, A., (2005) **Molekulare Untersuchungen zur Regulation der Expression sekretorischer Proteasen in *Candida albicans***. In: University of Wuerzburg. University of Wuerzburg.

Xie, J., L. Tao, C. J. Nobile, Y. Tong, G. Guan, Y. Sun, C. Cao, A. D. Hernday, A. D. Johnson, L. Zhang, F. Y. Bai & G. Huang, (2013) **White-opaque switching in natural *MTL*a/alpha isolates of *Candida albicans*: evolutionary implications for roles in host adaptation, pathogenesis, and sex**. *PLoS biology* 11: e1001525.

Zaman, S., S. I. Lippman, X. Zhao & J. R. Broach, (2008) **How *Saccharomyces* responds to nutrients**. *Annual review of genetics* 42: 27-81.

Zhang, Z. D., J. Rozowsky, H. Y. Lam, J. Du, M. Snyder & M. Gerstein, (2007) **Tilescope: online analysis pipeline for high-density tiling microarray data**. *Genome biology* 8: R81.

Zhu, C., K. J. Byers, R. P. McCord, Z. Shi, M. F. Berger, D. E. Newburger, K. Saulrieta, Z. Smith, M. V. Shah, M. Radhakrishnan, A. A. Philippakis, Y. Hu, F. De Masi, M. Pacek, A. Rolfs, T. Murthy, J. Labaer & M. L. Bulyk, (2009) **High-resolution DNA-binding specificity analysis of yeast transcription factors**. *Genome research* 19: 556-566.

Znaidi, S., K. S. Barker, S. Weber, A. M. Alarco, T. T. Liu, G. Boucher, P. D. Rogers & M. Raymond, (2009) **Identification of the *Candida albicans* Cap1p regulon**. *Eukaryotic cell* 8: 806-820.

Znaidi, S., S. Weber, O. Z. Al-Abdin, P. Bomme, S. Saidane, S. Drouin, S. Lemieux, X. De Deken, F. Robert & M. Raymond, (2008) **Genomewide location analysis of *Candida albicans* Upc2p, a regulator of sterol metabolism and azole drug resistance**. *Eukaryotic cell* 7: 836-847.

Appendix

Appendix A1: Stp1 targets

Stp1-HA binding events during growth in YCB-YE-BSA. List includes combined data from three independent experiments with a p-value cut-off of ≤0.01 and a log_2 pseudo-median signal intensity threshold of ≥1.5. Binding events, descending from highest binding intensities, with their respective fold binding ratios, Contig19 numbers, and binding event locations within the Contig19 are indicated. Assigned ORFs to each binding event are indicated with their Gene ID (orf19 numbers), gene names and their respective location in the Contig19 were taken from the *Candida* genome database (CGD). Genes IDs with no CGD name are described as their closest ortholog in *S. cerevisiae* (e.g. Sc*DUG1*) and alternative CGD names are separated by a slash. Binding events within 1 kb upstream (direct upstream), further upstream (distance indicated in parentheses), or overlapping with the ORF (upstream / ORF) relative to ATG^{start} codon of the assigned ORF are given in the column binding region. Note that only binding events assigned to the upstream region of an ORF are indicated and otherwise associated ORFs were excluded.

No.	Log_2 signal intensity	fold binding ratio	Contig 19 #	Location	Gene ID	CGD Gene Name	Binding region	gene location
1	3.068	8.386	Contig19-10259	28741..30361	orf19.6937	***PTR22***	direct upstream	28683 to 26953
2	2.734	6.653	Contig19-10151	121681..123181	orf19.2602	***OPT1***	direct upstream	121515 to 119164
3	1.742	3.345	Contig19-10190	46261..47401	orf19.3746	***OPT2***	direct upstream	47900 to 50689
4	1.658	3.156	Contig19-10194	38101..38821	orf19.3915	***ScDUG1***	upstream / ORF	38202 to 36745
5	1.658	3.156	Contig19-10194	38101..38821	orf19.3916	-	direct upstream	38944 to 40528
6	1.586	3.002	Contig19-10202	166561..167461	orf19.4309	***GRP2***	upstream / ORF	166658 to 165633
7	1.528	2.884	Contig19-10119	285841..286801	orf19.1585	***ZRT2***	direct upstream	287113 to 288225
8	1.483	2.795	Contig19-10125	63961..65041	orf19.1770	***CYC1***	direct upstream	63913 to 63581
9	1.366	2.578	Contig19-10188	9841..10741	orf19.3707	***YHB1***	direct upstream	9013 to 7817
10	1.363	2.572	Contig19-10087	3841..4561	orf19.1028	***ELA1***	upstream (1.6 kb)	6119 to 7297
11	1.363	2.572	Contig19-10087	3841..4561	orf19.1027	***PDR16***	direct upstream	3747 to 2638
12	1.328	2.511	Contig19-10131	22321..23281	orf19.1825	-	upstream (2.8 kb)	19564 to 17339
13	1.328	2.511	Contig19-10131	22321..23281	orf19.1826	***MDM34***	direct upstream	23245 to 25113
14	1.303	2.467	Contig19-10072	9361..10381	orf19.740	***HAP41***	upstream (1.5 kb)	8192 to 7047
15	1.272	2.415	Contig19-10233	137521..138181	orf19.5772	***AOR1***	upstream / ORF	137548 to 136532
16	1.272	2.415	Contig19-10233	137521..138181	orf19.5773	-	direct upstream	138321 to 140423
17	1.261	2.397	Contig19-2516	75121..75721	orf19.7498	***LEU1***	upstream / ORF	75645 to 77975
18	1.261	2.397	Contig19-2516	75121..75721	orf19.7497	***ScCUL3***	direct upstream	75110 to 72531
19	1.260	2.395	Contig19-2472	5461..6301	orf19.6659	***GAP6/GAP5***	upstream / ORF	6260 to 7990
20	1.260	2.395	Contig19-2472	5461..6301	orf19.6658	-	direct upstream	5054 to 3423
21	1.240	2.362	Contig19-10190	51721..53941	orf19.3749	***OPT3***	direct upstream	53984 to 56701
22	1.231	2.347	Contig19-10233	148681..149761	orf19.5775.3	-	direct upstream	150368 to 150811
23	1.212	2.317	Contig19-10014	37021..38161	orf19.34	***GIT1***	upstream (2.6 kb)	34817 to 33258
24	1.212	2.317	Contig19-1913	781..2761	orf19.2659	-	upstream / ORF	2220 to 2825
25	1.212	2.317	Contig19-1913	781..2761	orf19.2658	-	direct upstream	331 to 2
26	1.210	2.313	Contig19-10262	98221..98881	orf19.7043	-	direct upstream	99345 to 99854
27	1.210	2.313	Contig19-10262	98221..98881	orf19.7042	-	direct upstream	97997 to 97095
28	1.208	2.310	Contig19-10248	104881..105301	orf19.6514	***CUP9***	direct upstream	105683 to 106717
29	1.208	2.310	Contig19-10150	9961..10681	orf19.2435	***MSI3***	direct upstream	10638 to 12743
30	1.190	2.282	Contig19-10236	114841..115741	orf19.5917.3	***YRA1***	upstream (2.5 kb)	118231 to 119817
31	1.190	2.282	Contig19-10236	114841..115741	orf19.5917	***STP1***	direct upstream	114713 to 113403
32	1.186	2.275	Contig19-10158	212701..216421	orf19.2765	***PGA52/FLO1***	upstream / ORF	213017 to 212376
33	1.186	2.275	Contig19-10158	212701..216421	orf19.2766	-	upstream / ORF	214131 to 213823
34	1.179	2.264	Contig19-10236	289081..290521	orf19.6000	***CDR1***	direct upstream	290502 to 295007
35	1.179	2.264	Contig19-10236	289081..290521	orf19.5999	***DYN1***	direct upstream	288228 to 275743
36	1.172	2.253	Contig19-10176	76261..76921	orf19.3430	***BUD21***	direct upstream	75387 to 74353
37	1.172	2.253	Contig19-10176	76261..76921	orf19.3431	***MIP1***	direct upstream	77381 to 81067
38	1.165	2.242	Contig19-10057	83941..87361	orf19.610	***EFG1***	direct upstream	82527 to 80950
39	1.157	2.230	Contig19-10190	26101..27121	orf19.3734	***GEF2***	direct upstream	27973 to 30552
40	1.150	2.219	Contig19-10123	186961..187621	orf19.1690	***TOS1***	direct upstream	187827 to 189233
41	1.128	2.186	Contig19-10216	162181..163021	orf19.4980	***HSP70/SSA4***	direct upstream	163054 to 165024
42	1.124	2.180	Contig19-10193	20641..21181	orf19.3861	***SIS1***	upstream / ORF	21143 to 22174
43	1.123	2.178	Contig19-10219	16621..17821	orf19.5132	-	direct upstream	18606 to 18986
44	1.123	2.178	Contig19-10219	16621..17821	orf19.5131	***ScGID7***	direct upstream	16269 to 14107
45	1.122	2.176	Contig19-10070	27241..27781	orf19.723	***BCR1***	upstream (1.4 kb)	29228 to 31450
46	1.115	2.166	Contig19-10186	33001..34261	orf19.3672	***GAL10***	direct upstream	34326 to 36353
47	1.115	2.166	Contig19-10186	33001..34261	orf19.3670	***GAL1***	direct upstream	32964 to 31417
48	1.113	2.163	Contig19-10139	72481..74581	orf19.2026	***UBP13***	upstream (1.3 kb)	75836 to 77938
49	1.113	2.163	Contig19-10139	72481..74581	orf19.2023	***HGT7/HXT3***	direct upstream	72164 to 70524
50	1.104	2.149	Contig19-10215	403801..404221	orf19.4906	***ScBCK2***	upstream / ORF	403854 to 401548
51	1.101	2.145	Contig19-10173	30841..33121	orf19.3302	***ScGAC1***	direct upstream	30088 to 27986
52	1.098	2.141	Contig19-10070	67921..68650	orf19.734	***GLK1***	upstream / ORF	68068 to 66650
53	1.098	2.141	Contig19-10070	67921..68650	orf19.11	-	direct upstream	Contig19-10011:6820 to 6101
54	1.097	2.139	Contig19-10230	202981..205861	orf19.5626	-	direct upstream	206329 to 207558
55	1.097	2.139	Contig19-10230	202981..205861	orf19.5625	-	direct upstream	201767 to 201234
56	1.095	2.136	Contig19-2500	47281..47701	orf19.6982	***ScAIM32***	upstream (3.2 kb)	44067 to 42778
57	1.094	2.135	Contig19-10262	185821..187261	orf19.7085	-	upstream / ORF	186697 to 188016
58	1.094	2.135	Contig19-10262	185821..187261	orf19.7084	***DFI1***	direct upstream	185003 to 183990
59	1.093	2.133	Contig19-10087	42601..43201	orf19.1048	***IFD6***	upstream / ORF	43147 to 44181
60	1.086	2.123	Contig19-10137	108421..109561	orf19.1979	***GIT3/IFN1***	direct upstream	110304 to 111911
61	1.085	2.121	Contig19-10215	246001..246601	orf19.4833	***MLS1***	direct upstream	246665 to 248320
62	1.085	2.121	Contig19-10186	37981..38701	orf19.3675	***GAL7***	direct upstream	38913 to 40073
63	1.085	2.121	Contig19-10186	37981..38701	orf19.3674	***GAL102/TGD99***	direct upstream	37985 to 37023
64	1.075	2.107	Contig19-10254	193021..194101	orf19.6816	-	direct upstream	194310 to 195158

No.	Log_2 signal intensity	fold binding ratio	Contig 19 #	Location	Gene ID	CGD Gene Name	Binding region	gene location
65	1.075	2.107	Contig19-10254	193021..194101	orf19.6814	***TDH3***	direct upstream	192755 to 191748
66	1.074	2.105	Contig19-10194	189121..190441	orf19.3997	***ADH1***	upstream / ORF	190256 to 191560
67	1.070	2.099	Contig19-10087	68161..68701	orf19.1065	***SSA2***	direct upstream	68078 to 66141
68	1.065	2.092	Contig19-10185	28141..29041	orf19.3649	***ScFES1***	direct upstream	28039 to 27185
69	1.065	2.092	Contig19-10185	28141..29041	orf19.3651	***PGK1***	direct upstream	29063 to 30316
70	1.062	2.088	Contig19-10202	180301..181741	orf19.4322	***DAP2***	upstream (1.9 kb)	183636 to 186152
71	1.062	2.088	Contig19-10202	180301..181741	orf19.4318	***MIG1***	direct upstream	180286 to 178574
72	1.061	2.086	Contig19-10076	164401..165181	orf19.868	**ADAEC**	direct upstream	165275 to 166912
73	1.059	2.083	Contig19-10158	117721..118501	orf19.2723	***HIT1***	upstream (1.5 kb)	116245 to 115799
74	1.053	2.075	Contig19-10035	47881..48601	orf19.111	***CAN2***	direct upstream	47238 to 45532
75	1.053	2.075	Contig19-10113	9181..9901	orf19.1358	***GCN4***	direct upstream	8177 to 7206
76	1.050	2.071	Contig19-10227	143521..144781	orf19.5469	***YRF1***	direct upstream	145442 to 148636
77	1.050	2.071	Contig19-2513	90721..92101	orf19.7381	***AHR1/ZCF37***	upstream (2.0 kb)	94127 to 96001
78	1.044	2.062	Contig19-10212	111721..112981	orf19.4623.3	***NHP6A***	upstream / ORF	112939 to 113217
79	1.037	2.052	Contig19-10158	246841..247501	orf19.2775	***IDI1***	direct upstream	Cntg19-10158:243468 to 242614
80	1.037	2.052	Contig19-10158	246841..247501	orf19.2777	-	direct upstream	247698 to 248555
81	1.037	2.052	Contig19-10053	30001..30421	orf19.475	-	upstream (2.0 kb)	32435 to 33536
82	1.037	2.052	Contig19-10053	30001..30421	orf19.474	-	direct upstream	29767 to 28466
83	1.029	2.041	Contig19-10011	7081..7801	orf19.13	-	direct upstream	7651 to 9069
84	1.028	2.039	Contig19-10217	2281..2761	orf19.5038	***TRM3***	direct upstream	3338 to 7660
85	1.028	2.039	Contig19-10217	2281..2761	orf19.5037	***HRQ2***	direct upstream	2227 to 959
86	1.026	2.036	Contig19-10162	16681..17701	orf19.2877	***PDC11***	direct upstream	17859 to 19562
87	1.026	2.036	Contig19-10162	16681..17701	orf19.2876	***CBF1***	direct upstream	16237 to 15566
88	1.023	2.032	Contig19-10158	129661..131101	orf19.2726	***ScSFK1***	upstream (2.7 kb)	133754 to 134692
89	1.021	2.029	Contig19-10119	78421..79141	orf19.1486	-	direct upstream	78202 to 77705
90	1.018	2.025	Contig19-10248	169201..171181	orf19.6541	***RPL5***	direct upstream	171209 to 172105
91	1.009	2.013	Contig19-10236	202201..204361	orf19.5960	***NCE102***	direct upstream	201621 to 201109
92	1.000	2.000	Contig19-10215	259261..259681	orf19.4843	***ScFRE8***	direct upstream	259245 to 257050
93	0.995	1.993	Contig19-10080	112261..113041	orf19.968	***PGA14***	direct upstream	112221 to 111826
94	0.994	1.992	Contig19-10123	19021..19621	orf19.1613	***ILV2***	direct upstream	18943 to 16892
95	0.992	1.989	Contig19-10052	53281..54121	orf19.434	***PRD1***	direct upstream	53980 to 56088
96	0.988	1.983	Contig19-10248	258961..259621	orf19.6586	-	direct upstream	259819 to 260760
97	0.987	1.982	Contig19-2456	1921..3781	orf19.6614	***HPR5***	direct upstream	4341 to 8609
98	0.986	1.981	Contig19-10163	15841..17941	orf19.2929	***GSC1/FKS1***	upstream (1.2 kb)	14363 to 8670
99	0.982	1.975	Contig19-10215	166261..166921	orf19.4793	***ScTMA16***	upstream (2.4 kb)	169321 to 169920
100	0.982	1.975	Contig19-10215	166261..166921	orf19.4792	-	direct upstream	166088 to 164415
101	0.980	1.972	Contig19-2514	98761..99121	orf19.7448	***LYS9***	upstream / ORF	99091 to 100425
102	0.979	1.971	Contig19-10124	5341..6181	orf19.1736	-	direct upstream	6583 to 6885
103	0.979	1.971	Contig19-10124	5341..6181	orf19.1735	***ScCWC27***	direct upstream	5035 to 4631
104	0.972	1.962	Contig19-10163	167281..168361	orf19.3010.1	***ECM33***	upstream (1.1 kb)	166142 to 164904
105	0.969	1.957	Contig19-2506	37981..38641	orf19.7151	-	upstream (3.9 kb)	34084 to 33650
106	0.968	1.956	Contig19-10203	1621..2041	orf19.4376	-	upstream (1.6 kb)	Contig19-10203:62041 to 61304
107	0.966	1.953	Contig19-10064	36601..37681	orf19.670.2	-	upstream / ORF	37526 to 37838
108	0.965	1.952	Contig19-10230	45961..46381	orf19.5537	***WSC2***	direct upstream	45151 to 43748
109	0.964	1.951	Contig19-10052	82501..83161	orf19.450	-	upstream (1.5 kb)	84205 to 84573
110	0.963	1.949	Contig19-10119	76501..77041	orf19.1485	***ScMRPL31***	direct upstream	75195 to 74854
111	0.961	1.947	Contig19-10216	280441..280981	orf19.5032	***SIM1/SUN42***	direct upstream	281519 to 282637
112	0.957	1.941	Contig19-10137	77581..78001	orf19.1961	***SpJMJ4***	direct upstream	78058 to 79650
113	0.954	1.937	Contig19-10083	11701..12421	orf19.1013	-	upstream / ORF	12046 to 11735
114	0.953	1.936	Contig19-10216	76261..78301	orf19.4941	***TYE7***	upstream / ORF	77121 to 76312
115	0.953	1.936	Contig19-10216	76261..78301	orf19.4940	***HIP1***	direct upstream	75715 to 74036
116	0.952	1.935	Contig19-10057	5341..5761	orf19.568	***SPE2***	upstream (2.7 kb)	2643 to 1495
117	0.952	1.935	Contig19-10057	5341..5761	orf19.570	***IFF8***	direct upstream	6389 to 8533
118	0.950	1.932	Contig19-10097	56701..57241	orf19.1168	***ZCF3***	direct upstream	57221 to 57808
119	0.947	1.928	Contig19-10123	262141..262741	orf19.1728	-	upstream (1.8 kb)	264587 to 265219
120	0.947	1.928	Contig19-10123	262141..262741	orf19.1727	***PMC1***	direct upstream	261178 to 257543
121	0.947	1.928	Contig19-10215	307561..308581	orf19.4869	***SFU1***	direct upstream	309680 to 311233
122	0.947	1.928	Contig19-10215	307561..308581	orf19.4867	***SWE1***	direct upstream	306971 to 303435
123	0.947	1.928	Contig19-10254	39121..39781	orf19.6734	***TCC1***	upstream (1.5 kb)	37674 to 35428
124	0.946	1.927	Contig19-10139	36301..36901	orf19.2005	***REG1***	direct upstream	38214 to 41249
125	0.942	1.921	Contig19-10161	20761..21841	orf19.2823	***RFG1/ROX1***	upstream (1.8 kb)	23516 to 25319
126	0.941	1.920	Contig19-10254	161041..161581	orf19.6798	***SSN6/CYC8***	upstream (1.3 kb)	159688 to 156446
127	0.938	1.916	Contig19-10113	47401..47941	orf19.1375	***LEU42***	direct upstream	47242 to 45521
128	0.934	1.911	Contig19-10151	19081..19381	orf19.2530	-	upstream / ORF	19139 to 18807
129	0.934	1.911	Contig19-10151	19081..19381	orf19.2531	***CSP37***	upstream / ORF	19310 to 20275
130	0.931	1.907	Contig19-10220	4141..4621	orf19.5197	***APE2***	direct upstream	4646 to 7510
131	0.930	1.905	Contig19-10244	17761..18121	orf19.6311	-	direct upstream	17583 to 17278
132	0.922	1.895	Contig19-2514	70321..70681	orf19.7436	***AAF1/CAD1***	upstream (1.5 kb)	72283 to 74121
133	0.921	1.893	Contig19-10139	55921..56461	orf19.2014	***BCY1***	direct upstream	56937 to 58314
134	0.921	1.893	Contig19-10139	55921..56461	orf19.2013	***KAR2***	direct upstream	55829 to 53766
135	0.919	1.891	Contig19-10216	213301..213661	orf19.5005	***OSM1***	direct upstream	213767 to 215713
136	0.917	1.888	Contig19-10194	32761..33181	orf19.3912	***GLN3***	direct upstream	32468 to 30420
137	0.916	1.887	Contig19-10035	10981..11281	orf19.89	***PEX7***	direct upstream	11789 to 12931
138	0.916	1.887	Contig19-10035	10981..11281	orf19.88	***ILV5***	direct upstream	10857 to 9655
139	0.915	1.886	Contig19-10216	117181..118921	orf19.4960	***SPE4***	upstream (1.5 kb)	115739 to 114705
140	0.915	1.886	Contig19-10216	117181..118921	orf19.4961	***STP2***	direct upstream	119025 to 120779
141	0.915	1.886	Contig19-10262	131941..132601	orf19.7054	-	upstream (2.5 kb)	129964 to 129599
142	0.915	1.886	Contig19-10051	24061..24901	orf19.396	***EAF6***	upstream / ORF	24839 to 25474
143	0.915	1.886	Contig19-10051	24061..24901	orf19.395	***ENO1***	direct upstream	23877 to 22555
144	0.914	1.884	Contig19-10187	11401..11641	orf19.3695	***EPT1***	direct upstream	11657 to 12865
145	0.914	1.884	Contig19-10046	65461..66121	orf19.265	-	upstream (2.0 kb)	67497 to 68999
146	0.911	1.880	Contig19-2506	60661..61021	orf19.7166	-	direct upstream	60996 to 62339
147	0.911	1.880	Contig19-10262	70261..70621	orf19.7029	***ScGUD1***	direct upstream	69625 to 67793
148	0.909	1.878	Contig19-1914	1..601	orf19.2661	***TLO34/CTA218***	upstream (2.1 kb)	2763 to 3149
149	0.909	1.878	Contig19-2200	3001..5401	orf19.4552	-	direct upstream	5621 to 5944
150	0.907	1.875	Contig19-10234	19561..20041	orf19.5785	-	direct upstream	18967 to 18089
151	0.905	1.873	Contig19-10093	2041..2341	orf19.1105.3	-	direct upstream	2486 to 3198
152	0.905	1.873	Contig19-10093	2041..2341	orf19.1105.2	***PGA56/CSU51***	direct upstream	1611 to 1357
153	0.905	1.873	Contig19-2513	88321..89161	orf19.7380	-	upstream (4.3 kb)	83969 to 80967
154	0.902	1.869	Contig19-10143	5821..7021	orf19.2231	-	direct upstream	5396 to 4617
155	0.901	1.867	Contig19-10135	15781..16261	orf19.1867	-	direct upstream	13892 to 12693
156	0.901	1.867	Contig19-10135	15781..16261	orf19.1868	***RNR22***	direct upstream	15561 to 14377

No.	Log_2 signal intensity	fold binding ratio	Contig 19 #	Location	Gene ID	CGD Gene Name	Binding region	gene location
157	0.897	1.862	Contig19-10227	108721..109561	orf19.5438	***ScSLX8***	direct upstream	110199 to 110588
158	0.897	1.862	Contig19-10227	108721..109561	orf19.5437	***RHR2***	direct upstream	108424 to 107660
159	0.896	1.861	Contig19-10147	10561..11341	orf19.2356	***CRZ2***	upstream (4.0 kb)	14793 to 16346
160	0.893	1.857	Contig19-10248	255121..255721	orf19.6585	***ScAIM1***	upstream (1.2 kb)	253917 to 253549
161	0.892	1.856	Contig19-10237	192961..194641	orf19.6114	-	direct upstream	194887 to 195198
162	0.890	1.853	Contig19-10170	22681..23461	orf19.3171	***ACH1***	direct upstream	23686 to 25260
163	0.888	1.851	Contig19-10099	35521..36661	orf19.1193	***GNP1/AGP1***	upstream / ORF	35870 to 34131
164	0.888	1.851	Contig19-10206	38281..38821	orf19.4476	***IFD6***	direct upstream	38293 to 37259
165	0.887	1.849	Contig19-10230	164461..164941	orf19.5604	***MDR1***	direct upstream	164333 to 162639
166	0.887	1.849	Contig19-10227	58861..59161	orf19.5399	***IFF11***	direct upstream	57887 to 56352
167	0.887	1.849	Contig19-2518	98221..99481	orf19.7692	***FAA4***	upstream (2.5 kb)	9367 to 8780
168	0.886	1.848	Contig19-10169	11581..11881	orf19.3156	***MDS1***	upstream (2.5 kb)	9171 to 5908
169	0.886	1.848	Contig19-10136	17041..19021	orf19.1925	***TLO5/CTA222***	upstream (1.5 kb)	15386 to 14856
170	0.884	1.845	Contig19-10166	1201..3001	orf19.3074	***TLO10/CTA211***	upstream (2.5 kb)	5448 to 6107
171	0.884	1.845	Contig19-10166	1201..3001	orf19.3073	-	direct upstream	357 to 1
172	0.884	1.845	Contig19-2513	64381..64681	orf19.7374	***CTA4***	direct upstream	65440 to 68490
173	0.884	1.845	Contig19-10080	84841..85381	orf19.951	-	direct upstream	85943 to 86431
174	0.883	1.844	Contig19-10076	197701..198121	orf19.882	***HSP78***	direct upstream	198123 to 200489
175	0.882	1.843	Contig19-2500	55201..56281	orf19.6984	***AVT42***	upstream (4.0 kb)	59732 to 62020
176	0.880	1.840	Contig19-10253	10741..10921	orf19.6687	-	upstream (3.0 kb)	7867 to 5864
177	0.880	1.840	Contig19-10253	10741..10921	orf19.6688	-	direct upstream	11147 to 12127
178	0.880	1.840	Contig19-10158	169861..170281	orf19.2747	***RGT1***	direct upstream	169681 to 166592
179	0.880	1.840	Contig19-10186	18481..19081	orf19.3668	***HGT2/RGT2***	direct upstream	18212 to 16575
180	0.880	1.840	Contig19-10254	78781..79141	orf19.6757	***GCY1***	direct upstream	78720 to 77833
181	0.879	1.839	Contig19-1876	6301..6961	orf19.2226	-	direct upstream	7747 to 8217
182	0.878	1.838	Contig19-10080	2101..3181	orf19.921	***HMS1***	upstream (1.8 kb)	4811 to 6868
183	0.878	1.838	Contig19-10080	2101..3181	orf19.920	***RMT2***	direct upstream	1237 to 2
184	0.878	1.838	Contig19-10140	46621..47041	orf19.2157	***DAC1/NAG2***	upstream / ORF	46949 to 48190
185	0.878	1.838	Contig19-10140	46621..47041	orf19.2156	***NAG1***	direct upstream	46508 to 45960
186	0.876	1.835	Contig19-10203	94861..95461	orf19.4393	***CIT1***	direct upstream	95560 to 97056
187	0.873	1.831	Contig19-10257	19021..20521	orf19.6874	***BAS1***	upstream (2.3 kb)	22840 to 24663
188	0.873	1.831	Contig19-10076	97081..97621	orf19.837	***GNA1***	direct upstream	96644 to 96195
189	0.872	1.830	Contig19-10151	133381..134041	orf19.2608	***ADH5/SAD1***	direct upstream	133374 to 132295
190	0.870	1.828	Contig19-10147	13741..14101	orf19.2355	***ALS10***	direct upstream	2941 to 7701
191	0.870	1.828	Contig19-2506	2401..4441	orf19.7127	***TLO16/CTA227***	upstream (1.8 kb)	6229 to 6756
192	0.868	1.825	Contig19-10248	11101..11341	orf19.6457	-	upstream (1.5 kb)	12996 to 14546
193	0.868	1.825	Contig19-10248	11101..11341	orf19.6456	-	direct upstream	10904 to 9228
194	0.868	1.825	Contig19-10248	36421..36961	orf19.6470	***AHP2/AHP13***	direct upstream	36037 to 35480
195	0.868	1.825	Contig19-10248	36421..36961	orf19.6472	***CYP1/CPR1***	direct upstream	36968 to 37456
196	0.867	1.824	Contig19-10190	25321..25741	orf19.3733	***IDP2***	direct upstream	25053 to 23815
197	0.865	1.821	Contig19-10053	132421..132961	orf19.541	-	direct upstream	130913 to 129792
198	0.865	1.821	Contig19-10053	132421..132961	orf19.542	***HXK2***	direct upstream	133086 to 134540
199	0.865	1.821	Contig19-10212	223861..224281	orf19.4679	***AGP2***	direct upstream	224972 to 226678
200	0.865	1.821	Contig19-10196	34681..35881	orf19.4082	***DDR48***	upstream (1.5 kb)	36776 to 37414
201	0.865	1.821	Contig19-10196	34681..35881	orf19.4081	-	direct upstream	36062 to 36562
202	0.865	1.821	Contig19-2506	40081..40741	orf19.7152	***CYS4***	direct upstream	40932 to 42029
203	0.864	1.820	Contig19-10236	266341..266521	orf19.5994	***RHB1***	upstream (4.5 kb)	270925 to 271479
204	0.864	1.820	Contig19-1960	7801..8341	orf19.3887	-	upstream (1.2 kb)	Contig19-10193:66522 to 65971
205	0.862	1.818	Contig19-10233	20701..21121	orf19.5713	***YMX6/NDE1***	upstream / ORF	20812 to 22680
206	0.861	1.816	Contig19-10080	33841..34501	orf19.932	***DRS24/DNF2***	direct upstream	32926 to 27776
207	0.858	1.813	Contig19-10076	117181..117601	orf19.847	***YIM1***	direct upstream	116661 to 115573
208	0.857	1.811	Contig19-10193	68881..69421	orf19.3888	***PGI1***	direct upstream	68434 to 66782
209	0.855	1.809	Contig19-10194	267601..269941	orf19.4054	***CTA24/TLO12***	upstream (2.5 kb)	265502 to 264744
210	0.854	1.808	Contig19-10218	134221..135601	orf19.5114	***GRD19***	direct upstream	134301 to 133828
211	0.854	1.808	Contig19-10194	200221..200521	orf19.4000	***GRF10/PHO2***	upstream (1.2 kb)	201662 to 203719
212	0.849	1.801	Contig19-10212	204481..205141	orf19.4669	***AAT22***	upstream / ORF	205158 to 206219
213	0.849	1.801	Contig19-2500	84901..85261	orf19.6995	***ATO6/AFF4***	direct upstream	86069 to 86914
214	0.849	1.801	Contig19-2500	84901..85261	orf19.6994	***BAT22***	direct upstream	84760 to 83651
215	0.847	1.799	Contig19-10173	67981..69241	orf19.3325	***GLG21***	direct upstream	67774 to 65792
216	0.847	1.799	Contig19-10065	7261..7741	orf19.695	***RGS2***	upstream (1.5 kb)	6127 to 4829
217	0.846	1.798	Contig19-10236	260761..261061	orf19.5992	***WOR2***	upstream (2.1 kb)	263182 to 264522
218	0.845	1.796	Contig19-10241	98281..98461	orf19.6246	***NAT3***	direct upstream	98149 to 97583
219	0.841	1.791	Contig19-10046	126001..126361	orf19.304	-	direct upstream	126491 to 128008
220	0.841	1.791	Contig19-10200	18781..19921	orf19.4166	***ZCF21***	direct upstream	17972 to 16083
221	0.840	1.790	Contig19-2479	11941..13210	orf19.6834.10	***TAR1***	upstream (2.5 kb)	9613 to 9347
222	0.840	1.790	Contig19-2479	11941..13210	orf19.6835	-	upstream (2.0 kb)	10086 to 9760
223	0.840	1.790	Contig19-10262	134041..134401	orf19.7055	-	upstream (3.5 kb)	137428 to 137754
224	0.840	1.790	Contig19-2492	18181..21781	orf19.6965	***FGR30***	upstream / ORF	18287 to 17964
225	0.840	1.790	Contig19-10119	216181..216721	orf19.1544	***ScBUG1***	upstream (1.9 kb)	218627 to 219424
226	0.840	1.790	Contig19-10119	216181..216721	orf19.1543	***OPI1***	direct upstream	215820 to 214519
227	0.840	1.790	Contig19-10225	3901..4261	orf19.5292	***AXL2***	upstream (1.5 kb)	5464 to 8331
228	0.839	1.789	Contig19-10188	10921..11521	orf19.3708	***SAP2***	upstream (2.0 kb)	13535 to 14731
229	0.838	1.788	Contig19-10202	88381..88921	orf19.4263	-	upstream (1.3 kb)	87123 to 85960
230	0.838	1.788	Contig19-10202	88381..88921	orf19.4264	-	direct upstream	89544 to 90449
231	0.837	1.786	Contig19-10256	11881..12601	orf19.6844	***ICL1***	direct upstream	12743 to 14395
232	0.836	1.785	Contig19-10064	7501..8161	orf19.657	***SAM2***	direct upstream	8337 to 9494
233	0.831	1.779	Contig19-10076	157921..158101	orf19.866	***RAD32***	direct upstream	157862 to 155940
234	0.828	1.775	Contig19-10194	123181..123661	orf19.3967	***SpNSE1***	direct upstream	123809 to 126772
235	0.828	1.775	Contig19-10230	16441..16921	orf19.5520	***ASG7***	direct upstream	15932 to 15486
236	0.828	1.775	Contig19-10230	16441..16921	orf19.5521	***ISA1***	direct upstream	16993 to 17802
237	0.827	1.774	Contig19-10254	45001..45901	orf19.6736	***FMP38***	direct upstream	46395 to 48284
238	0.826	1.773	Contig19-10238	47941..48241	orf19.6146	***CLG1***	direct upstream	48465 to 49220
239	0.824	1.770	Contig19-10223	126541..127921	orf19.5282	-	direct upstream	125620 to 124178
240	0.824	1.770	Contig19-10193	12781..13321	orf19.3854	***SAT4***	direct upstream	14386 to 16278
241	0.823	1.769	Contig19-2500	51181..52021	orf19.6983	-	direct upstream	50324 to 49152
242	0.822	1.768	Contig19-10237	199261..199570	orf19.6115	-	upstream (4.0 kb)	195548 to 195210
243	0.821	1.767	Contig19-10259	31741..31921	orf19.6938	***MEU1***	direct upstream	31638 to 30604
244	0.820	1.765	Contig19-10104	43081..43501	orf19.1239	-	upstream (1.7 kb)	41358 to 40372
245	0.820	1.765	Contig19-10104	43081..43501	orf19.1240	-	direct upstream	43704 to 51911
246	0.819	1.764	Contig19-10070	11221..11521	orf19.717	***HSP60***	direct upstream	11586 to 13286
247	0.819	1.764	Contig19-10215	144661..145441	orf19.4784	***CRP1/CRD1***	direct upstream	145409 to 149002
248	0.819	1.764	Contig19-10215	144661..145441	orf19.4783	-	direct upstream	144354 to 142930

No.	Log_2 signal intensity	fold binding ratio	Contig 19 #	Location	Gene ID	CGD Gene Name	Binding region	gene location
249	0.817	1.762	Contig19-10146	19261..20401	orf19.2308	***ScPFK27***	direct upstream	19030 to 17945
250	0.816	1.761	Contig19-10166	78601..79501	orf19.3127	***CZF1/ZNF1***	upstream (3.6 kb)	83126 to 84283
251	0.815	1.759	Contig19-10241	66661..66841	orf19.6229	***CAT1/CCT1***	direct upstream	66645 to 65188
252	0.813	1.757	Contig19-10104	129361..130021	orf19.1277	-	direct upstream	128765 to 127587
253	0.812	1.756	Contig19-2506	96601..96841	orf19.7196	***PRB1***	direct upstream	96464 to 94983
254	0.811	1.754	Contig19-10241	35761..36301	orf19.6214	***ATC1/ATH1***	direct upstream	37010 to 40246
255	0.811	1.754	Contig19-10241	35761..36301	orf19.6213	***SUI2***	direct upstream	35229 to 34327
256	0.810	1.753	Contig19-2514	47101..47341	orf19.7417	***TSA1***	direct upstream	47448 to 48038
257	0.809	1.752	Contig19-10173	94081..94441	orf19.3336	-	upstream (1.9 kb)	96360 to 96818
258	0.807	1.750	Contig19-10174	13501..14161	orf19.3368	-	upstream (2.2 kb)	11269 to 10964
259	0.807	1.750	Contig19-10174	13501..14161	orf19.3369	***MOH1***	direct upstream	14893 to 15684
260	0.805	1.747	Contig19-10262	49141..50101	orf19.7021	***GPH1***	direct upstream	48832 to 46130
261	0.805	1.747	Contig19-10104	70801..71101	orf19.1253	***PHO4***	direct upstream	71866 to 73845
262	0.804	1.746	Contig19-10235	4981..5521	orf19.5844	***MEI5***	direct upstream	5622 to 6098
263	0.804	1.746	Contig19-10194	83821..84301	orf19.3945	-	direct upstream	84707 to 86137
264	0.804	1.746	Contig19-10194	83821..84301	orf19.3944	***GRR1***	direct upstream	83197 to 80855
265	0.803	1.745	Contig19-10076	246901..247441	orf19.909	***STP4***	direct upstream	247548 to 248678
266	0.802	1.744	Contig19-10186	70561..71281	orf19.3691	***TIM21/FMP17***	direct upstream	71513 to 72319
267	0.802	1.744	Contig19-10186	70561..71281	orf19.3690.2	***ScRPL26B***	direct upstream	70376 to 69527
268	0.801	1.742	Contig19-10202	163861..164341	orf19.4308	***HSL1***	direct upstream	162876 to 158488
269	0.798	1.739	Contig19-2285	1621..2161	orf19.5284	-	direct upstream	855 to 541
270	0.798	1.739	Contig19-10215	409381..409561	orf19.4908	-	direct upstream	409855 to 410190
271	0.798	1.739	Contig19-10215	409381..409561	orf19.4907	-	direct upstream	409086 to 407269
272	0.797	1.737	Contig19-10236	127861..128341	orf19.5924	***ZCF31***	upstream (1.1 kb)	129473 to 132865
273	0.797	1.737	Contig19-10216	247861..248461	orf19.5022	***SMF2***	direct upstream	248827 to 250842
274	0.797	1.737	Contig19-10216	247861..248461	orf19.5021	***PDX1***	direct upstream	247652 to 246399
275	0.797	1.737	Contig19-10190	34621..34981	orf19.3737	***ScMUK1***	direct upstream	35689 to 38070
276	0.796	1.736	Contig19-10162	61861..62941	orf19.2892	***ScSBE22***	direct upstream	61185 to 58549
277	0.794	1.734	Contig19-10215	187861..188161	orf19.4803	-	upstream (1.1 kb)	189261 to 189638
278	0.794	1.734	Contig19-10215	187861..188161	orf19.4802	***FTH1***	direct upstream	187746 to 186472
279	0.793	1.733	Contig19-10020	16381..16861	orf19.53	***UAF22***	upstream (1.5 kb)	14846 to 13713
280	0.793	1.733	Contig19-10020	16381..16861	orf19.54	***RHD1***	direct upstream	17659 to 19623
281	0.793	1.733	Contig19-1948	5701..6181	orf19.3071	***MIH1***	upstream (1.5 kb)	7750 to 10434
282	0.792	1.731	Contig19-10137	34561..34981	orf19.1944	***GPR1***	direct upstream	33678 to 31207
283	0.792	1.731	Contig19-10216	81181..81421	orf19.4943	***PSA1***	direct upstream	81570 to 82946
284	0.791	1.730	Contig19-10046	39721..40201	orf19.251	-	direct upstream	39573 to 38863
285	0.791	1.730	Contig19-10254	6661..7201	orf19.6715	-	upstream (2.3 kb)	9452 to 9760
286	0.791	1.730	Contig19-10254	6661..7201	orf19.6713	-	direct upstream	5809 to 4604
287	0.790	1.729	Contig19-10170	66601..67081	orf19.3193	***FCR3/YAP3***	upstream (2.3 kb)	64279 to 63080
288	0.790	1.729	Contig19-10170	66601..67081	orf19.3195	***HIP1/GAP3***	direct upstream	67622 to 69421
289	0.789	1.728	Contig19-1739	421..721	orf19.1289	***SCT1***	upstream (2.0 kb)	2464 to 4776
290	0.789	1.728	Contig19-1739	421..721	orf19.1288	***FOX2***	direct upstream	310 to 2
291	0.788	1.727	Contig19-10238	18061..18541	orf19.6126	***KGD2***	direct upstream	17026 to 15701
292	0.788	1.727	Contig19-10238	18061..18541	orf19.6127	***LPD1***	direct upstream	18685 to 20160
293	0.788	1.727	Contig19-10119	38161..38581	orf19.1461	-	direct upstream	38523 to 39764
294	0.788	1.727	Contig19-10119	38161..38581	orf19.1460	***ScQNS1***	direct upstream	38030 to 35886
295	0.787	1.725	Contig19-10257	16621..16921	orf19.6873	***RPS8A***	upstream (2.5 kb)	15135 to 14515
296	0.787	1.725	Contig19-10046	208141..208741	orf19.345	***UGA2***	direct upstream	211202 to 212677
297	0.787	1.725	Contig19-10046	208141..208741	orf19.344	-	direct upstream	208048 to 207233
298	0.787	1.725	Contig19-10054	3481..3841	orf19.556	-	direct upstream	2859 to 2440
299	0.787	1.725	Contig19-10054	3481..3841	orf19.557	-	direct upstream	3942 to 4967
300	0.787	1.725	Contig19-10196	82441..82801	orf19.4118	***CNT1/NNT1***	direct upstream	82152 to 80326
301	0.786	1.724	Contig19-10125	97021..97441	orf19.1355	***SOL2***	direct upstream	Contig19-10113:174 to 1217
302	0.786	1.724	Contig19-10125	97021..97441	orf19.1785	-	direct upstream	97018 to 96038
303	0.785	1.723	Contig19-10151	94981..95161	orf19.2583	***PTR2***	direct upstream	94244 to 92289
304	0.784	1.722	Contig19-2511	111241..111721	orf19.7341	-	direct upstream	110063 to 109164
305	0.784	1.722	Contig19-2134	541..1081	orf19.4155	***KAP114***	direct upstream	404 to 3
306	0.783	1.721	Contig19-10183	94681..95341	orf19.3574	***MDJ2***	direct upstream	93869 to 93438
307	0.783	1.721	Contig19-10183	94681..95341	orf19.3575	***CDC19/PYK1***	direct upstream	95445 to 96959
308	0.780	1.717	Contig19-10053	128281..128581	orf19.539	***LAP3***	direct upstream	128114 to 126585
309	0.780	1.717	Contig19-10125	32041..33061	orf19.1756	***GPD1***	direct upstream	30860 to 29649
310	0.780	1.717	Contig19-10241	64681..64861	orf19.6227	-	direct upstream	64456 to 63464
311	0.779	1.716	Contig19-10172	149461..149641	orf19.3283	***OAR1***	direct upstream	149804 to 150493
312	0.779	1.716	Contig19-10212	210781..211261	orf19.4673	***BMT9***	upstream (2.5 kb)	213774 to 216125
313	0.779	1.716	Contig19-10212	210781..211261	orf19.4672	-	direct upstream	210225 to 209923
314	0.779	1.716	Contig19-10131	24961..25201	orf19.1827	-	direct upstream	26050 to 27408
315	0.779	1.716	Contig19-10202	55681..56221	orf19.4245	-	upstream (2.0 kb)	53680 to 52334
316	0.779	1.716	Contig19-10202	55681..56221	orf19.4246	-	direct upstream	56331 to 58124
317	0.778	1.715	Contig19-10079	481..901	orf19.917	-	direct upstream	1566 to 1895
318	0.778	1.715	Contig19-10212	78661..78961	orf19.4602	***MDH1-1***	direct upstream	79031 to 80029
319	0.778	1.715	Contig19-10212	78661..78961	orf19.4601	***TFC1***	direct upstream	78175 to 76658
320	0.778	1.715	Contig19-10192	83221..83521	orf19.3812	***SSZ1/PDR13***	direct upstream	82551 to 80929
321	0.778	1.715	Contig19-10192	83221..83521	orf19.3813	-	direct upstream	83572 to 85075
322	0.777	1.714	Contig19-10176	123421..123601	orf19.3448	-	direct upstream	119245 to 119775
323	0.777	1.714	Contig19-10072	17821..18181	orf19.742	***ALD6***	upstream (1.5 kb)	16267 to 14594
324	0.776	1.712	Contig19-2506	32341..32641	orf19.7150	***NRG1***	upstream (1.5 kb)	30769 to 29837
325	0.775	1.711	Contig19-10162	32701..33061	orf19.2882	***XUT1/UAP2***	upstream (2.8 kb)	35870 to 37645
326	0.775	1.711	Contig19-10162	32701..33061	orf19.2881	***MNN4***	upstream (2.4 kb)	30302 to 27312
327	0.774	1.710	Contig19-10076	231841..232201	orf19.903	***GPM1***	direct upstream	231759 to 231013
328	0.773	1.709	Contig19-10248	178021..178561	orf19.6547	-	direct upstream	177553 to 177206
329	0.773	1.709	Contig19-10248	178021..178561	orf19.6548	***ISU1***	direct upstream	178807 to 179370
330	0.773	1.709	Contig19-10193	40021..40201	orf19.3868	-	direct upstream	39822 to 39469
331	0.773	1.709	Contig19-10193	40021..40201	orf19.3869	-	direct upstream	40248 to 42002
332	0.770	1.705	Contig19-10163	211861..212161	orf19.3038	***TPS2***	direct upstream	212194 to 214860
333	0.770	1.705	Contig19-10150	49081..49321	orf19.2454	***PHO87***	upstream (2.5 kb)	46682 to 43662
334	0.770	1.705	Contig19-10150	49081..49321	orf19.2455	***ScDUG2***	direct upstream	49405 to 52801
335	0.769	1.704	Contig19-2516	153901..154261	orf19.7542	***PGA25***	upstream (1.5 kb)	155614 to 156783
336	0.769	1.704	Contig19-2516	153901..154261	orf19.7539	***INO2***	direct upstream	153745 to 152606
337	0.768	1.703	Contig19-10248	117061..117361	orf19.6515	***HSP90***	direct upstream	117062 to 114939
338	0.768	1.703	Contig19-10052	46741..47101	orf19.430	***YPT522***	direct upstream	46237 to 45578
339	0.768	1.703	Contig19-10052	46741..47101	orf19.431	***ZCF2***	direct upstream	47160 to 49487

No.	Log_2 signal intensity	fold binding ratio	Contig 19 #	Location	Gene ID	CGD Gene Name	Binding region	gene location
340	0.768	1.703	Contig19-10184	50581..51181	orf19.3618	***YWP1/FlO1***	direct upstream	50017 to 48416
341	0.767	1.702	Contig19-10202	107101..107461	orf19.4273	***ScSLS1***	upstream (1.5 kb)	105970 to 103211
342	0.767	1.702	Contig19-10202	107101..107461	orf19.4274	***PUT1***	direct upstream	107581 to 109050
343	0.766	1.701	Contig19-10248	236221..236641	orf19.6577	***FLU1/TPO1***	direct upstream	236037 to 234205
344	0.761	1.695	Contig19-2516	117901..118201	orf19.7514	***PCK1***	direct upstream	117774 to 116113
345	0.760	1.693	Contig19-10254	95581..96181	orf19.6769	***ScOCA5***	upstream (1.2 kb)	94411 to 92261
346	0.760	1.693	Contig19-10254	95581..96181	orf19.6770	***ENT4***	direct upstream	96362 to 97318
347	0.758	1.691	Contig19-10158	221101..221281	orf19.2767	***PG59***	direct upstream	222188 to 222529
348	0.758	1.691	Contig19-10227	37261..37561	orf19.5389	***FKH1/FKH2***	direct upstream	38239 to 39819
349	0.758	1.691	Contig19-10212	4381..4741	orf19.4565	***BGL2***	direct upstream	4886 to 5812
350	0.758	1.691	Contig19-10173	48601..48841	orf19.3310	-	direct upstream	47722 to 46970
351	0.758	1.691	Contig19-10173	48601..48841	orf19.3311	***IFD3***	direct upstream	49125 to 50174
352	0.757	1.690	Contig19-1888	4741..5530	orf19.2295	***CTA226***	upstream (3.5 kb)	1544 to 1020
353	0.757	1.690	Contig19-10064	48061..48241	orf19.675	-	upstream (2.0 kb)	47516 to 46878
354	0.756	1.689	Contig19-10234	41761..42241	orf19.5801	***RNR21***	direct upstream	42463 to 43704
355	0.756	1.689	Contig19-10113	6001..6361	orf19.1357	***FCY21/FCY22***	upstream (1.5kb)	4636 to 3092
356	0.756	1.689	Contig19-10155	9121..10081	orf19.2638	-	upstream (2.0 kb)	7178 to 6351
357	0.756	1.689	Contig19-10155	9121..10081	orf19.2639	***ScMRPL20***	direct upstream	10548 to 11069
358	0.755	1.688	Contig19-10014	31861..32701	orf19.33	***LPF1***	upstream / ORF	31904 to 31599
359	0.754	1.686	Contig19-10064	61141..63181	orf19.682	-	upstream / ORF	61886 to 58323
360	0.754	1.686	Contig19-10064	61141..63181	orf19.683	-	direct upstream	63598 to 64347
361	0.753	1.685	Contig19-10035	56821..57121	orf19.118	***FAD2/ODE1***	direct upstream	57736 to 59046
362	0.752	1.684	Contig19-10227	151561..151801	orf19.5475	-	upstream (2.0 kb)	149540 to 148716
363	0.752	1.684	Contig19-2492	7801..8521	orf19.6961	-	direct upstream	7257 to 6271
364	0.752	1.684	Contig19-2492	7801..8521	orf19.6960	-	direct upstream	7257 to 5719
365	0.750	1.682	Contig19-10236	183301..183721	orf19.5953	***SFP1***	upstream (2.0 kb)	185788 to 187125
366	0.750	1.682	Contig19-10236	183301..183721	orf19.5952	-	direct upstream	183032 to 181716
367	0.749	1.681	Contig19-10192	102421..102781	orf19.3822	***SCS7***	direct upstream	102349 to 101213
368	0.748	1.679	Contig19-10141	121501..121861	orf19.2222	***YCK22***	upstream (1.5 kb)	120091 to 118955
369	0.748	1.679	Contig19-10141	121501..121861	orf19.2223	-	direct upstream	122158 to 123567
370	0.748	1.679	Contig19-10227	20761..21481	orf19.5383	***PMA1***	direct upstream	20418 to 17731
371	0.748	1.679	Contig19-10123	208861..209161	orf19.1701	***RKI1***	direct upstream	209315 to 210106
372	0.748	1.679	Contig19-10123	208861..209161	orf19.1700	***RPS7A/RPS7***	direct upstream	208717 to 208157
373	0.748	1.679	Contig19-10063	35581..35761	orf19.646	***GLN1***	direct upstream	35153 to 34032
374	0.748	1.679	Contig19-2500	72721..72961	orf19.6987	***DNM1***	direct upstream	71983 to 69383
375	0.748	1.679	Contig19-2500	72721..72961	orf19.6988	***OST1***	direct upstream	73113 to 74525
376	0.745	1.676	Contig19-10230	210421..210661	orf19.5628	***ScDIC1***	direct upstream	210742 to 211791
377	0.744	1.675	Contig19-10064	2761..3121	orf19.655	***PHO84***	upstream (2.0 kb)	748 to 2
378	0.744	1.675	Contig19-10064	2761..3121	orf19.656	***DPP1***	upstream (1.5 kb)	4742 to 5527
379	0.743	1.674	Contig19-10064	82681..83221	orf19.691	***GPD2***	direct upstream	82441 to 81326
380	0.742	1.672	Contig19-2285	10261..11221	orf19.5288	***IFE2/BDH2***	upstream / ORF	10976 to 12283
381	0.742	1.672	Contig19-10163	250981..251221	orf19.3060	***SWP1***	upstream (1.2 kb)	252319 to 253146
382	0.742	1.672	Contig19-10163	250981..251221	orf19.3059	***SUA71***	direct upstream	250490 to 249456
383	0.741	1.671	Contig19-10236	80101..80701	orf19.5903	***RAX1***	upstream (3.0 kb)	83603 to 85255
384	0.741	1.671	Contig19-10236	80101..80701	orf19.5902	***RAS2/RLP1***	direct upstream	79856 to 78894
385	0.740	1.670	Contig19-2208	10861..11761	orf19.4712	***FGR6-3/IFV12***	direct upstream	12167 to 13705
386	0.740	1.670	Contig19-10183	19021..19321	orf19.3533	***ScEMI1***	direct upstream	19719 to 20168
387	0.740	1.670	Contig19-10183	19021..19321	orf19.3532	***MRPL10***	direct upstream	18637 to 17786
388	0.740	1.670	Contig19-10241	30361..30721	orf19.6209	***ScMCH2***	direct upstream	30848 to 32281
389	0.740	1.670	Contig19-10241	30361..30721	orf19.6208	***MEF2***	direct upstream	29680 to 27257
390	0.739	1.669	Contig19-10014	31261..31681	orf19.32	-	direct upstream	30748 to 30407
391	0.739	1.669	Contig19-10139	6961..7321	orf19.1991	***PTM1***	direct upstream	6250 to 4391
392	0.739	1.669	Contig19-10139	6961..7321	orf19.1992	***SIR2***	direct upstream	7497 to 9056
393	0.739	1.669	Contig19-10237	72781..73021	orf19.6034	***TUB2***	direct upstream	74010 to 75738
394	0.737	1.667	Contig19-10233	145921..146701	orf19.5775	***IFV1***	direct upstream	145529 to 143991
395	0.736	1.666	Contig19-1859	2761..3181	orf19.1859	-	upstream (2.5 kb)	351 to 1
396	0.736	1.666	Contig19-10125	83521..83761	orf19.1778	-	upstream (1.5 kb)	82413 to 82099
397	0.736	1.666	Contig19-10125	83521..83761	orf19.1779	***MP65/SCW1***	direct upstream	84804 to 85121
398	0.735	1.664	Contig19-10190	67441..67861	orf19.3753	***SEF1***	direct upstream	68160 to 70913
399	0.733	1.662	Contig19-10202	154741..155161	orf19.4304	***GAP1***	direct upstream	154479 to 152731
400	0.733	1.662	Contig19-10133	15541..16141	orf19.1847	***ARO10***	direct upstream	16549 to 18438
401	0.732	1.661	Contig19-2518	10501..10741	orf19.7550	***IFA14***	direct upstream	9782 to 7746
402	0.732	1.661	Contig19-10218	138061..138301	orf19.5117	***OLE1***	direct upstream	137673 to 136213
403	0.732	1.661	Contig19-10230	42841..43081	orf19.5536	***AMD21***	upstream (3.0 kb)	39550 to 37832
404	0.730	1.659	Contig19-10230	47341..47641	orf19.5539	***ScUSE1***	upstream (1.5 kb)	48808 to 49650
405	0.730	1.659	Contig19-10251	7021..7261	orf19.6626	-	direct upstream	6706 to 6080
406	0.728	1.656	Contig19-2514	481..721	orf19.7398.1	***TSA1B***	direct upstream	313 to 1
407	0.728	1.656	Contig19-10150	77521..77701	orf19.2469	***RAD10/ERC1***	direct upstream	77954 to 78970
408	0.728	1.656	Contig19-10150	77521..77701	orf19.2468	***TMT1***	direct upstream	77397 to 76477
409	0.727	1.655	Contig19-10099	18481..19561	orf19.1189	-	direct upstream	19523 to 21577
410	0.727	1.655	Contig19-10200	21541..21961	orf19.4167	-	direct upstream	22802 to 23341
411	0.727	1.655	Contig19-10163	39121..39661	orf19.2942	***DIP5***	upstream (2.5 kb)	36879 to 35120
412	0.727	1.655	Contig19-10163	39121..39661	orf19.2943.5	-	direct upstream	39647 to 39946
413	0.725	1.653	Contig19-10117	1621..1921	orf19.1434	***DPB11***	direct upstream	2505 to 4652
414	0.725	1.653	Contig19-10117	1621..1921	orf19.1433	***ScLPX1***	direct upstream	1528 to 335
415	0.725	1.653	Contig19-10053	80161..80881	orf19.508	***QDR1***	upstream / ORF	80380 to 78851
416	0.723	1.651	Contig19-10150	132301..132481	orf19.2501	***FLC1/BOP1***	direct upstream	133070 to 135496
417	0.722	1.649	Contig19-10176	16321..16501	orf19.3405	***ZCF18***	direct upstream	16931 to 18523
418	0.722	1.649	Contig19-10176	16321..16501	orf19.3404	-	direct upstream	16142 to 14661
419	0.722	1.649	Contig19-10158	231541..232021	orf19.2770.1	***SOD1***	upstream / ORF	231911 to 232620
420	0.720	1.647	Contig19-2492	11221..13201	orf19.6962	-	upstream / ORF	11625 to 11302
421	0.720	1.647	Contig19-2511	118741..118921	orf19.7342	***AXL1***	direct upstream	119558 to 123670
422	0.720	1.647	Contig19-10122	23101..23881	orf19.1604	***ScLYS14***	upstream (3.0 kb)	20506 to 17756
423	0.719	1.646	Contig19-10097	28621..29281	orf19.1150.1	***ScYSF1***	direct upstream	29687 to 29908
424	0.719	1.646	Contig19-10097	28621..29281	orf19.1150	***ScGLN3***	direct upstream	28111 to 26693
425	0.718	1.645	Contig19-10136	1261..1681	orf19.1906	-	direct upstream	816 to 487
426	0.718	1.645	Contig19-10136	1261..1681	orf19.1907	***EMC9***	direct upstream	2024 to 4177
427	0.718	1.645	Contig19-10163	23341..23641	orf19.2935	***RPL10***	direct upstream	24005 to 24667
428	0.718	1.645	Contig19-10163	23341..23641	orf19.2934	***BUD20***	direct upstream	23303 to 22773
429	0.718	1.645	Contig19-10236	301081..301621	orf19.6003	***ScGIS3***	direct upstream	300665 to 298878
430	0.718	1.645	Contig19-10173	5221..5521	orf19.3291	***HMT1/RMT1***	direct upstream	5572 to 6591
431	0.717	1.644	Contig19-10123	117841..118081	orf19.1663	***MNT2/KRE2***	upstream (1.3 kb)	119444 to 120829

No.	Log_2 signal intensity	fold binding ratio	Contig 19 #	Location	Gene ID	CGD Gene Name	Binding region	gene location
432	0.717	1.644	Contig19-10123	117841..118081	orf19.1662	***MRP1***	direct upstream	117111 to 116200
433	0.717	1.644	Contig19-10097	24721..25141	orf19.1149	***MRF1/ETR2***	direct upstream	25376 to 26455
434	0.715	1.641	Contig19-10215	28861..29041	orf19.4737	***TPO3/DHA12***	direct upstream	29632 to 30972
435	0.714	1.640	Contig19-10230	112501..112681	orf19.5578	-	upstream (1.5 kb)	114161 to 115852
436	0.714	1.640	Contig19-10230	112501..112681	orf19.5576	***ScCAB1***	direct upstream	111927 to 110634
437	0.714	1.640	Contig19-10248	166801..167701	orf19.6540	***PFK2***	direct upstream	167794 to 170634
438	0.714	1.640	Contig19-10248	166801..167701	orf19.6539	***RVB2***	direct upstream	166245 to 164749
439	0.714	1.640	Contig19-10158	52081..52321	orf19.2684	***SLK19***	direct upstream	51806 to 49371
440	0.713	1.639	Contig19-10204	24241..24481	orf19.4410	***ALG1***	direct upstream	24579 to 25949
441	0.713	1.639	Contig19-10204	24241..24481	orf19.4409	***ScNPP1***	direct upstream	24014 to 21939
442	0.713	1.639	Contig19-2511	58021..58801	orf19.7314	***CDG1***	upstream (1.5 kb)	60145 to 60942
443	0.713	1.639	Contig19-2511	58021..58801	orf19.7313	***SSU1***	direct upstream	57766 to 56321
444	0.712	1.638	Contig19-10150	122461..122761	orf19.2496	***ATO2/FUN34***	upstream (1.2 kb)	123725 to 124522
445	0.712	1.638	Contig19-10150	122461..122761	orf19.2495	***GSL1/FKS1***	direct upstream	122127 to 117412
446	0.711	1.637	Contig19-10132	16501..16801	orf19.1836	***APN2***	direct upstream	17485 to 18840
447	0.711	1.637	Contig19-10132	16501..16801	orf19.1835	***ScPEA2***	direct upstream	15662 to 13758
448	0.711	1.637	Contig19-10126	5101..5581	orf19.1789.1	***LYS1***	direct upstream	5845 to 6992
449	0.710	1.636	Contig19-10163	221941..222121	orf19.3043	***TGL2***	direct upstream	222348 to 223403
450	0.710	1.636	Contig19-10139	66901..67501	orf19.2020	***HGT6/HXT4***	direct upstream	66413 to 64761
451	0.708	1.634	Contig19-10150	65341..65701	orf19.2459	-	direct upstream	64643 to 61725
452	0.707	1.632	Contig19-10052	119581..119941	orf19.461	-	direct upstream	120598 to 121590
453	0.707	1.632	Contig19-10052	119581..119941	orf19.460	***CEK2***	direct upstream	118908 to 117790
454	0.706	1.631	Contig19-10176	103381..103801	orf19.3439	-	direct upstream	104706 to 105659
455	0.706	1.631	Contig19-10186	26821..27001	orf19.3669	***SHA3/SKS1***	direct upstream	26399 to 24612
456	0.706	1.631	Contig19-10236	541..1021	orf19.5854	***SBP1***	direct upstream	1293 to 2141
457	0.706	1.631	Contig19-10073	57301..57961	orf19.778	***PIL1/EBP1***	direct upstream	57138 to 56212
458	0.705	1.630	Contig19-10080	24241..24541	orf19.930	***PET9***	direct upstream	23304 to 22399
459	0.705	1.630	Contig19-10070	48061..48721	orf19.727	***IFV1***	direct upstream	49228 to 50766
460	0.705	1.630	Contig19-10146	58141..58441	orf19.2333	***ScTDA3***	upstream (1.5 kb)	59846 to 61336
461	0.705	1.630	Contig19-10146	58141..58441	orf19.2332	-	direct upstream	57462 to 56668
462	0.703	1.628	Contig19-10137	96721..97141	orf19.1972	***SET5***	direct upstream	97226 to 98647
463	0.703	1.628	Contig19-10137	96721..97141	orf19.1971	***TRY3***	direct upstream	96293 to 94809
464	0.701	1.626	Contig19-10215	115381..115681	orf19.4772	***SSU81/SHO1***	direct upstream	115019 to 113856
465	0.701	1.626	Contig19-10141	31921..32341	orf19.2179	***SIT1/ARN1***	upstream (1.5 kb)	33831 to 35645
466	0.700	1.625	Contig19-10123	102241..102541	orf19.1655	***PXP2/POX102***	upstream (2.0 kb)	100816 to 98642
467	0.700	1.625	Contig19-10123	102241..102541	orf19.1655.3	***ScPMP3***	upstream (1.5 kb)	103270 to 103437
468	0.700	1.625	Contig19-10080	91381..91801	orf19.954	***XDJ1***	direct upstream	91992 to 93311
469	0.700	1.625	Contig19-10080	91381..91801	orf19.953.1	***COF1***	direct upstream	90439 to 89783
470	0.698	1.622	Contig19-10141	62221..62581	orf19.2192	***GDH2***	direct upstream	61761 to 58591
471	0.697	1.621	Contig19-10225	112261..112621	orf19.5348	***TPS3***	direct upstream	112727 to 115812
472	0.697	1.621	Contig19-2516	139441..139921	orf19.7529	***EPL1***	upstream / ORF	139889 to 142150
473	0.697	1.621	Contig19-2516	139441..139921	orf19.7527	-	direct upstream	138922 to 136742
474	0.697	1.621	Contig19-10184	48121..48361	orf19.3617	***GTR1***	upstream (1.5 kb)	46700 to 45810
475	0.696	1.620	Contig19-10216	203881..204241	orf19.5000	***CYB2***	direct upstream	204501 to 206183
476	0.694	1.618	Contig19-10233	124021..124201	orf19.5763	***SPS19***	direct upstream	124903 to 125685
477	0.694	1.618	Contig19-10233	124021..124201	orf19.5762	***PGA61***	direct upstream	123429 to 122758
478	0.694	1.618	Contig19-10231	42241..42661	orf19.5664	***HOF1***	direct upstream	43349 to 45172
479	0.694	1.618	Contig19-10231	42241..42661	orf19.5663	***RCH1***	direct upstream	42082 to 40847
480	0.694	1.618	Contig19-10080	68881..69121	orf19.941	***SEC14***	direct upstream	69794 to 70699
481	0.694	1.618	Contig19-2212	8821..9121	orf19.4718	***TRP5***	upstream (1.5 kb)	10836 to 12944
482	0.694	1.618	Contig19-2212	8821..9121	orf19.4716	***GDH3/GDH1***	direct upstream	8485 to 7115
483	0.692	1.616	Contig19-2511	45841..46081	orf19.7306	-	direct upstream	45647 to 44598
484	0.692	1.616	Contig19-10195	6001..6601	orf19.4056	***BRG1/GAT2***	upstream (2.0 kb)	4405 to 3065
485	0.692	1.616	Contig19-10262	7921..8161	orf19.7003	-	upstream (2.0kb)	6461 to 6123
486	0.691	1.614	Contig19-10219	134701..135421	orf19.5191	***FGR6-1/IFV3***	direct upstream	134179 to 132641
487	0.691	1.614	Contig19-10209	36361..36781	orf19.4540	***UBC8***	direct upstream	36868 to 37440
488	0.689	1.612	Contig19-10103	6301..6481	orf19.1223	***DBF2***	upstream (4.0 kb)	2262 to 130
489	0.689	1.612	Contig19-10103	6301..6481	orf19.1224	***FRP3/AFF1***	direct upstream	7446 to 8303
490	0.689	1.612	Contig19-10183	841..1201	orf19.3522	-	upstream (2.0 kb)	2993 to 3298
491	0.689	1.612	Contig19-10183	841..1201	orf19.3521	***ARH2***	direct upstream	656 to 3
492	0.687	1.610	Contig19-10225	64261..65101	orf19.5315	***FGR6***	direct upstream	66025 to 67062
493	0.686	1.609	Contig19-1286	1..301	orf19.72	***CTR2***	direct upstream	673 to 1161
494	0.686	1.609	Contig19-10137	80341..80641	orf19.1963	***GDS1***	upstream (3.0 kb)	83442 to 84965
495	0.685	1.608	Contig19-10219	136381..137341	orf19.5192	-	upstream / ORF	137210 to 137734
496	0.685	1.608	Contig19-10230	138301..138481	orf19.5588	***PGA60***	upstream (1.2 kb)	139710 to 142007
497	0.685	1.608	Contig19-10230	138301..138481	orf19.5587	-	direct upstream	138087 to 136687
498	0.684	1.607	Contig19-1960	1621..2401	orf19.3144	-	direct upstream	2975 to 3775
499	0.683	1.605	Contig19-10236	307681..308101	orf19.6007	-	direct upstream	307029 to 305968
500	0.683	1.605	Contig19-10150	60781..61201	orf19.2458	***SIP5***	direct upstream	59951 to 58410
501	0.682	1.604	Contig19-1832	1981..2161	orf19.1809	***FOX2***	direct upstream	2293 to 5013
502	0.682	1.604	Contig19-2411	3541..5221	orf19.6300	***RSP620A***	direct upstream	3464 to 3141
503	0.681	1.603	Contig19-10192	143641..143821	orf19.3845	***FGR3***	upstream (1.2 kb)	142525 to 141002
504	0.681	1.603	Contig19-10192	143641..143821	orf19.3846	***LYS4***	direct upstream	143960 to 146014
505	0.681	1.603	Contig19-10257	37861..38041	orf19.6882	***OSM1***	direct upstream	38243 to 39754
506	0.681	1.603	Contig19-10257	37861..38041	orf19.6881	***YTH1***	direct upstream	37550 to 36903
507	0.679	1.601	Contig19-10212	102901..103141	orf19.4618	***FBA1***	direct upstream	103441 to 104520
508	0.679	1.601	Contig19-10212	102901..103141	orf19.4617	***MAK3***	direct upstream	102343 to 101807
509	0.679	1.601	Contig19-10202	223681..223981	orf19.4342	***ScSUT1***	direct upstream	224026 to 225096
510	0.678	1.600	Contig19-10035	2521..2761	orf19.85	***GPX2***	upstream (2.5 kb)	4559 to 5050
511	0.678	1.600	Contig19-10035	2521..2761	orf19.84	***CAN3***	upstream (1.5 kb)	1308 to 2
512	0.678	1.600	Contig19-10196	25501..25981	orf19.4076	***MET10***	upstream (3.0 kb)	22798 to 19514
513	0.678	1.600	Contig19-10196	25501..25981	orf19.4077	***MIT1/SUR1***	upstream (1.5 kb)	27331 to 28965
514	0.678	1.600	Contig19-2011	6361..7021	orf19.3490	***FGR6-4/IFV10***	direct upstream	7591 to 9129
515	0.676	1.598	Contig19-10262	10321..10621	orf19.7005	***IFV5***	direct upstream	11498 to 13036
516	0.676	1.598	Contig19-2175	10321..11041	orf19.4485	***IFV11***	direct upstream	11538 to 13076
517	0.675	1.597	Contig19-10139	104521..104881	orf19.2048	-	direct upstream	105143 to 105508
518	0.675	1.597	Contig19-10139	104521..104881	orf19.2047	-	direct upstream	104450 to 103824
519	0.675	1.597	Contig19-10183	56101..56701	orf19.3555	***BUD14***	upstream (4.0 kb)	60587 to 62992
520	0.675	1.597	Contig19-10183	56101..56701	orf19.3554	***AAT1***	direct upstream	55842 to 54529
521	0.675	1.597	Contig19-10166	96841..97801	orf19.3134	-	upstream (2.5 kb)	100282 to 100722
522	0.675	1.597	Contig19-10166	96841..97801	orf19.3133	***GUT2***	direct upstream	96169 to 94217
523	0.673	1.594	Contig19-2518	140341..140881	orf19.7611	***TRX1***	direct upstream	140272 to 139961

No.	Log_2 signal intensity	fold binding ratio	Contig 19 #	Location	Gene ID	CGD Gene Name	Binding region	gene location
524	0.673	1.594	Contig19-10216	4321..4561	orf19.4914	***ScMHF1***	direct upstream	5193 to 5546
525	0.673	1.594	Contig19-10216	4321..4561	orf19.4913	***ScDUF1***	direct upstream	3759 to 130
526	0.672	1.593	Contig19-10123	185821..186061	orf19.1687	***PRP43***	upstream (2.5 kb)	183467 to 181164
527	0.672	1.593	Contig19-10104	25981..26641	orf19.1234	***FGR6-10/IFV2***	direct upstream	27086 to 28624
528	0.671	1.592	Contig19-10251	11401..12241	orf19.6630	***ScLCL2***	direct upstream	12673 to 13077
529	0.668	1.589	Contig19-10185	4561..4981	orf19.3642	***SUN41***	direct upstream	4022 to 2766
530	0.668	1.589	Contig19-10143	70981..71461	orf19.2268	***RCK2***	upstream (4.0 kb)	67366 to 65597
531	0.668	1.589	Contig19-10143	70981..71461	orf19.2270	***SMF12***	direct upstream	71809 to 73563
532	0.668	1.589	Contig19-2506	83581..83821	orf19.7186	***CLB4***	upstream (1.2 kb)	84816 to 86276
533	0.667	1.588	Contig19-10259	2041..2641	orf19.6922	-	upstream (1.5 kb)	352 to 2
534	0.667	1.588	Contig19-10225	49981..50521	orf19.5313	-	upstream (1.5 kb)	48398 to 45891
535	0.667	1.588	Contig19-2514	91321..91801	orf19.7445	***VID24***	upstream / ORF	91386 to 92873
536	0.667	1.588	Contig19-2514	91321..91801	orf19.7444	***ScTFB6***	upstream (1.5 kb)	89879 to 88854
537	0.666	1.587	Contig19-10212	277801..278101	orf19.4698	***PTC8/DHP99***	upstream (1.5kb)	276095 to 274830
538	0.666	1.587	Contig19-10212	277801..278101	orf19.4699	***ScTGL3***	direct upstream	279033 to 281081
539	0.665	1.586	Contig19-10148	30241..30781	orf19.2397.3	-	direct upstream	30061 to 28980
540	0.664	1.584	Contig19-10212	293401..293581	orf19.4705	***CCA1***	direct upstream	293264 to 291621
541	0.664	1.584	Contig19-10212	293401..293581	orf19.4706	***ScPIN2***	direct upstream	294175 to 294672
542	0.663	1.583	Contig19-10212	282241..282421	orf19.4702	-	direct upstream	282931 to 283833
543	0.663	1.583	Contig19-10212	282241..282421	orf19.4701	***ScELP1***	direct upstream	282142 to 281144
544	0.663	1.583	Contig19-10163	8461..9241	orf19.2928	-	direct upstream	7926 to 6853
545	0.662	1.582	Contig19-10173	154441..154741	orf19.3361	***YAT11***	upstream (2.5 kb)	157604 to 158392
546	0.662	1.582	Contig19-2449	34381..34861	orf19.6608	-	direct upstream	35157 to 37325
547	0.662	1.582	Contig19-10109	36421..36661	orf19.1314	-	direct upstream	37007 to 38416
548	0.661	1.581	Contig19-10181	8941..9361	orf19.3498	-	upstream (1.2 kb)	7731 to 6640
549	0.660	1.580	Contig19-2513	10261..10441	orf19.7350	***RCT1***	direct upstream	10693 to 11268
550	0.660	1.580	Contig19-2405	23281..23461	orf19.6191	***TLO8/CTA223***	upstream (3.5 kb)	20247 to 19738
551	0.660	1.580	Contig19-2516	38881..39361	orf19.7481	***MDH1***	upstream / ORF	39240 to 40253
552	0.660	1.580	Contig19-2516	38881..39361	orf19.7480	-	direct upstream	38013 to 37414
553	0.657	1.577	Contig19-10262	50521..51001	orf19.7022	-	direct upstream	51430 to 52458
554	0.657	1.577	Contig19-1800	6181..6361	orf19.1593	***RIM11***	direct upstream	5913 to 4684
555	0.656	1.576	Contig19-10057	59581..60541	orf19.599	-	upstream (2.2 kb)	62825 to 63184
556	0.655	1.575	Contig19-10125	90421..90781	orf19.1781	-	upstream (2.5 kb)	88359 to 88039
557	0.655	1.575	Contig19-10125	90421..90781	orf19.1783	***YOR1***	direct upstream	91278 to 95744
558	0.654	1.574	Contig19-10063	31681..31861	orf19.645.1	***VMA13***	direct upstream	31040 to 29564
559	0.653	1.572	Contig19-10109	26341..26641	orf19.1312	-	upstream (4.0 kb)	31554 to 34412
560	0.653	1.572	Contig19-10109	26341..26641	orf19.1311	***SPO75***	direct upstream	26169 to 23584
561	0.653	1.572	Contig19-1340	541..721	orf19.83	***OLE2***	direct upstream	915 to 1562
562	0.652	1.571	Contig19-10090	39541..40261	orf19.1093	***FLO8***	direct upstream	38683 to 36230
563	0.652	1.571	Contig19-2479	4501..4981	orf19.6834	-	upstream (1.5 kb)	3155 to 2844
564	0.651	1.570	Contig19-10014	38581..39061	orf19.35	***SKY2***	direct upstream	39987 to 43031
565	0.651	1.570	Contig19-10227	83881..84301	orf19.5416	***ESA1***	direct upstream	83471 to 81846
566	0.651	1.570	Contig19-10227	83881..84301	orf19.5417	***DOT5***	direct upstream	84702 to 85493
567	0.650	1.569	Contig19-10218	140461..141121	orf19.5118	***SDS24***	direct upstream	141198 to 143084
568	0.645	1.564	Contig19-1504	2761..3241	orf19.381	***CTA27***	direct upstream	3361 to 3750
569	0.645	1.564	Contig19-10194	61501..61681	orf19.3931	***SFC1/ACR1***	direct upstream	60558 to 59647
570	0.643	1.562	Contig19-2518	213721..214561	orf19.7676	***XYL2***	upstream / ORF	214240 to 213158
571	0.642	1.560	Contig19-10160	2761..3121	orf19.2803	***HEM13***	direct upstream	3763 to 4734
572	0.640	1.558	Contig19-2506	109801..109981	orf19.7203	***MRP7***	upstream (1.2 kb)	108745 to 107576
573	0.640	1.558	Contig19-2506	109801..109981	orf19.7204	***NPD1***	direct upstream	110022 to 111383
574	0.640	1.558	Contig19-10113	16261..17161	orf19.1363	-	direct upstream	17877 to 19055
575	0.640	1.558	Contig19-10113	16261..17161	orf19.1362	***SMM1***	direct upstream	15291 to 13990
576	0.638	1.556	Contig19-10141	109921..110281	orf19.2216	***PDS5***	upstream (2.0 kb)	108110 to 104199
577	0.637	1.555	Contig19-1553	2161..2641	orf19.631	***CTA217***	direct upstream	2013 to 1018
578	0.636	1.554	Contig19-2485	2521..3361	orf19.6896	-	direct upstream	2124 to 586
579	0.629	1.546	Contig19-10230	169021..169441	orf19.5607	-	upstream (1.2 kb)	170419 to 171360
580	0.629	1.546	Contig19-10230	169021..169441	orf19.5605	***ScALY2***	direct upstream	168530 to 165540
581	0.627	1.544	Contig19-10135	1441..1801	orf19.1862	***ScRTC3***	upstream (2.5 kb)	4715 to 5080
582	0.627	1.544	Contig19-2500	87001..87241	orf19.6996	***ScMNT4***	direct upstream	87613 to 89670
583	0.626	1.543	Contig19-2350	20641..21001	orf19.5700	***TLO11/CTA224***	upstream (1.5 kb)	19166 to 18657
584	0.626	1.543	Contig19-10215	215461..215701	orf19.4818	-	upstream (1.5 kb)	216982 to 218565
585	0.624	1.541	Contig19-2413	18541..19141	orf19.6338	-	upstream (2.0 kb)	16608 to 16222
586	0.623	1.540	Contig19-10225	94561..94981	orf19.5335	***SGS1***	direct upstream	95201 to 98770
587	0.623	1.540	Contig19-10225	94561..94981	orf19.5334	***TIS11***	direct upstream	94266 to 93655
588	0.622	1.539	Contig19-10254	172381..172621	orf19.6804	***SRP68***	direct upstream	171790 to 169970
589	0.621	1.538	Contig19-10215	116461..117001	orf19.4773	***AOX2***	upstream (1.5 kb)	119171 to 120267
590	0.619	1.536	Contig19-10045	12781..12961	orf19.204	-	upstream (1.5 kb)	14507 to 15121
591	0.619	1.536	Contig19-10045	12781..12961	orf19.203	***STB3***	direct upstream	11777 to 10266
592	0.613	1.529	Contig19-10227	142921..143341	orf19.5467	***TLO7/CTA225***	upstream (3.0 kb)	139783 to 139274
593	0.605	1.521	Contig19-10246	4021..4261	orf19.6342	-	direct upstream	3086 to 2601
594	0.605	1.521	Contig19-10246	4021..4261	orf19.6343	***FEN1***	direct upstream	4449 to 5462
595	0.598	1.514	Contig19-10192	35221..35401	orf19.3788.1	***RPL30***	direct upstream	34669 to 34267
596	0.598	1.514	Contig19-10192	35221..35401	orf19.3789	***RPL24A***	direct upstream	35592 to 36059
597	0.592	1.507	Contig19-10076	162481..162721	orf19.867	-	upstream (2.0 kb)	160458 to 158845
598	0.582	1.497	Contig19-10194	169261..169621	orf19.3983	-	upstream (4.0 kb)	165633 to 163423
599	0.582	1.497	Contig19-10194	169261..169621	orf19.3984	-	upstream (1.5 kb)	171134 to 173662
600	0.576	1.491	Contig19-10123	113881..114061	orf19.1659	***ALG8***	direct upstream	113534 to 111771
601	0.576	1.491	Contig19-10123	113881..114061	orf19.1661	***DBP5***	direct upstream	114198 to 115820
602	0.571	1.486	Contig19-10035	21721..22021	orf19.92	-	upstream (1.5 kb)	20572 to 17882
603	0.571	1.486	Contig19-10035	21721..22021	orf19.93	***ScMIC17***	direct upstream	22228 to 22683
604	0.570	1.485	Contig19-10161	37981..38161	orf19.2827	***TID3***	direct upstream	39111 to 41477
605	0.570	1.485	Contig19-10161	37981..38161	orf19.2826	-	direct upstream	37750 to 36350
606	0.566	1.480	Contig19-10247	28561..28801	orf19.6385	***ACO1***	direct upstream	27779 to 25446
607	0.560	1.474	Contig19-10254	206581..206761	orf19.6818	-	direct upstream	207055 to 211167
608	0.502	1.416	Contig19-10212	184981..185161	orf19.4656	-	direct upstream	184415 to 182517
609	0.451	1.367	Contig19-2511	52381..52561	orf19.7311	-	direct upstream	52989 to 53573
610	0.451	1.367	Contig19-2511	52381..52561	orf19.7310	***ScMSC1***	direct upstream	52269 to 49903

Appendix A2: *SAP2* sequences from plasmids pSAP2KS4 and pSAP2KS5

SAP2 reference sequence: Allelic sequence from _SAP2-1_ derived from plasmid pSAP2KS5 and from _SAP2-2_ derived from plasmid pSAP2KS4. Consensus sequence represents the SAP2 superalignment including all insertions. Nucleotide positions are relative to the ATG^{start} (highlighted as framed ATG) of the _SAP2_ ORF and the stop codon is highlighted as framed TAA. Allelic polymorphisms are shaded in light gray and identical nucleotides are depicted as dots in _SAP2-2_. Note: due to the cloning strategy the C at position +1179 of _SAP2-2_ was replaced by a T, which is otherwise only present in _SAP2-1_ and the Poly-T stretch approx. -1900 upstream of the _SAP2_ ATG^{start} contained 15 instead of 16 Thymidine residues, compared to the online genome sequence (CGD; www.candidagenome.org). Introduced restriction sites which represent no actual _SAP2_ sequences are underlined, i.e. the ApaI-site 5'-GGGCCC-3' and the BglII-site 5'-AGATCT-3'.

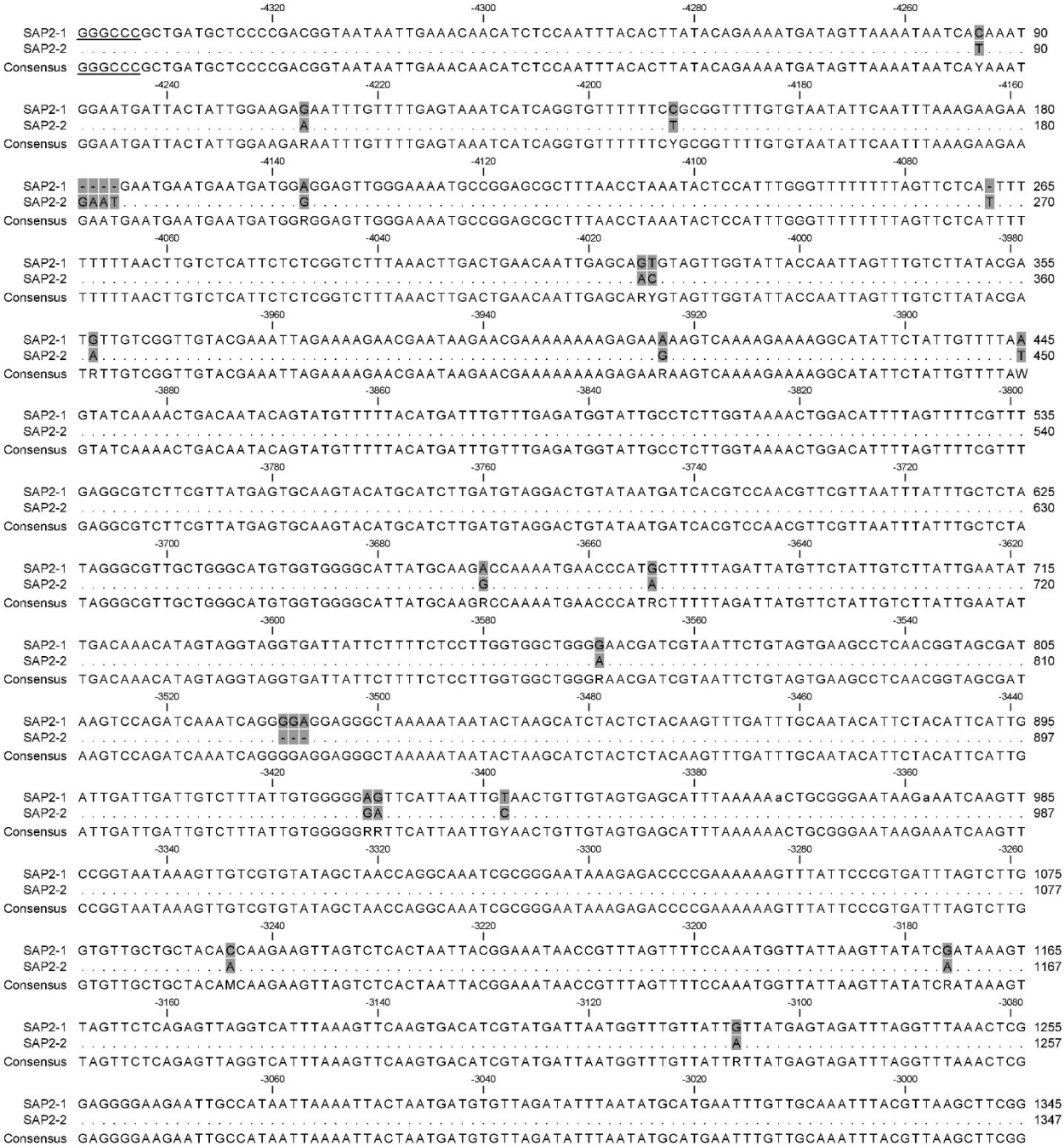

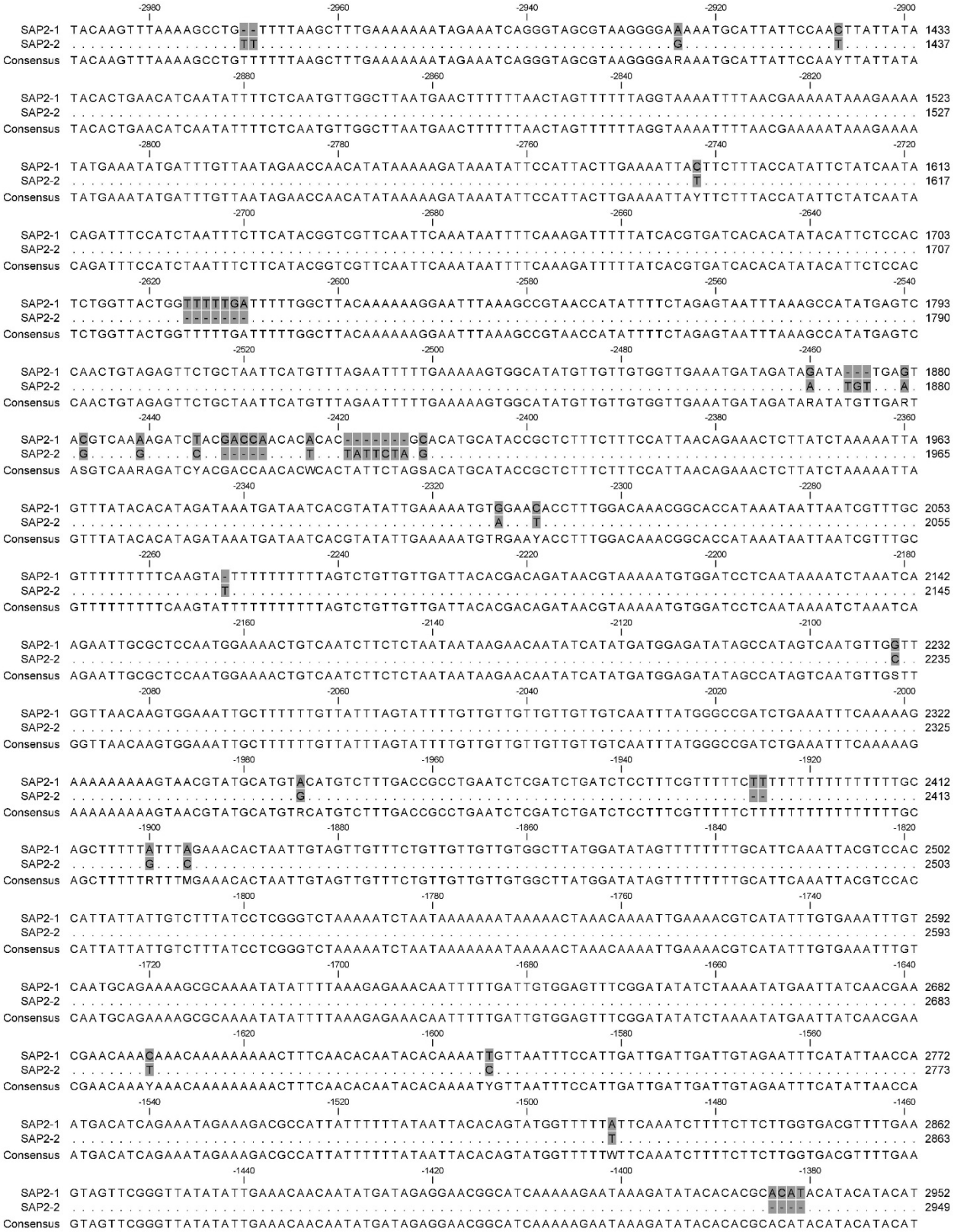

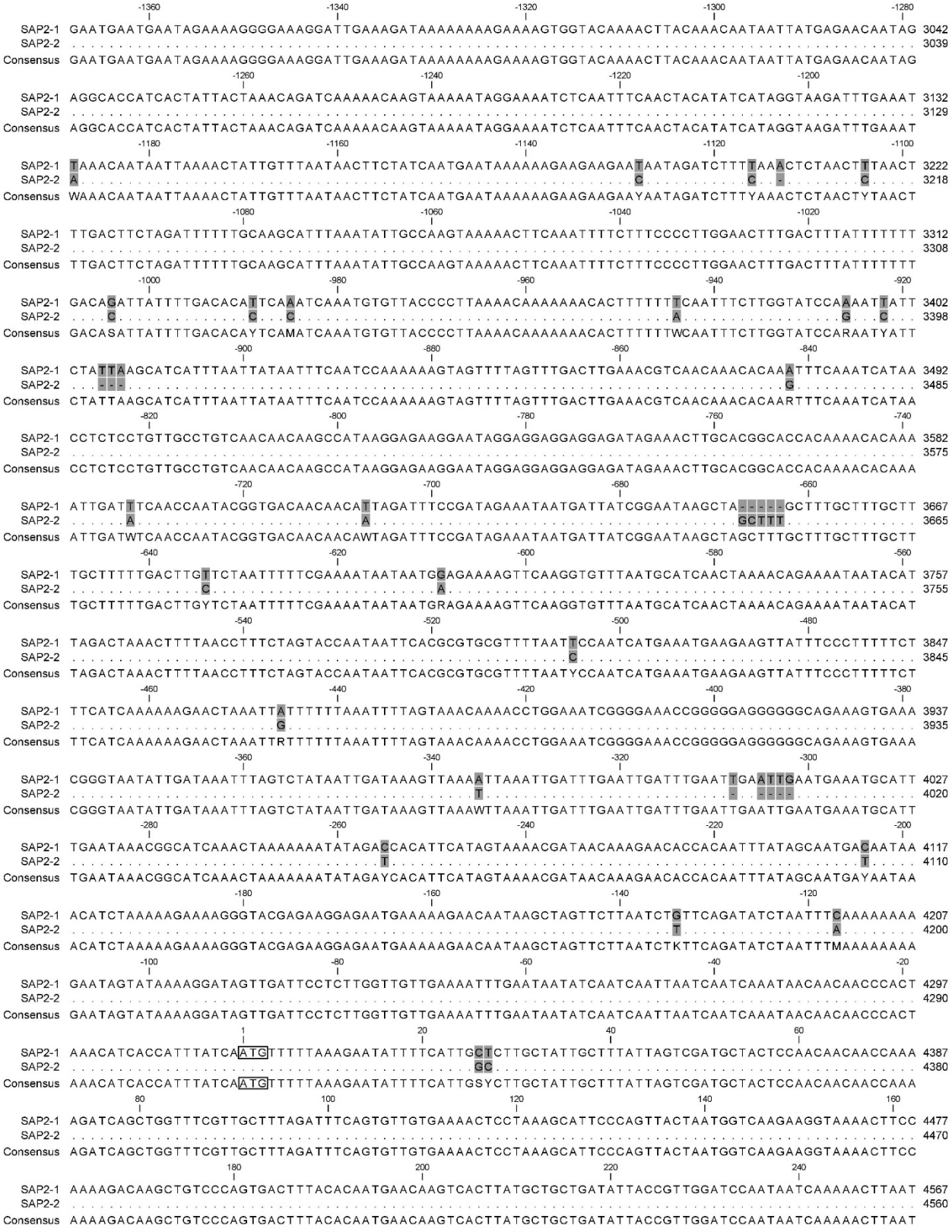


SAP2-1 GTTATTGTTGATACTGGATCATCTGATTTATGGGTTCCTGATGTTAATGTTGATTGTCAAGTCACTTATAGTGATCAAACTGCAGATTTC 4657
SAP2-2 A 4650
Consensus GTTATTGTTGATACTGGATCATCWGATTTATGGGTTCCTGATGTTAATGTTGATTGTCAAGTCACTTATAGTGATCAAACTGCAGATTTC
SAP2-1 TGTAAACAAAAGGGGACATATGATCCAAGTGGTTCATCAGCTTCACAAGATTTGAATACTCCATTCAAAATTGGTTATGGTGATGGATCT 4747
SAP2-2 4740
Consensus TGTAAACAAAAGGGGACATATGATCCAAGTGGTTCATCAGCTTCACAAGATTTGAATACTCCATTCAAAATTGGTTATGGTGATGGATCT
SAP2-1 TCATCTCAAGGTACTTTATATAAGGATACCGTTGGATTTGGTGGTGTTTCGATTAAAAATCAAGTTTTAGCTGATGTTGATTCTACTTCA 4837
SAP2-2 4830
Consensus TCATCTCAAGGTACTTTATATAAGGATACCGTTGGATTTGGTGGTGTTTCGATTAAAAATCAAGTTTTAGCTGATGTTGATTCTACTTCA
SAP2-1 ATTGATCAAGGTATTTTAGGGGTTGGTTATAAAACCAATGAAGCCGGTGGTAGTTATGATAATGTCCCTGTCACTTTAAAAAAACAAGGA 4927
SAP2-2 4920
Consensus ATTGATCAAGGTATTTTAGGGGTTGGTTATAAAACCAATGAAGCCGGTGGTAGTTATGATAATGTCCCTGTCACTTTAAAAAAACAAGGA
SAP2-1 GTCATTGCTAAGAATGCTTATTCACTTTATCTTAATTCTCCAGATGCTGCCACGGGACAAATAATTTTCGGTGGGGTTGATAATGCTAAA 5017
SAP2-2 C 5010
Consensus GTCATTGCTAAGAATGCTTATTCACTTTATCTTAATTCTCCAGATGCTGCCACGGGACAAATMATTTTCGGTGGGGTTGATAATGCTAAA
SAP2-1 TATAGTGGTTCATTAATTGCATTACCAGTTACTTCTGATCGTGAATTAAGAATTAGTTTGGGTTCAGTTGAAGTTTCTGGTAAAACCATC 5107
SAP2-2 5100
Consensus TATAGTGGTTCATTAATTGCATTACCAGTTACTTCTGATCGTGAATTAAGAATTAGTTTGGGTTCAGTTGAAGTTTCTGGTAAAACCATC
SAP2-1 AATACTGATAATGTCGATGTTCTTGTGGATTCAGGTACCACCATTACTTATTTGCAACAAGATCTTGCTGATCAAATCATTAAAGCTTTC 5197
SAP2-2 T 5190
Consensus AATACTGATAATGTCGATGTTCTTKTGGATTCAGGTACCACCATTACTTATTTGCAACAAGATCTTGCTGATCAAATCATTAAAGCTTTC
SAP2-1 AATGGTAAATTAACTCAAGATTCCAATGGTAATTCATTCTATGAAGTTGATTGTAATTTGTCAGGGGATGTTGTATTCAATTTTAGTAAA 5287
SAP2-2 5280
Consensus AATGGTAAATTAACTCAAGATTCCAATGGTAATTCATTCTATGAAGTTGATTGTAATTTGTCAGGGGATGTTGTATTCAATTTTAGTAAA
SAP2-1 AATGCTAAAATTTCCGTTCCAGCTTCCGAATTTGCTGCTTCTTTACAAGGTGATGATGGTCAACCATATGATAAATGTCAATTACTTTTC 5377
SAP2-2 5370
Consensus AATGCTAAAATTTCCGTTCCAGCTTCCGAATTTGCTGCTTCTTTACAAGGTGATGATGGTCAACCATATGATAAATGTCAATTACTTTTC
SAP2-1 GATGTTAATGATGCTAACATTCTTGGTGATAACTTTTTGAGATCAGCTTATATTGTTTATGATTTGGATGATAATGAAATTTCTTTGGCT 5467
SAP2-2 5460
Consensus GATGTTAATGATGCTAACATTCTTGGTGATAACTTTTTGAGATCAGCTTATATTGTTTATGATTTGGATGATAATGAAATTTCTTTGGCT
SAP2-1 CAAGTCAAATATACTTCTGCTTCCAGTATTTCTGCCTTGACCTAAGATCT 5517
SAP2-2 5510
Consensus CAAGTCAAATATACTTCTGCTTCCAGTATTTCTGCCTTGACCTAAGATCT